DNA Block Copolymers – Synthesis, Morphologies and Applications

Dissertation
zur Erlangung des Grades
"Doktor der Naturwissenchaften"

am Fachbereich
Chemie, Pharmazie und Geowissenschaften
der Johannes Gutenberg-Universität Mainz

Fikri E. Alemdaroglu
geb. in Adana

Mainz 2007

Dedicated to my wife, Ceren…

Hayatta en hakiki mürşit ilimdir!
(The real guide in life is science!)
M. Kemal ATATÜRK, 1923

Yaşamayı ciddiye alacaksın
Yani o derece, öylesine ki,
Kocaman gözlüklerin,
Beyaz gömleğinle bir laboratuarda insanlar için ölebileceksin.
Hem de yüzünü bile görmediğin insanlar için,
Hem de hiç kimse seni buna zorlamamışken,
Hem de en güzel, en gerçek şeyin yaşamak olduğunu bildiğin halde...

Nazım HİKMET, 1947

TABLE OF CONTENTS

List of Abbreviations

A	adenine
AFM	atomic force microscopy
ASO	antisense oligonucleotide
bp	base pair
Caco-2	human colon adenocarcinoma cell line
C	cytosine
CCD	charge coupled device
CLSM	confocal laser scanning microscopy
CMC	critical micelle concentration
DBC	DNA block copolymer
DCC	*N,N'*-dicyclohexylcarbodiimide
DIPEA	diisopropyl ethylamine
DLS	dynamic light scattering
DMEM	Dulbecco's modified Eagle's medium
DMF	*N,N*-dimethylformamide
DMSO	dimethylsulfoxide
DMT-MM	4-(4,6-dimethoxy-1,3,5-triazin-2-yl)-4-methylmorpholinium chloride)
DNA	deoxyribonucleic acid
Dox	Doxorubicin
DSMZ	Deutsche Sammlung von Mikroorganismen und Zellkulturen GmbH
DTS	DNA templated synthesis
dNTP	deoxynucleotide triphosphate
ds	double stranded
dTTP	deoxythymidine triphosphate
EDC	*N*-(3-dimethylaminopropyl)-*N'*-ethylcarbodiimide
FA	folic acid
FACS	fluorescence-activated cell-sorting
FBS	fetal bovine serum
FCS	fluorescence correlation spectroscopy
FR	Folate receptor
G	guanine

GPC	gel permeation chromatography
HBSS	Hank's balanced salt solution
HEPES	(4-(2-hydroxyethyl)-1-piperazineethanesulfonic acid)
HOPG	highly oriented pyrolytic graphite
HPLC	high pressure liquid chromatography
LCST	lower critical solution temperature
MALDI-TOF MS	matrix assisted laser desorption / ionization – time of flight mass spectrometry
MES	2-(*N*-morpholino)ethanesulfonic acid
M_n	number average molecular weight
M_w	weight average molecular weight
MW	molecular weight
MWCO	molecular weight cut-off
MOPS	3-(*N*-morpholino)propanesulfonic acid
NHS	*N*-hydroxysuccinimide
NIPAM	*N*-isopropylacrylamide
NMR	nuclear magnetic resonance
OD	optical density
ODN	oligodeoxynucleotide
PAGE	polyacrylamide gel electrophoresis
PCR	polymerase chain reaction
PDI	polydispersity index
PEG	poly(ethylene glycol)
PEI	polyethyleneimine
PEO	poly(ethylene oxide)
PLGA	poly(D,L-lactic-co-glycolic acid)
PLL	poly(L-lysine)
PNIPAM	poly(*N*-isopropylacrylamide)
PPO	poly(propylene oxide)
PS	polystyrene
RFC	reduced folate carrier
RNA	ribonucleic acid
ROMP	ring-opening metathesis polymerization

RP	reverse phase
RT	reverse transcription
SCK	shell cross-linked nanoparticle
SEC	size exclusion chromatography
SEM	scanning electron microscopy
SFM	scanning force microscopy
SNP	single nucleotide polymorphism
ss	single stranded
sulfo-NHS	sulfo-*N*-hydroxysuccinimide ester
T	thymidine
TBE	tris-borate-EDTA buffer
TdT	terminal deoxynucleotidyl transferase
T_G	glass transition temperature
THF	tetrahydrofuran
Tris	tris(hydroxymethyl)aminomethane
U	unit
UV/Vis	ultraviolet/visible spectroscopy
XTT	(2,3-bis(2-methoxy-4-nitro-5-sulfophenyl)-2H-tetrazolium-5-carboxanilide)

1 DNA Meets Synthetic Polymers – Highly Versatile Hybrid Materials*

-A literature review-

"The nucleic-acid 'system' that operates
in terrestrial life is optimized through evolution. Why not use it [...]
to allow human beings to sculpt something new,
perhaps beautiful, perhaps useful, certainly unnatural."

Prof. Dr. Roald Hoffmann, Nobel laureate in chemistry, 1981

Hybrids are a combination of dissimilar components arranged at the nanometric and molecular level.[1, 2] Throughout evolution nature has evolved a large variety of hybrid materials if one thinks of the post-transcriptional modifications of proteins, where peptidic structures are functionalized with carbohydrates or lipids,[3] and the process of biomineralization,[4, 5] which combines organic and inorganic materials within biological systems. Natural hybrids containing nucleic acids as a major class of biomacromolecules are also known. One important example is the ribosome which consists of a RNA structure into which proteins are interdispersed by non-covalent bonds.[6] Especially the complex function of this entity, i.e. the catalysis of protein biosynthesis, underlines the importance and potency of such biological hybrids. Involved in this process is another type of molecular chimeras, the so-called tRNAs. They consist of RNA that is covalently linked to small organic molecules, the amino acids.[7] Beside these naturally occuring examples, chemists have created artificial nucleic acid hybrid structures. DNA has been combined with inorganic materials like gold nanoparticles but also with small organic moieties like organic dyes or electrochemically

* Parts of this chapter were published as an "*Emerging Area*" article: *Org. Biomol. Chem.* **2007**, *5*, 1311.

active units.[8, 9] With such DNA hybrids new detection strategies[10] and nanoelectronic structures,[11, 12] as well as nanomechanical devices[13] were realized. In recent years a new type of nucleic acid hybrids has emerged, which consists of the combination of synthetic oligodeoxynucleotides (ODNs) and organic polymers. As a consequence of joining these two classes of materials, DNA block copolymers (DBCs) originate that maintain the special features of the biomacromolecule DNA and at the same time represent polymeric block type architectures that have attractive material properties in their own right.

The special features of DNA that are important in regard to the corresponding polymeric hybrids are the following: 1) Solid phase organic synthesis methods allow the preparation of single stranded (ss) DNA with almost any desired sequence of more than 100 bases.[14] 2) Hybridization of complementary sequences leads to the formation of a helical, semiflexible double stranded (ds) polymer with a diameter of about two nanometers and a pitch of about 3.4-3.6 nm in the B-form. 3) In addition to the famous double helix[15, 16], DNA can adopt other superstructures like triple helices or quadruplexes up to sophisticated artificially created 2-D and 3D-nanostructures.[17-20] 4) Finally, enzymes allow site specific modifications of the DNA strands.

In contrast, synthetic block copolymers usually self-assemble into well ordered periodic structures, a phenomenon called microphase separation.[21] This process is driven by the enthalpy of demixing of the constituent components of the block copolymers, whilst the macroscopic separation is hindered by the connectivity of the two blocks. Hence, the domain size of the ordered structures is of similar magnitude to that of the molecular dimensions. The morphologies which are adopted range from spherical, through cylindrical and gyroidal, to lamellar structures and can be controlled by the block length ratio of the constituent components. Beside the formation of nanostructures in bulk, block copolymers also form nano-objects in solution. This is the case when one of the blocks dissolves in the solvent, while the other block is insoluble (selective solvents). Especially polyelectrolyte block copolymers, which combine structural features of polyelectrolytes, block copolymers, and surfactants, show a rich association behaviour. The formation of micelles, strings, and networks of sometimes quite complicated topology has been described.[22] This class of polymers is important to mention in the context of DNA block copolymers since DNA from a polymer chemist's point of view represents a polyelectrolyte.

DNA and synthetic polymers were combined to bring out or enhance advantageous chemical and biological behaviours and at the same time to reduce or wholly suppress undesirable properties. An additional target is the evolution of entirely new material behaviour.

Within this chapter, first the different synthetic routes to prepare DNA block copolymers are described. Special attention will be paid to the synthesis of linear topologies and graft architectures where ODNs are attached as side chains to a synthetic polymer backbone. Common to all of these structures is that the nucleic acid segments and the organic polymer moieties are connected by covalent bonds. There is a considerable amount of literature describing electrostatic complexes of DNA with various polycations,[23, 24] however, this is beyond the scope of this introduction. In the second part the focus lies on the properties of these materials and their applications in the fields of biology, biotechnology and nanoscience are described.

Synthesis of DNA Block Copolymers

For the generation of linear DNA block copolymers one end of an ODN needs to be coupled to a terminal functionality of an organic polymer block. This synthetic goal is achieved by grafting onto strategies either by connecting the biological and the organic polymer segments in solution (**Figure 1.1A**) or on a solid support (**Figure 1.1B**). Three different coupling reactions in solution have been reported: amide [25-28] and disulfide bond formation[29] as well as Michael addition.[29] When a peptide bond is formed to join both segments, terminally amino-functionalized ODNs were coupled to active ester containing polymers. Several activating reagents including *N*,*N*′-dicyclohexylcarbodiimide (DCC), *N*-hydroxysuccinimide ester (NHS) or *N*-(3-dimethylaminopropyl)-*N*'-ethylcarbodiimide (EDC) and sulfo-*N*-hydroxysuccinimide ester (sulfo-NHS) were used for the coupling reaction. The formation of a disulfide bridge between DNA and the polymer required a terminal thiol-modification at the ODN as well as at the polymer, which were reacted at slightly alkaline conditions in aqueous phase. In the case of the Michael addition, thiol functionalized ODNs were reacted with a malimido functionalized polymer at neutral pH. Attaching the biological and the organic segment in solution is an easy procedure and does not require an expensive DNA synthesizer. Amino or thiol functionalized ODNs are available from commercial sources which makes DBCs available to conventionally equipped laboratories. This coupling strategy proceeds with high yields as long as water-soluble polymers such as poly(ethylene oxide) (PEO) and

poly(N-isopropylacrylamide) (PNIPAM) are employed.[28, 30-38] However, the yields are drastically lower when hydrophobic polymers are used. A reason for poor coupling efficiencies is the incompatibility of the hydrophilic DNA and the hydrophobic polymers in the solvent. To overcome these synthetic difficulties, solid phase synthesis was employed for the preparation of amphiphilic DBCs by several groups (See **Figure 1.1**).[39-42]

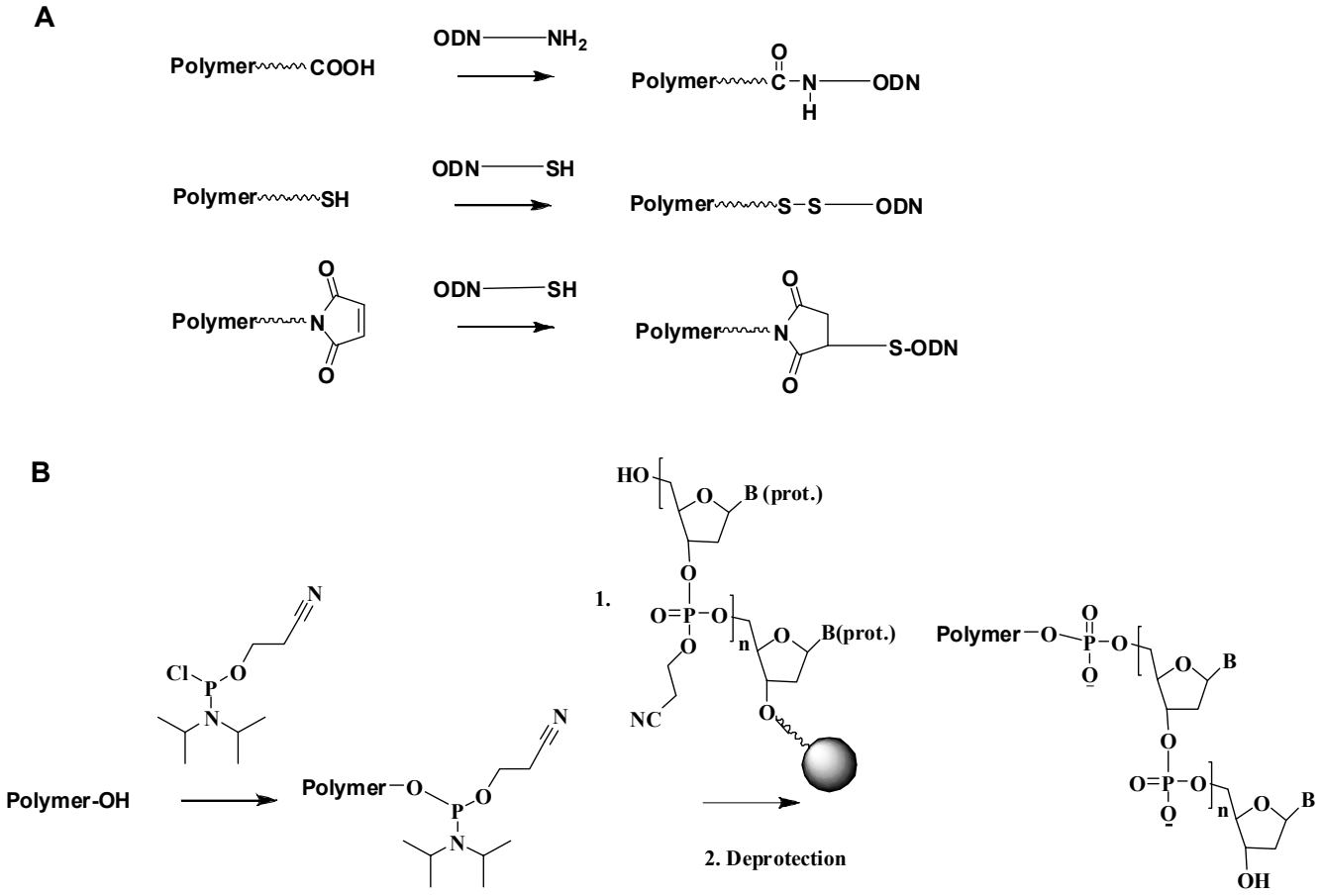

Figure 1.1 *The synthesis of DBCs by (A) in solution and (B) on solid support.*

The grafting onto approach on the solid support started with hydroxyl-terminated PS that was reacted with phosphoramidite chloride to yield the corresponding phosphoramidite-polymer. This key reagent was then coupled to the detrytilated 5' hydroxyl-end of the ODN on the solid support by the so-called "syringe-synthesis-technique". After liberation from the solid

support, deprotection of the protecting groups and purification by polyacrylamide gel electrophoresis (PAGE) or by HPLC the DBCs were obtained. This synthetic route offers one advantage for the preparation of amphiphilic DBCs. The incompatibility of the biological and the synthetic moiety is avoided because the coupling step is carried out in organic solvents in which the organic polymer is readily soluble. However the syringe synthesis technique[43, 44] might have some drawbacks because high reproducibility and efficient exposure of the phosphoramidite polymer to the solid phase cannot be guaranteed with a manual method employing two syringes containing the reactants. Interestingly, Mirkin and coworkers[43, 44] have never reported the yields of the DBCs prepared by this technique and only mentioned the quantity of the materials they used.

Another structurally important class of DBCs consists of graft architectures where several ODNs are attached to the polymer backbone to form a comb-like topology (**Figure 1.2**). Three different synthetic routes were developed to realize these structures. In the first approach, the synthetic polymer was prefabricated and in a subsequent grafting step the ODNs were coupled in solution. One way to attach the ODNs to the synthetic backbone is amide bond formation. Therefore, during the synthesis the polymer backbone was equipped with active ester groups that were reacted with terminal amino-modified ODNs.[45] Like in the previous procedure, a covalent bond between the organic polymer and the nucleic acid units was realized with the help of amino-modified ODNs. They were reacted with an alternating copolymer consisting of ethylene- and maleic anhydride units representing the backbone.[46] A second route for the preparation of graft architectures relies on coupling the synthetic polymer to the ODN on a solid support. This procedure is similar to the one described above for the fabrication of linear amphiphilic DBCs using phosphoramidite polymers. A major difference was that several phosphoramidite groups along the polynorbonene backbone served as attachment points for the ODNs.[43, 44] A third variant for the preparation of DNA side chain polymers is based on polymerizable ODN-macromonomers. An acrylamide monomer was functionalized via an alkyl spacer as phosphoramidite that can be reacted with the 5’ end of an ODN. This polymerizable nucleic acid moiety was transformed into a graft architecture by copolymerization with acrylamide.[47, 48] The multimerization of nucleic acid segments along a single organic macromolecule offers important advantages in some applications including DNA detection and DNA hydrogels which are discussed later in this chapter.

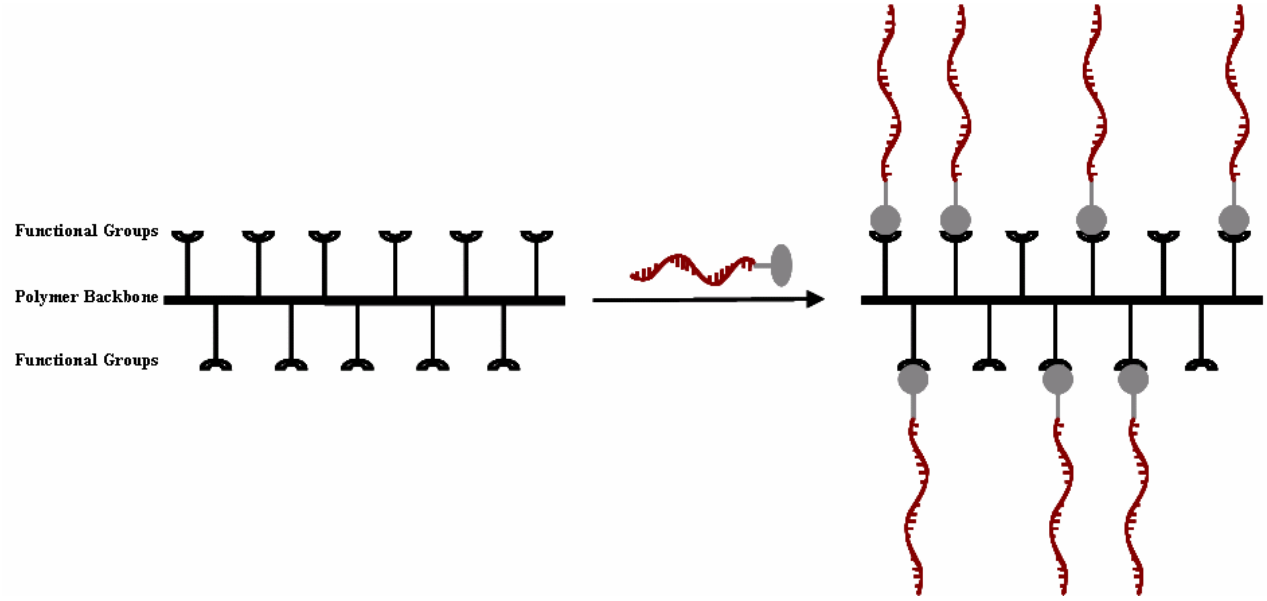

Figure 1.2 *The covalent attachment of end functionalized ODN to a polymer backbone.*

DBCs as new Gene Delivery System

A wide variety of antisense oligonucleotides (ASOs) have attracted considerable attention due to their specific interaction with cytoplasmic mRNA and connected therewith the blocking of specific gene products. ASOs are not only a useful experimental tool in protein target identification and validation for drug development, but also a highly selective therapeutic strategy for diseases with dysregulated protein expression.[49] Practical applications of ASOs as therapeutic agents encounter two important problems: poor cellular uptake and enzymatic hydrolysis.[50] This is the point where DBCs come into play because cellular uptake of ODNs can be enhanced and nuclease activity on ODN substrates can be reduced.

Park and coworkers[51] have addressed the issue of poor cellular uptake by employing micellar aggregates of different DBCs as ASOs delivery systems. They prepared a DNA-*b*- poly(D,L-lactic-co-glycolic acid) (PLGA) block copolymer by reacting amine-terminated ASO with an activated PLGA. This amphiphilic DBC formed micelles readily in aqueous solution with

PLGA segments as a hydrophobic core and ODN segments as a surrounding hydrophilic corona. Atomic force microscopy (AFM) and dynamic light scattering (DLS) analysis revealed spherical-shaped micelles with a diameter of 80 nm. The *in vitro* uptake studies with NIH3T3 mouse fibroblast cells showed that the micelles were transported into the cells more efficiently than the pristine ODN. Due to the biodegradable nature of the organic polymer, these micelles could release the ASO in a controlled manner.[51] The use of micelles as ASO carriers encouraged the same group to extend their delivery system to biocompatible DNA-*b*-PEO block copolymer systems. In this case nanoscopic aggregates were prepared by complexation with polycations like the positively charged fusogenic peptide, KALA,[52] and polyethyleneimine (PEI).[30] Both electrostatic complexes exhibited a core containing the charged moieties whereas the corona was composed of PEO. The effective hydrodynamic diameter of both micelle aggregates was around 70 nm with a very narrow size distribution. In the first conjugate, the ODN was coupled to PEO via an acid-cleavable linkage (phosphoramidite) so that the ODN could be released in the acidic endosomal environment and interacts with the target mRNA sequence to inhibit protein expression. In particular, the cellular uptake behaviour and antiproliferation effects of the *c-myb* antisense ODN containing polyion complex micelles on smooth muscle cells were investigated. It was shown that the micelles were incorporated into the cells far more efficiently than the non-polymer-modified ODN. Alternatively, the PEI cationic polymer was complexed with DNA-*b*-PEO that codes for *c-raf* antisense and the corresponding electrostatic aggregate was applied to tumor-bearing nude mice. Significant antitumor activities against human lung cancer were measured. Interestingly, the polyion complex micelles showed a higher accumulation level in the tumor cells than the pristine ODN. Kataoka *et al.* as well synthesized electrostatic complexes of DNA-*b*-PEO and polycationic moieties like PEI and poly(L-lysine) (PLL).[33, 38] The micelle systems containing PEI were desigend in such a fashion that the ODN can be released by hydrolysis from the PEO segment. Moreover, the stability of the DNA-*b*-PEO within the polyion complex micelles against deoxyribonuclease (DNase I) was demonstrated. Important findings in regard to design effective antisense ODN delivery systems were made with the electrostatically trapped micelles bearing PLL as the polycation. Structural features of the DNA block copolymer were also an acid labile linker between the PEO and the nucleic acid moiety and a lactose targetting moiety attached to the PEO segment. A significant antisense effect against luciferase gene expression could be observed. Micelles with a targetting unit showed a more pronounced antisense effect than control complexes without the lactose unit. The acid-labile linkage was found to be crucial for high antisense activity since control

experiments with a non-cleavable control DNA block copolymer showed decreased performance. Beside targeting mRNA, recently so called anti gene ODNs that interact with ds DNA have been developed. These ODNs are designed to bind to polypurine-polypyrimidine sequences through triple helix formation and manipulate gene function.[53-61] A comprehensive study to use DNA-*b*-PEO conjugates as anti gene ODN delivery systems for inhibiting the expression of the Ki-*ras* gene and the proliferation of pancreatic cancer cells was carried out by Xodo and coworkers.[36] A high molecular weight PEO was conjugated to a G-rich oligonucleotide as previously reported by the same group. [62, 63] The uptake of DNA-*b*-PEO, which was supposed to form a triplex with the promoter region of the KI-*ras* gene, was investigated by fluorescence-activated cell-sorting (FACS) and confocal fluorescence microscopy showing that the cells harboured the conjugate 6-7 times higher than the pristine ODN (**Figure 1.3**). Of equal importance is that the DNA-*b*-PEO efficiently inhibited the transcription of Ki-*ras* mRNA and associated therewith the proliferation of pancreatic cancer cells was reduced by 50%. It is important to mention that the ODN-PEO conjugate itself did not promote any inhibition of transcription by the anticipated interaction with the ds DNA. Instead, the antiproliferative activity was induced by binding of the DNA-*b*-PEO to a nuclear factor recognizing the KI-*ras* promotor sequence by an aptameric mechanism. In this regard, the study introduced a new antiproliferative strategy based on the use of aptamers against nuclear proteins. On the other hand, this was the first report of an aptamer consisting of a DNA block copolymer.

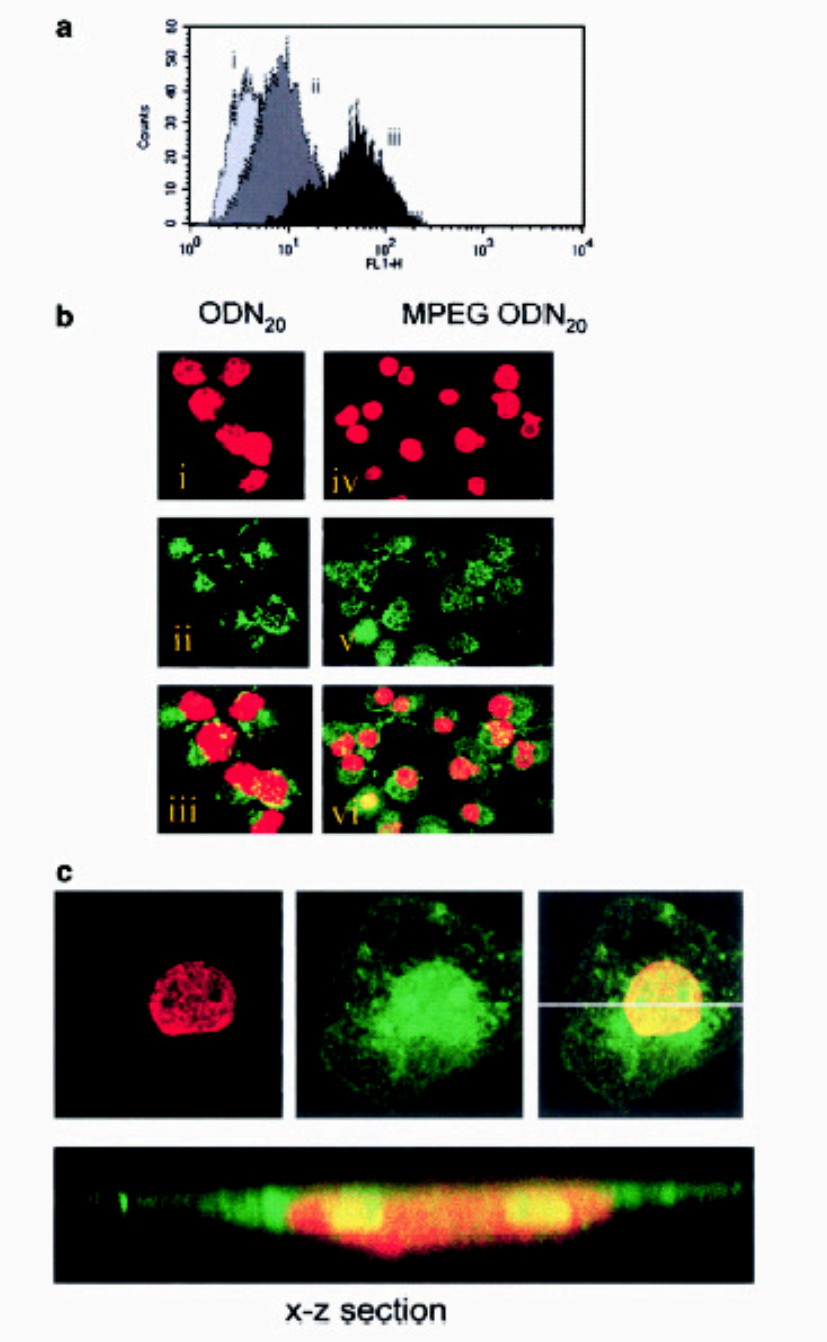

Figure 1.3 *Uptake of conjugated and unconjugated ODNs. **(a)** FACS analysis of Panc-1 cells untreated and treated with 5 mM ODN20 and MPEG ODN20. Cells were analyzed by FACS 48 hours after the oligonucleotides were delivered to the cells. Peak i, untreated cells; peak ii, cells treated with ODN20-F; peak iii, cells treated with MPEG ODN20-F. **(b)** Confocal images of Panc-1 cells treated for 24 hours with 5 mM ODN20-F (panels i, ii, iii) and MPEG ODN20-F (panels iv, v,vi). Panels i and iv show the nuclei of Panc-1 cells stained in red with propidium iodide; panels ii and v show the green fluorescence light emitted by the fluorescein-conjugated oligonucleotides; panels iii and vi are superimposed views obtained*

*from i‡ii and iv‡v. (**c**) Confocal views of a Panc-1 cell showing that MPEG ODN20-F is harbored in the nucleus. Note the presence of the conjugate in the nucleoli. The x–z panel shows a cumulative projection of x–z crosssections corresponding to the line depicted in the magnified cell.*[36]

DBCs used in Purification of Biomaterials

An important class of DBCs consists of the DNA-*b*-PNIPAM conjugates, which are used for purification of biomacromolecules employing a thermal stimulus. It is well known that PNIPAM exhibits a remarkable phase transition in aqueous media in response to changes in temperature and therefore exhibiting a lower critical solution temperature (LCST).[64, 65] This fully reversible temperature-responsive behaviour has found application in the purification of bioconjugates from reactants and other solutes employing small temperature increases above the LCST.[26-28, 31, 32, 66-71] In an important report, Freitag and coworkers[70] synthesized a DNA-*b*-PNIPAM conjugate, of which the nucleic acid segment was capable of recognizing a sequence of plasmid DNA by triple helix formation (**Figure 1.4**). After complexation below the LCST, the plasmid target DNA could be precipitated quantitatively from the solution by raising the temperature to 40°C. After redissolution at lower temperatures, DNA-*b*-PNIPAM was released from the plasmid by changing the pH of the solution. The target DNA molecule was obtained in yields of 70 to 90% in good purity. Plasmid DNA offers an attractive way to deliver therapeutic genes for gene therapy and genetic immunization due to its simplicity and excellent safety profile.[72, 73] However, the dosage which has been used in gene therapy is high,[74-76] and the current purification techniques will probably not meet the demands if these drugs are routinely administered in the future. The triple-helix affinity precipitation of plasmid DNA by DNA-*b*-PNIPAM conjugates could serve as a practical system to provide large amounts of pharmaceutical grade plasmid DNA.

Beside for the isolation of plasmid DNA, DNA-*b*-PNIPAM conjugates were applied for the affinty precipitation and separation of DNA-binding proteins.[69] For that purpose, PNIPAM terminally functionalized with a psoralene group was photochemically crosslinked with ds DNA to form a graft architecture. When this side chain polymer containing a ds DNA backbone was enzymatically ligated to a non-PNIPAM-modified DNA segment encoding the so-called TATA-box, the corresponding TATA-box binding protein could be selectively

separated from a protein mixture by thermal affinity precipitation. In the future, this elegant approach might be extended for the detection of unknown DNA binding proteins like transcription factors from cell lysates.

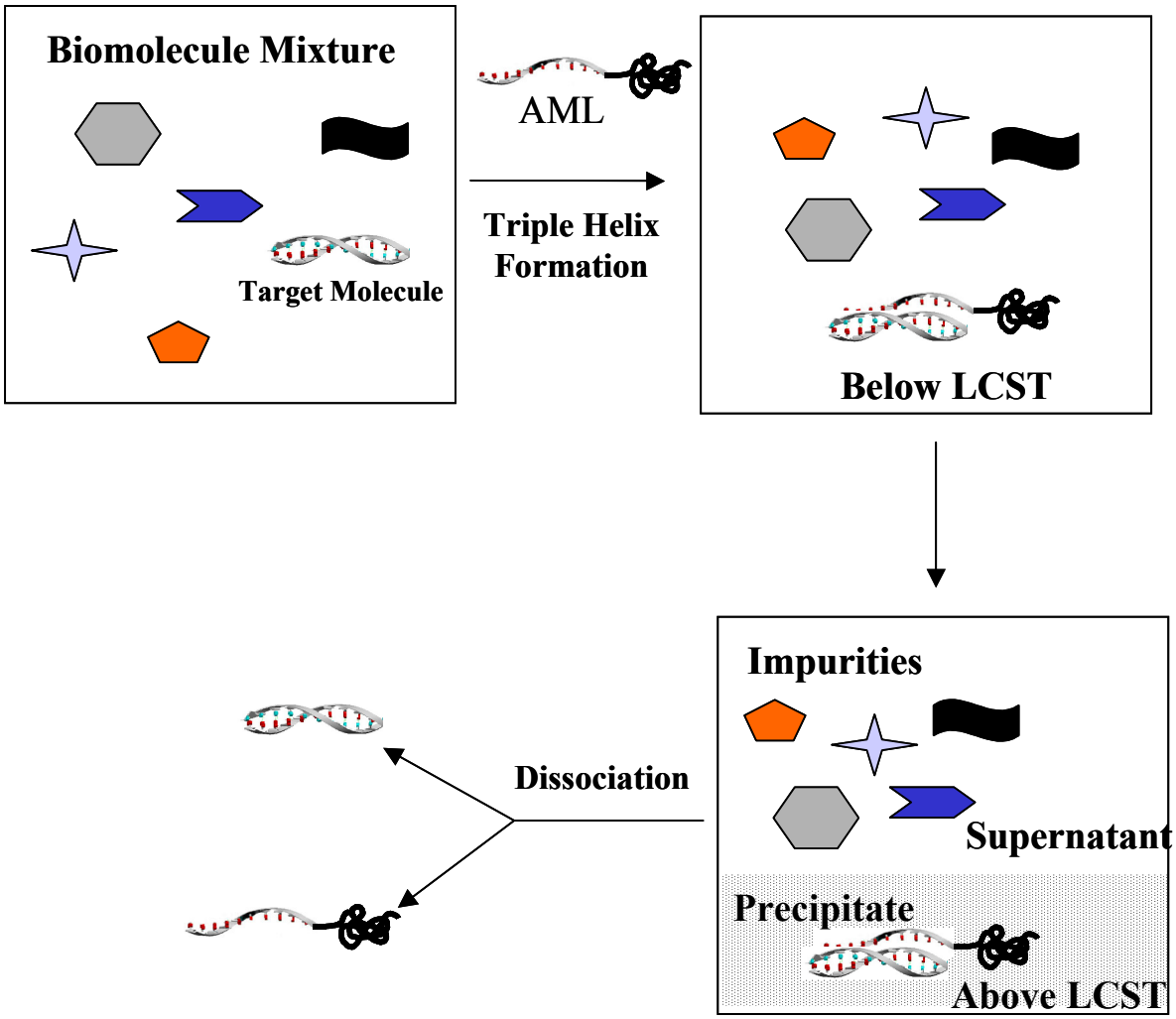

Figure 1.4 *Purification of pharmaceutical grade plasmid DNA by triplex-helix affinity precipitation procedure.*

DBCs used in Sensitive DNA Detection

Sensitive DNA detection is important in the fields of gene analysis, tissue matching, and forensic applications. The key challenge is to develop a material that efficiently senses the presence of ss or ds DNA and converts it to a detectable signal, either electrochemically or by means of fluorescence. A first approach towards using DNA block copolymers as probes for DNA detection were undertaken by Haralambidis and coworkers.[77] The rationalization behind the use of employing a block copolymer architecture was that the nucleic acid part is needed for molecular recognizion while the polymer block allows the incorporation of multiple labels along the backbone. A synthetically challenging method was developed for realizing the linkage between the ODN and the organic polymer segment, since the polyamide was attached to the base of the nucleotide at the 5' end.[77] The polyamide unit was synthesized employing standard Fmoc-chemistry. This allowed the incorporation of several pyrenylated amino acid building blocks into the peptide segment.[78] Significant excimer fluorescence from the DNA-*b*-polyamide was detected due to the close proximity of the chromophores. The multimerization of labels resulted in an increase of the emission intensity proving the concept of a polylabel strategy. Hybridization of DNA-*b*-polyamide with complementary sequences affected the luminescence intensity of the probe, however, a real DNA detection was not realized.

Instead of DNA diblock copolymers, the Müllen group[79] developed a triblock architecture for DNA detection. This novel structural concept is based on fluorescence dequenching upon hybridization (**Figure 1.5A**). The so-called "twin probe" consists of a central fluorene derivative as fluorophore to which two identical oligonucleotides were covalently attached. This probe architecture was applied in a homogenous hybridization assay with subsequent fluorescence spectroscopic analysis. The bioorganic hybrid structure was well suited for sequence specific DNA detection and even single nucleotide polymorphisms (SNPs) were identified with high efficiency. The covalent attachment of two single stranded oligonucleotides leads to strong quenching of the central fluorescence dye induced by the nucleobases whereas when one oligonucleotide is coupled to the central fluorophore no dequenching upon hybridization occurs. The twin probe is characterized by supramolecular aggregate formation accompanied by red-shifted emission and broad fluorescence spectra. In the future, the central emitter unit will be extended to oligomeric conjugated materials with the aim of increasing the sensitivity of the probe.

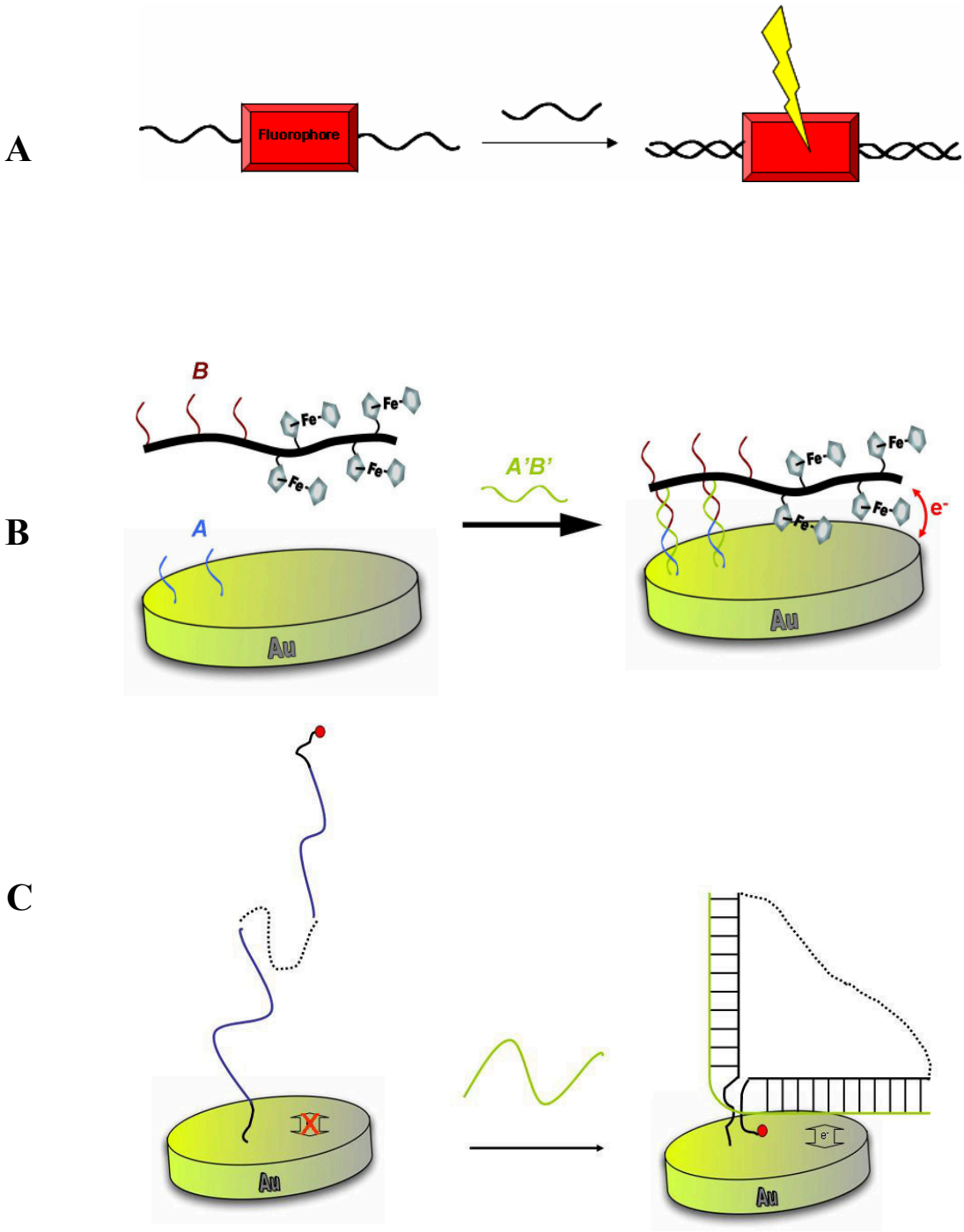

Figure 1.5 *DNA block copolymers used in sensitive DNA detection. A) Twin probe is applied for DNA detection by means of fluorescence in a homogenous hybridization essay. B) Electrochemical detection of DNA by graft architecture. C) Triblock architecture for the reagentless DNA detection.*

In contrast to linear structures, a graft architecture for sensitive DNA detection was realized by Mirkin and co-workers who reported the electrochemical detection of DNA by polynorbornene-DNA hybrids (**Figure 1.5B**).[43, 44] Two kinds of DBCs with either ferrocenyl or dibromoferrocenyl groups as well as ODNs were prepared by ring-opening metathesis polymerization (ROMP). With these DBCs target concentrations as low as 100 pM could be detected which is one order of magnitude more sensitive than the previously reported system based on ferrocene containing oligonucleotides.[80]

A structural alternative to graft architectures of DBCs used for electrochemical DNA detection is a linear topology (**Figure 1.5C**). Grinstaff *et al.* prepared an A-B-A type triblock copolymer containing two DNA strands linked via a small, flexible PEO linker.[40] The capture strand was functionalized with a terminal thiol for immobilization on a gold electrode. The probe strand contained the 5'-terminal redox-active reporter group, ferrocene. Upon binding of the target strand to the immobilized capture strand the distance between the 5'-terminal ferrocene and the electrode surface was decreased resulting in an electrochemical signal. This DNA triblock copolymer gives rise to a sensitive reagentless electrochemical assay which is ideally suited for the continuous, rather than batch, monitoring of a flow of analyte.[81] Compared to the above described graft architecture, the estimated detection limit of the assay was 200 pM of DNA.

DBCs in Nanoscience

Nanotechnology has been one of the fastest developing research areas in recent years. One of the key objectives in this fascinating multidisciplinary field are nanoparticles, which most commonly exhibit sizes in the range of 10-100 nm and size dependent properties different from the bulk materials. These objects can either be composed of inorganic[82-84] or organic materials.[85] Synthetic chemists have been extremely creative in finding new methods for the preparation of nanoparticles. The chemical synthesis techniques can, in principle, be divided into two general strategies: 1) the mechanical milling of raw material down to nanosized particles and 2) the conversion of the products or educts dissolved in suitable solvents into nanodispersed systems by precipitation, condensation or chemical synthesis. Especially, within the chemical routes towards nanoparticles, polymers are often involved, if one considers the preparation of polymer dispersions[86-88] and dendrimers[89, 90] or the aggregation of block polymers.[22, 91] When the solvent environment of a linear block copolymer system is

a selective solvent for one of the segments while the other polymer unit is insoluble, typically spherical micelles of nearly uniform size and shape are obtained, which can be regarded as nanoparticle systems.[92]

Translated into the context of amphiphilic DNA block copolymers, this means that nanoparticles containing a hydrophobic polymeric core and a ss DNA corona are obtained. In a previous paragraph, the advantages of such systems containing a hydrophobic core of PLGA and a shell of ss nucleic acids have been discussed in regard to delivery of antisense ODNs.[51] But amphiphilic DBC systems with polystyrene (PS)[39] have also been synthesized. The organic segment of DNA-*b*-PS polymers exhibited an M_n of 5.600 g/mol while the lengths of the ODNs was adjusted to be a 5 mer, 10 mer and 25 mer. The diameter of the resulting micelles was measured by AFM and dynamic light scattering which are important tools for the characterization of superstructures formed from amphiphilic DBCs (**Figure 1.6**). The different lengths of the DNA segments resulted in tailorable diameters of the micelles ranging from 8 – 30 nm. The AFM measurements that were carried out in tapping mode on a mica surface in air were consistent with the DLS data. These well-defined block copolymer micelles were employed to build up sequence specific aggregates with DNA modified gold nanoparticles. The aggregates could be reversibly disassembled by heating them above the melting temperature of the double stranded DNA. This result paves the way to higher ordered nanostructures defined by the recognition properties of DNA and the hydrophobic-hydrophobic interactions of the water insoluble polymer segments. In such a fashion, hybrid structures consisting of three classes of materials, organic polymers, biological entities and inorganic moieties were realized.

DNA Hydrogels Based on DBCs

In general, hydrogels are defined as crosslinked polymer networks. Two different network architectures containing DNA are known. The first class of DNA hydrogels was built up by chemically crosslinking ds DNA strands.[93] As a crosslinking agent ethylene glycol diglcidyl ether was employed. Such DNA gels showed a discontinuous volume transition when acetone was added to the network that was swollen in aqueous medium. At a concentration of 63% acetone the gel shrinked 15 times of its volume. The process was proven to be reversible. Such phase transitions are one reason why polymer networks have attracted the attention of

many researchers. Recently, several groups have investigated synthetic polymer hydrogels and tried to induce phase transitions by external stimuli.[94]

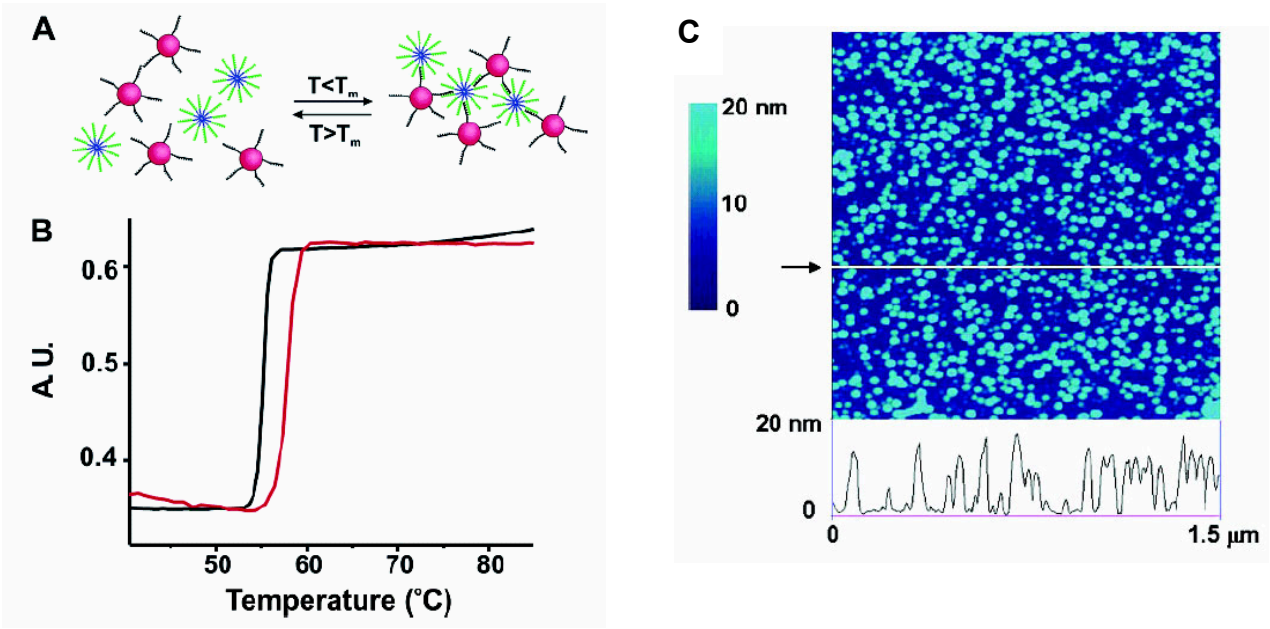

Figure 1.6 *(A) DNA directed sequence specific assembly of DBC micelles and DNA modified gold nanoparticles. The assembled aggregates can be reversibly disassembled by heating them above the "melting temperature" of the duplex strand interconnects. (B) The sharp melting transitions (melting curves) as monitored by the surface plasmon band of the Au nanoparticles at 520 nm vs solution temperature. The red line shows the melting curve for the assemblies formed from the DNA micelles and gold nanoparticles modified with complementary DNA. The black line shows the melting curve for the assemblies formed from DNA micelles and gold nanoparticles modified with single base mismatch DNA strands. (C)Tapping mode AFM image showing the spherical micelle structures constructed from polymer-DNA amphiphiles.*

Gels can expand or contract when triggered by tiny changes in temperature, light, solvent composition, or when target molecules are bound. The ability of the gels to undergo huge but reversible changes in volume allows unique new systems to be created mainly for the purpose of encapsulating and releasing materials. Since synthetic polymer chains of the gels cannot

bind with the target molecules selectively, conjugates of the receptors and the chain are needed. In contrast, DNA has inherently a unique chain structure able to bind with specific bio- and synthetic molecules.[93, 95] At this point the second class of DNA networks is introduced. Characteristic for these structures is that not the polymer network but the crossing points consist of DNA. Nagahara and coworkers prepared two different kinds of DBCs. Poly(*N*,*N*-dimethylacrylamide-*co*-*N*-acryloyloxysuccinimide) was reacted with either an amino-terminated 10mer ODN exclusivly containing adenine (oligoA) or thymine bases (oligoT) to form graft architectures.[45] A first hydrogel was realized by hybridizing the side chain polymer carrying oligoA with the conjugate containing oligoT. In a second route, a hydrogel was formed by hybridizing two oligoT derivatized copolymers with a 20mer adenine crosslinking strand. Nagahara *et. al* prepared films of these hydrogel materials and characterized the hybridization behaviour by UV-monitored melting curves. The material exhibits two important properties. First, gel formation is reversible and the temperature of dissociation can be controlled by the composition and length of the ODN. Second, during the gelation process that can be carried out at room temperature a target molecule remains intact because of the mild and selective hydrogen bond formation between coplementary DNA strands. Release of the target molecule might be achieved by denaturing the double stranded DNA crosslinks. Inspired by this approach, Langrana *et al*. prepared DNA gels by adding a crosslinking strand to a mixture of two DNA-polyacrylamide graft architectures.[47, 48] This DNA sequence was designed in such a fashion that it was complementary to both ODNs of the DNA graft polymers. As described for the previous example, hydrogel formation was thermoreversible. But it was also possible to dissociate the DNA crosslinks without a thermal stimulus. This was achieved by introducing a toehold at the crosslinking strand or so called fuel strand consisting of an additional ss DNA segment that does not hybridize with the DNA sidechains attached to the polyacrylamide. When a so called removal strand that is a full complement to the fuel strand was added the crosslinks could be efficiently disintegrated. This change in the degree of crosslinking was accompanied by a switch of the mechanical properties of the hydrogel. It needs to be pointed out here that all environmental parameters like temperature and buffer conditions remained constant while just a DNA strand was added which induced a change in the stiffness of the network. This kind of sequence responsive materials with modifiable bulk properties might be promising candidates for biotechnology applications.

Summary

The combination of DNA and synthetic polymers in a covalent fashion leads to engineered material properties of the hybrids that cannot be realized with the polymer or the nucleic acid as single entities. Several synthetic routes and coupling strategies are now available to produce ss DNA di- and triblock architectures. These methods especially allow one to vary the nature of the organic polymer to exhibit hydrophilic, hydrophobic as well as thermoresponsive properties. Generally, solution coupling strategies have been employed to prepare DBCs with water-soluble polymers. So far, only two amphiphilic structures are reported with remarkable properties which suffer from low yields. In order to exploit the DNA in combination with hydrophobic polymers robust coupling strategies with high yields need to be developed. Another limitation remains regarding the nucleic acid segments. Until now, the length of the DNA blocks is limited to around 40 nucleotides, which is rather small in comparison to naturally occuring nucleic acid like genomic or plasmid DNA. In 2006, Pickett has proposed to use DNA to obtain high molecular weight and monodisperse macromolecules.[96] Based on physical theories and assumptions, he theoretically showed that the Watson-Crick base pairing can be employed to obtain ds DBCs with complex structures. However, except di- and triblock linear DBCs, which were prepared by grafting-onto techniques, no complex DNA copolymer architectures have been realized. Owing to its specific hydrogen bonding, DNA is an important building block for programmable material synthesis. Hydrophobic polymers in combination with this biological entity have been employed to prepare nanoparticles as mentioned above. However, until now, only spherical nanoparticles have been assembled. More work should be dedicated to tailor the size and the shape of the micelles.

DBCs have found promising applications in the field of antisense and antigene delivery, DNA detection and in nanoscience. More efforts must be devoted to optimize these applications and broaden their use in the fields of bio- and nanotechnology. With using DBCs in the context of nucleic acid delivery, a promising research direction namely investigating the interaction of these materials with living cells has been started. Now it is the time to study uptake and transport properties of the systems in cells and through biological barriers in regard to their physical parameters.

References

[1] P. Y. W. Dankers, M. C. Harmsen, L. A. Brouwer, M. J. A. Van Luyn, E. W. Meijer, *Nat. Mater.* **2005**, *4*, 568.

[2] T. Kokubo, H. M. Kim, M. Kawashita, *Biomaterials* **2003**, *24*, 2161.

[3] V. Schreiber, F. Dantzer, J. C. Ame, G. de Murcia, *Nat. Rev. Mol. Cell Biol.* **2006**, *7*, 517.

[4] G. Krampitz, G. Graser, *Angew. Chem. Int. Ed.* **1988**, *27*, 1145.

[5] L. Addadi, S. Weiner, *Angew. Chem. Int. Ed.* **1992**, *31*, 153.

[6] G. L. Conn, D. E. Draper, E. E. Lattman, A. G. Gittis, *Science* **1999**, *284*, 1171.

[7] P. Nissen, M. Kjeldgaard, S. Thirup, G. Polekhina, L. Reshetnikova, B. F. C. Clark, J. Nyborg, *Science* **1995**, *270*, 1464.

[8] S. J. Park, A. A. Lazarides, C. A. Mirkin, P. W. Brazis, C. R. Kannewurf, R. L. Letsinger, *Angew. Chem. Int. Ed.* **2000**, *39*, 3845.

[9] S. J. Park, T. A. Taton, C. A. Mirkin, *Science* **2002**, *295*, 1503.

[10] T. A. Taton, C. A. Mirkin, R. L. Letsinger, *Science* **2000**, *289*, 1757.

[11] E. Braun, Y. Eichen, U. Sivan, G. Ben-Yoseph, *Nature* **1998**, *391*, 775.

[12] K. Keren, R. S. Berman, E. Buchstab, U. Sivan, E. Braun, *Science* **2003**, *302*, 1380.

[13] C. D. Mao, W. Q. Sun, Z. Y. Shen, N. C. Seeman, *Nature* **1999**, *397*, 144.

[14] M. H. Caruthers, *Science* **1985**, *230*, 281.

[15] J. D. Watson, F. H. C. Crick, *Nature* **1953**, *171*, 737.

[16] J. D. Watson, F. H. C. Crick, *Nature* **1953**, *171*, 964.

[17] P. W. K. Rothemund, *Nature* **2006**, *440*, 297.

[18] N. C. Seeman, *Nature* **2003**, *421*, 427.

[19] C. X. Lin, Y. Liu, S. Rinker, H. Yan, *Chemphyschem* **2006**, *7*, 1641.

[20] M. K. Beissenhirtz, I. Willner, *Org. Biomol. Chem.* **2006**, *4*, 3392.

[21] I. W. Hamley, *The physics of block copolymers*, Oxford University Press, Oxford, **1998**.

[22] S. Forster, V. Abetz, A. H. E. Muller, *Adv. Polym. Sci.* **2004**, *166*, 173.

[23] T. K. Bronich, H. K. Nguyen, A. Eisenberg, A. V. Kabanov, *J. Am. Chem. Soc.* **2000**, *122*, 8339.

[24] M. Thomas, A. M. Klibanov, *Proc. Natl. Acad. Sci. U. S. A.* **2002**, *99*, 14640.

[25] J. H. Jeong, S. H. Kim, S. W. Kim, T. G. Park, *Bioconjugate Chem.* **2005**, *16*, 1034.

[26] Y. G. Takei, T. Aoki, K. Sanui, N. Ogata, T. Okano, Y. Sakurai, *Bioconjugate Chem.* **1993**, *4*, 42.

[27] Y. G. Takei, M. Matsukata, T. Aoki, K. Sanui, N. Ogata, A. Kikuchi, Y. Sakurai, T. Okano, *Bioconjugate Chem.* **1994**, *5*, 577.

[28] R. B. Fong, Z. L. Ding, C. J. Long, A. S. Hoffman, P. S. Stayton, *Bioconjugate Chem.* **1999**, *10*, 720.

[29] M. Oishi, T. Hayama, Y. Akiyama, S. Takae, A. Harada, Y. Yarnasaki, F. Nagatsugi, S. Sasaki, Y. Nagasaki, K. Kataoka, *Biomacromolecules* **2005**, *6*, 2449.

[30] J. H. Jeong, S. W. Kim, T. G. Park, *J. Controlled Release* **2003**, *93*, 183.

[31] D. Umeno, T. Mori, M. Maeda, *Chem. Commun.* **1998**, 1433.

[32] D. Umeno, M. Kawasaki, M. Maeda, *Bioconjugate Chem.* **1998**, *9*, 719.

[33] M. Oishi, S. Sasaki, Y. Nagasaki, K. Kataoka, *Biomacromolecules* **2003**, *4*, 1426.

[34] M. Murata, W. Kaku, T. Anada, Y. Sato, T. Kano, M. Maeda, Y. Katayama, *Bioorg. Med. Chem. Lett.* **2003**, *13*, 3967.

[35] J. H. Jeong, S. H. Kim, S. W. Kim, T. G. Park, *Journal of Biomaterials Science-Polymer Edition* **2005**, *16*, 1409.

[36] S. Cogoi, M. Ballico, G. M. Bonora, L. E. Xodo, *Cancer Gene Ther.* **2004**, *11*, 465.

[37] J. Sanchez-Quesada, A. Saghatelian, S. Cheley, H. Bayley, M. R. Ghadiri, *Angew. Chem. Int. Ed.* **2004**, *43*, 3063.

[38] M. Oishi, F. Nagatsugi, S. Sasaki, Y. Nagasaki, K. Kataoka, *ChemBioChem* **2005**, *6*, 718.

[39] Z. Li, Y. Zhang, P. Fullhart, C. A. Mirkin, *Nano Lett.* **2004**, *4*, 1055.

[40] C. E. Immoos, S. J. Lee, M. W. Grinstaff, *J. Am. Chem. Soc.* **2004**, *126*, 10814.

[41] B. de Lambert, C. Chaix, M. T. Charreyre, A. Laurent, A. Aigoui, A. Perrin-Rubens, C. Pichot, *Bioconjugate Chem.* **2005**, *16*, 265.

[42] C. Minard-Basquin, C. Chaix, C. Pichot, B. Mandrand, *Bioconjugate Chem.* **2000**, *11*, 795.

[43] K. J. Watson, S. J. Park, J. H. Im, S. T. Nguyen, C. A. Mirkin, *J. Am. Chem. Soc.* **2001**, *123*, 5592.

[44] J. M. Gibbs, S. J. Park, D. R. Anderson, K. J. Watson, C. A. Mirkin, S. T. Nguyen, *J. Am. Chem. Soc.* **2005**, *127*, 1170.

[45] S. Nagahara, T. Matsuda, *Polym. Gels Networks* **1996**, *4*, 111.

[46] C. Minard-Basquin, C. Chaix, C. Pichot, *Nucleosides Nucleotides & Nucleic Acids* **2001**, *20*, 895.

[47] D. C. Lin, B. Yurke, N. A. Langrana, *Journal of Biomech. Eng.-Tasme* **2004**, *126*, 104.

[48] D. C. Lin, B. Yurke, N. A. Langrana, *J. Mater. Res.* **2005**, *20*, 1456.

[49] C. A. Stein, Y. C. Cheng, *Science* **1993**, *261*, 1004.

[50] J. B. Opalinska, A. M. Gewirtz, *Nature Rev. Drug Dis.* **2002**, *1*, 503.

[51] J. H. Jeong, T. G. Park, *Bioconjugate Chem.* **2001**, *12*, 917.

[52] J. H. Jeong, S. W. Kim, T. G. Park, *Bioconjugate Chem.* **2003**, *14*, 473.

[53] C. Morassutti, B. Scaggiante, L. E. Xodo, B. Dapas, G. Paroni, G. Tolazzi, F. Quadrifoglio, *Antisense & Nucleic Acid Drug Development* **1999**, *9*, 261.

[54] S. Cogoi, C. Suraci, E. Del Terra, S. Diviacco, G. Van der Marel, J. Van Boom, F. Quadrifoglio, L. Xodo, *Antisense & Nucleic Acid Drug Development* **2000**, *10*, 283.

[55] S. Cogoi, V. Rapozzi, F. Quadrifoglio, L. Xodo, *Biochemistry* **2001**, *40*, 1135.

[56] V. Rapozzi, S. Cogoi, P. Spessotto, A. Risso, G. M. Bonora, F. Quadrifoglio, L. E. Xodo, *Biochemistry* **2002**, *41*, 502.

[57] J. Joseph, J. C. Kandala, D. Veerapanane, K. T. Weber, R. V. Guntaka, *Nucleic Acids Res.* **1997**, *25*, 2182.

[58] E. M. McGuffie, D. Pacheco, G. M. R. Carbone, C. V. Catapano, *Cancer Res.* **2000**, *60*, 3790.

[59] F. X. Barre, S. Ait-Si-Ali, C. Giovannangeli, R. Luis, P. Robin, L. L. Pritchard, C. Helene, A. Harel-Bellan, *Proc. Natl. Acad. Sci. U. S. A.* **2000**, *97*, 3084.

[60] A. M. Stutz, J. Hoeck, F. Natt, B. Cuenoud, M. Woisetschlager, *J. Biol. Chem.* **2001**, *276*, 11759.

[61] F. Rininsland, T. R. Johnson, C. L. Chernicky, E. Schulze, P. Burfeind, J. Ilan, J. Ilan, *Proc. Natl. Acad. Sci. U. S. A.* **1997**, *94*, 5854.

[62] G. M. Bonora, E. Ivanova, V. Zarytova, B. Burcovich, F. M. Veronese, *Bioconjugate Chem.* **1997**, *8*, 793.

[63] M. Ballico, S. Drioli, F. Morvan, L. Xodo, G. M. Bonora, *Bioconjugate Chem.* **2001**, *12*, 719.

[64] M. Heskins, J. E. Guillet, *J. Macromol. Sci-Chem. A2* **1968**, *8*, 1441.

[65] Y. H. Bae, T. Okano, R. Hsu, S. W. Kim, *Makromolekulare Chemie-Rapid Communications* **1987**, *8*, 481.

[66] Y. G. Takei, T. Aoki, K. Sanui, N. Ogata, T. Okano, Y. Sakurai, *Bioconjugate Chem.* **1993**, *4*, 341.

[67] D. Umeno, M. Maeda, *Chem. Lett.* **1999**, 381.

[68] T. Mori, D. Umeno, M. Maeda, *Biotechnol. Bioeng.* **2001**, *72*, 261.

[69] N. Soh, D. Umeno, Z. L. Tang, M. Murata, M. Maeda, *Anal. Sci.* **2002**, *18*, 1295.

[70] M. D. Costioli, I. Fisch, F. Garret-Flaudy, F. Hilbrig, R. Freitag, *Biotechnol. Bioeng.* **2003**, *81*, 535.

[71] M. Murata, W. Kaku, T. Anada, N. Soh, Y. Katayama, M. Maeda, *Chem. Lett.* **2003**, *32*, 266.

[72] A. Mountain, *Trends Biotechnol.* **2000**, *18*, 119.

[73] F. Berger, C. Canova, A. L. Benabid, D. Wion, *Nat. Biotechnol.* **1999**, *17*, 517.

[74] D. Robertson, *Nat. Biotechnol.* **2001**, *19*, 604.

[75] E. Sheu, S. Rothman, M. German, X. G. Wang, M. Finer, B. M. McMahon, *Current Opinion in Molecular Therapeutics* **2003**, *5*, 420.

[76] H. Aihara, J. Miyazaki, *Nat. Biotechnol.* **1998**, *16*, 867.

[77] G. Tong, J. M. Lawlor, G. W. Tregear, J. Haralambidis, *J. Org. Chem.* **1993**, *58*, 2223.

[78] G. Tong, J. M. Lawlor, G. W. Tregear, J. Haralambidis, *J. Am. Chem. Soc.* **1995**, *117*, 12151.

[79] E. Ergen, M. Weber, J. Jacob, A. Herrmann, K. Müllen, *Chem-Eur. J.* **2006**, *12*, 3707.

[80] C. J. Yu, Y. J. Wan, H. Yowanto, J. Li, C. L. Tao, M. D. James, C. L. Tan, G. F. Blackburn, T. J. Meade, *J. Am. Chem. Soc.* **2001**, *123*, 11155.

[81] C. Fan, K. W. Plaxco, A. J. Heeger, *Proc. Natl. Acad. Sci. U. S. A.* **2003**, *100*, 9134.

[82] V. Lindberg, B. Hellsing, *Journal of Physics-Condensed Matter* **2005**, *17*, S1075.

[83] T. Trindade, P. O'Brien, N. L. Pickett, *Chem. Mater.* **2001**, *13*, 3843.

[84] A. Eychmuller, *J. Phys. Chem. B* **2000**, *104*, 6514.

[85] D. Horn, J. Rieger, *Angew. Chem. Int. Ed.* **2001**, *40*, 4331.

[86] D. Distler, *Waessrige Polymerdispersionen : Synthese, Eigenschaften, Anwendungen*, Wiley-VCH, Weinheim ; Chichester, **1999**.

[87] J. M. Asua, *Polymeric dispersions : principles and applications*, Kluwer Academic, Dordrecht ; London, **1997**.

[88] T. Kietzke, D. Neher, K. Landfester, R. Montenegro, R. Guntner, U. Scherf, *Nature Materials* **2003**, *2*, 408.

[89] C. Zhisheng, S. L. Cooper, *Adv. Mater.* **2000**, *12*, 843.

[90] G. R. Newkome, C. N. Moorefield, F. Voegtle, *Dendrimers and dendrons : concepts, syntheses, applications*, Wiley-VCH, Weinheim Chichester, **2001**.

[91] I. W. Hamley, *Nanotechnology* **2003**, *14*, R39.

[92] S. Forster, M. Antonietti, *Adv. Mater.* **1998**, *10*, 195.

[93] T. Amiya, T. Tanaka, *Macromolecules* **1987**, *20*, 1162.

[94] J. Elisseeff, A. Ferran, S. Hwang, S. Varghese, Z. Zhang, *Stem Cells and Development* **2006**, *15*, 295.

[95] E. Takushi, *Thermochim. Acta* **1998**, *308*, 75.

[96] G. T. Pickett, *Macromolecules* **2006**, *39*, 9557.

2 Motivation and Objective

"**DNA is the secret of life.**"

-Prof. Dr. James Watson, Nobel Prize in 1962

The highly specific base pairing of DNA serves not only as the genetic code for life but also as the building block in the design of novel materials owing to its remarkable features. In the last decade significant research has focused on using DNA as a synthetically programmable binding motif for the preparation of new materials with preconceived architectural parameters and properties.[1-5] Such materials have led to the development of new biological detection schemes,[6-8] novel nanostructures,[9-11] and the construction of nanoelectronic devices.[12]

Recently, polymer chemistry and molecular biology have converged to create a new type of hybrid material, made of oligodeoxynucleotides (ODNs) and organic polymers.[13] Within short time, applications of these bioorganic hybrids have been explored for their potential use in biodiagnostics, biomaterial purification and nucleic acid delivery.[7, 14, 15] However, the synthetic methods to prepare such polymeric materials were insufficient to produce large amounts and to elucidate structure-morphology relationships. Nevertheless, as outlined in the introduction, practical routes for water soluble DNA block copolymers (DBCs) are available, but amphiphilic DBCs seem only be accessible in low yields.[13, 16] Therefore, a major part of this work was dedicated to the development of new strategies towards such DBC structures. Special attention was paid to obtain amphiphilic DBCs in high yields. Different synthetic strategies that rely on coupling the nucleic acid moiety and the organic polymer in solution or on solid support were developed and are described in *Chapter 3*.

DBCs of higher complexity like multiblock architectures have never been reported. This synthetic challenge in block copolymer synthesis has been approached by exploiting the self-

recognition properties of DNA. Two DNA diblock copolymers with complementary sequences were hybridized to form triblock architectures. The combination of diblock and triblock structures led to well-defined pentablock architectures. The assembly of ds multiblock copolymers is detailed in *Chapter 4*.

The DNA block copolymers known to date are restricted with respect to the length of their nucleic acid segments when compared to genomic or plasmid DNA. This synthetic limitation has been overcome by introducing the polymerase chain reaction (PCR) into polymer chemistry. This method provides a simple tool to build well-defined multiblock copolymers with extended DNA segments. The use of a ss DNA-PEG-ss DNA triblock copolymer primer and a conventional ODN primer in the amplification process resulted in ds DNA triblock copolymers. When the primer set consisted of the ss triblock copolymer and a ss DNA diblock copolymer, ds DNA pentablock architectures were obtained. The lengths of the DNA blocks, which ranged from tens of base pairs (bp) to more than 500 bp, were adjusted by the annealing sites of the primers on the template. Common to all architectures are the high molecular weight and the monodispersity of the nucleic acid units. Furthermore, these nanostructures were visualized by scanning force microscopy (SFM) and manipulated by the SFM tip to investigate their mechanical properties on the single molecule level. The synthesis as well as the characterization of these materials are described in *Chapter 5*.

After establishing the synthetic routes for preparing amphiphilic DBCs, the morphology of these novel architectures was investigated. In *Chapter 6*, the structural properties of DNA-*b*-polystyrene (PS) copolymers were characterized on different substrate surfaces by SFM. For some of these biological organic hybrid structures, novel microscale DNA arrays with nanoscale features were observed.

For the DNA-*b*-PS diblock copolymer system, the morphologies could be altered by changing the processing conditions. However, in *Chapter 7*, a mild stimulus was employed to manipulate the supramolecular architectures of DNA-b-poly(propylene oxide) (PPO). The specific hydrogen bonding of the nucleic acid segment in DNA block copolymers offers the possibility to change such morphologies sequence specifically. It is described how DNA block copolymer morphologies can be varied by hybridization with short and long ss DNA templates. The resultant nanostructures were visualized by SFM on a substrate surface and further characterized by fluorescence correlation spectroscopy (FCS) in solution.

Besides switching structural properties of DNA block copolymer micelles, in *Chapter 8* it was demonstrated how the size of spherical nanoparticles could be adjusted by an enzyme. For this purpose, terminal deoxynucleotidyl transferase (TdT), a template independent enzyme that randomly adds deoxynucleotide triphosphate (dNTP) to an ODN primer sequence was employed. ss DNA(22mer)-*b*-PPO copolymers were used as priming species which are known to form micelles in aqueous solution. By incubating spherical DNA block copolymer micelles for different reaction times the size of these nanoparticles could be increased up to 2.5 fold as analyzed by SFM and FCS.

In addition to performing enzymatic reactions on DBC nanoparticles, such micelles were successfully employed as scaffolds for DNA-templated synthesis. The template consisted of amphiphilic DNA-block copolymer micelles with a hydrophobic core and a ss DNA-shell. Instead of Watson-Crick base pairing, aggregation of hydrophobic polymer blocks aligned the DNA of the corona to act as a scaffold in DNA-templated organic synthesis. The ss DNA of the corona was hybridized with ODNs that were equipped with different reactants. Depending on the functionalization site, i.e. the 5' or 3' ends, various organic reactions were performed sequence specifically either on the surface of the micelles (5') or at the hydrophobic/hydrophilic interface (3'). The yields of these reactions as well as structural analysis of the micelles before and after the chemical bond formation are given in *Chapter 9*.

Apart from the synthesis and the morphologies, an important requirement for a new bioorganic hybrid material is its biocompatibility and interaction with living systems, i.e. human cells. In *Chapter 10*, the toxicity of the DNA-*b*-PPO block copolymers was analyzed by a cell proliferation assay. Diverse shapes of nanoparticles showed slightly different toxicity. The uptake of chemically equivalent, structurally different DNA block copolymers into human colon adenocarcinoma (Caco-2) cells was then studied. It was shown that the Caco-2 cells, which are used as a drug transport model for assessing intestinal transport, internalize DNA block copolymer micelles of various shapes to different extents.

Motivated by the non-toxic nature of the amphiphilic DBCs, in *Chapter 11* these nanoobjects were employed as drug delivery vehicles to transport an anticancer drug to tumor cells. The micelles obtained from DNA block copolymers were conveniently functionalized with targeting units by hybridization. This facile route allowed studying the effect of the amount of

targeting units on the targeting efficacy. Additionally, the micelles were loaded with the anticancer drug, doxorubicin, and then applied to tumor cells. The viability of the cells was measured in the presence and absence of targeting units. The outcome of these drug delivery experiments with DNA block copolymer micelles are detailed in the last chapter of this work.

References

[1] C. A. Mirkin, R. L. Letsinger, R. C. Mucic, J. J. Storhoff, *Nature* **1996**, *382*, 607.

[2] A. P. Alivisatos, K. P. Johnsson, X. G. Peng, T. E. Wilson, C. J. Loweth, M. P. Bruchez, P. G. Schultz, *Nature* **1996**, *382*, 609.

[3] N. L. Rosi, C. A. Mirkin, *Chem. Rev.* **2005**, *105*, 1547.

[4] J. J. Storhoff, C. A. Mirkin, *Chem. Rev.* **1999**, *99*, 1849.

[5] N. L. Rosi, D. A. Giljohann, C. S. Thaxton, A. K. R. Lytton-Jean, M. S. Han, C. A. Mirkin, *Science* **2006**, *312*, 1027.

[6] Y. C. Cao, R. C. Jin, J. M. Nam, C. S. Thaxton, C. A. Mirkin, *J. Am. Chem. Soc.* **2003**, *125*, 14676.

[7] C. E. Immoos, S. J. Lee, M. W. Grinstaff, *J. Am. Chem. Soc.* **2004**, *126*, 10814.

[8] E. Ergen, M. Weber, J. Jacob, A. Herrmann, K. Müllen, *Chem.-Eur. J.* **2006**, *12*, 3707.

[9] N. C. Seeman, *Nature* **2003**, *421*, 427.

[10] A. Condon, *Nat. Rev. Gen.* **2006**, *7*, 565.

[11] P. W. K. Rothemund, *Nature* **2006**, *440*, 297.

[12] K. Keren, R. S. Berman, E. Buchstab, U. Sivan, E. Braun, *Science* **2003**, *302*, 1380.

[13] F. E. Alemdaroglu, A. Herrmann, *Org. Biomol. Chem.* **2007**, *5*, 1311.

[14] K. J. Watson, S. J. Park, J. H. Im, S. T. Nguyen, C. A. Mirkin, *J. Am. Chem. Soc.* **2001**, *123*, 5592.

[15] J. H. Jeong, T. G. Park, *Bioconjugate Chem.* **2001**, *12*, 917.

[16] Z. Li, Y. Zhang, P. Fullhart, C. A. Mirkin, *Nano Lett.* **2004**, *4*, 1055.

3 Synthesis of ss DNA Block Copolymers

"**Creation is wonderful.**"

Prof. Hoffmann, 1954

Synthetic approaches towards novel hybrid materials that are purposed to be implemented in various bio- and nanotechnological applications have to be straightforward and accomplishable on at least milligram scale. This is an important requirement to provide enough material for exploiting the necessary morphological studies which might be crucial for subsequent biotechnological and biomedical applications.

For the fabrication of linear DNA block copolymers one end of an ODN needs to be coupled to a terminal functionality of an organic polymer block. This synthetic goal is achieved by grafting onto strategies either by connecting the biological and the organic polymer segments in solution or on a solid support. The first method has been extensively explored as described in the literature for amide [1-4] and disulfide bond formation[5] as well as Michael addition.[5] The coupling on solid supports has been investigated to a less extent. In this work, several different ss DNA block copolymers have been synthesized. The organic polymer segment was chosen to be **hydrophilic**, **thermoresponsive** or **hydrophobic**. Below, the synthesis of such block copolymers is detailed.

In-Solution Coupling

The coupling strategy in solution was employed for all three kinds of organic polymer segments mentioned above. Such a synthetic route is easy and straightforward because end-functionalized ODNs can be obtained commercially and an expensive DNA synthesizer is not required.

ss DNA-*b*-PEG Block Copolymers

For the coupling of the hydrophilic PEG and the terminally functionalized ODN, amide bond formation was employed. Therefore, carboxyl-end-functionalized PEGs (M_n = 5000 **1a** and 20000 g/mol **1b**, polydispersity index (PDI) < 1.1) and amino terminated ODNs (5'-TAACAGGATTAGCAGAGCGAGG-3' **2,** 22mer, MW = 6950 g/mol) were obtained from commercial sources and used without further purification. A variety of different activation reagents were utilized to prepare the hybrids. The following activating reagents have been reported for constructing DNA block copolymer hybrids: DCC, NHS or EDC and sulfo-NHS.[3, 4, 6, 7] However, during the course of the work, it was found that a new and cheap activating reagent called 4-(4,6-dimethoxy-1,3,5-triazin-2-yl)-4-methylmorpholinium chloride) (DMT-MM)[8, 9] was superior compared to others. This coupling agent is a crystalline, air stable, non-hygroscopic and an easy-to-handle compound (**Figure 3.1**).

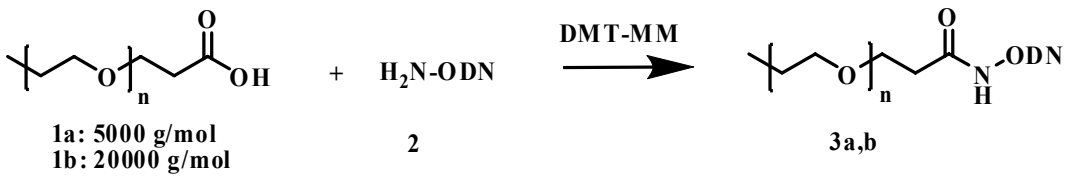

Figure 3.1 *The synthesis of ss DNA-b-PEG block copolymers by amide bond formation.*

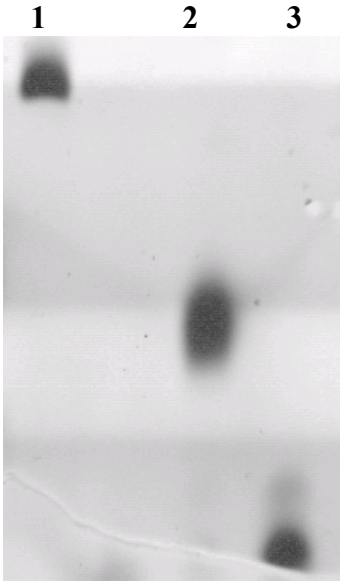

Figure 3.2 *PAGE analysis of purified DNA-b-PEG diblock copolymers Lane 1: ss DNA-b-PEG(20K)* ***3b****. Lane 2: ss DNA-b-PEG(5K)* ***3a****. Lane 3: ss DNA* ***2***

The DNA-*b*-PEG diblock copolymers were obtained in high yields of 75 and 90 % for the PEG moieties with molecular weights of 20000 and 5000 g/mol, respectively. The resulting conjugates were purified by PAGE and characterized by MALDI-TOF MS and HPLC. The electrophoretic analysis was performed at denaturing conditions where the polyacrylamide gel contained 7 M urea to exclude any secondary structure formation (**Figure 3.2**). The ss DNA-*b*-PEG block copolymers appeared as discrete bands in the gel. Their electrophoretic mobilities differed significantly from that of the ODN starting materials. Further structural analysis was performed by HPLC and MALDI-TOF MS together with *M. Safak*. A prepacked reverse phase (RP) column (Amerhsam Biosciences, Sweden) was employed to prove the purity of the compound. For the HPLC analysis the gradient was held constant for 7 min. at 0% eluent **B** and then increased to 100% **B** in 42.5 min. with a flow rate of 1.0 ml/min. Eluent **A** was 0.1 M triethylamine ammonium acetate (TEAAc pH: 7.0) and eluent **B** was 0.1 M TEAAc/ACN (20:80) mixture (**Figure 3.3**). Both ss DNA-b-PEG polymers elute as single peaks. No contamination by the starting materials was detected.

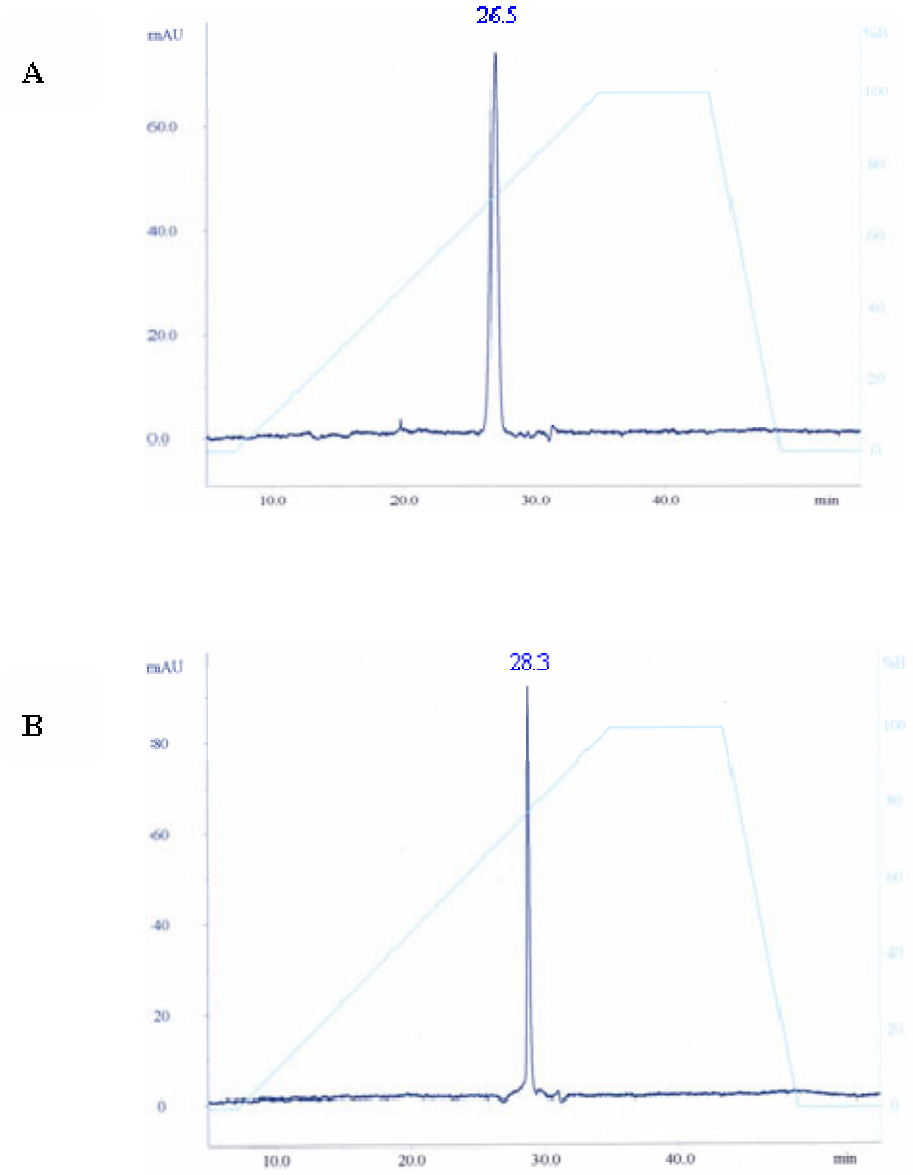

Figure 3.3 *The HPLC elugrams represent* ***(A)*** *ss DNA-PEG(5K) and* ***(B)*** *ss DNA-PEG(20K). At 26.5 min. and 28.3 min. ss DNA-PEG(5K) and ss DNA-PEG(20K) elute, respectively.*

Additionally, the bioorganic hybrids were characterized by MALDI-TOF MS (**Figure 3.4**). For the analysis hydroxypicolonic acid was employed as a matrix.

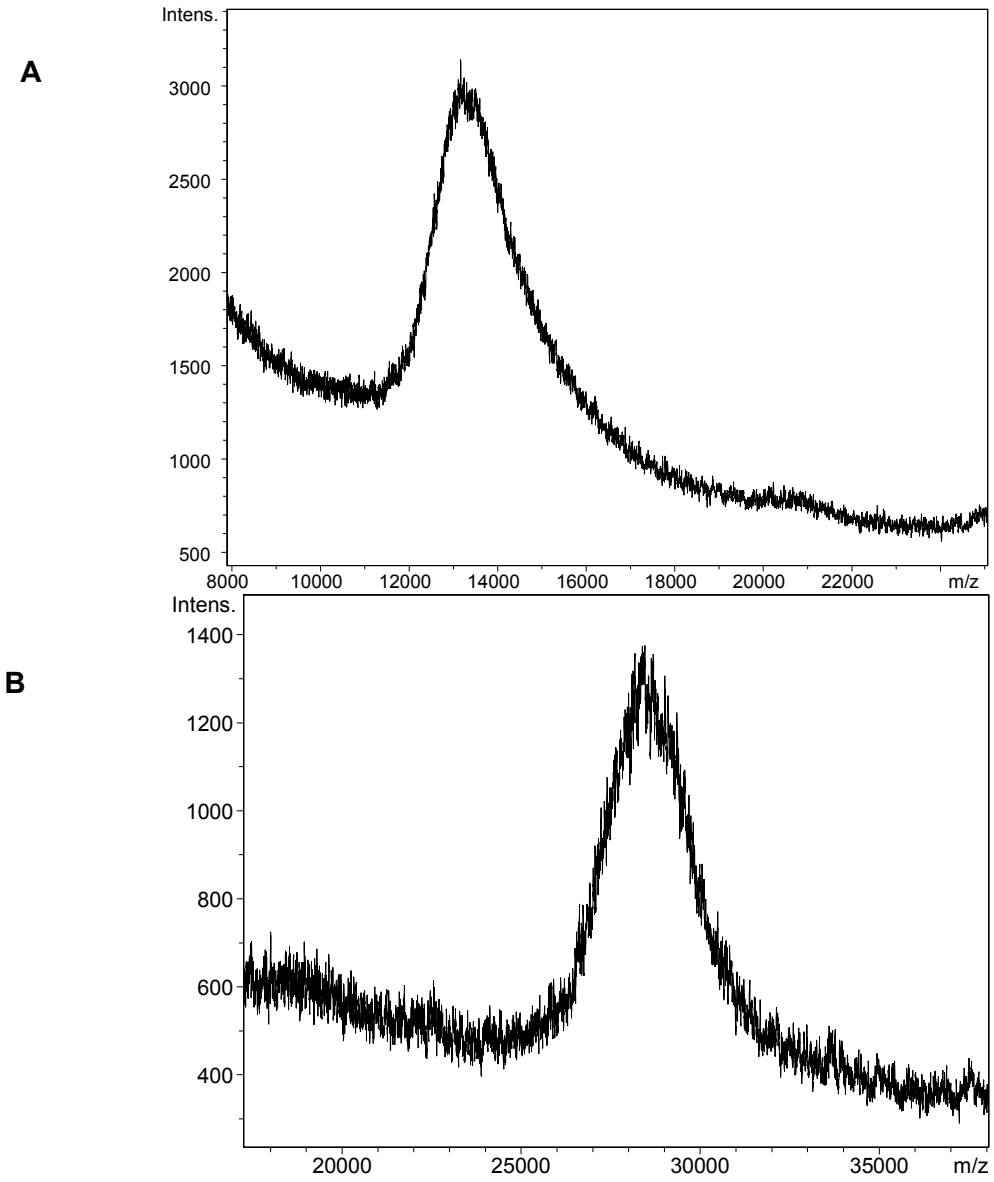

Figure 3.4 *The MALDI-TOF spectrum of* ***(A)*** *ss DNA-PEG(5K) (found: 13200 g/mol, calculated: 13100 g/mol) and* ***(B)*** *ss DNA-PEG(20K) (found: 28300 g/mol, calculated: 28100 g/mol).*

The mass spectra of ss DNA-b-PEG diblock copolymers (**Figure 3.4**) show the expected mass peaks with only small deviations from the calculated molecular weights.

ss DNA-*b*-PNIPAM Diblock Copolymers

An important class of DNA block copolymers consists of DNA-*b*-PNIPAM conjugates, which are mainly used for purification of biomacromolecules employing a thermal stimulus.[10, 11] Instead of amide bond formation, for the synthesis of DNA-*b*-PNIPAM a different coupling reaction was employed here. The amino-terminated PNIPAM (M_n = 2000 and 6000 g/mol, PDI = 2.03 and 2.32) was prepared by free radical polymerization of NIPAM applying 2,2'-azobisisobutyronitrile and amino-ethanethiol as initiator and chain transfer reagent, respectively.[12] Subsequently, the amino-terminated PNIPAM was reacted with maleimido butyric acid chloride for incorporation of the thiol-reactive group. The final grafting of the thiol-modified ss DNA (5'-TAACAGGATTA GCAGAGCGAGG-3', 22mer, MW = 6950 g/mol) onto the maleimido functionalized PNIPAM was realized with yields of 39 and 52 % for organic polymer segment of 6000 and 2000 g/mol, respectively (**Figure 3.5**).

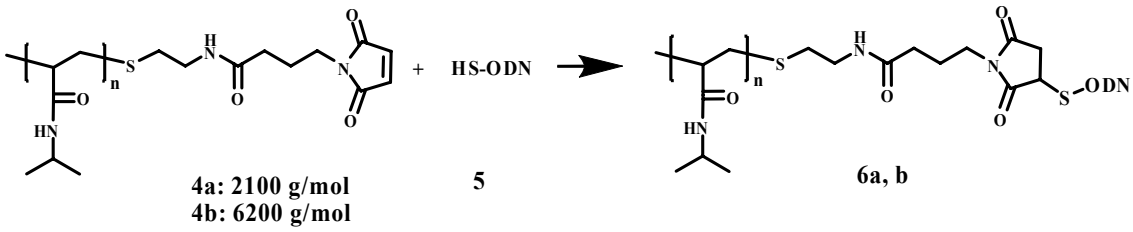

Figure 3.5 *The synthesis of ss DNA-b-PNIPAM conjugates by Michael addition.*

Ss DNA-*b*-PNIPAM block copolymers were analyzed by denaturing PAGE (**Figure 3.6**). The DNA block copolymers appeared as discrete bands in the gel. Their electrophoretic mobilities differed significantly from that of the ODN starting materials.

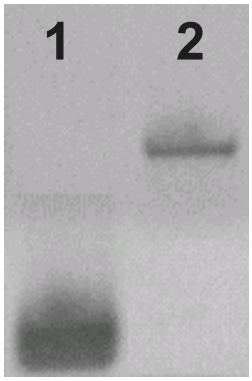

Figure 3.6 *Denaturing PAGE analysis of ss DNA-b-PNIPAM diblock copolymer. Lane 1: ss DNA (22mer)* ***5****. Lane 2: ss DNA-b-PNIPAM diblock copolymer* ***6b****.*

ss DNA-*b*-PS Diblock Copolymers

In addition to hydrophilic and thermo responsive organic polymer segments, hydrophobic PS was also conjugated to an ODN (16mer, Sequence: 5'-TAG TTGTGATGTACAT-3' MW: 5100 g/mol). For this purpose amino terminated PS (M_w: 5500, 10000, 56000 g/mol; PDI < 1.1) was synthesized anionically by *J. Thiel* according to the literature.[13] These polymers were end-functionalized with a maleimido group.[14] In contrast to the preparation of the DNA-*b*-PEG- and DNA-*b*-PNIPAM conjugates, the coupling of the hydrophilic ss DNA to the hydrophobic PS was carried out in a solvent mixture of THF and water (**Figure 3.7**). Although different solvent compositions with varying ratios were employed for the reaction, the coupling efficiencies were low yielding DNA-*b*-PS only in 10-15 %.

The purity of the DNA-*b*-PS block copolymers was demonstrated by PAGE (**Figure 3.8**). These hybrids appeared as discrete bands in the gel. Their electrophoretic mobilities differed significantly from that of the starting material, ODN.

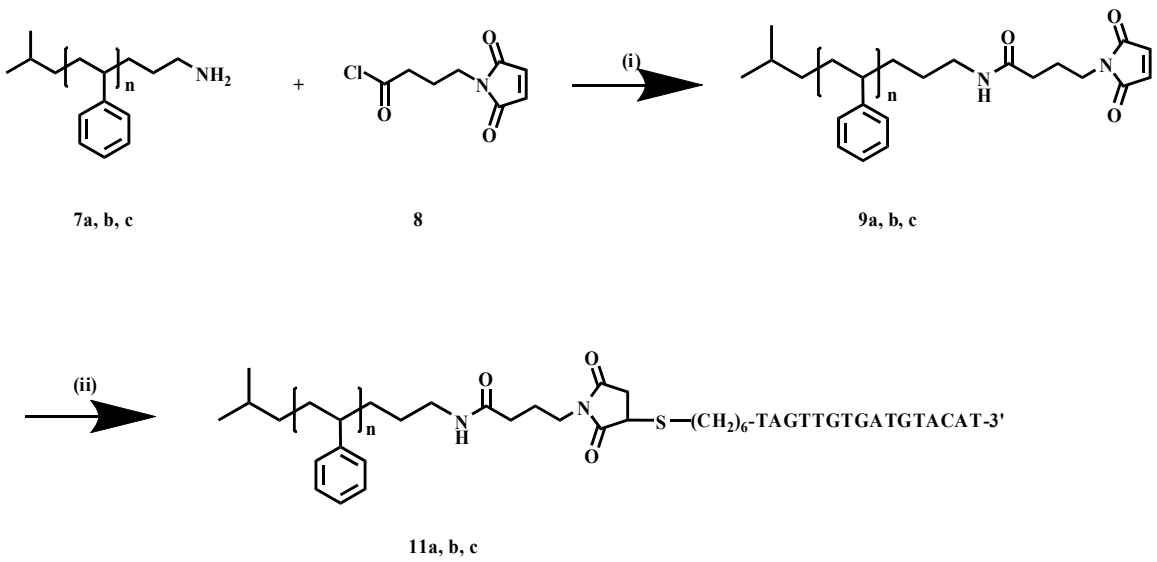

Figure 3.7 *Synthesis of DNA-PS diblock copolymers 10a-c. (i) Triethylamine, dry DMF, RT, overnight. (ii) 5'-HS-$(CH_2)_6$-TAGTTGTGATGTACAT-3' **10**, H_2O/THF, RT, 2 days.*

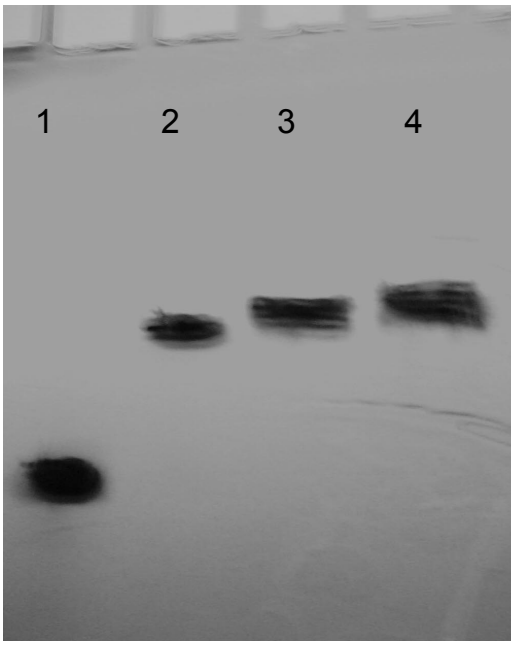

Figure 3.8 *PAGE (20%) of DNA-b-PS block copolymers. Lane 1: ODN **10**, lane 2: DNA-b-PS (5.100/5.500) **11a**, lane 3: DNA-b-PS (5.100/10.000) **11b**, lane 4: DNA-b-PS (5.100/56.000) **11c**.*

Although the molecular weight of the PS block increased more than tenfold (compare **Figure 3.8 Lane 2 and 4**), their mobilities in the gel were only slightly influenced. The characterization of the ss DNA-*b*-PS hybrids was also carried out by mass spectrometry. For the block copolymer with the lowest molecular weight, a MALDI-TOF mass spectrum was recorded (**Figure 3.9**). The mass spectrum of ss DNA-*b*-PS diblock copolymer **11a** show the expected mass peak with only small deviations from the calculated molecular weight.

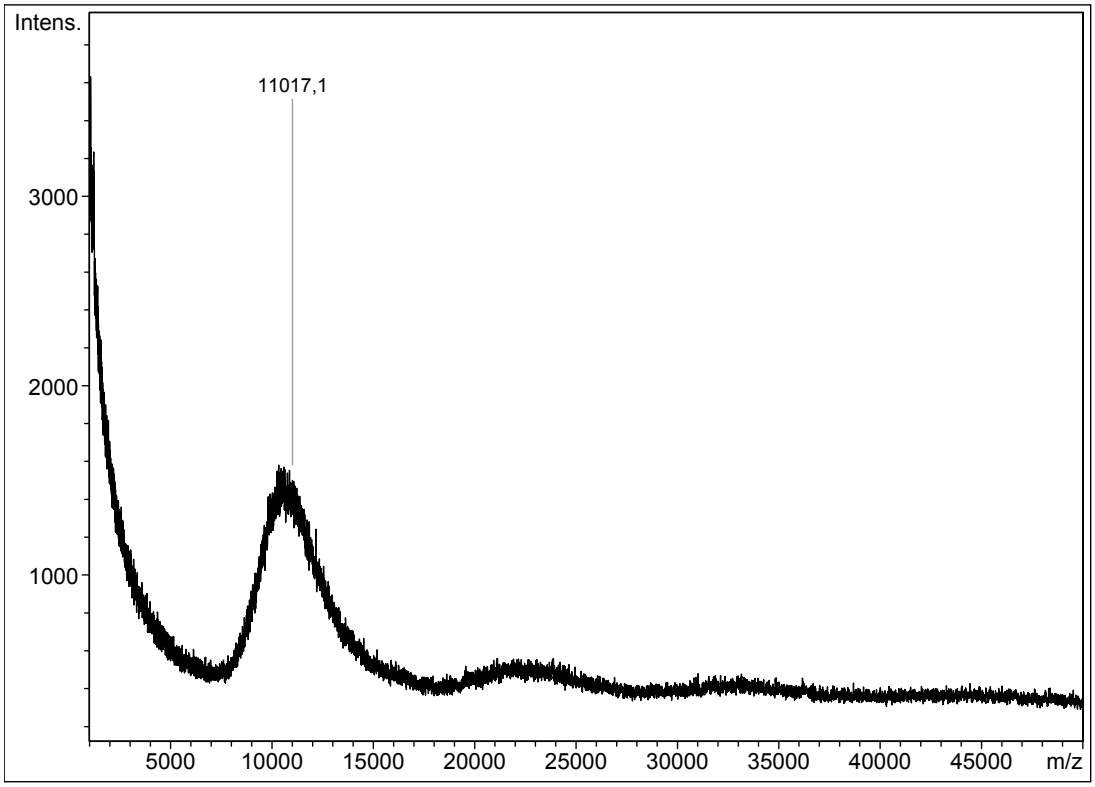

Figure 3.9 *MALDI-TOF mass spectrum of the diblock copolymer **11a** (matrix: indoleacrylic acid). (found: 11017 g/mol, calculated: 11370 g/mol).*

Solid Phase Synthesis of ss DNA Block Copolymers

The yields of the in-solution coupling were reasonable when water soluble polymers were employed. However, the grafting-onto strategy in solution failed and gave low yields when hydrophobic polymers were coupled with nucleic acid segments. A reason for poor coupling

efficieny is the incompatibility of the hydrophilic DNA and the hydrophobic polymers in the solvent. Therefore, a new strategy was developed which is based on solid phase synthesis.

ss DNA-*b*-PPO Block Copolymers

Inspired by the synthetic strategy of Mirkin,[15] hydroxyl-terminated PPOs (M_n: 1000 and 6800 g/mol; PDI: 1.3 and 1.9, respectively) were reacted with phosphoramidite chloride to yield the corresponding phosphoramidite-PPO derivatives. The activated PPOs were then coupled to the 5' end of an ODN (22mer, sequence: 5'- CCTCGCTCTGCTAATCCTGTTA-3') on a solid support using a DNA-synthesizer (**Figure 3.10**).

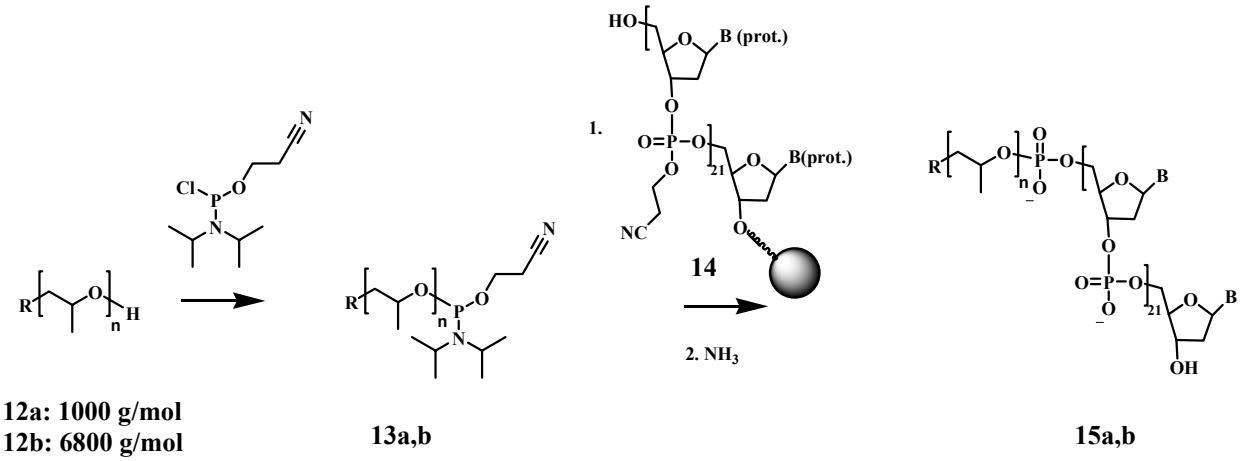

Figure 3.10 *The synthesis of DNA-b-PPO on the solid support.*

For the automated attachment of phosphoramidite functionalized PPOs to the 5' end of the ODN, a modified procedure was undertaken. The contact time of the activated polymer that was dissolved in dichloromethane with the solid support was increased to 1 min. compared to 0.25 min for the standard attachment of nucleotides. The recycling time of this reagent was raised to 30 min. in contrast to 3 min. as used for the standard procedure. After deprotection and purification by PAGE the DNA-*b*-PPOs were obtained. Coupling efficiencies of the large polymer moieties were remarkably high with yields reaching up to 65% for PPO with a

molecular weight of 1000 g/mol. With higher molecular weight slightly lower yields were obtained like 60 % for PPO of M_w: 6800 g/mol.

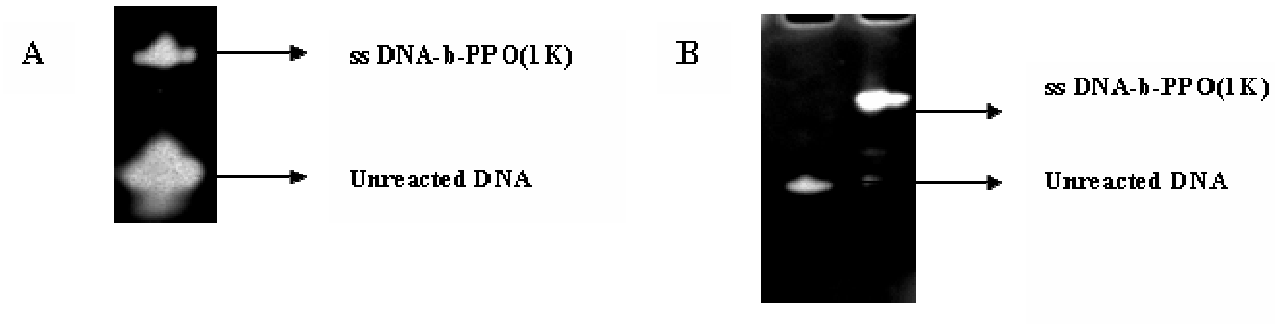

Figure 3.11 *PAGE analysis of **A)** crude reaction mixture and **B)** the purified compound **13a.***

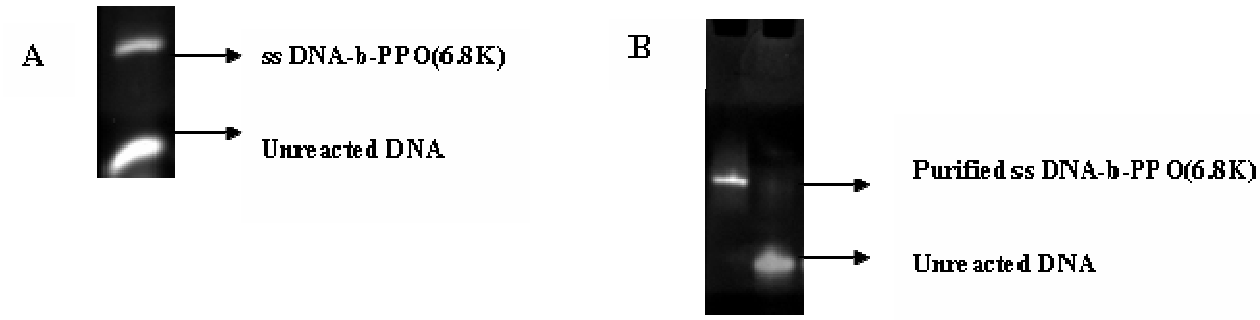

Figure 3.12 *PAGE analysis of **A)** crude reaction mixture and **B)** the purified compound **15b.***

After the electrophoretic purification the products were characterized by denaturing PAGE (**Figure 3.11 and 3.12**) and MALDI-TOF MS (**Figure 3.13**). The DNA block copolymers appeared as discrete bands in the gel. Their electrophoretic mobilities differed significantly from that of the ODN starting materials. The mass spectrum of ss DNA-*b*-PPO diblock copolymer **15b** show the expected mass peak with only small deviations from the calculated molecular weight.

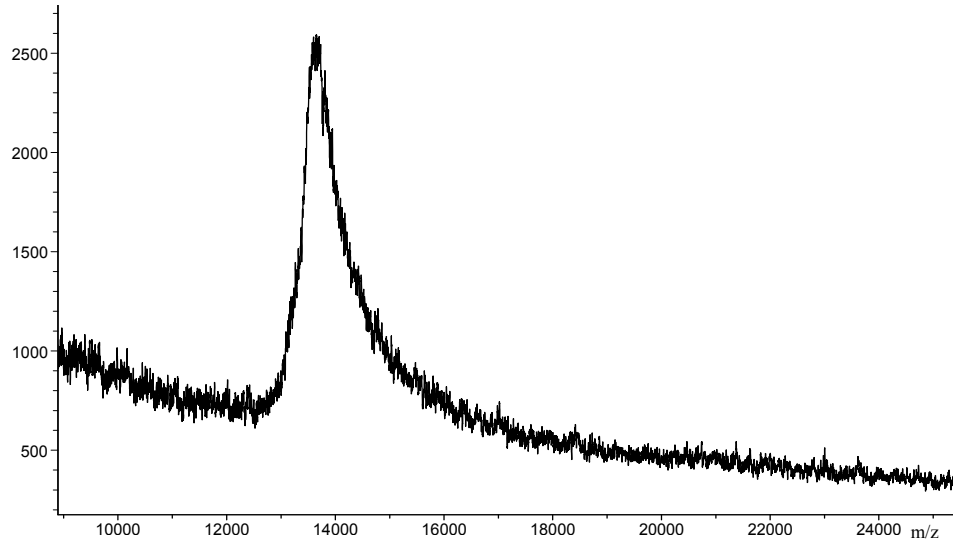

Figure 3.13 *MALDI-TOF spectrum of **15b** (found: 13600 g/mol, calculated: 13870) (Matrix: 3-hydroxypicolinic acid).*

ss DNA-*b*-PEG-*b*-ss DNA Triblock Copolymers

Beside the preparation of diblock copolymer hybrids, linear triblock architectures have also been realized on the solid support with the help of a DNA synthesizer. For the generation of the triblock copolymer, bis-phosphoramidite functionalized PEGs (M_n: 1000, 2000 and 4000 g/mol; PDI < 1.5) were synthesized and attached to the 5' terminus of the nucleic acid segment employing solid phase synthesis (**Figure 3.14**).

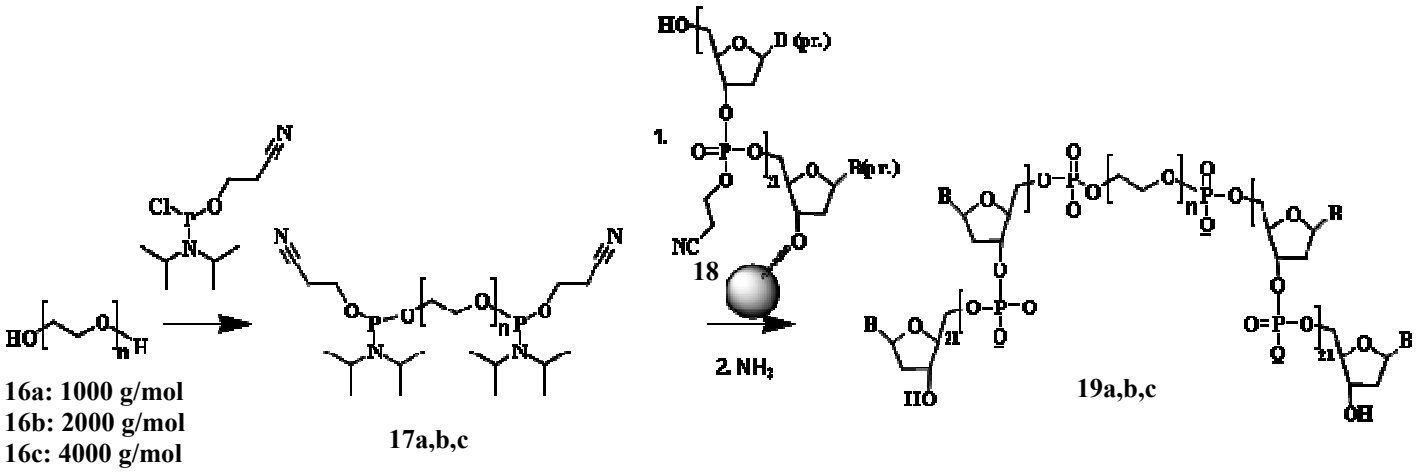

Figure 3.14 *The synthesis of ss DNA-b-PEG-b-ss DNA on the solid support.*

For the attachment of bis-phosphoramidite functionalized PEGs **17a, b, c,** which were dissolved in dicholoromethane, to the 5' end of the ODN **18** on the solid phase, a modified procedure was carried out similar to the attachment of PPO in the DNA synthesizer. This time, the recycling time was increased further to 45 min. in comparison to 30 min. for PPO coupling. After deprotection and purification by PAGE the ss DNA-*b*-PEG-*b*-ss DNAs were obtained. The samples were analyzed by denaturing PAGE (**Figure 3.15**) and MALDI-TOF MS (**Figure 3.16**).

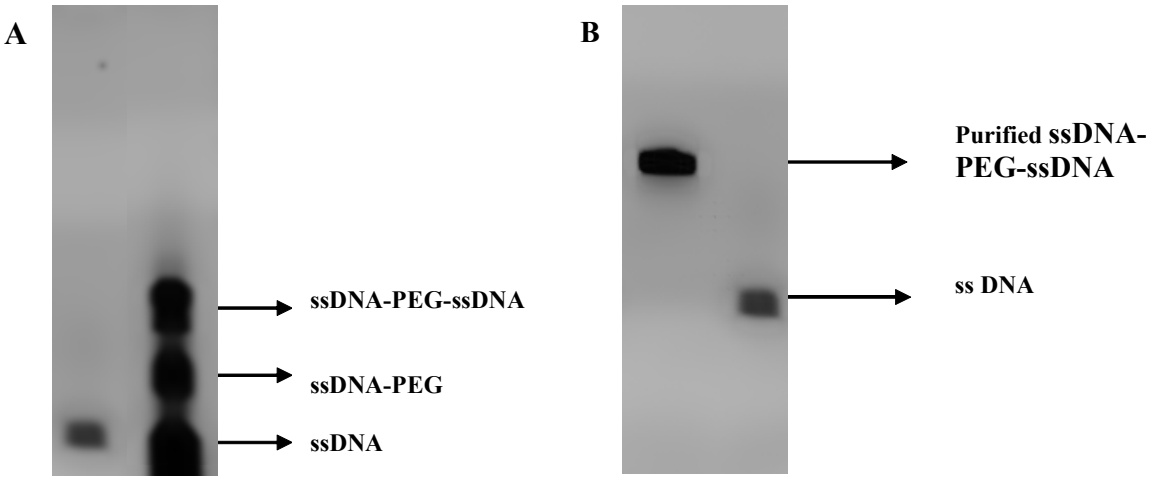

Figure 3.15 *PAGE analysis of* ***(A)*** *crude reaction mixture and* ***(B)*** *the purified product* ***19a****.*

The yields decreased slightly to 29 % when the organic polymer block exhibited a molecular weight of 4000 g/mol. **Figure 3.15A** and **3.15B** show the electrophoretic analysis of the reaction mixture and the purified product **19a** compared to ss DNA. The MALDI-TOF MS analysis reveals the expected molecular weight.

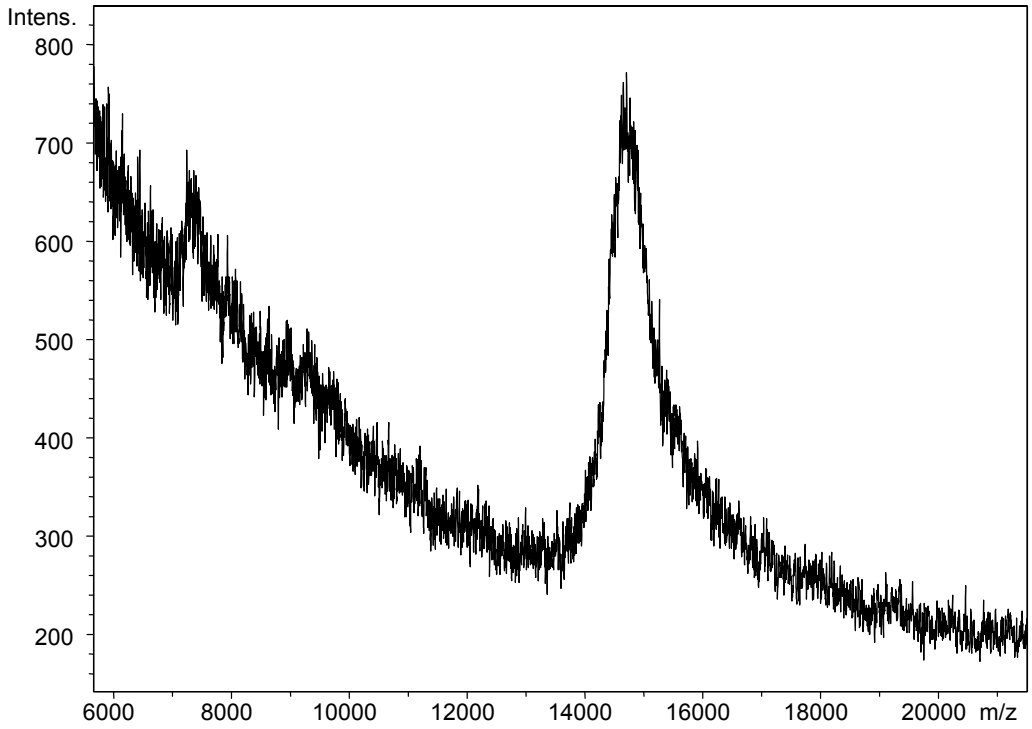

Figure 3.16 *MALDI-TOF spectrum of **19a** (found: 15100 g/mol calculated 15100 g/mol; Matrix: hydroxypicolinic acid).*

The experimental outcome of the coupling reaction suggests that using a DNA-synthesizer is superior to a grafting onto approach in solution[16] or a manual attachment procedure[15] because automation guarantees high reproducibility and efficient exposition of the phosphoramidite-polymer to the solid phase. Moreover, the problem of finding a common solvent for the hydrophilic DNA and the hydrophobic polymer is avoided.

Experimental Section

I. Materials and Methods

Unless otherwise stated, materials were obtained from commercial suppliers and were used without further purification. PEG, *N*-diisopropyl-2-cyanoethyl-chlorophosphoramidite, diisopropylethylamine were purchased from Aldrich. Succinimide activated carboxy-terminated PEGs were obtained from Nektar (USA). The dimethoxytrityl protected phosphoramadites were purchased from Link Technologies (UK) or SAFC (Germany). ss DNA block copolymers were synthesized using Äkta Oligopilot DNA synthesizer (Amersham Biosciences, Sweden). Tetramethylenesilane and triphenylphosphine were used as the references for the ^{1}H NMR and ^{31}P NMR spectra, respectively. The spectra were recorded on Bruker AMX 250 (250MHz) or DRX 500 (500 MHz) spectrometers. Molecular weights were determined using matrix-assisted laser desorption/ionisation time of flight (MALDI-TOF). The spectra were recorded on a Bruker MALDI-TOF (Reflex-TOF) mass spectrometer. HPLC analysis and purifications were performed on an Äkta Purifier (Amersham Biosciences, Sweden) using a C-18 column with UV detection at 260 nm. In all experiments, MilliQ standard water (Millipore Inc., USA) with a typical resistivity of 18.2 MΩ/cm was used. Oligonucleotides were quantified spectrophotometrically at a wavelength of 260 nm (SpectraMax M2, Molecular Devices, USA) and by denaturing PAGE followed by staining with ethidium bromide and UV transillumination. The densiometric quantification was done using GelPro programme distributed from Intas GmbH (Germany).

II. Synthesis of DNA-PEG Diblock Copolymers

The synthesis of DNA-PEG diblock copolymers was carried out by mixing 5'-amino-modified oligonucleotide (5'-TAACAGGATTAGCAGAGCGAGG-3', 22mer, MW = 6950 g/mol) (1 μmol) with carboxy-terminated PEG (M_n = 5000 or 20000 g/mol) (5 μmol) in the presence of DMT-MM (5.5 μmol) in water. The mixture was allowed to react for 12 h at room temperature. The block copolymer products were purified using 8 % denaturing PAGE. After excision of the bands, they were dialyzed against water for 24 hours. Subsequently, the DNA block copolymers were lyophilized yielding 0.7 μmol (70 %) ss DNA-*b*-PEG(5K) and

0.5 μmol (50 %) ss DNA-*b*-PEG(20K), respectively. Characterization of the products was carried out by PAGE, HPLC and MALDI-TOF MS.

III. Synthesis of ss DNA-*b*-PNIPAM Diblock Copolymers

Amino-terminated PNIPAM (M_n: 2100 and 6200 g/mol) and 4-maleimido butyric acid chloride[14] were synthesized according to the literature. For the maleimide functionalization of PNIPAM, amino-terminated PNIPAM (0.016 mmol) and 4-maleimido butyric acid chloride (30 mg, 0.16 mmol) were dissolved in a mixture of dry DMF (5 ml) and triethylamine (0.5 ml, 3.5 mmol). The solution was stirred at room temperature under an argon atmosphere overnight. Then excess maleimido butyric acid was removed by precipitation in water. Maleimido-terminated PNIPAMs were obtained after freeze drying. MALDI TOF MS: m/z = 2213 and 6311 g/mol.

For the preparation of the ss DNA-*b*-PNIPAM, PNIPAM (1.67 μmol) and thiol end-functionalized DNA (5 mg, 0.98 μmol) were allowed to react in water for 2 d on a shaker. The product was purified using preparative PAGE. Subsequently, the salt was exchanged using a dialysis membrane with molecular weight cut-off (MWCO) of 1000 g/mol yielding 2.1 mg (0.95 μmol) **6a** (42%) and 1.8 mg (0.28 μmol) **6b** (22%). **6a** and **6b** were then analyzed by PAGE.

IV. Synthesis of ss DNA-*b*-PS diblock Copolymers

Compound 7a-c: The amino terminated polymers were synthesized according to the literature.[13] **7a**: MALDI-TOF MS: 6100 g/mol, SEC: M_w: 5500 g/mol, PDI = 1.1; **7b**: MALDI-TOF MS: 9500 g/mol, SEC: M_w: 10000 g/mol, PDI = 1.1; **7c**: MALDI-TOF MS: 50000 g/mol, SEC: 56000 g/mol, PDI = 1.3.

Compound 8: 4-Maleimidobutyric acid chloride was prepared according to the literature.[14]

Compound 9a: 4-Maleimidobutyric acid chloride **8** (30 mg, 0,16 mmol) and **7a** (100 mg, 0,016 mmol) were dissolved in a mixture of dry DMF (5 ml) and triethylamine (0,5 ml, 3,5

mmol). The solution was stirred overnight at room temperature under an argon atmosphere. Then the product was purified by precipitation in methanol to give a slightly yellow powder. Yield: 90 mg (89 %). MALDI-TOF MS: m/z =6300 g/mol ($M(Ag^+)$), SEC: 5200 g/mol, D = 1.2.

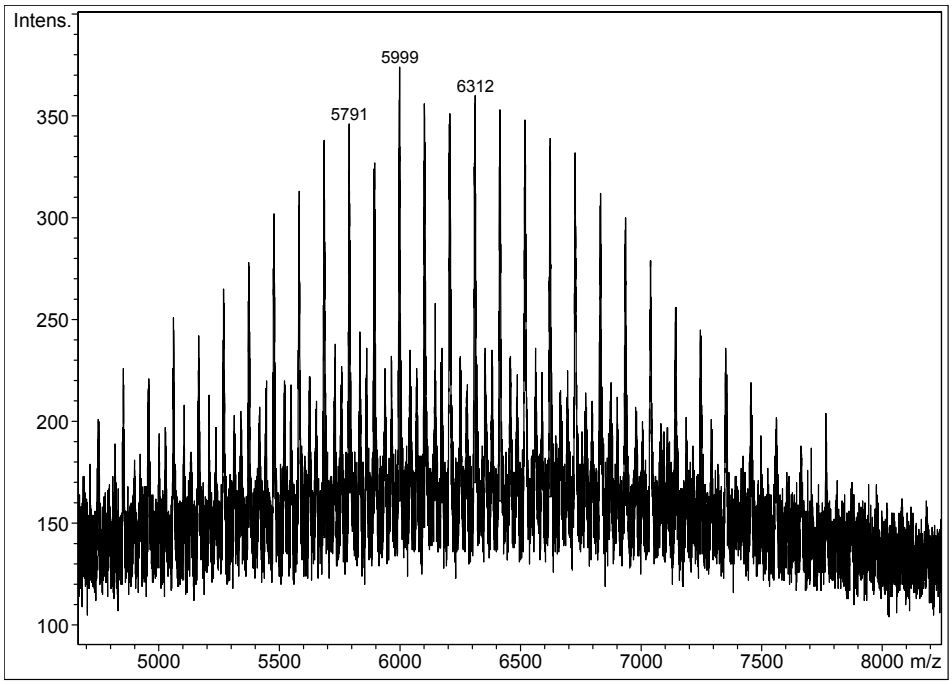

Figure 3.17 *MALDI-TOF spectrum of the malimido-functionalized polymer* ***9a*** *(Dithranol, Ag^+).*

Compounds 9b and 9c: The malimido functionalized polystyrenes of higher molecular weight were synthesized as described for **3a**. **3b**: Yield: 85 mg (87 %), SEC: M_w: 10500 g/mol; PDI = 1.2. **3c**: Yield: 80 mg (83 %), SEC: 58000 g/mol, PDI = 1.3.

Compound 10 (ODN) : The thiol modified oligonucleotide 5'-HS-$(CH_2)_6$-TAGTT GTGATGTACAT-3' was synthesized in 15 µmol scale using a DNA Synthesizer by standard phosphoramidite method.[17] Subsequently, the ODN was cleaved from the support with 37% ammonia at 50 °C, overnight. The trityl group was deprotected using the procedure of the manufacturer. The oligonucleotide was dried overnight under vacuum and was purified using HPLC equipped with a RP18 reverse phase column. MALDI-TOF MS: m/z = 5140 g/mol ($M(Na^+)$) (calc. 5123 g/mol).

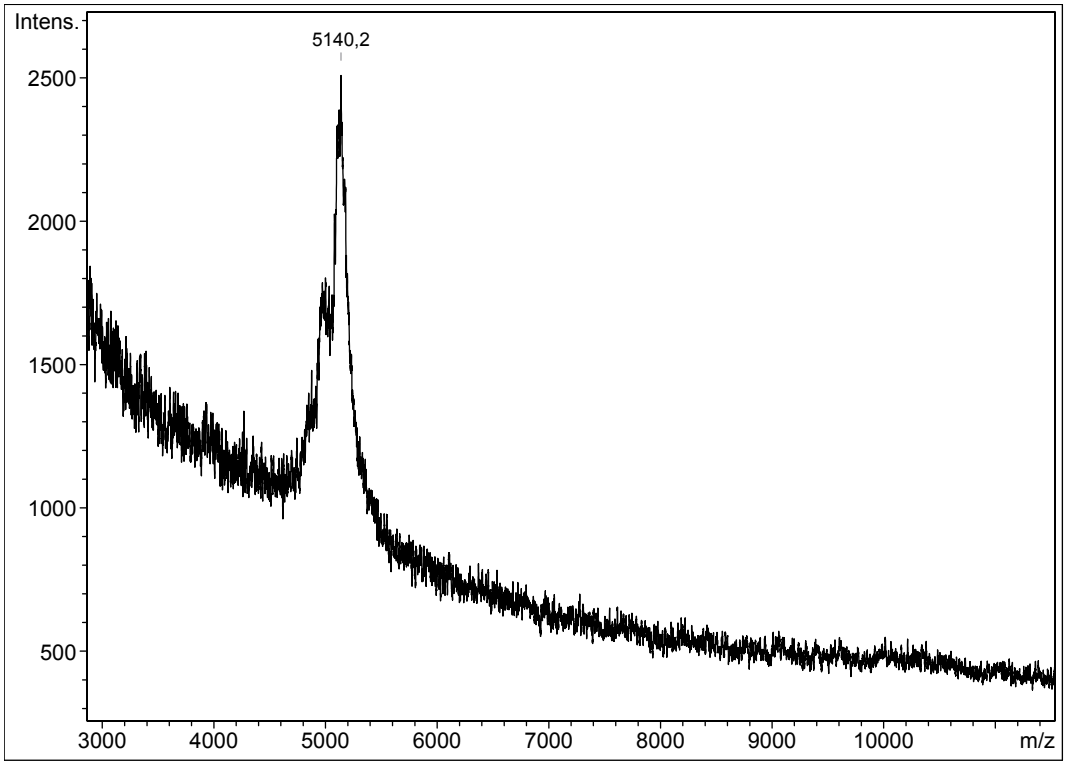

Figure 3.18 *MALDI-TOF spectrum of the oligonucleotide **10** (matrix: 2,4,6 trihydroxy-acetophenone and ammonium citrate).*

Compound 11a: For the preparation of the DNA-PS diblock copolymer compound **9a** (10 mg, 1.67 μmol) and compound **10** (5 mg, 0.98 μmol) were allowed to react in a H_2O/THF mixture for 2 d on a shaker. The coupled product was purified using preparative PAGE. Subsequently, the salt was exchanged using a dialysis membrane (Float-A-Lyzer, Spectrum Laboratories Inc.,USA) with MWCO of 8.000 g/mol, and pure product was obtained. Optical density (OD) obtained for this reaction was 300 at 260 nm. (Due to the fact that DNA and PS have absorption maxima at similar wavelength only ODs are given to express the yield of this reaction. A similar determination of yield is done elsewhere [18]) MALDI-TOF MS: m/z = 11017 g/mol.

Compound 11b: The synthesis of the DNA-PS diblock copolymer was performed similar to that of compound **11a** starting with 5 mg of **10**. OD_{260}: 210.

Compound 11c: The synthesis of the DNA-PS diblock copolymer was performed similar to that of compound **11a** starting with 5 mg of **10**. OD_{260}: 160.

V. Synthesis of DNA-*b*-PPO Diblock Copolymers

a) Synthesis of Phosphoramidite Functionalized PPOs (13a, b)

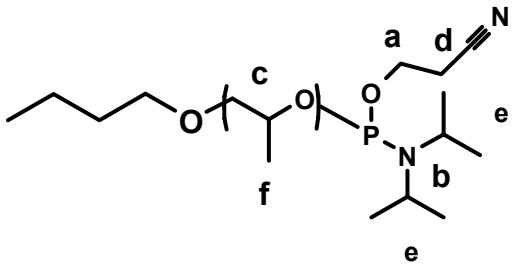

Compound 13a: Poly(propyleneglycol) monobutyl ether **12a** with a molecular weight of 1.000 g/mol (1.0 mmoles, 1.0 g) was dissolved in dry THF and reacted with N-diisopropyl-2-cyanoethyl-chlorophosphoramidite (4.2 mmol, 1.0 g) in the presence of diisopropylethylamine at room temperature under argon atmosphere for 2h. The crude product was dried and dissolved in ethyl acetate and extracted with Na_2CO_3 solution, water (3x) and brine (3x). The solution was dried over $MgSO_4$. After evaporation of the solvent the product was dried under high vacuum. (Yield: 99%)

^{31}P NMR (200 MHz, THF-d_8): 146.1 ppm

^{1}H-NMR (500 MHz, $CDCl_3$): 3.88 (t, 2H, J = 2.9 Hz, a), 3.55-3.67 (broad, 2H, b) 3.51-3.36 (broad, 70H, c), 2.61 (t, 2H, J=2.4 Hz, d), 1.16 (d, 12H, e), 1.09 (broad, 70H, f)

^{13}C-NMR (125MHz, $CDCl_3$): 13.86, 17.02, 20.09, 20.65, 24.27, 24.39, 42.62, 73.06, 75.02, 117.48

Compound 13b: Poly(propyleneglycol) monobutyl ether **12b** with a molecular weight of 6.800 g/mol (1.0 mmol, 6.8 g) was dissolved in dry THF and reacted with N-diisopropyl-2-cyanoethyl-chlorophosphoramidite (4.2 mmoles, 1.0 g) in the presence of diisopropylethylamine at room temperature under argon atmosphere for 3 h. The crude product was dried and dissolved in ethyl acetate and extracted with Na_2CO_3 solution, water (3x) and brine (3x). The solution was dried over $MgSO_4$. After evaporation of the solvent the product was dried under high vacuum. (Yield: 95%)

^{31}P NMR (200 MHz, THF-d_8): 145.7 ppm

^{1}H-NMR (500 MHz, $CDCl_3$): 3.84 (t, 2H, J = 2.8 Hz, a), 3.51-3.69 (broad, 2H, b) 3.47-3.26 (broad, 348H, c), 2.55 (t, 2H, J=2.5 Hz, d), 1.14 (d,12H, e), 0.89-1.07 (broad, 348H, f)
^{13}C-NMR (125MHz, $CDCl_3$): 13.77, 18.12, 20.17, 20.75, 24.25, 24.42, 42.62, 73.11, 75.04, 115.53

b) Grafting Onto On the Solid Support

Compound 15a: 5'-CCTCGCTCTGCTAATCCTGTTA-3' was synthesized in 120 μM scale using a standard phosphoramidite DNA synthesis protocol.[17] Compound **3a** was dissolved in dry acetonitrile and attached to the 5' end of the sequence by an optimized coupling procedure, which is as follows: The coupling time of this step was increased to 1 minute whereas the coupling time was 0.25 min for the standard DNA phosphoramidites. Compound **13a** was recycled through the solid support for 25 min to achieve high coupling efficiency. After that, **15a** was liberated from the solid support using concentrated ammonia for 16 h accompanied by deprotection of the bases. The solid support was removed by filtering and was then washed with ethanol/water mixture. After evaporation of the solvent the conjugate was purified by denaturing PAGE, filtered and desalted. Finally, the product was analysed by PAGE followed by ethidium bromide staining and MALDI-TOF MS. (Yield: 65%)
MALDI-TOF MS: 7,815 m/z

Compound 15b: 5'- CCTCGCTCTGCTAATCCTGTTA-3' was synthesized in 120 μM scale using a standard phosphoramidite DNA synthesis protocol.[19] Compound **13b** was dissolved in dry dichloromethane and attached to the 5' end of the sequence by optimising the coupling procedure, which is as follows: The coupling time of this step was increased to 1 minute whereas the coupling time was 0.25 minute for the standard DNA phosphoramidites. Compound **13b** was recycled through the solid support for 25 minutes to achieve high coupling efficiency. After that, **15b** was liberated from the solid support using concentrated ammonia for 16 h accompanied by deprotection of the bases. The solid support was removed by filtering and was then washed with ethanol/water mixture. After evaporation of the solvent the conjugate was purified by denaturing PAGE, filtered and desalted. (Yield: 60%)
MALDI-TOF MS: 13,593 m/z

VI. Synthesis of ss DNA-*b*-PEG-*b*-ss DNA Triblock Copolymers

a) Synthesis of Bisphosphoramidite Functionalized PEG (17 a,b,c)

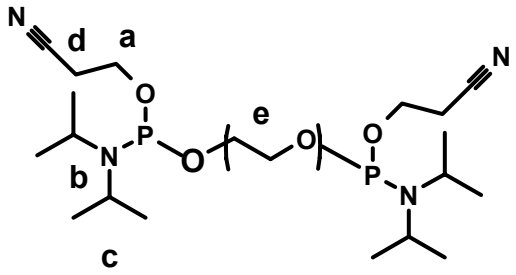

Compound 17a: Poly(ethyleneglycol) with a molecular weight of 1000 g/mol (1.0 mmoles, 1.0 g) was dissolved in dry THF and reacted with N-diisopropyl-2-cyanoethyl-chlorophosphoramidite (2.10 mmol, 500 mg) in the presence of diisopropylethylamine (1 ml) at room temperature under argon atmosphere for 2h. The solution was filtered and then the filtrate was dried under high vacuum. (Yield: 99%)

^{31}P NMR (200 MHz, THF): 144.1, 144.7 ppm
^{1}H-NMR (500 MHz, $CDCl_3$): 1.10 (d, 24H, **c**), 2.65 (t, 2H, **d**), 3.04 (m, 2H, **b**), 3.60-3.86 (b, 105H, **e**), 3.94 (t, 2H, **a**),
^{13}C-NMR (125MHz, $CDCl_3$): 20.2, 23.6, 23.9, 44.3, 59.1, 65.1, 65.6, 116.6, 117.5

Compound 17b: Poly(ethyleneglycol) with a molecular weight of 2000 g/mol (1.0 mmoles, 2.0 g) was dissolved in dry THF and reacted with N-diisopropyl-2-cyanoethyl-chlorophosphoramidite (2.10 mmol, 500 mg) in the presence of diisopropylethylamine at room temperature under argon atmosphere for 2h. The solution was filtered and then the filtrate was dried under high vacuum. (Yield: 99%)

^{31}P NMR (200 MHz, THF): 145.9, 146.5 ppm

Compound 17c: Poly(ethyleneglycol) with a molecular weight of 4000 g/mol (1.0 mmoles, 4.0 g) was dissolved in dry THF and reacted with N-diisopropyl-2-cyanoethyl-chlorophosphoramidite (2.10 mmol, 500 mg) in the presence of diisopropylethylamine at

room temperature under argon atmosphere for 2h. The solution was filtered and then the filtrate was dried under high vacuum. (Yield: 99%)

^{31}P NMR (200 MHz, THF): 143.2, 144.1 ppm

b) Synthesis of ssDNA-*b*-PEG-*b*-ssDNA Triblock Copolymers

Compound 18a: 5'-CCTCGCTCTGCTAATCCTGTTA-3' (22mer, MW = 6780 g/mol) was synthesized in 120 micromole scale using a standard phosphoramidite DNA synthesis protocol. Phosphoramidite functionalized polymer **17a** was dissolved in dry dichloromethane and attached to the 5' ends of the sequence by an optimized coupling procedure.[10] After that, ss DNA-PEG-ss DNA was liberated from the solid support using concentrated ammonia for 16 h accompanied by deprotection of the bases. The solid support was removed by filtering and was then washed with an ethanol/water mixture to completely liberate from the resin. After evaporation of the solvent the conjugate was purified by denaturing PAGE, filtered and desalted. Finally, the product was analyzed by PAGE followed by ethidium bromide staining and MALDI-TOF MS. (Yield: 35 %)
MALDI-TOF MS: 15100 m/z

Compound 18b: The synthesis of the DNA-PEG triblock copolymer was performed similar to that of compound **18a** yielding 35 % pure product.

Compound 18c: The synthesis of the DNA-PEG triblock copolymer was performed similar to that of compound **18a** yielding 29 % pure product.

References

[1] J. H. Jeong, S. H. Kim, S. W. Kim, T. G. Park, *Bioconjugate Chem.* **2005**, *16*, 1034.

[2] Y. G. Takei, T. Aoki, K. Sanui, N. Ogata, T. Okano, Y. Sakurai, *Bioconjugate Chem.* **1993**, *4*, 42.

[3] Y. G. Takei, M. Matsukata, T. Aoki, K. Sanui, N. Ogata, A. Kikuchi, Y. Sakurai, T. Okano, *Bioconjugate Chem.* **1994**, *5*, 577.

[4] R. B. Fong, Z. L. Ding, C. J. Long, A. S. Hoffman, P. S. Stayton, *Bioconjugate Chem.* **1999**, *10*, 720.

[5] M. Oishi, T. Hayama, Y. Akiyama, S. Takae, A. Harada, Y. Yarnasaki, F. Nagatsugi, S. Sasaki, Y. Nagasaki, K. Kataoka, *Biomacromolecules* **2005**, *6*, 2449.

[6] J. H. Jeong, S. H. Kim, S. W. Kim, T. G. Park, *J. Biomat. Sci.*. **2005**, *16*, 1409.

[7] Y. G. Takei, T. Aoki, K. Sanui, N. Ogata, T. Okano, Y. Sakurai, *Bioconjugate Chem.* **1993**, *4*, 341.

[8] M. Kunishima, C. Kawachi, J. Morita, K. Terao, F. Iwasaki, S. Tani, *Tetrahedron* **1999**, *55*, 13159.

[9] M. Kunishima, C. Kawachi, F. Iwasaki, K. Terao, S. Tani, *Tetrahedron Lett.* **1999**, *40*, 5327.

[10] M. Heskins, J. E. Guillet, *J. Macromol. Sci-Chem. A2* **1968**, *8*, 1441.

[11] Y. H. Bae, T. Okano, R. Hsu, S. W. Kim, *Makromol. Chem. Rapid Comm.* **1987**, *8*, 481.

[12] A. Chilkoti, G. H. Chen, P. S. Stayton, A. S. Hoffman, *Bioconjugate Chem.* **1994**, *5*, 504.

[13] K. Ueda, A. Hirao, S. Nakahama, *Macromolecules* **1990**, *23*, 939.

[14] A. Herrmann, G. Mihov, G. W. M. Vandermeulen, H. A. Klok, K. Müllen, *Tetrahedron* **2003**, *59*, 3925.

[15] K. J. Watson, S. J. Park, J. H. Im, S. T. Nguyen, C. A. Mirkin, *J. Am. Chem. Soc.* **2001**, *123*, 5592.

[16] J. H. Jeong, T. G. Park, *Bioconjugate Chem.* **2001**, *12*, 917.

[17] M. H. Caruthers, *Acc. Chem. Res.* **1991**, *24*, 278.

[18] M. A. Abdalla, J. Bayer, J. O. Radler, K. Müllen, *Angew. Chem. Int. Ed.* **2004**, *43*, 3967.

4 Synthesis of DNA Multiblock Copolymers by Hybridization*

"**In the light of this new knowledge of macromolecular chemistry, the wonder of Life in its chemical aspect is revealed in the astounding abundance and masterly macromolecular architecture of living matter.**"

Prof. Hermann Staudinger, Nobel laureate in chemistry (1953)

DNA block copolymer structures, morphologies and applications have generated considerable scientific interest over the past decade. These hybrids consist of DNA as biological component covalently linked to organic polymer segments either in linear or graft architectures. Applications of the linear topologies range from gene delivery,[1-5] DNA detection,[6, 7] to biomaterial purification.[8, 9] In extension to linear diblock structures only two A-B-A type DNA triblock architectures have been reported.[6, 10] Their central organic units consisting of fluorene and ethylene oxide moieties are limited with respect to molecular weight. Furthermore, no complex DNA multiblock copolymers have been reported so far. Herein, we describe a novel concept for the fabrication of DNA multiblock architectures by hybridization. Thereby Watson-Crick base pairing is employed for the formation of triblock and pentablock structures (**Figure 4.1**).

For the generation of DNA triblock copolymers, two ss DNA diblock polymers were synthesized as described in *Chapter 3*. The sequences of the two ODNs (22 mer) were selected to be complementary to each other. The DNA-*b*-PEG diblock copolymers were synthesized by

* Parts of this chapter have been published: *Chem. Commun.* **2007**, *13*, 1358.

reacting carboxyl chain-end functionalized PEGs (M_n = 5000 and 20000 g/mol, polydispersity index (PDI) < 1.1) with 5' amino-modified ODNs in the presence of DMT-MM as activating reagent to yield the corresponding conjugates DNA-*b*-PEG(5K) and DNA-*b*-PEG(20K).

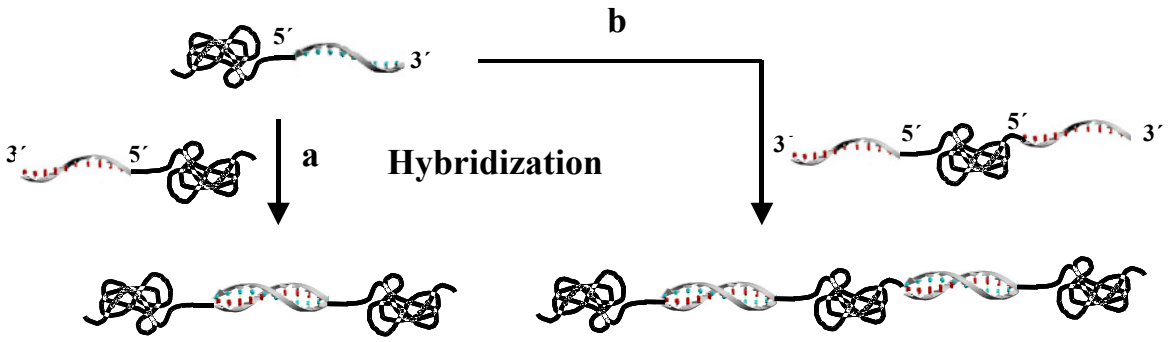

Figure 4.1 *Schematic representation of building up DNA multiblock copolymers by hybridization. Fabrication of (**a**) triblock- and (**b**) pentablock architectures.*

The resulting conjugates were purified by denaturing polyacrylamide gel electrophoresis (PAGE) and characterized by MALDI-TOF MS and HPLC (see *Chapter 3* for experimental details). The DNA-*b*-PEG diblock copolymers bearing complementary sequences were hybridized in TAE buffer (20 mM tris(hydroxymethyl)aminomethane-HCl, pH 8.0; 10 mM acetic acid; 0,5 mM EDTA) in the presence of 100 mM NaCl and 20 mM $MgCl_2$. Equimolar quantities of these block copolymers were mixed, heated up 95°C and then slowly cooled down to room temperature over the course of three days by using a thermocycler. The resulting triblock architectures were characterized by 5 % denaturing PAGE (**Figure 4.2**). In order to assess the electrophoretic mobility, these hybrids were compared with DNA-*b*-PEG containing ss or double stranded (ds) nucleic acid segments. Lanes 1 and 2 contain the ss DNA-*b*-PEGs where the organic polymer segment exhibits a molecular weight of 5000 and 20000 g/mol, respectively. Lanes 3 and 4 consist of the corresponding ds DNA-*b*-PEGs that were generated by hybridization of the ss DNA-*b*-PEGs from lanes 1 and 2 with the complementary ODN. Lanes 5-7 represent the triblock structures of PEG(5K)-ds DNA(22bp)-PEG(5K), PEG(5K)-ds

DNA(22bp)-PEG(20K) and PEG(20K)-ds DNA(22bp)-PEG(20K). With increasing molecular weight of the synthetic polymer segments, reduced electrophoretic mobilities were detected.

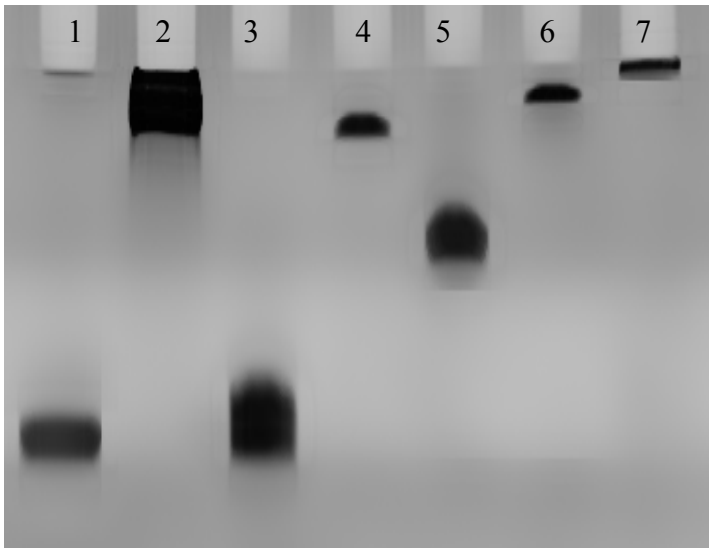

Figure 4.2 *Gel analysis of the di-, and triblock copolymers. (A) Lanes 1-4 contain diblock copolymers of ss DNA-b-PEG(5K), ss DNA-b-PEG(20K), ds DNA-b-PEG(5K) and ds DNA-b-PEG(20K), respectively. Lanes 5-7 contain the triblock architectures of PEG(5K)-DNA-PEG(5K), PEG(5K)-DNA-PEG(20K) and PEG(20K)-DNA-PEG(20K), respectively.*

In order to realize more complex multiblock architectures containing ds DNA, a novel building block was prepared by a straightforward synthetic route. This triblock architecture is composed of a central PEG domain (M_n = 1000 g/mol, PDI < 1.1) onto which two identical ss ODNs were covalently attached at their 5' ends. These ODNs encode the complementary sequence of the ss DNA-*b*-PEG. For the generation of the triblock copolymer, a bis-phosphoramidite functionalized PEG was synthesized and attached to the 5' terminus of the nucleic acid fragment employing solid phase synthesis similar as reported previously.[11]

Figure 4.3 *Lane 1 and 2 contain the triblock copolymers of ss DNA-PEG-ss DNA and ds DNA-PEG-ds DNA, respectively. Lane 3 and 4 contain the pentablock architectures of PEG(5K)-DNA-PEG-DNA-PEG(5K) and PEG(20K)-DNA-PEG-DNA-PEG(20K), respectively.*

This ss DNA triblock architecture was analyzed and purified by denaturing PAGE and the molecular weight was confirmed by MALDI-TOF MS (see *Chapter 3* for experimental details). This building block was used to construct ds DNA pentablock copolymers with varying molecular weights of the terminal synthetic polymer units. These multiblock architectures were synthesized by hybridizing two equivalents of the ss DNA-*b*-PEG with one equivalent of the ss DNA triblock copolymer applying the same conditions as described above. The multiblock bioorganic hybrids were analyzed by denaturing PAGE (**Figure 4.3**). Lanes 1 and 2 correspond to the triblock architectures DNA-PEG-DNA exhibiting either ss or ds nucleic acid segments, respectively. Lanes 3 and 4 represent the A-B-A-B-A type pentablock structures with terminal PEG segments of 5000 and 20000 g/mol, respectively. Again, an increase in the molecular weight of the DNA block copolymers resulted in lower gel shifts. As an additional structural proof, MALDI-TOF MS was used to confirm the formation of the ds DNA pentablock structures (**Figure 4.4**).

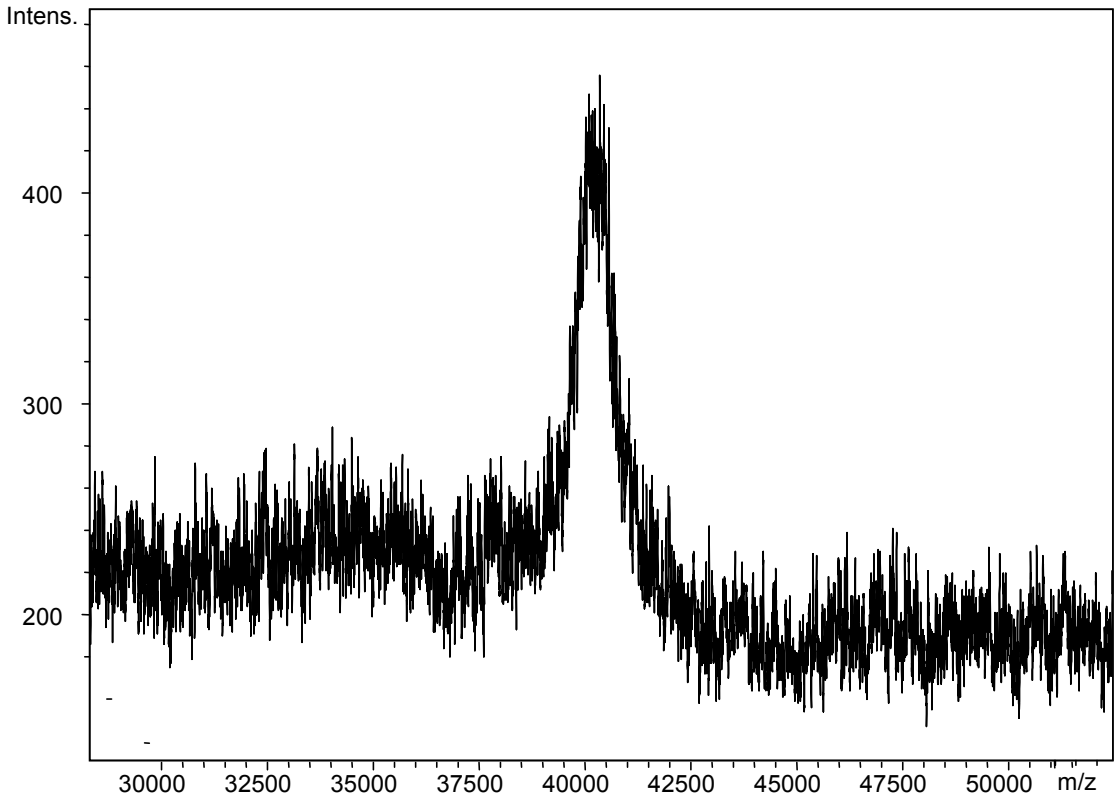

Figure 4.4 *The MALDI-TOF spectrum of the pentablock copolymer, PEG(5K)-DNA-PEG-DNA-PEG(5K) (found: 40500 g/mol, calculated 41000 g/mol).*

Multiblock copolymers are very attractive materials due to their rich varieties of morphologies in bulk and in selective solvents. However, the synthesis of well-defined multiblock architectures, usually prepared by living polymerization techniques, is difficult and laborious. These complex structures can be realized by sequential addition of monomers, the use of difunctional linking agents or difunctional intiators and by combinations thereof.[12] Nevertheless, control over the molecular weight and low polydispersity are hard to achieve.[13] Moreover, the products are sometimes contaminated with homopolymers and further purification is crucial to obtain pure materials.[12] In contrast, the assembly of DNA multiblock copolymers by molecular recognition has some striking advantages. First, contamination with homopolymers is avoided when pure ss building blocks are employed. Second, dry and inert conditions for multiblock assembly are not required. Third, highly well defined structures are obtained due to the monodispersity of the nucleic acid segments.

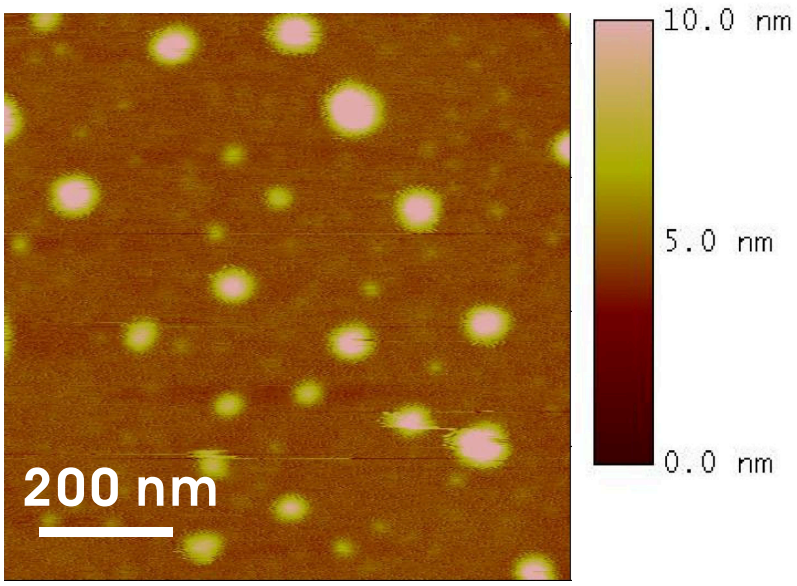

Figure 4.5 *SFM topographical image of DNA-triblockcopolymer PEG(20K)-DNA(22bp)-PEG(20K). The height is indicated with a color scale bar on the right. The z-scale in this image is 10 nm.*

To elucidate the resulting morphologies in a selective solvent preliminary experiments with a ds DNA triblock copolymer were carried out. Therefore, SFM measurements were carried out by *J. Wang* in the group of *Dr. R. Berger*. These analyses revealed the formation of spherical micelles in dichloromethane, which is a selective solvent for the organic polymer segment. The maximum height of individual micelles was calculated by means of local roughness analysis (**Figure 4.5**).

The maximum height of the micelles varied from 3 nm to 11 nm. The diameter of the micelles was determined to lie between 15 and 77 nm. A detailed study of the influence of the molecular parameters like ss and ds nucleic acid segments or block length ratios on structural properties in solution as well as the investigation of bulk morphologies are subject of further studies. In conclusion, Watson-Crick base pairing was employed to construct multiblock copolymer architectures in a highly modular manner. In the future, this approach will be also used to connect synthetically incompatible organic polymer segments.

Experimental Section

I. Synthesis of Multiblock Architectures

General Hybridization Procedure

The hybridization was carried out by dissolving the desired stoichiometric quantities of ss entities in in TAE buffer (20 mM tris(hydroxymethyl)aminomethane-HCl, pH 8.0; 10 mM acetic acid, 0,5 mM EDTA) containing Na^+ (100 mM) and Mg^{2+} (20 mM). The mixture was heated to 95°C and was slowly cooled to room temperature over the course of 3 days (1 degree per hour) by using a polymerase chain reaction thermocycler (Biometra GmbH, Germany). The final concentration of DNA was between 2-5 μM.

DNA Sequences:

ss DNA-PEG-ss DNA: 5'- CCTCGCTCTGCTAATCCTGTTA-3'

Complementary: 5'- TAACAGGATTAGCAGAGCGAGG -3'

II. Scanning Force Microscopy (SFM) Measurements of DNA Triblock Copolymer Micelles

20 microliters of a 0.2 nM DNA-triblockcopolymer solution in dichloromethane were deposited onto silicon wafer (Si-Mat-Silicon Materials, Landsberg am Lech, Germany). After evaporation of the solvent, the sample was mounted in the SFM.

The images were recorded using a commercial SFM (Multimode, Nanoscope IIIa, Veeco Instruments, California, USA) in tapping mode in air with an E-scanner. Silicon cantilevers (OMCLAC 160 TS-W2, Olympus, Japan; 160 μm long, 50 μm wide, 4.6 μm thick) with resonance frequencies of ~300 kHz were used. The height of the tip was 7-15 μm, and the tip radius of curvature was < 10 nm.

SFM images (512×512 pixels) were recorded at a scan rate of 1 Hz. The raw data has been modified by applying the second order "flatten" filter.

References

[1] J. H. Jeong, T. G. Park, *Bioconjugate Chem.* **2001**, *12*, 917.

[2] M. Murata, W. Kaku, T. Anada, Y. Sato, T. Kano, M. Maeda, Y. Katayama, *Bioorg. Med. Chem. Lett.* **2003**, *13*, 3967.

[3] S. Cogoi, M. Ballico, G. M. Bonora, L. E. Xodo, *Cancer Gene Ther.* **2004**, *11*, 465.

[4] J. H. Jeong, S. H. Kim, S. W. Kim, T. G. Park, *Bioconjugate Chem.* **2005**, *16*, 1034.

[5] M. Oishi, F. Nagatsugi, S. Sasaki, Y. Nagasaki, K. Kataoka, *ChemBioChem* **2005**, *6*, 718.

[6] C. E. Immoos, S. J. Lee, M. W. Grinstaff, *J. Am. Chem. Soc.* **2004**, *126*, 10814.

[7] Z. Li, Y. Zhang, P. Fullhart, C. A. Mirkin, *Nano Lett.* **2004**, *4*, 1055.

[8] R. B. Fong, Z. L. Ding, C. J. Long, A. S. Hoffman, P. S. Stayton, *Bioconjugate Chem.* **1999**, *10*, 720.

[9] M. D. Costioli, I. Fisch, F. Garret-Flaudy, F. Hilbrig, R. Freitag, *Biotechnol. Bioeng.* **2003**, *81*, 535.

[10] E. Ergen, M. Weber, J. Jacob, A. Herrmann, K. Müllen, *Chem.-Eur. J.* **2006**, *12*, 3707.

[11] F. E. Alemdaroglu, K. Ding, R. Berger, A. Herrmann, *Angew. Chem. Int. Ed.* **2006**, *45*, 4206.

[12] N. Hadjichristidis, M. Pitsikalis, H. Iatrou, *Adv. Polym. Sci.* **2005**, *189*, 1.

[13] C. Y. Wang, M. H. Cui, *J. Appl. Polym. Sci.* **2003**, *88*, 1632.

5 Generation of Multiblock Copolymers by PCR: Synthesis, Visualization and Nanomechanical Properties*

"**DNA is not merely the secret of life.**"

-Prof. Dr. N. C. Seeman, 1997

Block copolymers are attractive materials due to their variable and predictable morphologies and broad range of applications in the field of nanostructured materials.[1-3] Although the first block copolymer has been synthesized nearly half a century ago, the development of new synthetic strategies of highly defined and complex block copolymer topologies is still progressing.[4, 5] Recently, a novel class of linear block copolymers was introduced that contains DNA as a biological segment covalently linked to synthetic polymer units.[6] As a consequence of the conjugation of these two different classes of materials, DBCs originate that are outfitted with engineered material properties that cannot be realized with polymers or nucleic acids alone. Therefore, DBCs have rapidly found remarkable applications ranging from gene delivery,[7] sensitive DNA detection[8] to biomaterial purification.[9] Several synthetic routes and coupling strategies were established to produce ss DBCs allowing to vary the nature of the organic polymer and the sequence composition of the ODN segment.[6] Employing these as building blocks, linear ds tri- and pentablock architectures were assembled by hybridization which has been described in the previous chapter.[10]

* Parts of this chapter have been submitted for publication. (June 2007)

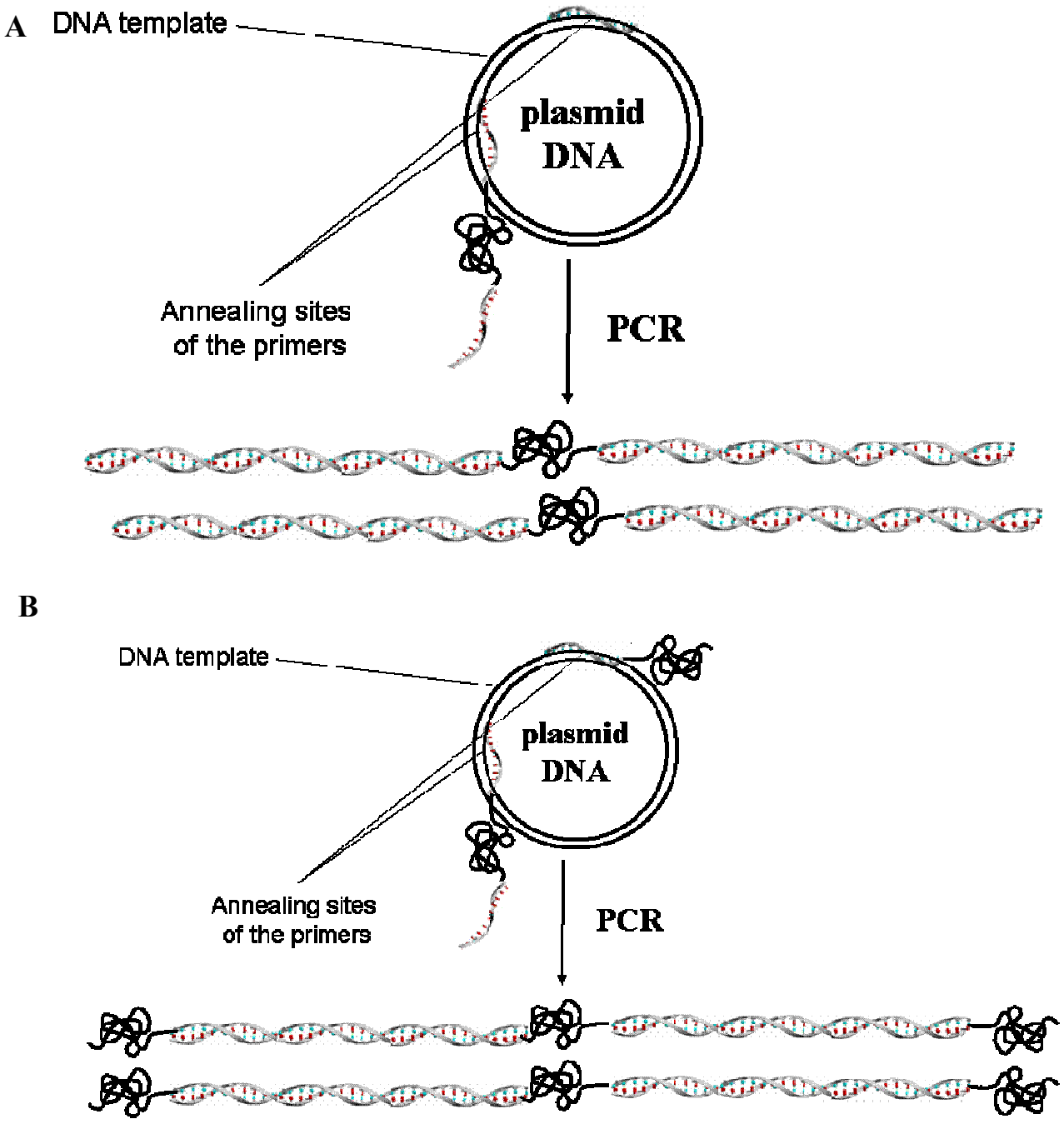

Figure 5.1 *Schematic representation of the built-up of (A) DNA triblock- and (B) DNA pentablock copolymers by polymerase chain reaction.*

Although this method provided complex and well-defined block copolymer topologies, a synthetic limitation remains regarding the nucleic acid segments. The ODNs were generated by solid-phase synthesis therefore the lengths of these segments were limited to several tens of nucleotides. This is rather small in comparison to naturally occurring polynucleotides like

genomic or plasmid DNA. In the following paragraphs it will be demonstrated how to overcome this synthetic limitation by employing the PCR for the preparation of high molecular weight DNA multiblock copolymer architectures with extended ds DNA segments. Moreover, significant extension of the nucleic acid segments allows direct visualization of single block copolymers by SFM, and even the nanomechanical properties of single bioorganic hybrids could be investigated by SFM.

In molecular biology PCR is an efficient technique to produce a specific DNA sequence *in vitro* by employing a DNA-template, two oligonucleotide primers, the four deoxynucleotide triphosphates (dNTPs) and a thermostable DNA polymerase in a three-step amplification process over several cycles.[11, 12] Due to its extreme sensitivity and specificity it is commonly used in medical and biological research for a variety of tasks, such as the detection of hereditary diseases, the identification of genetic fingerprints, the diagnosis of infectious diseases, the cloning of genes and paternity testing.[13] It was hypothesized that this technique could be transferred to polymer chemistry for obtaining well-defined block copolymers with monodisperse, high molecular weight nucleic acid blocks. It was postulated that a triblock copolymer of type ss DNA-A-ss DNA (A denotes the organic polymer unit) as one primer and a conventional ODN as a second primer would lead to triblock copolymers of type ds DNA-A-ds DNA with extended nucleic acid segments. When instead of the ODN a ss DNA diblock copolymer is employed as a second primer pentablock copolymers are generated. The lengths of the nucleic acid segments are determined by the annealing sites of the primers on the template (**Figure 5.1**).

Since PEG is known to function as an enhancer in PCR,[14] PEG was selected as the organic component of the ss DBCs. The triblock copolymer primer **ssTB1** was synthesized using a DNA synthesizer with a bisphosphoramidite PEG polymer as the key intermediate like described in *Chapter 3*. Onto the central PEG domain (Mn = 2000 g/mol, PDI = 1.1) two identical ss ODNs were attached. (22mer, sequence: 5'-CCTCGCTCTGCTAATCCTGTTA-3', Mw: 6670 g/mol). For the PCR were employed: **ssTB1** as forward primer, a conventional ODN as a backward primer, the plasmid **pBR322** as the template, 4 dNTPs, and a thermostable DNA polymerase. This set of reagents resulted in formation of triblock copolymers of type ds DNA-*b*-PEG-*b*-ds DNA exhibiting nucleic acid units with lengths of 167, 225 and 500 bp. To achieve effective amplification an optimized PCR procedure was developed with an annealing time of 4 min, in contrast to a period of 30 sec for denaturation

and extension. Otherwise standard times and temperatures were employed[15] (4 min at 95 °C and then 30 cycles of 30 sec at 95 °C for denaturation, 1-4 min at 55-59 °C for annealing and 30 sec - 2 min at 72 °C for extension). The triblock copolymers were analyzed by 1 % agarose gel electrophoresis followed by ethidium bromide staining (**Figure 5.2**).

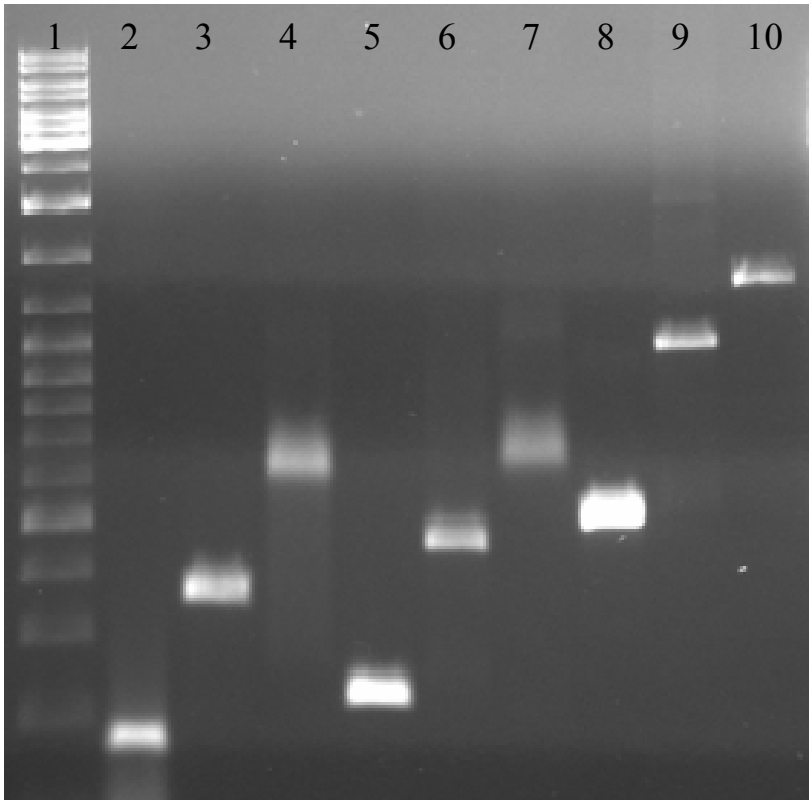

Figure 5.2 *Gel analysis of the tri- and pentablock copolymers. Lane 1 is DNA ladder (10000bp-100bp). Lane 2, 5 and 8 are the ds DNA controls with 167, 225 and 500 bp. Lane 3, 6 and 9 are the triblock copolymers with 167, 225 and 500 bp nucleic acid blocks, respectively. Lanes 4, 7 and 10 represent DNA pentablock copolymers with 167, 225 and 500 bp DNA segments, respectively, and terminal PEG segments (Mw: 20000 g/mol).*

The non-polymer functionalized primers were selected to hybridize in increasing distance from **ssTB1** on the template which resulted in nucleic acid blocks of increasing length. As controls, amplicons were generated that have the same sequence as the nucleic acid block present in the triblock structures. As expected, the triblock copolymers showed lower electrophoretic mobilities than the pristine DNA. In the case of DNA(167 bp)-*b*-PEG(2K)-*b*-

DNA(167 bp) (**Figure 5.2, lane 3**) the largest shift was detected whereas DNA(500 bp)-*b*-PEG(2K)-*b*-DNA(500 bp) (**Figure 5.2, lane 9**) exhibited the lowest mobility. For DNA(225 bp)-*b*-PEG(2K)-*b*-DNA(225 bp) (**Figure 5.2, lane 6**) an intermediate mobility was observed. Beside characterization by gel electrophoresis, DNA-PEG-DNA triblock copolymers were characterized by restriction analysis with a sequence specific endonuclease to confirm the triblock copolymer structures (see Experimental Section). Furthermore, the triblock copolymers were verified by direct visualization of single DBCs employing SFM, which recently has been used as a powerful tool for visualizing micelles of amphiphilic DBCs.[7, 16-18] These measurements were carried out by *J. Wang*. The samples were scanned in soft tapping mode in buffer on mica (**Figure 5.3**). A mean contour length of 344 ± 22 nm was measured for DNA(500 bp)-*b*-PEG(2K)-*b*-DNA(500 bp) as an average from 100 polymer molecules. This yields a rise per bp of 0.34 ± 0.02 nm which is in good agreement with the expected value for ds DNA in the B-form.[19] Frequently a kink of the polymer chain was observed at half contour length, which can be explained by the presence of a flexible polymer bridging the equally sized DNA blocks. In the case of triblock copolymers with a nucleic acid block of 225 bp a mean length of 159 ± 13 nm was measured which results in a rise per bp of 0.35 ± 0.03 nm. For the triblock copolymer with DNA blocks of 167 bp a contour length of 123 ± 11 nm was determined that is slightly higher (~10 nm) than the theoretically expected value. Control experiments with pristine ds DNA of 167 bp, 225 bp and 500 bp showed only single DNA fragments of stretched polymer chains as expected for a semiflexible polymer with a persistence length of 50 nm.[20] Kinks within these structures were not observed (See Experimental Section).

In order to realize pentablock architectures, **ssTB1** and several ss DNA diblock copolymers (**ssDB1, ssDB2 and ssDB3**) were employed in the PCR process. In contrast to the ss triblock structure **ssTB1**, the diblock copolymers were synthesized in solution
by coupling an active ester functionalized PEG (Mn = 20 000 g/mol, PDI = 1.1) with amino modified ODNs as shown in *Chapter 3*.[10] The combination of ss triblock copolymer and ss diblock copolymers as set of primers resulted in three different PEG-*b*-DNA-*b*-PEG-*b*-DNA-*b*-PEG pentablock copolymers with varying DNA segment lengths of 167, 225 and 500 bp employing similar PCR conditions as described for the corresponding triblock architectures.

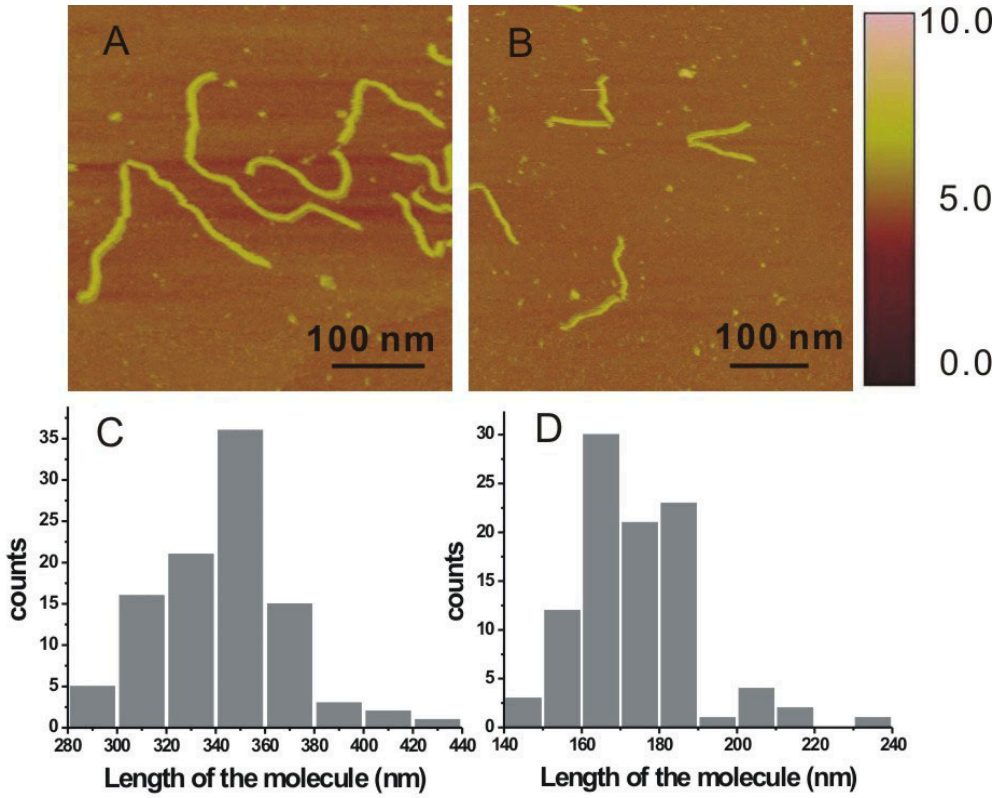

Figure 5.3 *Tapping mode SFM topographical images in buffer on mica with length distributions of DNA (500 bp)-b-PEG-b-DNA (500 bp) (A, C) and DNA (225 bp)-b-PEG-b-DNA (225 bp) (B, D). The height scale in (A, B) is indicated with a color bar (10 nm) on the right. The height of the center of molecule is ~0.3 nm.*

The structures of the pentablock copolymers were assessed by agarose gel electrophoresis (**Figure 5.2**) and restriction analysis with a sequence specific endonuclease (see Experimental Section). In analogy to the triblock copolymers, an increase in the molecular weights of the biological segments induced a decrease in the electrophoretic mobilities. It is noteworthy to mention that the pentablock architecture with a DNA segment length of 500 bp exhibits a molecular weight of more than 600 000 g/mol as calculated for the exact sequence composition and is constituted of monodisperse biological segments. In the context of block copolymer synthesis this is a remarkable result because ultrahigh molecular weight multiblock architectures with almost perfect structural precision were obtained.

In order to investigate their nanomechanical properties single blockcopolymers were also manipulated by the SFM tip. These measurements were carried out by *W. Zhuang* in the group of *Prof. Dr. J. P. Rabe*. **Figure 5.4A** displays a tapping mode SFM image of a triblock copolymer with two nucleic acid blocks of 500 bp connected by the PEG block with a measured contour length of 356 nm. The sample was deposited on an HOPG surface pre-coated with a sub-monolayer of dodecylamine ($C_{12}H_{25}NH_2$: from 300mg/l chloroform solution). The manipulation was carried out in contact mode,[21] similarly as recently demonstrated for neat ds DNA on such a modified HOPG surface [22]. As shown in **Figure 5.4B**, the triblock polymer was elongated to 432 nm after dragging by the SFM tip along the moving trace marked with a dotted arrow. **Figure 5.4C** shows the resulting structures after dragging the triblock copolymer in the direction perpendicular to its stretching axis. As a consequence the hybrid was broken due to the large pulling force. From several of these experiments and careful contour length measurements it became apparent that the breaking point was located at the center of the triblock rather than at the tip-molecule contact point. The total length of two broken pieces amounts to 483 nm, which means that compared to the original length of 356 nm the triblock polymer was 1.4 times elongated upon dragging across the surface. The PEG polymer incorporated in the middle of the triblock was not distinguishable from ds DNA. This may be attributed to the low molecular weight of the PEG unit and/or that it formed a flexible random coil on the surface. However, the PEG moiety could be clearly distinguished from ds DNA by SFM after a blowing manipulation. In this experiment a thin film of chloroform was spin-coated on the same surface, in order to generate a surface pressure inside a topological crossover triblock loop by a tapping SFM tip,[23] which can stretch and overstretch the triblock chain.

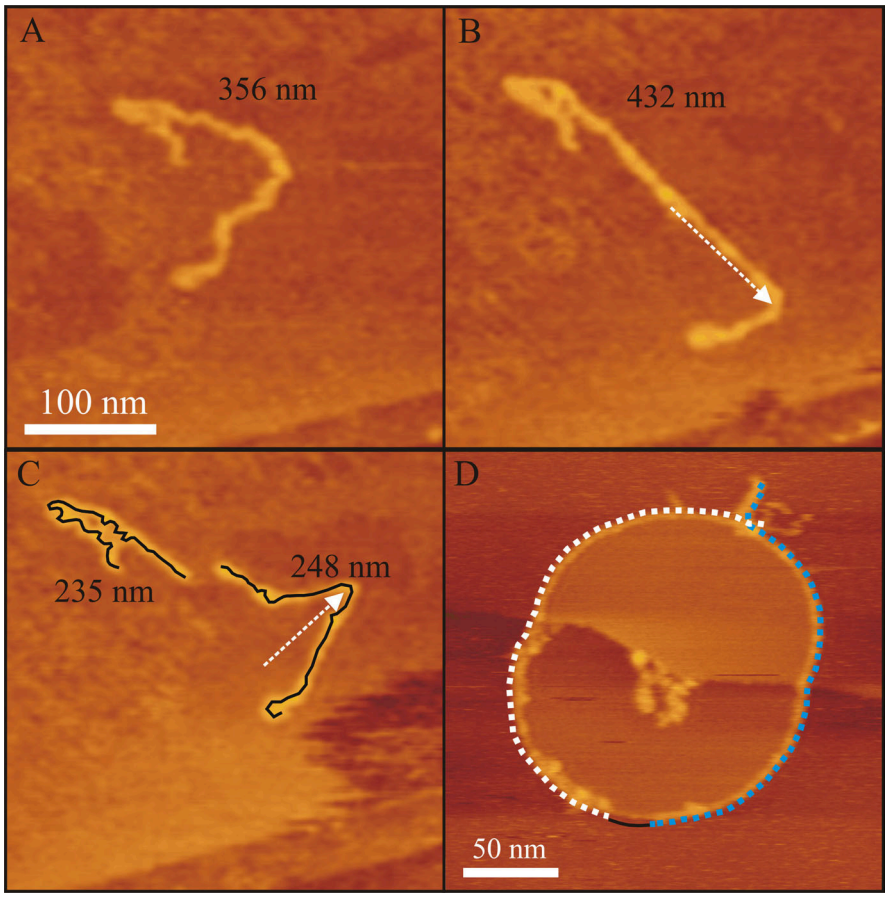

Figure 5.4 *Tapping mode SFM topographical images of a DNA (500 bp)-b-PEG-b-DNA (500 bp) triblock molecule on $C_{12}H_{25}NH_2$ pre-coated HOPG before (A) and after (B and C) manipulation. White dotted arrows in (B) and (C) indicate the moving traces of SFM tip during manipulation in contact mode. The black solid lines in (C) following the triblock contours were used to calculate the contour lengths. (D) Tapping mode SFM image of a DNA (500 bp)-b-PEG-b-DNA (500 bp) triblock molecule, which formed a topological crossover loop across a step edge of the HOPG surface covered by an ultrathin chloroform layer, and which had been blown by the tapping SFM tip. [23] The white and blue dotted lines sketch the contours of the two ds DNA blocks while the black solid line sketches the PEG contour. The unidentified material inside the loop is attributed to impurities deposited from the solution.*

Figure 5.4D displays a blown triblock hybrid loop, where the thin PEG polymer with about 18 nm length bridges two thick overstretched ds DNA chains aside. The elongation of the single triblock molecule reveals the unique mechanical properties of ds-DNA, i.e. B-form ds DNA can be overstretched to the S-form by factor of 1.7 times in solution[24, 25] or 2 times on a surface.[23, 26] In the triblock dragging experiment it was noticed that both ends of the

triblock were almost immobilized on the surface, which may be due to high surface friction resulting from high concentration of dodecylamine underneath.The final elongation of the triblock chain of 1.4 times is therefore the average elongation of different pieces along the whole chain. On the other hand, the manipulation of ds DNA by an SFM tip has shown that the maximum force acting on the molecule is at the position where the SFM tip contacts the molecular chain. Interestingly, the scission of the triblock does not occur at the position loaded by the maximum force but almost at the center region of the triblock. It is consistent with the fact that ss DNA has a much smaller Young's modulus than ds DNA under the same force loading conditions.[24] SFM cantilever pulling experiments have also proven that the covalent bond in polysaccharide can be ruptured at about 1000 pN while ds DNA remains unbroken at the same force.[27] Similarly, in the triblock molecules the single PEG backbone breaks at a lower force than ds DNA, which is consistent with a weaker break force.

In summary, PCR was successfully implemented into polymer chemistry to produce complex linear multiblock architectures. Salient characteristics of the DNA polymer hybrids were the high molecular weights exceeding 600 000 g/mol and their structural accuracy. Noteworthy are the modularity of the approach and the ease of adjusting the molecular weights of the biological blocks that can be adjusted by the annealing sites of the polymer functionalized or conventional ODN primers on the template. Besides gel electrophoresis and restriction analysis the DNA multiblock architectures were characterized by SFM. Direct visualization revealed single polymer chains with the theoretically expected contour lengths for the DNA blocks and a characteristic bending at the central organic polymer unit bridging them. Furthermore, the triblock hybrids were manipulated by SFM, which so far has only been demonstrated for neat DNA and dendronized polymers. Upon blowing circular topologies, the DNA and the organic polymer chain have been extended and could thereby be displayed. To the best of our knowledge, this experiment afforded for the first time to visualize the three blocks of a single linear triblock copolymer chain by SFM. Moreover, dragging-breaking experiments revealed that the single PEG backbone breaks at a force at which the ds DNA backbones keep unbroken, thereby identifying the mechanical weak point of the DNA-polymer hybrids.

Experimental Section

The Sequences

Id.	DNA sequence 5'-3'-direction
ssTB1	CCTCGCTCTGCTAATCCTGTTA
ssDB1	CCTCGCTCTGCTAATCCTGTTA
ssDB2	CATCCATACCGCCAGTTGTTTA
ssDB3	CATCCATACCGCCAGTTGTTTA

Synthesis of ds DNA triblock copolymers

ds DNA triblock copolymers were synthesized by standard PCR procedure employing a polymer functionalized triblock primer (**ssTB1**) and a conventional oligonucleotide primer. A total of 200 µl PCR reaction mixture containing 0.5 mM dNTPs, 1 U Taq DNA polymerase, 50 pg plasmid DNA pBR322, 1 µM forward and backward primers, PCR buffer (100 mM Tris-HCl, 500 mM KCl and 0.8% Nonidet P40), and 2-2.5 mM of magnesium chloride were subjected to thermal cycling (4 min at 95 °C and then 30 cycles of 30 sec at 95 °C for denaturation, 1-4 min at 55-59 °C for annealing and 30 sec-2 min at 72 °C for extension) in a thermocycler. The PCR amplified products were purified by QIAquick Gel Extraction Kit from Qiagen GmbH (Germany) using deionized water for eluting the amplicons. The PCR products were characterized by agarose gel electrophoresis.

Synthesis of ds DNA pentablock copolymers

ds DNA pentablock copolymers were synthesized by standard PCR protocols employing polymer functionalized triblock forward (**ssTB1**) and diblock backward (**ssDB1, ssDB2** and **ssDB3**) primers. PCR was carried out in 200 µl PCR reaction mixture containing 0.5 mM dNTPs, 4 U Taq DNA polymerase, 200 pg plasmid DNA pBR322, 1 µM forward and backward primers, PCR buffer (100 mM Tris-HCl (pH 8.8 at 25 °C), 500 mM KCl and 0.8% Nonidet P40), and magnesium chloride (2-3 mM). The PCR conditions were as follows:

95 °C, 4 min; (95 °C, 30 sec; 59 °C, 4 min; 72 °C, 1 min) / 30 cycles; 72 °C, 7 min. The amplified products were purified by electroelution into dialysis bags. The ds DNA triblock copolymers were characterized by agarose gel electrophoresis.

Purification of ds DNA Pentablock Copolymers

The purification was done according to the literature with a few modifications.[15] The procedure is detailed below. After the PCR reaction, the reaction mixture was run in a 1.5% agarose gel. Before the band was excised, the gel was photographed to establish a record of which band was removed. By using a sharp scalpel a small slice of agarose gel containing the band of pentablock copolymers were cut out, and placed on a square of Parafilm wetted with 0.25x TBE. One end of a piece of dialysis tubing was sealed with a secure knot. The dialysis bag was filled with 0.25x TBE. By using a thin spatula, the gel slice was transferred into the buffer-filled bag. The gel slice was allowed to sink to the bottom of the bag. Some of the buffer inside the bag was squeezed out, leaving just enough to keep the gel slice in constant contact with the buffer. A dialysis clip was placed just above the gel slice to seal the bag. Trapping air bubbles must be avoided. The bag was immersed in a shallow layer of 0.25x TBE in a horizontal electrophoresis tank. The gel fragments should be maintained parallel to the electrodes. Electric current through the bag (7.5 V/cm) was passed for 45-60 minutes. By using a long-wavelength UV lamp the movement of the DNA fragment out of the gel slice was monitored. The polarity of the current was reversed for 20 sec. to release the DNA from the wall of the bag. After turning off the electric current the bag was recovered from the electrophoresis chamber. After the reverse electrophoresis, the buffer surrounding the gel slice was transferred to a plastic tube. The gel slice was removed from the bag and stained. It was examined by UV illumination to confirm that the entire block copolymer has eluted. The product was then desalted by Microspin G25 Columns (Amersham Biosciences, Sweden).

Characterization of ds DNA Tri- and Pentablock copolymers

Several of the ds DNA tri- and pentablock copolymers were characterized by sequence specific endonuclease digestion.

Restriction endonuclease analysis of ds DNA triblock copolymers

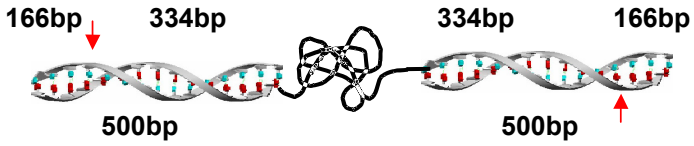

Figure 5.5 *The graphical representation of restriction endonuclease analysis of ds DNA triblock copolymer.*

Several DNA triblock have been analyzed by a sequence specific restriction endonuclease. As an example, the restriction analysis of the triblock copolymer ds DNA(500bp)-*b*-PEG(1K)-*b*-DNA(500 bp) is described below.

The DNA triblock copolymer was digested by the enzyme AasI (DrdI) at 37 °C for 15 h in the reaction buffer containing 10 mM Tris-HCl, 10 mM MgCl2 and 0.1 mg/ml BSA. The digested product was analyzed by agarose gel electrophoresis (**Figure 5.6**). Lanes 1 and 2 show the DNA ladder and the triblock copolymer, respectively.

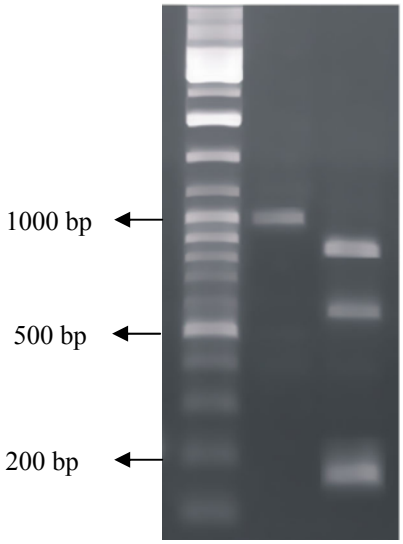

Figure 5.6 *Gel anaylsis of the digestion of a DNA triblock copolymer. Lane 1: DNA Ladder (10000-100 bp). Lane 2: ds DNA triblock copolymer with 500 bp nucleic acid segments. Lane 3: The digestion products of the DNA triblock copolymer.*

The digestion resulted in three different products which are shown in Lane 3. The band with the lowest electrophoretic mobility represents the triblock hybrid digested once. Other digestion products are the copolymer digested twice with an intermediate mobility and the nucleic acid segment of 166 bp with the highest mobility.

SFM Measurements of DNA Block Copolymers in Buffer

20 µl of a 10 µg/ml DNA-*b*-PEG-*b*-DNA solution in buffer (10 mM Tris PH 7.4, 1 mM $NiCl_2$) were deposited onto freshly cleaved mica (Plano GmbH, Germany). After 5 min incubation the samples were rinsed with 200 µl of buffer solution. The mica sheet was then mounted in the SFM keeping the surface always covered by buffer solution.

All images were recorded using a commercial SFM (Multimode, Nanoscope IIIa, Veeco Instruments, California USA) in soft tapping mode in liquid. Oxide-sharpened silicon nitride cantilevers (NP-S, Veeco Instruments, California; 115 µm long, 17 µm wide, 0.6 µnm thick) with an integrated tip (a spring constant of 0.32 N/m and a resonance frequency of 56 kHz in air) were used. The height of the tip was 2.5 to 3.5 µm. The tip radius was confirmed by scanning electron microscopy after having performed the SFM measurements. We found tip radii of curvatures < 20 nm in all cases. A piezoelectric E-scanner (Veeco Instruments, California) was used, which supplies a maximum x-, y-scan of 12.5 µm and a z-extension of 2.5 µm. The scanner was calibrated by imaging a rectangular grid of 1 µm * 1 µm mesh size.

In liquids, we selected a driving frequency between 8 – 10 kHz for imaging. SFM images (512 × 512 pixels) were recorded at a scan rate of 1 Hz. Images were processed by flattening to remove the background slope. Contour lengths measured from 100 molecules were plotted together in the histograms.

Control experiments

The DNA segments having 500 and 225 bp have been prepared by PCR. A mean length of 180.1 ± 11.1 nm was measured for the 500 bp fragments, yielding a rise of 0.36 ± 0.02 nm per bp, and a mean length of 86.3 ± 5.7 nm was measured for the 225 bp fragments, yielding a rise of 0.38 ± 0.03 nm per bp. The height of the molecules is ~2 nm. The width was determined to be 6~8 nm (**Figure 5.7**).

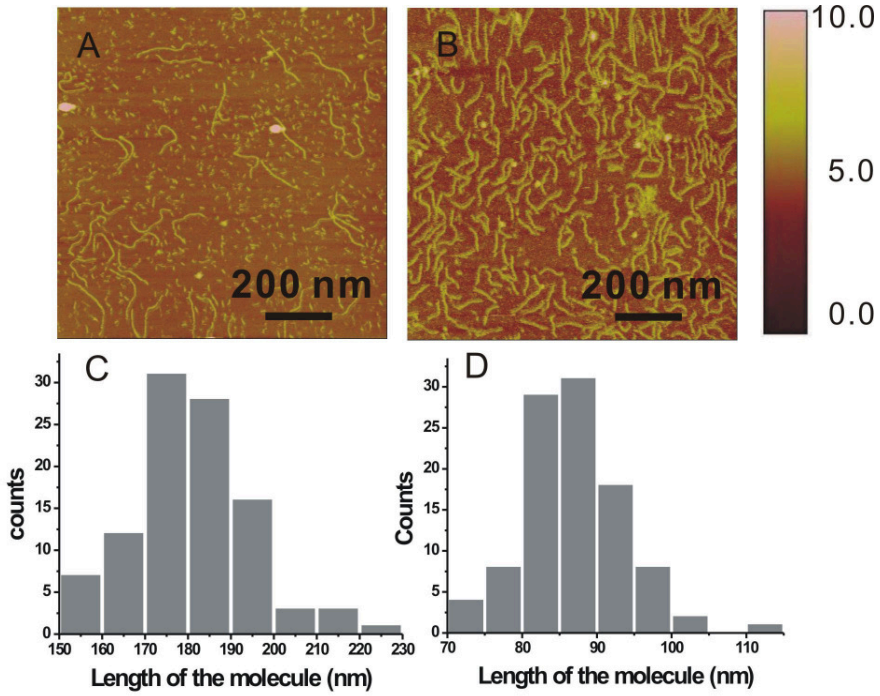

Figure 5.7 *Structural properties of DNA of 500 bp (A, C) and 225 bp DNA (B, D) investigated by Scanning Force Microscopy. (A, B) Tapping mode SFM topographical images in buffer. The height is indicated with a color scale bar on the right. The z-scale of the images is 10 nm. (C, D) Histograms of contour length distribution.*

Manipulation of Block Copolymers by SFM

For pre-coating the surface of highly oriented pyrolytic graphite (HOPG), a droplet (ca. 10 µl) of $C_{12}H_{25}NH_2$ (dodecylamine) in chloroform solution (0.3 g/l) was spin coated onto HOPG at spinning rate of 40 rps. The amphiphile pre-coated surface was annealed afterwards at 40°C for 20 min in order to evaporate the solvent remaining on the surface. 10 µl of a 5 µg/ml DNA (500 bp)-*b*-PEG-*b*-DNA (500 bp) solution in distilled water were deposited onto the precoated HOPG surface for 10 sec and spun off subsequently. SFM images were recorded before and after manipulation using a MultiMode scanning probe microscope (Digital Instruments, Inc., Santa Barbara, CA, USA) operated in tapping-mode. Height and phase images were recorded with scan rate of 2-4 lines/sec. and a resolution of 512*512 pixels. Olympus etched silicon cantilevers were used with a typical resonance frequency in the range of 200-400 kHz and a spring constant around 42 N/m. All samples were investigated at room

temperature open to the air. The contour length of single polymer molecule was determined by a home made software.

For dragging the molecules across the surface (lateral manipulation), a commercial SFM lithography program "Litho" (from Digital Instruments) based on the Multimode head and Nanoscope III controller was used. For the purpose of manipulation, the SFM can be gently switched from tapping mode to contact mode at predefined point while the tip is passing along the prededetermined trace. From the tip-molecule contact point, the interaction between SFM tip and sample is enhanced, and thus can be used to drag a molecule across the surface.

For blowing circular topologies, a droplet of chloroform liquid was additionally spin-coated at 40 rps onto the triblock molecules deposited on the HOPG surface for 20 sec. Then the sample was immediately scanned by SFM in tapping mode with scan rate of 4-5 lines/sec. Height and phase images were recorded while the blowing manipulation was performed.

References

[1] F. S. Bates, G. H. Fredrickson, *Ann. Rev. Phys. Chem.* **1990**, *41*, 525.

[2] F. S. Bates, G. H. Fredrickson, *Physics Today* **1999**, *52*, 32.

[3] I. W. Hamley, *The Physics of Block Copolymers*, Oxford University Press, Oxford, **2003**.

[4] N. Hadjichristidis, H. Iatrou, M. Pitsikalis, J. Mays, *Prog. Polym. Sci.* **2006**, *31*, 1068.

[5] N. Hadjichristidis, M. Pitsikalis, H. Iatrou, *Adv. Polym. Sci.* **2005**, *189*, 1.

[6] F. E. Alemdaroglu, A. Herrmann, *Org. Biomol. Chem.* **2007**, *5*, 1311

[7] J. H. Jeong, T. G. Park, *Bioconjugate Chem.* **2001**, *12*, 917.

[8] C. E. Immoos, S. J. Lee, M. W. Grinstaff, *J. Am. Chem. Soc.* **2004**, *126*, 10814.

[9] M. D. Costioli, I. Fisch, F. Garret-Flaudy, F. Hilbrig, R. Freitag, *Biotechnol. Bioeng.* **2003**, *81*, 535.

[10] F. E. Alemdaroglu, M. Safak, J. Wang, R. Berger, A. Herrmann, *Chem. Commun.* **2007**, 1358.

[11] R. K. Saiki, D. H. Gelfand, S. Stoffel, S. J. Scharf, R. Higuchi, G. T. Horn, K. B. Mullis, H. A. Erlich, *Science* **1988**, *239*, 487.

[12] K. B. Mullis, *Angew. Chem. Int. Ed.* **1994**, *33*, 1209.

[13] H. Ahern, *Scientist* **1996**, *10*, 18.

[14] D. Pomp, J. F. Madrano, *BioTechniques* **1991**, *10*, 58.

[15] J. Sambrook, D. W. Russel, *Molecular Cloning*, Cold Spring Harbour Laboratory Press, New York, **2001**.

[16] Z. Li, Y. Zhang, P. Fullhart, C. A. Mirkin, *Nano Lett.* **2004**, *4*, 1055.

[17] F. E. Alemdaroglu, K. Ding, R. Berger, A. Herrmann, *Angew. Chem. Int. Ed.* **2006**, *45*, 4206.

[18] K. Ding, F. E. Alemdaroglu, M. Börsch, R. Berger, A. Herrmann, *Angew. Chem. Int. Ed.* **2007**, *46*, 1172.

[19] W. Saenger, *Principles of nucleic acid structure*, Springer-Verlag, New York, **1984**.

[20] C. Rivetti, M. Guthold, C. Bustamante, *J. Mol. Biol.* **1996**, *264*, 919.

[21] L. Shu, A. D. Schlüter, C. Ecker, M. Severin, J. P. Rabe, *Angew. Chem. Int. Ed.* **2001**, *40*, 4666.

[22] M. Severin, J. Barner, A. A. Kalachev, J. P. Rabe, *Nano Lett.* **2004**, *4*, 577.

[23] N. Severin, W. Zhuang, C. Ecker, A. A. Kalachev, I. M. Sokolov, J. P. Rabe, *Nano Lett.* **2006**, *6*, 2561.

[24] S. B. Smith, Y. J. Cui, C. Bustamante, *Science* **1996**, *271*, 795.

[25] H. Clausen-Schaumann, M. Seitz, R. Krautbauer, H. E. Gaub, *Curr. Opin. Chem. Biol.* **2000**, *4*, 524.

[26] D. Bensimon, A. J. Simon, V. Croquette, A. Bensimon, *Phys. Rev. Lett.* **1995**, *74*, 4754.

[27] M. Grandbois, M. Beyer, M. Rief, H. Clausen-Schaumann, H. E. Gaub, *Science* **1999**, *283*, 1727.

6 Dendritic Nanopatterns from DNA-Diblock Copolymers

"There is plenty of room at the bottom"

Prof. Richard Feynmann, a visionary talk in 1959

DNA has been employed as the skeleton of 2D- and 3D-nanostructures[1-4] and has served as an interconnect or template to form DNA-hybrid-nanostructures with other materials.[5-9] Applications of DNA thereby range from new nucleic acid detection strategies[10] to nanoelectronic and nanomechanical structures and devices.[8, 11, 12] A combination of synthetic ODNs and organic polymers, as one class of DNA-hybrid-structures, consisted of graft polymers containing a polypyrrole [13-16] or a polynorbonene[17] backbone to which a number of synthetic ODNs were attached. Some of these systems were used for the development of amperometric DNA detection methods.[13-16, 18] In contrast to this graft polymer architectures, only two linear block polymer topologies containing DNA are known.[19, 20] A PLGA was chain end-coupled to an amine-terminated ODN, coding for *c-myc* antisense. This amphiphilic diblock structure could form micelles in the aqueous phase, which were applied as vectors for antisense ODNs.[19] The second linear DNA diblock copolymer consisted of an ODN and a PS-fragment. Micelles formed in aqueous solution from these amphiphilic polymers were utilized as a DNA detection system in combination with DNA-coated gold nanoparticles.[20]

Although the preparation of DNA-PS diblock copolymers is known, a novel facile synthesis of these materials was presented in *Chapter 3*. Surface-mediated self assembly of these biological-organic hybrid structures was then investigated by scanning force microscopy. Depending on the molecular weight of the PS-fragment, various nanostructures have been observed. In particular, it is noteworthy that some of the diblock copolymers containing single stranded DNA form dendritic nanostructures consisting of rectilinear fibers and represent a novel class of 2D-nanosized materials.

Besides their chemical characterization, the morphological behavior of the DNA-b-PS polymers **11a, b, c** were investigated on different substrates. Surface analytical techniques such as SFM are widely used to probe the topography properties of molecularly thin layers. In particular, SFM is a well established tool for the investigation of block copolymer systems[21-23] because different structural phases could be identified on the nanoscale. DNA-PS diblock copolymers **11a-c** were dissolved in water and formed a transparent solution. After drop casting onto silicon or mica and allowing the samples to dry under ambient conditions for two days, imaging of the surface structures was carried out by tapping mode SFM in collaboration with *Dr. D. Ke* in the group of *Prof. Dr. H. J. Butt*.

For the diblock copolymer **11a**, four different kinds of structures were visualized on a silicon wafer depending on the surface processing conditions (**Figure 6.1 and 6.2**): spherical micelles, fibers, leaf-like structures, and continuous layers. Spherical micelles with a hydrophobic PS core and a hydrophilic DNA corona were formed when the drop casted DNA-b-PS films were annealed at 100°C for 12 h. The average height of the micelles is 10.88 ± 1.36 nm. For the other structures different processing conditions were applied. The samples were drop casted and allowed to evaporate for 2 d. at 25°C. The fibers, which in some cases were curved and crossed, appeared singly separated (I), as bundles (II), or as stacks of bundles (III). The height and width of single fibers were measured as 3 nm and 50 nm, respectively. In the case of fiber bundles, the mean distance between the fibers is around 50 nm. The leaf-like structures (IV) showed no preferential orientation and covered on average an area of 0.2 to 2.5 μm^2. In an area of 400 μm^2, 20 leaf-like structures consisting of shorter fiber bundles were observed, resulting in a density of 0.05 μm^{-2}. The height of these structures is typically 10 nm decreasing at the end of the branches to 5 nm. This indicated that fibers were stacked in layers. The fibers and leaf-like structures bordered the thin continuous layers (V), which exhibited a height between 1.5 and 7 nm. Continuous layers were not detected without the presence of the other structures, which is evidence that the material in these areas could be the resource of fibers and leaf-like structures.

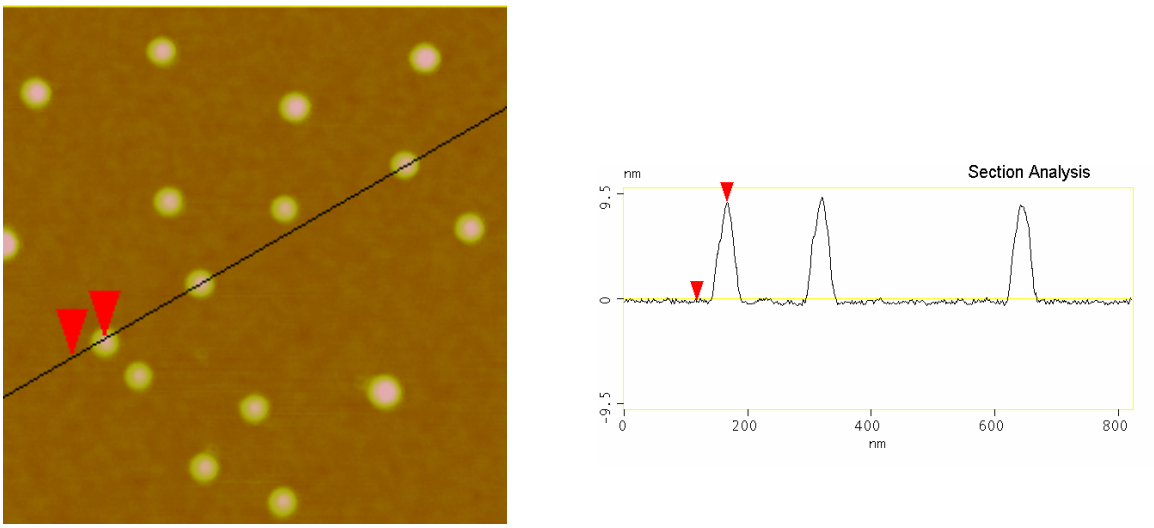

Figure 6.1 *SFM height images of DNA-b-PS with a PS segment of 5500 g/mol.*

Structures I-IV are attributed to the formation of cylindrical micelles. The micelles aggregated into bundles or leaf-like structures which were flattened upon solvent evaporation. This resulted in a vertical deformation of the cylindrical shape. Previously, primarily spherical micellar morphologies were detected for DNA-PS block copolymer morphologies. Occasionally, rod-like structures within these samples were found.[20] The different phase behavior of **11a** is likely influenced by the sample preparation, the surface, the length of the DNA fragment, as well as the sequence that varied significantly from that presented here.

In contrast to the DNA-PS block copolymer DNA-*b*-PS(5K), **11b** exhibited unique highly branched dendron structures (**Figure 6.3 a**) with random orientations on the silicon surface. The structures were prepared according to the following conditions. Briefly, 50 µl drop from 2 OD concentrated sample was placed on top of untreated silicon or a freshly cleaved mica substrate. Then, the substrate was placed inside a Petri dish allowing the drop to evaporate slowly (ambient temperature 23 °C, humidity inside the Petri dish 80%). After 5-6 h, the drop evaporated and the resulting samples were investigated by SFM. 245 of such structures were detected in an area of 6.400 μm^2 resulting in a density of 0.038 μm^{-2}. Single dendrons have a lateral extension of 1 to 10 μm^2. The shape of the dendritic structures suggests that their growth began at single sites (**Figure 6.3a**, pentagons). In the shown SFM images, two dendron structures were formed from two origins separated by approximately 1 µm. The dendrons consisted of straight fibers, which upon branching resulted in ramified structures (**Figure 6.3a**, squares).

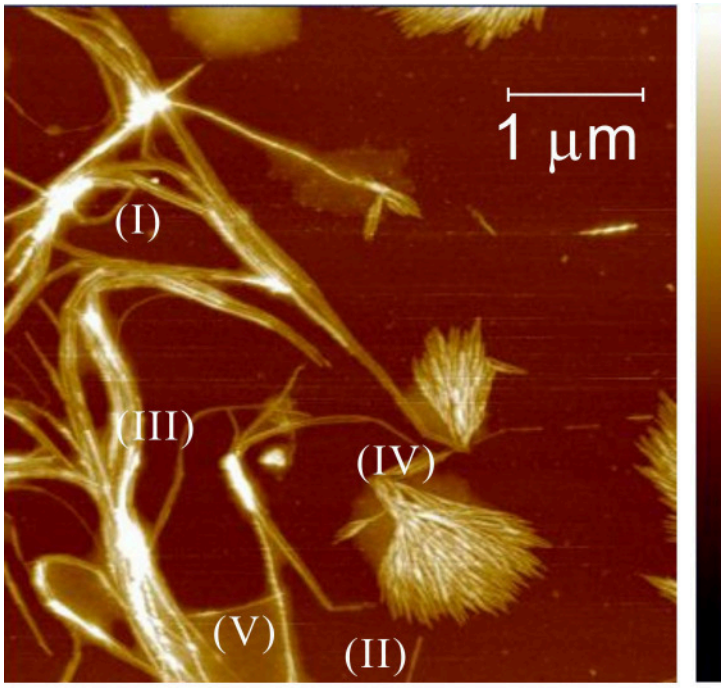

Figure 6.2 *SFM topographical image with color scale bar on the right. The z-scale in this image is 25 nm. (I)-(V) represent typical structures of the DNA-PS block copolymers 11a, on silicon.*

Droplets were sometimes visible at the ends of the branches (**Figure 6.3a**, circles), which exhibited a height between 7 and 16 nm. The dendritic structure was imaged at higher resolution in **Figure 6.3b**. Individual, parallel lamellae consisting of up to 9 single rods were formed. From a cross sectional analysis, the distance between neighboring lamellar rods was measured to be 13 nm (**Figure 6.3c**). The height above the substrate surface was 5 nm. The branch angles in **Figure 6.3b** are displayed in a histogram resulting in a peak value of 135° (**Figure 6.3d**). At the ends of the dendritic rod structures, more branches occurred and the distance between branching points decreased. At nanometer resolution, two additional features were detected. First, along individual rods, kinks within the fibers occurred. Those structural elements are marked by triangles. Second, the dendritic structures were self-avoiding, since crossing of branches was detected only rarely.

Also for the block copolymer DNA-*b*-PS(50K) on silicon and on mica, dendritic structures comparable to those of **11b** were obtained (**Figure 6.4**). They exhibited directional growth and covered surface areas of typically 7 μm^2. The height of the dendritic structures was 4 nm.

The width of an individual rod as well as the periodicity between neighboring rods was measured to be 12 nm. As detected for **11b**, at some positions of the rectilinear fibers of **11c**, kinks were observed in the otherwise self-avoiding, nanosized, dendritic surface pattern. A geometric analysis of the angles of the branches resulted in a peak value of 136°, which is very close to that of **11b**.

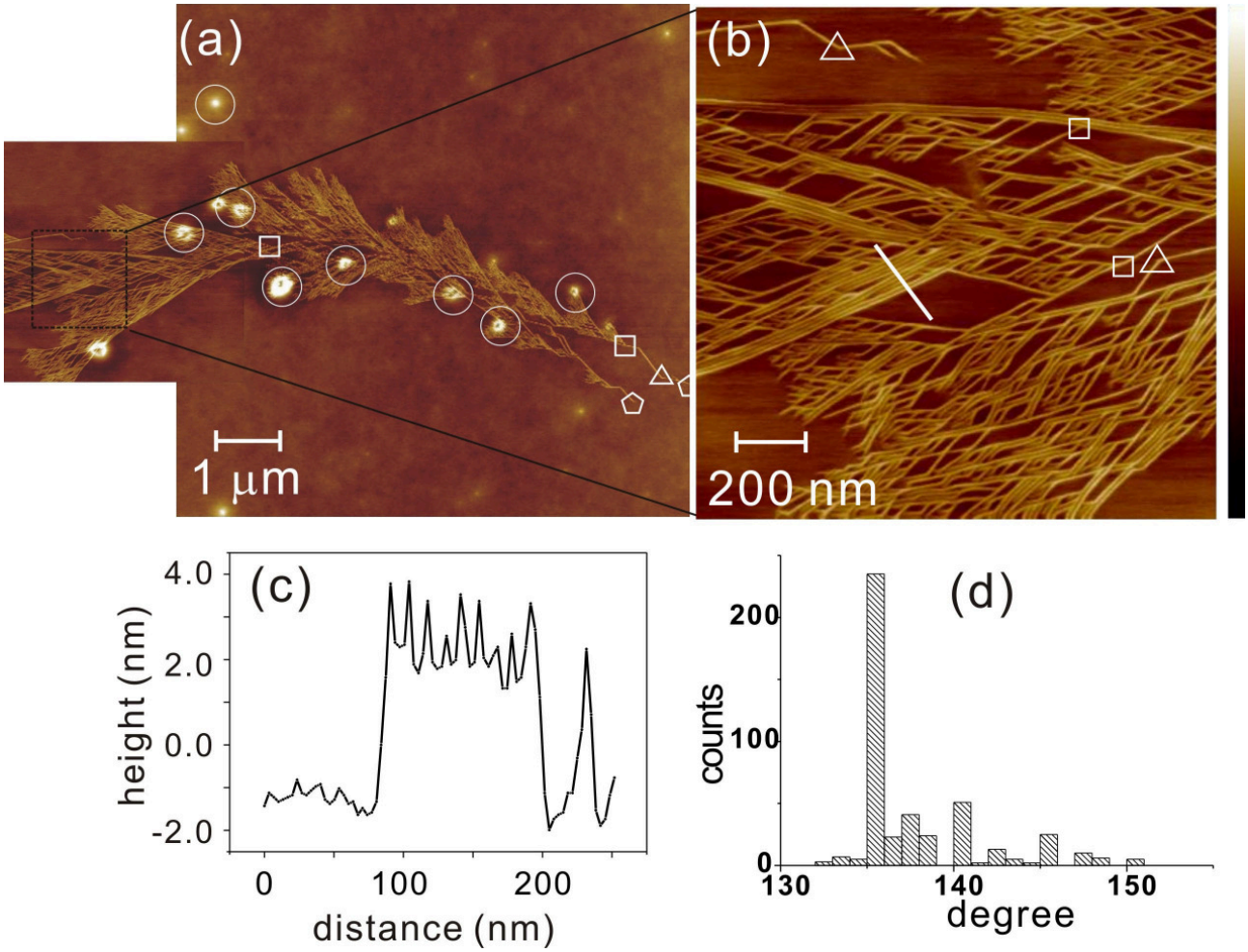

Figure 6.3 *(a)-(b) SFM topography images of a **11b** DNA-PS block copolymer on silicon. The z-scale of both images is 15 nm. (c) The cross section along the indicated line from (b). The width of the side by side packed 9 rods is 113 nm. (d) The histogram of branch angles as imaged in (b).*

Dendritic structures, arising from ultra-thin films of polymers on inorganic substrates, have been observed for poly(ethylene glycol),[24-26] poly(ethylene terephthalate), [27, 28] and PS,[29, 30] which is also one integral part of the diblock architectures described herein. Diffusion-limited

aggregation is a generally accepted model to explain the origin of such fractal morphologies which appear far away from thermodynamic equilibrium.[31] However, the DNA-PS block copolymers **11b** and **11c** exhibited some remarkable differences concerning their surface topologies compared to the polymers mentioned above. The rectilinearity of the nanosized dendritic framework, the discrete bending without the appearance of branching, and the unidirectional propagation of the dendrons have not been previously observed and were exclusively characteristic for surface morphologies of polymers **11b** and **11c**.

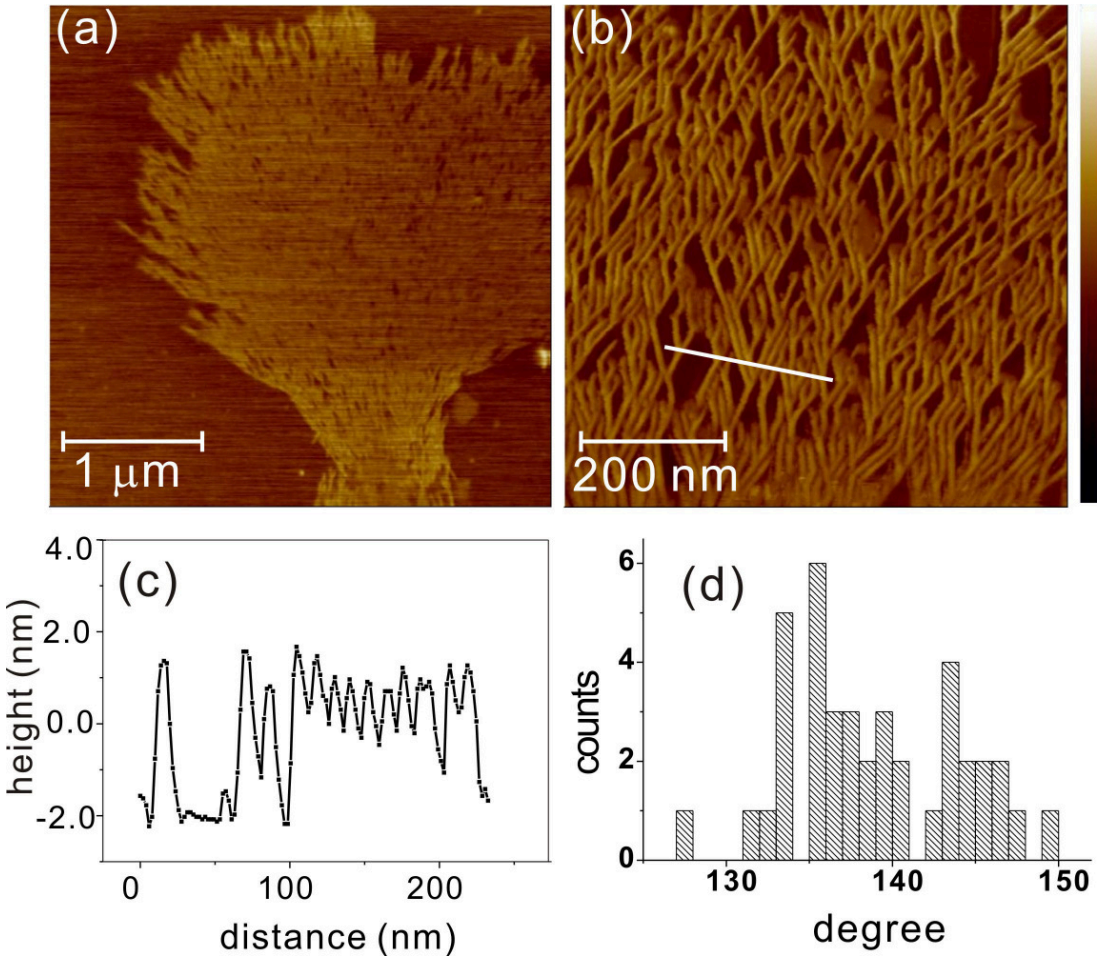

Figure 6.4 *(a)-(b) SFM topography images of a* ***11c*** *DNA-PS block copolymer on silicon. The z-scale of both images is 15 nm. (c) The cross section along the sketched line from (b). (d) The histogram of branch angles as imaged in (b).*

The straight morphologies did not appear to be induced by any templating effect of the underlying substrate. For poly(ethylene oxide), alignment of branched topologies was

achieved on alkali halide substrates through the underlying crystal lattice.[32] For polymers **11b** and **11c**, such an effect could be excluded; instead the rectilinear patterns as well as the kinking must be an intrinsic property of the materials. If the diffusion limited aggregation model is valid for the DNA-PS block copolymers, the unidirectional growth could be explained by the geometry of the polymers. Rod-like particles were assumed to form a two-dimensional pattern with only one growth direction.[33] The surface area coverage of the herein described structures was comparable to those obtained for other 2D nucleic acid arrays such as DNA double-crossover molecules,[3] DNA triple crossover complexes,[34] and DNA Holliday junctions.[35]

In conclusion, a simple preparation method for DNA-PS diblock copolymers was presented, with the possibility of obtaining the ODN from commercial sources. Three different block polymers **11a-c** with varying sizes of the PS-fragment ranging from 5500 to 56000 g/mol were synthesized by coupling the ODN and the PS block in solution. The morphologies of the DNA block copolymers were characterized on different substrate surfaces by SFM. For the DNA diblock copolymer DNA-*b*-PS(5K), depending on the processing conditions different nanostructures were obtained. Annealing at higher temperatures generated spherical micelles on a silicon surface, however, sample preparation at ambient conditions resulted bundles of fibers and leaf-like structures. For block copolymers **11b** and **11c** with higher molecular weights, novel microscale DNA arrays with nanoscale features were discovered. Dendritic architectures were observed on silicon as well as on mica substrates. It should be noted that structure formation originates from driving forces other than conventional Watson-Crick base pairing. Salient features of this novel class of 2D materials covering surface areas of several square micrometers are the straightness and periodicity of the nanoscopic dendritic patterns, bending of rectilinear topologies, and the unidirectional growth of dendrons. Future studies will be directed towards the origin and the growth process of these morphologies as well as towards the application of these non-equilibrium structures for the construction of more sophisticated and complex nanostructures. As single stranded DNA is present in the dendritic structures, hybridization is a major feature of which can be taken advantage for further control over morphology and function.

Experimental Section

Sample preparations for SFM measurements. All investigated samples were prepared by drop casting. First, DNA-PS diblock copolymers **11a-c** were dissolved in Milli-Q type water at 0.5 – 2 OD to give transparent solutions. From this solution, a 50 µl drop was placed on top of untreated silicon or a freshly cleaved mica substrate. The route mean square (RMS) roughness of the silicon wafer was determined as 0.158 nm over an area of 0.7 μm^2. The substrate was placed inside a Petri dish allowing the drop to evaporate slowly (ambient temperature 23 °C, humidity inside the Petri dish 80%). After 5-6 h, the drop evaporated and the resulting samples were investigated by SFM. For the formation of spherical micelles with a hydrophobic PS core and a hydrophilic DNA corona, the drop casted DNA-b-PS films were annealed at 100°C for 12 h.

Scanning Force Microscopy. Samples were imaged in air at room temperature with a commercial SFM (Multimode equipped with a Nanoscope IIIa controller, Veeco Instruments, California) in tapping mode. Rectangular silicon cantilevers (Olympus, Japan; 160 µm long, 50 µm wide, 4.6 µm thick, a nominal spring constant of 42 N/m and a resonance frequency of 300 KHz) were used. The height of the tip is around 11 µm and the tip radius is nominally less than 10 nm. A piezoelectric scanner was used, which allows the recording of high resolution images at a maximum scan range of 12.5 µm and a maximal z-extension of 2.5 µm. To increase the z-resolution we operated the SFM with a z-limit of 500 nm. All images were captured as raw data and for display purposes the images are flattened by a first order plane fit.

References

[1] T. J. Fu, N. C. Seeman, *Biochemistry* **1993**, *32*, 3211.

[2] X. Li, X. Yang, J. Qi, N. C. Seeman, *J. Am. Chem. Soc.* **1996**, *118*, 6131.

[3] E. Winfree, F. Liu, L. A. Wenzler, N. C. Seeman, *Nature* **1998**, *394*, 539.

[4] M. Scheffler, A. Dorenbeck, S. Jordan, M. Wüstefeld, G. von Kiedrowski, *Angew. Chem. Int. Ed.* **1999**, *38*, 3312.

[5] C. A. Mirkin, R. L. Letsinger, R. C. Mucic, J. J. Storhoff, *Nature* **1996**, *382*, 607.

[6] A. P. Alivisatos, K. P. Johnsson, X. Peng, T. E. Wilson, C. J. Loweth, M. P. Bruchez, P. G. Schultz, *Nature* **1996**, *382*, 609.

[7] J. J. Storhoff, C. A. Mirkin, *Chem. Rev.* **1999**, *99*, 1849.

[8] K. Keren, R. S. Berman, E. Buchstab, U. Sivan, E. Braun, *Science* **2003**, *302*, 1380.

[9] C. M. Niemeyer, *Appl. Phys. A* **1999**, *69*, 119.

[10] T. A. Taton, C. A. Mirkin, R. L. Letsinger, *Science* **2000**, *289*, 1757.

[11] E. Braun, Y. Eichen, U. Sivan, G. Ben-Yoseph, *Nature* **1998**, *391*, 775.

[12] C. Mao, W. Sun, Z. Shen, N. C. Seeman, *Nature* **1999**, *397*, 144.

[13] H. Bazin, T. Livache, *Nucleosides Nucleotides* **1999**, *18*, 1309.

[14] G. Bidan, M. Billon, K. Galasso, T. Livache, G. Mathis, A. Roget, L. M. Torres-Rodriguez, *Appl. Biochem. Biotechnol.* **2000**, *89*, 183.

[15] H. Korri-Youssoufi, F. Garnier, P. Srivastava, P. Godillot, A. Yassar, *J. Am. Chem. Soc.* **1997**, *119*, 7388.

[16] T. Livache, B. Fouque, A. Roget, J. Marchand, G. Bidan, R. Teoule, G. Mathis, *Anal. Biochem.* **1998**, *255*, 188.

[17] K. J. Watson, S.-J. Park, J.-H. Im, S. T. Nguyen, C. A. Mirkin, *J. Am. Chem. Soc.* **2001**, *123*, 5592.

[18] D. J. Caruana, A. Heller, *J. Am. Chem. Soc.* **1999**, *121*, 769.

[19] J. H. Jeong, T. G. Park, *Bioconjugate Chem.* **2001**, *12*, 917.

[20] Z. Li, P. Fullhart, C. A. Mirkin, *Nano Lett.* **2004**, *4*, 1055.

[21] J. C. Meiners, A. Ritzi, M. H. Rafailovich, J. Sokolov, J. Mlynek, G. Krausch, *Applied Physics A* **1995**, *61*, 519.

[22] M. A. van Dijk, R. van den Berg, *Macromolecules* **1995**, *28*, 6773.

[23] A. Knoll, A. Horvat, K. S. Lyakhova, G. Krausch, G. J. A. Sevenik, A. V. Zvelindovsky, R. Magerle, *Physical Review Letters* **2002**, *89*, 35501.

[24] S. Nettesheim, D. Zeisel, M. Handschuh, R. Zenobi, *Langmuir* **1998**, *14*, 3101.

[25] G. Reiter, J.-U. Sommer, *J. Chem. Phys.* **2000**, *112*, 4376.

[26] M. Wang, H.-G. Braun, E. Meyer, *Macromol. Rapid Commun.* **2002**, *23*, 853.

[27] Y. Sakai, M. Imai, K. Kaji, M. Tsuji, *J. Cryst. Growth* **1999**, *203*, 244.

[28] Y. Sakai, M. Imai, K. Kaji, M. Tsuji, *Macromolecules* **1996**, *29*, 8830.

[29] K. Taguchi, H. Miyaji, K. Izumi, A. Hoshino, Y. Miyamoto, R. Kokawa, *J. Macromol. Sci. B* **2002**, *41*, 1033.

[30] K. Taguchi, H. Miyaji, K. Izumi, A. Hoshino, Y. Miyamoto, R. Kokawa, *Polymer* **2001**, *42*, 7743.

[31] T. A. J. Witten, L. M. Sander, *Physical Review Letters* **1981**, *47*, 1400.

[32] R. Kurimoto, A. Kawaguchi, *Journal of Polymer Science: Part B: Polymer Physics* **2002**, *40*, 2421.

[33] J. Parkinson, K. E. Kadler, A. Brass, *Physical Review Letters* **1994**, *50*, 2963.

[34] T. H. LaBean, H. Yan, J. Kopatsch, F. Liu, E. Winfree, J. H. Reif, N. C. Seeman, *J. Am. Chem. Soc.* **2000**, *122*, 1848.

[35] C. Mao, W. Sun, N. C. Seeman, *J. Am. Chem. Soc.* **1999**, *121*, 5437.

7 Engineering the Structural Properties of DNA Block Copolymer Micelles*

"At the nanoscale there is no difference between chemistry and physics, engineering, biology or any subset thereof."

Prof. Mauro Ferrari, 2006

In solution amphiphilic block copolymers self-assemble into a large variety of different morphologies. These include most commonly spheres, rods and vesicular assemblies.[1, 2] Occasionally, also lamellae, tubes, large compound vesicles, hexagonally packed hollow hoops, large compound micelles and onions were obtained.[3] In recent years, it has become a challenge to manipulate these morphologies in solution by different strategies. For a given block copolymer composition reorganization of the micelle architectures was achieved by changing the salinity as well as the solution pH,[4-6] the polymer concentration,[7, 8] and the solvent composition.[9-11] Other approaches to change the structures of block copolymer supramolecular assemblies include the in situ chemical modification of the polymers[12] and thermally-induced melting and crystallization.[13]

Recently, a new type of block copolymer materials, so called "molecular chimeras" or "hybrids", has emerged that beside the synthetic polymer component contain a biological segment which is either composed of an amino acid[14, 15] or ODN sequence.[16-18] Amphiphilic DNA block copolymers, like other polyelectrolyte block copolymers, form micelles of spherical shape in aqueous solution. These micelles with a corona of ss DNA were applied for the delivery of ASOs,[19] for the hybridization with DNA-coated gold

* Parts of this chapter were published in *Angew. Chem. Int. Ed.* **2007**, *46*, 1172-1175.

nanoparticles[20] and as programmable, three dimensional scaffolds for DNA-templated organic reactions.[21]

In this chapter, a new concept for engineering the association behaviour of block copolymers is introduced. Spherical DNA block copolymer micelles are hybridized with long ss DNA template molecules that encode multiple times the complementary sequence of the micelle corona. Upon this molecular recognition event the shape of the micelles changes from spheres to uniform rods (**Figure 7.1**). Even perfect control over the length of the rod aggregates is achieved by the template. The supramolecular reorganization process is visualized by SFM and is verified by measuring the dimensions of the different block copolymer aggregates by FCS in solution.

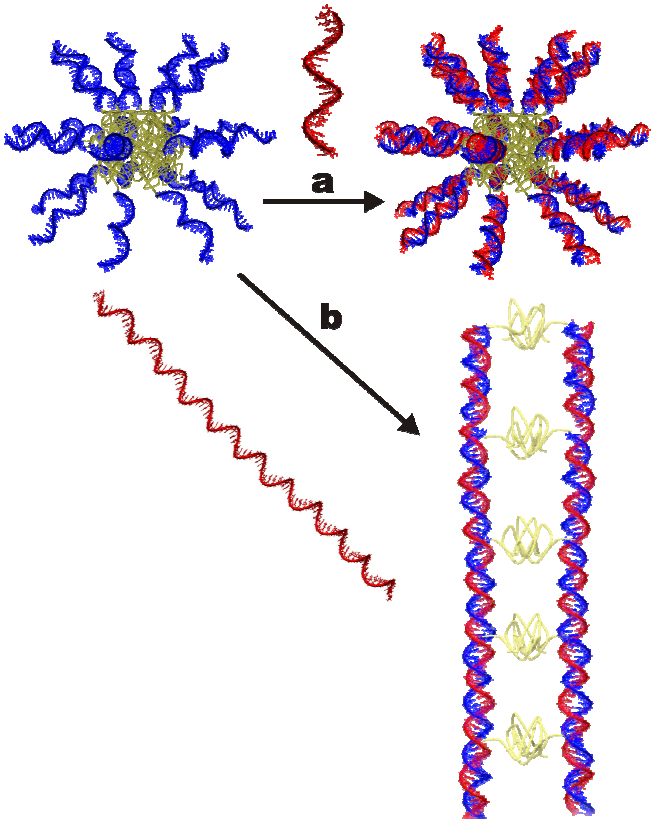

Figure 7.1 *Schematic representation of hybridization of ss DNA-b-PPO micelles with different DNA molecules. a) Base pairing with a short complementary sequence yields micelles with a ds corona maintaining the overall shape of the aggregates. b) Hybridization with long DNA templates results in rod-like micelles consisting of two parallel aligned double helices.*

The aim of this study was to explore how the structural properties of DNA block copolymer micelles can be altered by hybridization, transforming the ss nucleic acid shell of the micelles into ds DNA by employing Watson-Crick base pairing. For that purpose, DNA-*b*- PPO polymers were selected for the following reasons. Firstly, they can be produced in milligram quantities, fully automated in a single process using a DNA-synthesizer.[21] Secondly, the organic polymer block, PPO, exhibits a low glass transition temperature (T_G = -70°C). This guarantees that the block copolymers can be easily dissolved without using organic co-solvents and avoiding the subsequent dialysis. Moreover, the formation of kinetically trapped so called "frozen" micelles as they are known for block copolymers with a glassy hydrophobic domain is avoided allowing to study micelle aggregates at their thermodynamic equilibrium. A ss DNA-*b*-PPO polymer was synthesized as described previously in *Chapter 3*. The biological segment consists of a 22mer ODN (sequence: 5'-CCTCGCTCTGCTAATCCTGTTA-3') whereas the organic PPO block exhibits a molecular weight of 6.800 g/mol.

Micelles composed of this material were hybridized with its complementary sequence (5'-TAACAGGATTAGCAGAGCGAGG-3'). As a result, DNA block copolymer micelles were formed which contain a shell of ds DNA (**Figure 7.1a**). To investigate if hybridization with the complementary sequence influenced the structural features of the micelles, they were visualized by SFM in soft tapping mode in the hybridization buffer on a mica surface in collaboration with *Dr. D. Ke*. Although, the immobilization and the imaging process might alter the morphologies of the micelles, SFM has been proven a powerful tool to image amphiphilic DNA block copolymer aggregates.[19-21] Before and after double helix formation SFM topography images show spherical micelles (**Figure 7.2a** and **7.2b**). Histograms of the height distribution of the micelles before and after base pairing were compiled (**Figure 7.2c**). In both cases, the maximum height of the micelles ranged from 2 to 11 nm. A mean height value for ss micelles of 5.2 ± 1.8 nm (calculated from 117 micelles from 5 SFM pictures) was obtained. For ds micelles a mean height of 5.8 ± 1.6 nm was determined (calculated from 116 micelles from 9 SFM images).

The SFM measurements suggest that hybridization of ss DNA block copolymer micelles with the complementary sequence does not change the overall shape of the spherical aggregates. The deviations in the mean heights of ss and ds micelles might result from different charge

densities in the corona and micelle deformations induced by variations in the adjusted soft tapping mode parameters.

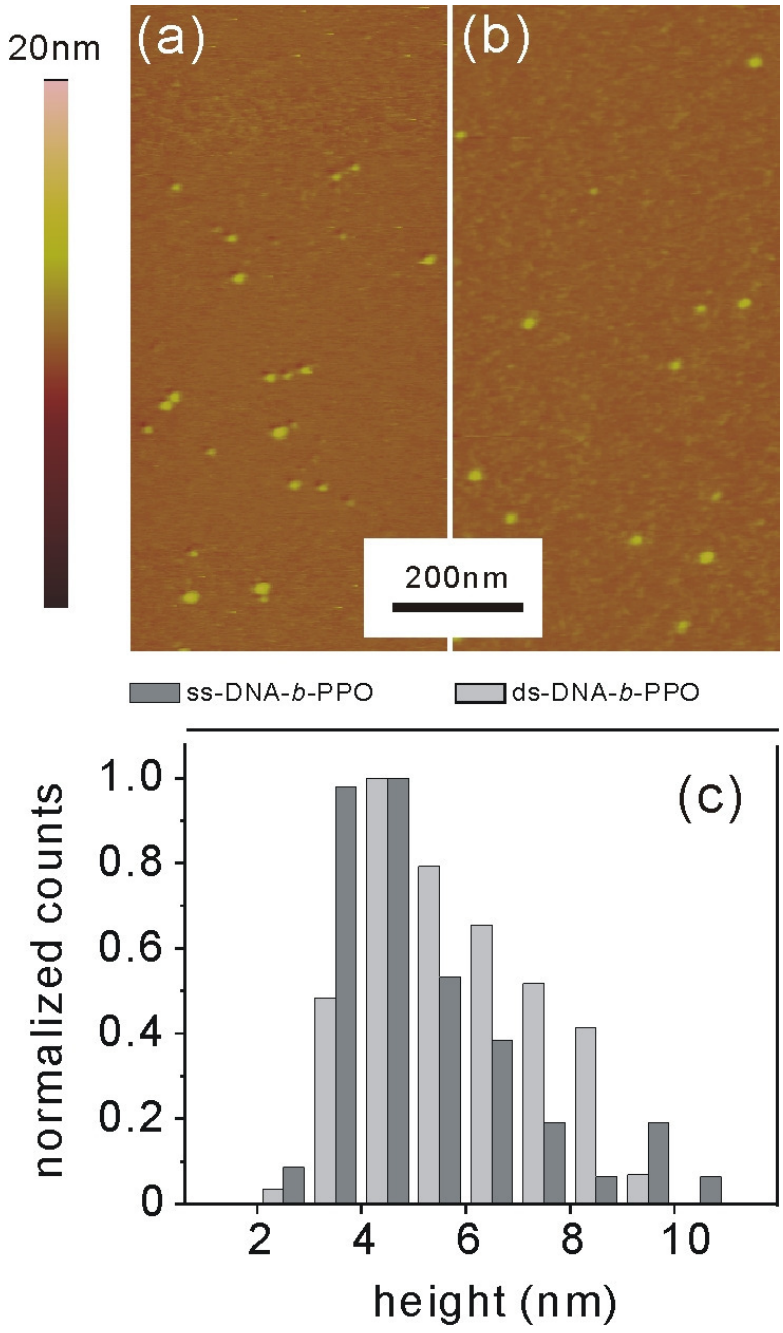

Figure 7.2 *SFM images of spherical DNA-b-PPO micelles before a) and after b) hybridization with a short complementary sequence. c) Height profiles of spherical ss and ds DNA-b-PPO micelles. The height is indicated with a color scale bar on the left. The z-scale in the images is 20 nm.*

To exclude also surface effects, it is necessary to investigate the structural properties of the micelles in solution. For that reason, FCS experiments with ss and ds micelles were carried out. This required labelling of the micelles by hybridization applying ODNs functionalized with a fluorescent dye (Alexa-488).

FCS is an ultrasensitive analysis method[22] that is generally used to monitor binding affinities of fluorescence-labelled biomacromolecules. For instance DNA hybridization events have been detected at the single-molecule level.[23] Furthermore, FCS has been employed to detect conformational transitions of enzymes[24] or polymers[25] by changes in the diffusion properties. The transit times of the freely diffusing fluorescent micelles through the excitation volume of 4.5 fl were measured in buffer using a confocal microscope setup.[26] The translational diffusion coefficients D were calculated from the mean diffusion times. As the diffusion coefficient D is related to the frictional coefficient f of the hydrated micelles, the shape information of the immobilized DNA block copolymer aggregates could be used to calculate the radius r_0 for the spherical micelles from the FCS diffusion data (see Experimental Section). This measurement was carried out by *Dr. M. Börsch* from University of Stuttgart. A mean radius of 5.6 ± 0.5 nm was found for the ss DNA micelles. The radius of the ds DNA micelles was 5.3 ± 0.5 nm. These values are in good agreement with the AFM measurements since they confirm similar dimensions for ss and ds micelles. Moreover, it can be concluded from the FCS data that upon immobilization, the micelles are flattened owing to the interaction with the surface and/or the SFM imaging process.

After hybridization of ss micelles with the complementary sequence, the changes of the morphology of the DNA block copolymer assemblies were investigated employing long DNA molecules. The sequence of these templates was chosen so that they encode several times the complementary sequence of DNA-*b*-PPO. On the template T110 (sequence: 5'-$(TAACAGGATTAGCAGAGCGAGG)_5$-3') and T88 (sequence: 5'-$(TAACAGGATTAGCAGAGCGAGG)_4$-3'), five and four DNA-*b*-PPO polymers can be annealed, respectively. For the hybridization experiments, the ratios of block copolymers to long DNA molecules were adjusted so that the templates were completely hybridized. The resulting structures were visualized by SFM on a mica surface. For the DNA-*b*-PPO-T110 hybridization product, no spherical objects were detected anymore. Instead, rod-like structures were observed (**Figure 7.3a**). Histograms of the height distribution of the rod-like objects were compiled which revealed an average height of 1.95 ± 0.1 nm (**Figure 7.3c**). Most

of the rods measured exhibited a length of 37 ± 1 nm. The shape and the dimensions of these structures is consistent with the model shown in **Figure 7.1b**. Upon hybridization, disintegration of the spherical ss DNA block copolymer micelles occurs and DNA-*b*-PPOs are organized in a linear fashion along the template molecule. Thereby, the nucleic acid segment of the DNA block copolymer is involved in forming the double helix with the template while the hydrophobic blocks stick out of the ds DNA. To minimize the hydrophobic contacts of the PPO with the aqueous environment, dimerization of two of these DNA-PPO hybrids occurs in most cases (**Figure 7.3b**) and rod-like micelles are formed. The parallel alignment of two double helices can be proven by a cross sectional analysis perpendicular to the long axis of the assembly (**Figure 7.3d**). On average the two DNA molecules are separated by 4.5 nm. The height of the rod-like aggregates is in very good agreement with values that have been obtained previously for ds DNA.[27] The length of the rod-like micelles corresponds very well with the length of ds DNA exhibiting the same number of nucleotides as present in the template T110 (37.4 nm) when assuming a contribution of 0.34 nm per bp.

Two different control experiments were carried out. On the one hand, DNA-*b*-PPO micelles were incubated with a 110mer ODN that did not show any sequence complementarity with that of the micelles. As a result the structural properties of the spherical micelles remained unchanged. On the other hand, the template T110 was hybridized with a non-polymer-modified ODN encoding the complementary sequence of the micelles. By SFM the expected ds DNA molecules were detected but no dimer formation occured.

To prove that in general spherical DNA block copolymer micelles can be transformed into amphiphilic rods using long DNA templates, DNA-*b*-PPO was hybridized with T88. Again, SFM analysis revealed the disappearance of spherical micelles and the formation of rod-like structures consisting of two parallel aligned double helices exhibiting a length of 30.4 ± 1.0 nm and a height of 1.72 ± 0.2 nm (Experimental Section). The longitudinal extension fits very well the theoretically expected value for ds DNA containing 88 nucleotides (29.9 nm).

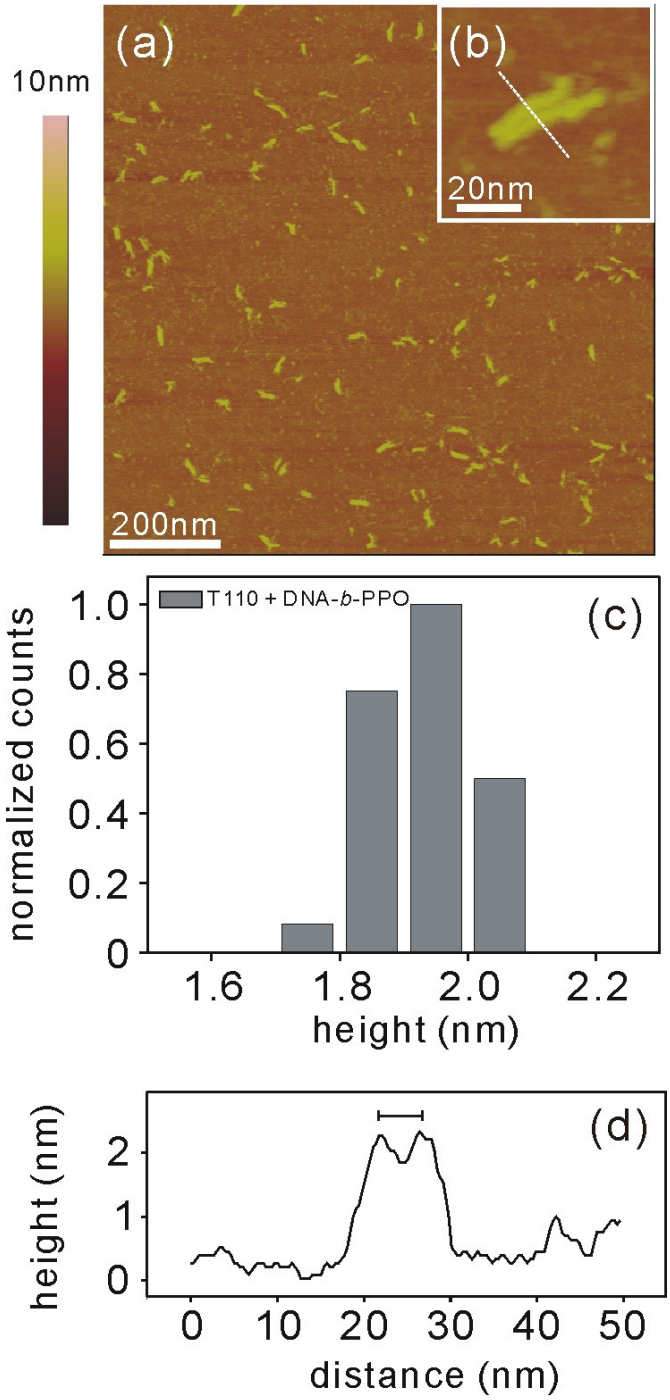

Figure 7.3 *a) SFM topography image of the hybridization products of DNA-b-PPO and T110. b) Close-up of a rod-like micelle consisting of two DNA helices arranged parallel to each other forming a dimer. c) The height of the rod-like aggregates was expressed in a histogram. d) The cross section along the indicated line from (b).*

The SFM results were again complemented by FCS experiments to prove the formation of rod-like micelles also in solution. For that purpose, spherical ss DNA block copolymer

micelles were hybridized with T110 templates carrying a fluorophore (Cy3). As a control, the labelled template T110 was hybridized with the DNA sequence present in DNA-*b*-PPO but without polymer attachment which results in the formation of a ds DNA molecule.

The shapes of the dimer DNA-rods and the ds DNA controls were investigated in buffer solution by diffusion measurements. Similar to the spherical micelles, the frictional coefficient f_{rod} of rod-like micelles is related to an effective radius of these objects. Using the measured aspect ratio P_{dimer} = 8.8 of the dimer and P_{DNA} = 19 of the ds DNA molecule, the diffusion times were predicted to increase by a factor of 1.3 from the control to the amphiphilic DNA dimer aggregate (Experimental Section).

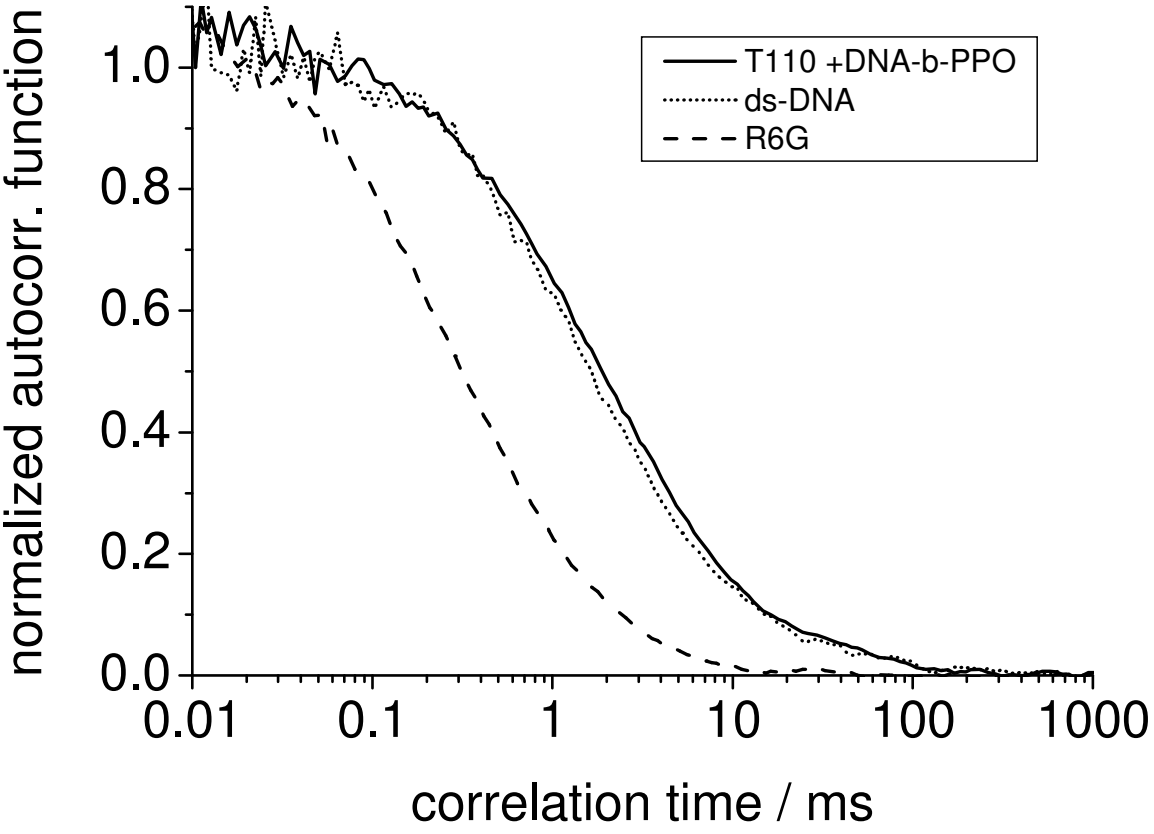

Figure 7.4 *Normalized autocorrelation functions of the hybridization products of DNA-b-PPO and T110 in solution (solid line), the ds-DNA from T110 and oligonucleotides as the control (dotted line), and rhodamine 6G in water (dashed line) as the reference.*

In **Figure 7.4** the autocorrelation functions of the dimers and the ds DNA controls are shown with mean diffusion times of τ_D = 1.9 ± 0.1 ms for the DNA-*b*-PPO-T110 hybridization products and τ_D = 1.47 ± 0.1 ms for the controls. The diffusion time ratio of 1.29 strongly supports the expectation that the rod-like properties of the hydrated dimers and of the ds DNA molecule are also maintained in solution. Usually, the superstructures of block copolymers are controlled by the primary sequence of monomers along the polymer chain. The parameters which even allow to predict the structural features of block copolymer aggregates are the block length ratio and the absolute length of the polymers.[28] Herein, a conceptually new approach for selectively manipulating the structural features of polyelectrolyte block copolymer micelles has been presented, which relies on molecular recognition. While hybridization of DNA block copolymer aggregates with short DNA has no significant impact on the structural properties, base pairing with long DNA templates induced a transformation from spherical into rod-like micelles. The Watson-Crick motif aligned the hydrophobic polymer segments along the DNA double helix, which resulted in selective dimer formation. Even the length of the resulting rod-like micelles could be precisely adjusted by the number of nucleotides of the templates. Characteristics of this novel strategy are the sequence specificity and the structural uniformity of the resulting micelle aggregates. This study, for the first time, demonstrates that DNA nanostructures, which are usually generated using base pairing of complementary ss ODN sequences,[29-31] can be built up employing hydrophobic interactions adding a new tool to the field of DNA nanotechnology in respect to structure formation.

Experimental Section

I. Material Preparation

General Hybridization Procedure

The hybridization was carried out by dissolving ss DNA-*b*-PPO diblock copolymer and the complementary strand or the long ss DNA templates, T110 and T88, in TAE buffer (20 mM tris(hydroxymethyl)aminomethane-HCl, pH 8.0; 10 mM acetic acid, 0,5 mM EDTA) containing Na^+ (100 mM) and Mg^{2+} (60 mM). The mixture was heated to 95°C and was slowly cooled to room temperature over the course of 3 days (1 degree per hour) by using a Biometra PCR thermocycler (Biometra GmbH, Germany). The final concentration of DNA was between 2-5 μM.

Material Preparation for FCS Experiments

ss DNA-*b*-PPO: Ss DNA-*b*-PPO micelles were hybridized with the complementary sequence which was functionalized with Alexa488 (Invitrogen, USA) at the 5' end. The ratio of ss DNA-*b*-PPO to ODN carrying the dye was adjusted to be 1 % so that the predominant form of DNA within the corona remains single stranded.

ds DNA-*b*-PPO: ss DNA-*b*-PPO was first hybridized with the dye as described above, then they were completely hybridized with the complementary sequence to obtain double stranded micelles.

DNA-*b*-PPO-T110: ss DNA-*b*-PPO was hybridized with equimolar amounts of Cy3 modified T110. The final dye concentration was 1 μM.

DNA-*b*-PPO-T88: ss DNA-*b*-PPO was hybridized with equimolar amounts of Cy3 modified T88. The final dye concentration was 1 μM.

DNA Sequences:

ss DNA-*b*-PPO: 5'-CCTCGCTCTGCTAATCCTGTTA-3'

Complementary: 5'-TAACAGGATTAGCAGAGCGAGG-3'

T110 : 5'- $(TAACAGGATTAGCAGAGCGAGG)_5$-3'

T88 : 5'- $(TAACAGGATTAGCAGAGCGAGG)_4$-3'

II. FCS Measurements

FCS measurements were carried out on a confocal setup of local design based on an Olympus IX71 inverted microscope. The 488 nm line of an argon ion laser (model 2020, Spectra Physics) was attenuated to 150 µW before focussing into the buffer solution by a water immersion objective (40 x, N.A. 1.15, Olympus). The solution was placed on a microscope coverslide as a droplett of 25 to 50 µl. Scattered laser light was blocked by a dichroic beam splitter (DCXR 488, AHF, Tübingen, Germany), and fluorescence was collected in the spectral range from 532 to 570 nm using interference filters (AHF). Single photons were detected by an avalanche photodiode (SPCM AQR-14, Perkin Elmer) and registered by a TCSPC device (PC card SPC-630, Becker & Hickl, Berlin, Germany) for software calculation of the autocorrelation functions, or by a real time hardware correlator (PC card ALV-5000 E, ALV, Langen, Germany).

The fluorescence intensity autocorrelation functions, $G(\tau_c)$, were fitted with a single diffusion time, τ_D, for the sample according to

$$G(\tau_c) = 1/N_f\,[1/(1 + \tau_c/\tau_D)]\,[1/(1 + (\omega/z)^2(\tau_c/\tau_D))]^{1/2}[1 - T + T\exp(-\tau_c/\tau_T)] \qquad \textbf{(Equation 7.1)}$$

with N_F, average number of fluorescent molecules in the confocal detection volume, τ_c, correlation time, ω/z, the ratio of the $1/e^2$ radii of the detection volume in radial and axial directions, T, average fraction of fluorophores in the triplet state, and τ_T, lifetime of the triplett state of the fluorophore. The ω/z was measured with a R6G solution as the reference and was kept fixed at this value during the subsequent fitting of the autocorrelation functions of the DNA-PPO micelle solutions (**Figure 7.5**).

The diffusion coefficient, D, is related to the diffusion time by

$$\tau_D = \omega^2 / 4D \qquad \textbf{(Equation 7.2)}$$

and to the frictional coefficient, f_{sphere}, of a sphere with radius R_0 by

$$f_{sphere} = kT / D = 6\pi\eta R_o \qquad \textbf{(Equation 7.3)}$$

which allows for the calculation of the radii of the spherical micelles.

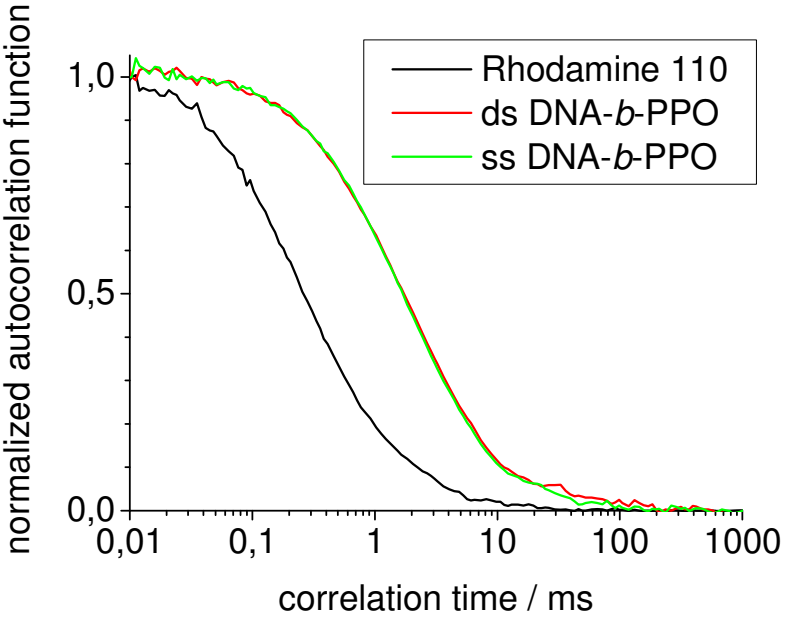

Figure 7.5 *Normalized autocorrelation functions of the DNA-b-PPO micelles in buffer solutions with an ss DNA corona (green curve), and with a ds DNA shell (red curve). As a reference Rhodamine 110 in water (black curve) was measured.*

Extrapolation of the diffusion times from the rod-like structures measured by AFM

The parallel-aligned dimers of the DNA-PPO hybrids on the T110 template can be treated as a cylinder of length $a/2$ and radius b. The volume, V_{dimer}, of the rod is

$$V_{rod} = 2\pi\, a\, b^2 \qquad \textbf{(Equation 7.4)}$$

which corresponds to a hypothetical spherical Volume with an apparent radius, R_0,

$$R_0 = (1.5\, a\, b^2)^{1/3} \qquad \textbf{(Equation 7.5)}$$

The axial ratio of length and radius of the cylinder, P, is:

$$P = a / b \qquad \textbf{(Equation 7.6)}$$

The frictional coefficient f_{rod} of the cylinder is related to the apparent radius R_0 and the axial ratio P by

$$f_{rod} = 6 \pi \eta R_0 [(2/3)^{1/3} P^{2/3}]/[\ln (2P) - 0.30] \qquad \textbf{(Equation 7.7)}$$

with η, viscosity of the solvent.
The frictional coefficient is related to the diffusion time τ_D combining (**Equation 7.2**) and (**Equation 7.3**) to

$$f_{rod} = \tau_D (4 kT / \omega^2) \qquad \textbf{(Equation 7.8)}$$

with ω, radial $1/e^2$ radius of the detection volume in the FCS measurements.

Accordingly the expected ratio of the diffusion times for the aggregates of the hybridization products DNA-*b*-PPO-T110 to ds T110 was calculated using the AFM structural information. For the DNA-*b*-PPO-T110 the length of the rod resulted in *a* = 18.5 nm, a mean radius of *b* = 2.1 nm and an axial ratio of P = 8.8 which yielded $V''_{rod} = \pi$ 82 nm^3 and R_o'' = 4.965 nm. The frictional coefficient was f'' = 6πη 4.965 nm 1.45 = 6πη 7.199 nm. For the controls we used a = 18.5 nm, b = 0.975 nm and P = 19 yielding $V'_{rod} = \pi$ * 35 nm^3 and R_o' = 2.977 nm. The frictional coefficient was calculated to f' = 6πη 2.977 nm 1.864 = 6πη * 5.481 nm.
The relative diffusion time changes predicted from the AFM structure resulted in a factor $\tau_{D,dimer}/\tau_{D,controls}$ = 1.298 for the T110-associated DNA-PPO and for the T110 controls.

However, if we assume that the dimeric rods would have a doubled hydrodynamic volume, the expected ratio of the diffusion times should be $\tau_{D,\,dimer} / \tau_{D,\,controls}$ = 1.26 which is also in good agreement with the FCS data.

III. SFM Measurements

AFM imaging of DNA block copolymers in buffer

A drop of 20 µl block copolymer buffer solution (10 mM Tris-HCl pH 7.4, 1 mM $NiCl_2$) was deposited on freshly cleaved mica (Plano GmbH, Germany) and left to incubation for 5 min. Then the surface was washed with 200 µl buffer solution and mounted onto a piezoelectric E-scanner (Veeco Instruments, California). In particular we ensured that the sample was always kept wet during the sample handling. Imaging was performed under tapping mode AFM in a liquid cell on a Multimode Nanoscope IIIa (Veeco Instruments, California USA). Oxide-sharpened silicon nitride cantilevers (NP-S, Veeco Instruments, California; 115 µm long, 17 µm wide, 0.6 µm thick) with an integrated tip (a spring constant of 0.32 N/m and a resonance frequency of 56 kHz in air) were applied. A driving frequency between 8 – 10 kHz for imaging was selected in existence of buffer solution. The images (512x512 pixels) were recorded with a scan size of 1 x 1 μm^2 at a scan rate of 1 Hz and by adjusting soft tapping mode. Raw topography data has been modified by applying the first order "flatten" filter. The maximum height of aggregates was calculated by means of local roughness analysis.

The tip radii were measured by scanning electron microscopy (SEM) after having performed the SFM measurements. For the images presented we determined tip radii of curvatures < 20 nm (**Figure 7.6a**). In some cases double tips have been found (**Figure 7.6b**). These tips can produce imaging artifacts appearing as double structures in the topography. Therefore all measurements where we found double tips were not considered. In addition, we can exclude artifacts from a double tip since the appearing aggregates show different orientation relative to the scanning direction in one image.

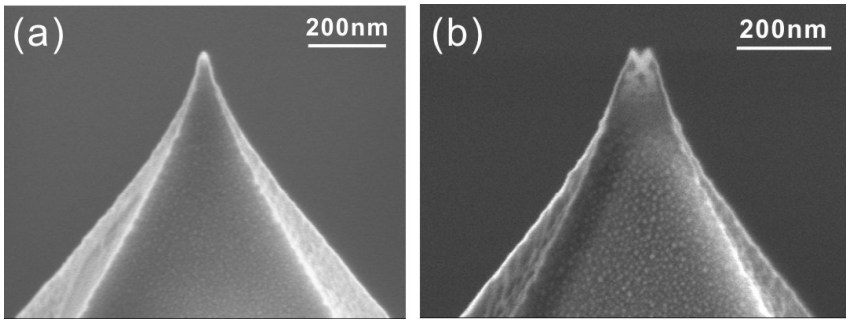

Figure 7.6 *The SEM image of the tip* ***(a)*** *with a radius of curvature < 20 nm,* ***(b)*** *showing a double-tip.*

Hybridization Experiments of ss DNA-*b*-PPO micelles with Template T88

To demonstrate the generality of our approach and to control the length of the rod-like micelles we have measured the structures arising from a shorter template (T88), which has the sequence in backbone as 5'-(TAACAGGATTAGCAGAGCGAGG)$_4$-3'). The AFM study was performed under 25 ng/µl in buffer. Similar to T110, they formed rod like structures on mica surface. The average length of the rods was measured to be 30.34 ± 0.22 nm, which is close to the theoretical value (29.92 nm). The height distribution shows an average value at 1.72 ± 0.03 nm (**Figure 7.7**).

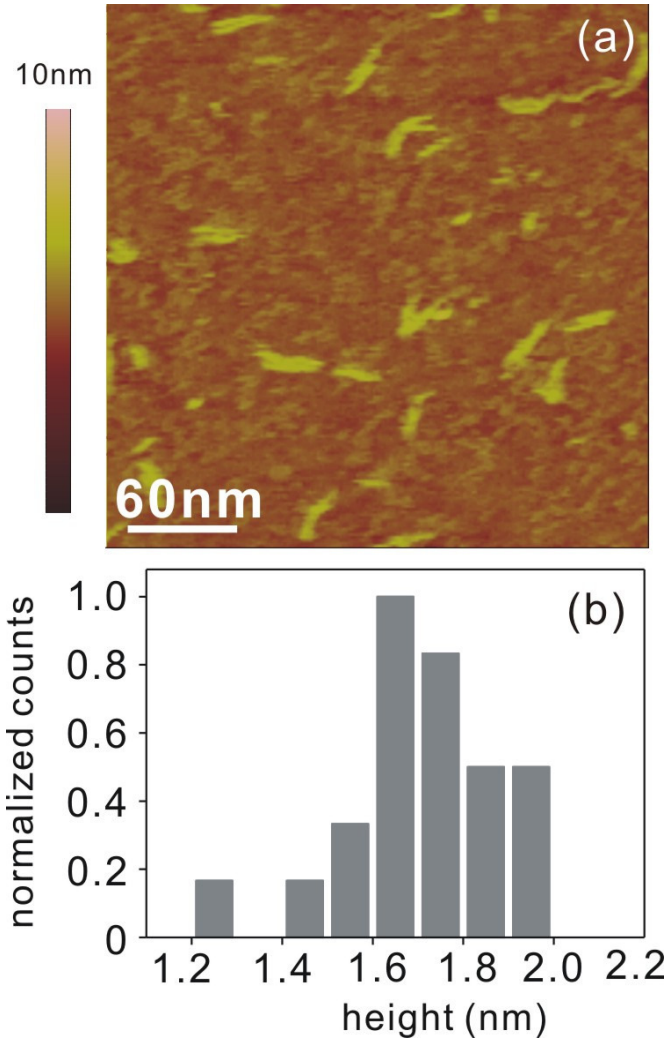

Figure 7.7 *Dimer formation by using a shorter template (T88)*

References

[1] D. E. Discher, A. Eisenberg, *Science* **2002**, *297*, 967.

[2] S. Förster, V. Abetz, A. H. E. Müller, *Adv. Polym. Sci.* **2004**, *166*, 173.

[3] H. W. Shen, A. Eisenberg, *Angew. Chem. Int. Ed.* **2000**, *39*, 3310.

[4] L. F. Zhang, K. Yu, A. Eisenberg, *Science* **1996**, *272*, 1777.

[5] T. J. Martin, K. Prochazka, P. Munk, S. E. Webber, *Macromolecules* **1996**, *29*, 6071.

[6] H. W. Shen, L. F. Zhang, A. Eisenberg, *J. Am. Chem. Soc.* **1999**, *121*, 2728.

[7] Y. Z. Liang, Z. C. Li, F. M. Li, *Chem. Lett.* **2000**, 320.

[8] L. F. Zhang, A. Eisenberg, *Macromolecules* **1999**, *32*, 2239.

[9] Y. S. Yu, L. F. Zhang, A. Eisenberg, *Macromolecules* **1998**, *31*, 1144.

[10] Y. S. Yu, A. Eisenberg, *J Am Chem Soc* **1997**, *119*, 8383.

[11] A. Stamouli, E. Pelletier, V. Koutsos, E. vanderVegte, G. Hadziioannou, *Langmuir* **1996**, *12*, 3221.

[12] Q. G. Ma, E. E. Remsen, C. G. Clark, T. Kowalewski, K. L. Wooley, *PNAS* **2002**, *99*, 5058.

[13] Q. Zhang, C. G. Clark, M. Wang, E. E. Remsen, K. L. Wooley, *Nano Lett.* **2002**, *2*, 1051.

[14] H. Schlaad, M. Antonietti, *Eur. Phys. J. E* **2003**, *10*, 17.

[15] H. A. Klok, *Angew. Chem. Int. Ed.* **2002**, *41*, 1509.

[16] J. Sanchez-Quesada, A. Saghatelian, S. Cheley, H. Bayley, M. R. Ghadiri, *Angew. Chem. Int. Ed.* **2004**, *43*, 3063.

[17] J. H. Jeong, S. W. Kim, T. G. Park, *Bioconjugate Chem.* **2003**, *14*, 473.

[18] R. B. Fong, Z. L. Ding, C. J. Long, A. S. Hoffman, P. S. Stayton, *Bioconjugate Chem.* **1999**, *10*, 720.

[19] J. H. Jeong, T. G. Park, *Bioconjugate Chem.* **2001**, *12*, 917.

[20] Z. Li, P. Fullhart, C. A. Mirkin, *Nano Lett.* **2004**, *4*, 1055.

[21] F. E. Alemdaroglu, K. Ding, R. Berger, A. Herrmann, *Angew. Chem. Int. Ed.* **2006**, *45*, 4206.

[22] E. Haustein, P. Schwille, *Methods* **2003**, *29*, 153.

[23] M. Kinjo, R. Rigler, *Nucleic Acids Res.* **1995**, *23*, 1795.

[24] M. Börsch, P. Turina, C. Eggeling, F. J.R., C. A. M. Seidel, A. Labahn, P. Gräber, *FEBS Lett.* **1998**, *437*, 251.

[25] A. Laguecir, S. Ulrich, J. Labille, N. Fatin-Rouge, S. Stoll, J. Buffle, *Eur. Polymer J.* **2006**, *42*, 1135.

[26] M. G. Düser, N. Zarrabi, Y. Bi, B. Zimmermann, S. D. Dunn, M. Börsch, *Proc. SPIE* **2006**, *6092*, 60920H.

[27] D. V. Nicolau, P. D. Sawant, *Scanning Probe Microscopy Studies of Surface-Immobilized DNA/Oligonucleotide Molecules, Vol. 1*, Berlin, **2005**.

[28] S. Förster, M. Antonietti, *Adv. Mater.* **1998**, *10*, 195.

[29] N. C. Seeman, *Angew. Chem. Int. Ed.* **1998**, *37*, 3220.

[30] N. C. Seeman, *Chemistry & Biology* **2003**, *10*, 1151.

[31] P. W. K. Rothemund, *Nature* **2006**, *440*, 297.

8 Controlling the Size of Nanoparticles by an Enzymatic Reaction*

**"Judging by current rates of progress […]
the emergence of atomic-precision manufacturing
on an industrial scale is still some decades away.
Nevertheless, it will happen …"**

Dr. Thomas Theis, 2006.

Chemists have been extremely creative in finding strategies for the preparation of organic nanoparticles. In many of these routes polymers are involved, including the preparation of polymer dispersions[1, 2] dendrimers[3, 4] or the aggregation of block polymers.[5, 6] As shown in *Chapters 6* and *7*, when for the latter approach amphiphilic DBCs are employed, nanoparticles are formed that exhibit a core of the hydrophobic polymer while the shell consists of ss DNA..[7, 8] These systems have been used for the delivery of ASOs,[9] to build thermoreversible organic/inorganic nanoparticle networks[10] and as programmable nanocontainers for a variety of chemical reactions.[11] Here we demonstrate that the size of these DNA block copolymer aggregates can be perfectly adjusted by the enzymatic reaction of a non-template dependent DNA polymerase. By incubating spherical DNA block copolymer micelles for different reaction times the size of these nanoparticles can be adjusted from a diameter of 10 nm to 25 nm.

Terminal deoxynucleotidyl transferase (TdT) (**Figure 8.1**)[12] is a template independent DNA polymerase responsible for the generation of random genetic information that is essential for

* Parts of this chapter were submitted for publication. (May 2007)

the efficacious function of the vertebrate adaptive immune system.[13] The physiological role of TdT is to catalyze the addition of random dNTPs onto the 3' hydroxyl terminus of single stranded DNA. In order to perform template-independent polymerase activity, TdT requires a primer at least as large as a trinucleotide and a free 3'-OH group for extension.[14] Until now, TdT has been exclusively used for the extension of pristine DNA [15] and has never been applied on a DNA hybrid. To the best of our knowledge, adjusting the size of nanoparticles by a DNA polymerase has so far never been explored.

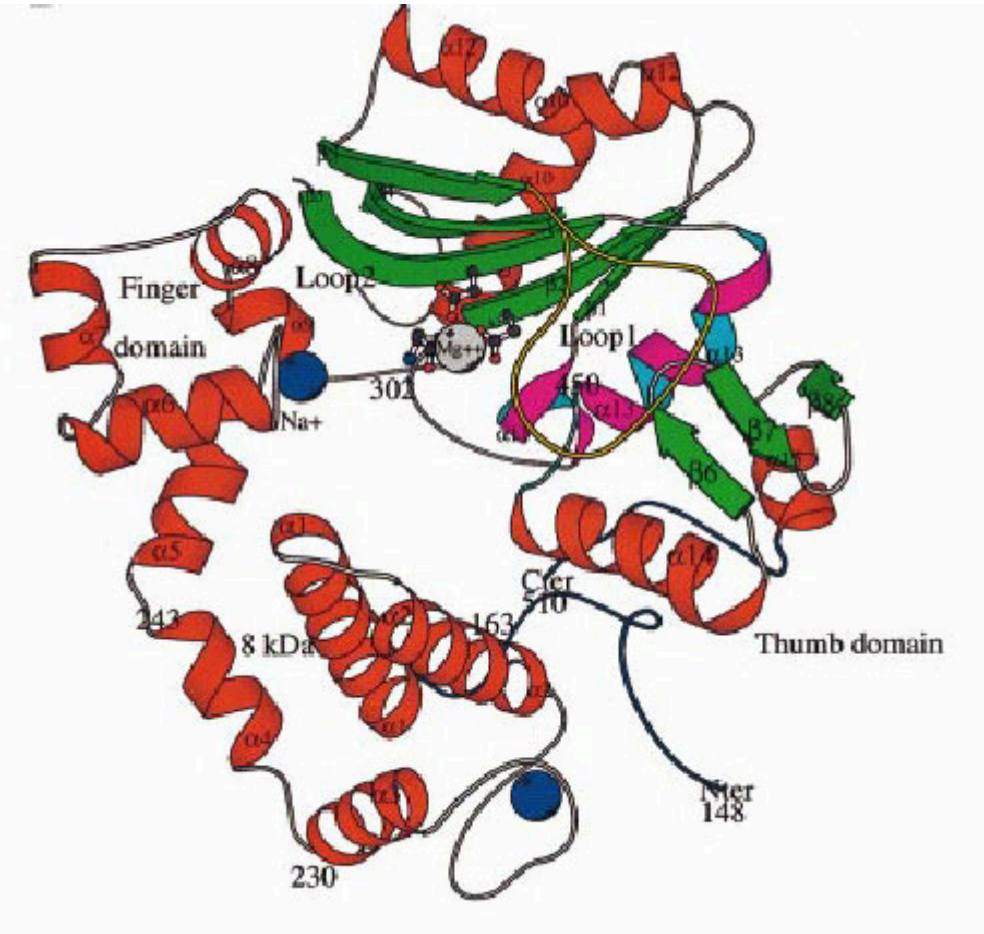

Figure 8.1 *The crystal structure of TdT.*[12]

We hypothesized that the nanoparticles formed by amphiphilic DBCs could be good candidates for increasing the size by TdT. These block copolymers can be synthesized in fully automated fashion and possess free 3'-OH groups since the organic polymer is attached to the 5' end. For this purpose DNA-*b*-PPO was synthesized employing a DNA synthesizer

according to the method described in *Chapter 3*.[11] The DNA-*b*-PPO contained a nucleic acid unit consisting of 22 nucleotides (Sequence: 5'-CCTCGCTCTGCTAATCCTGTTA-3', Mw: 6670 g/mol) and a synthetic polymer block of Mw: 6800 g/mol. This amphiphilic block copolymer hybrid is known to form micelles in aqueous solution. The diameter of the micelles is around 10 nm. [8]

Micelles composed of this material were incubated with TdT at 37°C using the standard procedure. Briefly, the enzymatic reactions were carried out by mixing Co^{+2} containing reaction buffer, DNA-*b*-PPO block copolymers, dTTP and TdT (see Experimental Section for the amounts). At certain time intervals (15, 30, 60, 180, 300, 960 min), the reaction was stopped and the growth of the nanoparticles was analyzed. The increase in micelle size was assessed by SFM, FCS, and PAGE.

To investigate whether the extension of the nucleic acid segment influenced the structural features of the micelles, these objects were visualized in the reaction buffer solution on a mica surface by SFM in soft tapping mode. These measurements were carried out by *J. Wang*. The nanoparticles were analyzed before the reaction, revealing spherical nanoparticles (**Figure 8.2A**). A histogram of the height distribution of the micelles was collected and a mean height value of 4.9 ± 1.2 nm was obtained (**Figure 8.2B**). **Figures 8.2C** and **8.2E** show the height profiles after TdT reaction of 60 min and 16 h. Histograms of the heights were compiled for at least 100 nanoobjects that are shown in **Figures 8.2D** and **8.2F**. Mean heights of 6.6 ± 1.4 and 11.2 ± 1.9 nm were obtained for 1 h and 16 h, respectively. In a similar way the mean heights for the other reaction times were determined. The results of the SFM measurements are summarized in **Table 8.1**. Although SFM has proven to be a powerful tool for imaging amphiphilic DBC aggregates, the exact dimensions can not be measured by this method. This is due to the fact that the immobilization, the imaging process and the tip broadening might slightly change the size of the micelles. Therefore, it is necessary to measure the dimensions of the DNA block copolymer aggregates in solution. Thus, FCS experiments with the nanoparticles were carried out.

Table 8.1 *Characterization of DNA block copolymer micelles that were blown up by TdT reaction. The results were [(a)] based on FCS analysis, [(b)] derived from SFM measurements and [(c)] determined by PAGE.*

Time (min)	Diameter[a] (nm)	Height[b] (nm)	T segments added[c]
15	9.9 ± 1.1	5.1 ± 1.4	6 ± 4
30	10.8 ± 1.6	5.2 ± 1.3	11 ± 3
60	12.4 ± 0.8	6.6 ± 1.4	22 ± 5
180	13.7 ± 1.3	7.2 ± 1.5	35 ± 8
300	17.5 ± 1.4	8.3 ± 1.6	43 ± 7
9600	23.0 ± 0.8	11.2 ± 1.9	62 ± 11

FCS is an ultrasensitive analysis method which was introduced in the early 1970s to study chemical kinetics at very dilute concentrations in biological systems.[16] Since then, the technique has developed into a powerful tool in analytical chemistry and biological research. For instance, DNA-hybridization events have been detected at the single-molecule level.[17] Furthermore, FCS has been employed to detect the mobility of proteins and DNA- or RNA-fragments within the cytosol or other cell organelles. Recently, we reported that FCS can be used to assess the change of micelle shape of DBCs from spherical to rod-like aggregates.[8] In this chapter the transit times of the freely diffusing fluorescent micelles that were processed by TdT through the excitation volume of 4.5 fl were measured in buffer solution by using a confocal microscope setup.[18] FCS analyses were carried out by *Dr. M. Börsch* from University of Stuttgart. The translational diffusion coefficients D were calculated from the mean diffusion times. As the diffusion coefficient D is related to the frictional coefficient f of the hydrated micelles, the shape information from the SFM experiments could be used to calculate the radius r_0 of the spherical micelles from the FCS diffusion data (see Experimental Section).

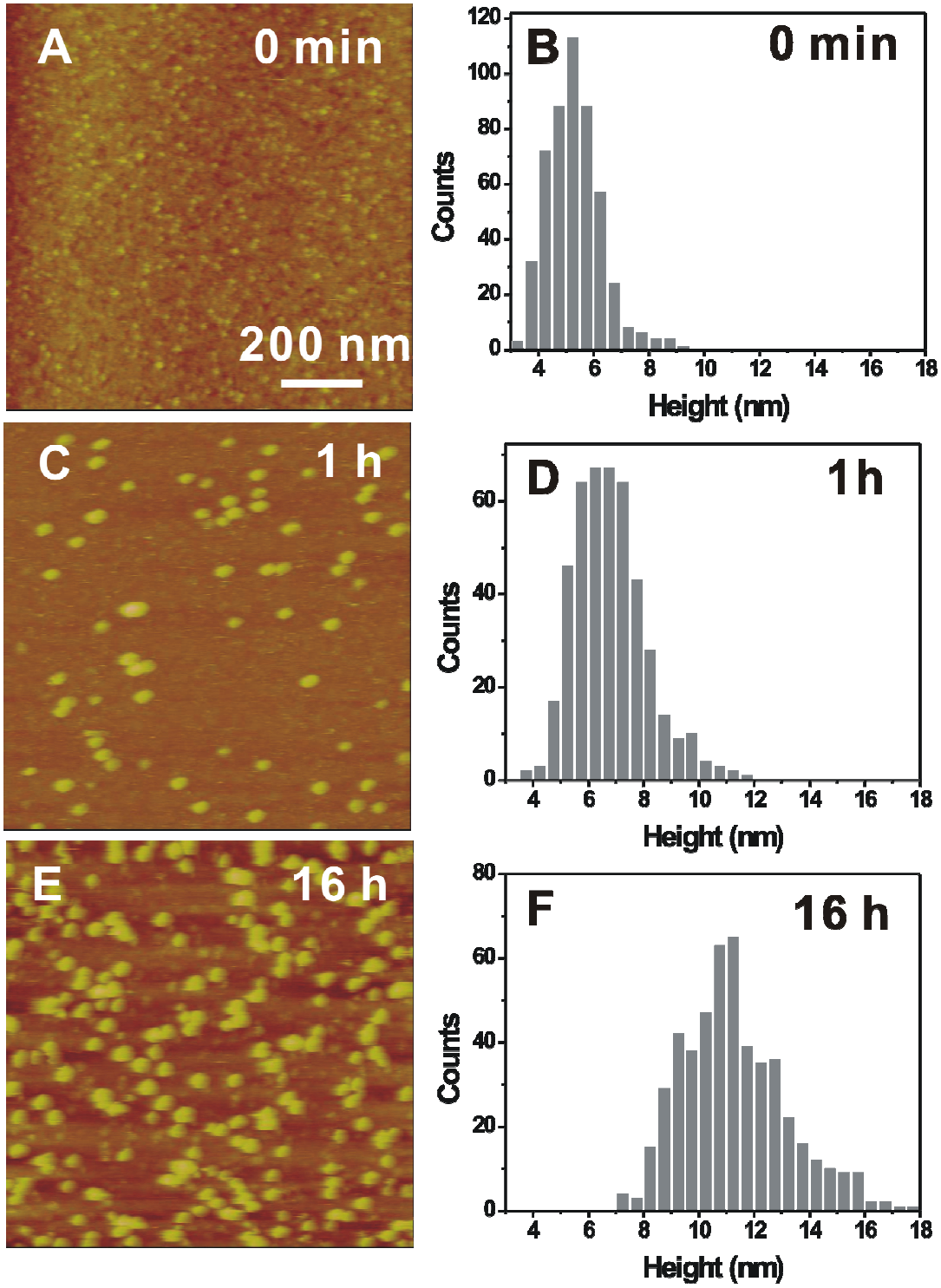

Figure 8.2 *SFM analysis of DNA block copolymer micelles that were incubated with TdT. A, C and E are height profiles of the nanoparticles after 0, 1 and 16 h of reaction time. B, D and E are the histograms of the maximum heights of the corresponding aggregates.*

Prior to TdT reaction the DBC micelles were labeled with the complementary sequence that was functionalized with Alexa488 (Invitrogen, USA) at the 5' end by hybridization. 1 % of the DNA-*b*-PPOs were equipped with the chromophore so that the predominant form of DNA within the corona remained single stranded. In the presence of TdT and deoxythymidine triphosphate (dTTP) the enzymatic extension of the single stranded DNA chains resulted in increasing diffusion times and corrected therewith in a growth of the hydrodynamic radius of the micelles. After 16 h reaction time, the FCS curve showed a 2.6-fold increase of the mean diffusion time, τ_D. However, for a detailed analysis of the autocorrelation functions a two-diffusing-components fit had to be used.[19, 20] The longer diffusion times of the labeled micelles varied from $\tau_{D2} \sim 280$ µs for a TdT reaction time of 15 minutes up to $\tau_{D2} \sim 650$ µs for 16 h reaction time. The short diffusion time component with $\tau_{D1} \sim 60 \pm 12$ µs was similar to the value of the reference dye rhodamine 110 ($\tau_D = 43 \pm 1$ µs) and most likely originated from fluorescent impurities.

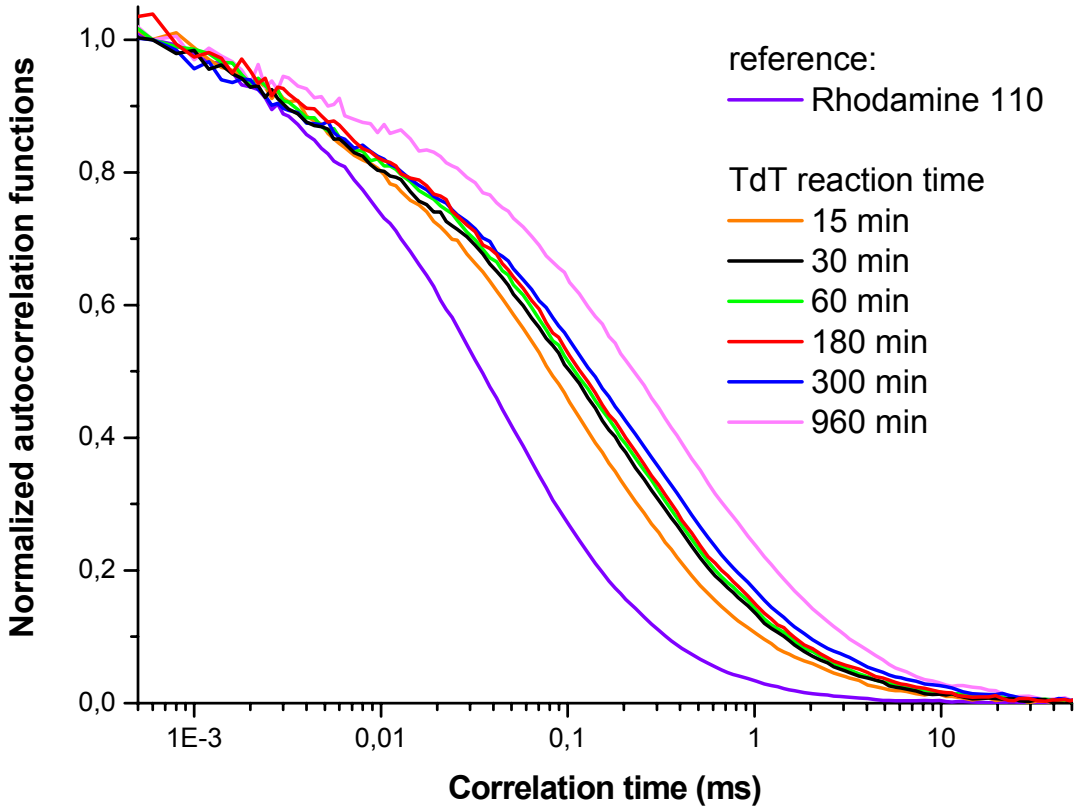

Figure 8.3 *The autocorrelation functions of the Alexa488 labeled nanoparticles that were extended by TdT.*

A mean diameter of 9.9 ± 1.1, 10.8 ± 0.6, 12.4 ± 0.8 nm was found for the DBC micelles after 15 min, 30 min and 60 min of incubation with TdT, respectively. With increasing reaction time, the micelles enlarged further to diameters of 13.7 ± 1.3 nm and 17.5 ± 1.4 nm for 3 h and 5 h, respectively. Extension with TdT for 16 h resulted in a micelle diameter of 23.0 ± 0.8 nm (**Figure 8.3** and **Table 8.1**). These values are in good agreement with the AFM measurements as they confirm similar trends of the growth of the micelles (**Figure 8.4**). It can be concluded from the FCS data that upon immobilization, the micelles are flattened owing to the interaction with the surface and/or the SFM imaging process. The constituent being mostly responsible for the deformation might be the soft hydrophobic polymer, PPO.

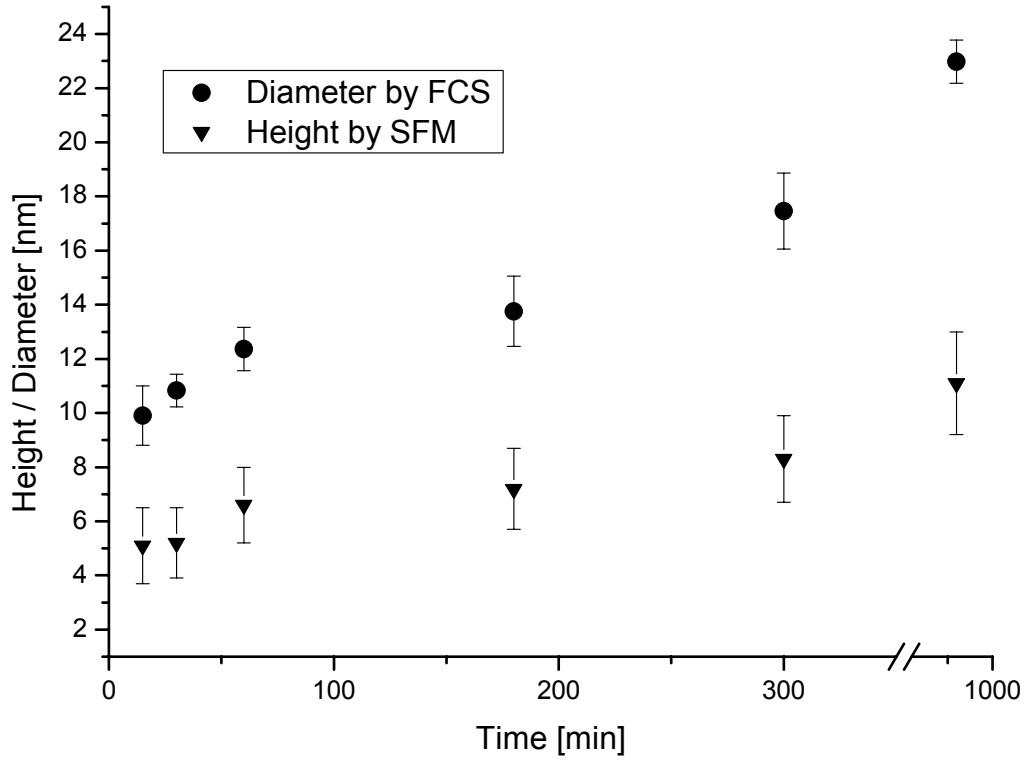

Figure 8.4 *The graph representing the diameters of the nanoparticles obtained by FCS and the maximum heights of the micelles measured by SFM.*

In order to correlate the size of the nanoparticles with the number of nucleotides attached to the DNA block copolymers, molecular weight markers were synthesized. A ladder of DNA-*b*-PPO block copolymer was prepared consisting of a 22mer and an additional thymidine (T) segment of variable length at the 3' end (0, 10, 20, 40 and 60 Ts). These markers were separately synthesized on the solid phase, purified and then mixed together in a stock

solution. The DNA block copolymer ladder was run together in a polyacrylamide gel with the reaction products of the TdT extended DNA polymer hybrids to estimate the amount of enzymatically attached nucleotides after different time intervals (**Figure 8.5**). Comparing the ladder with the incubation products provided the following results:

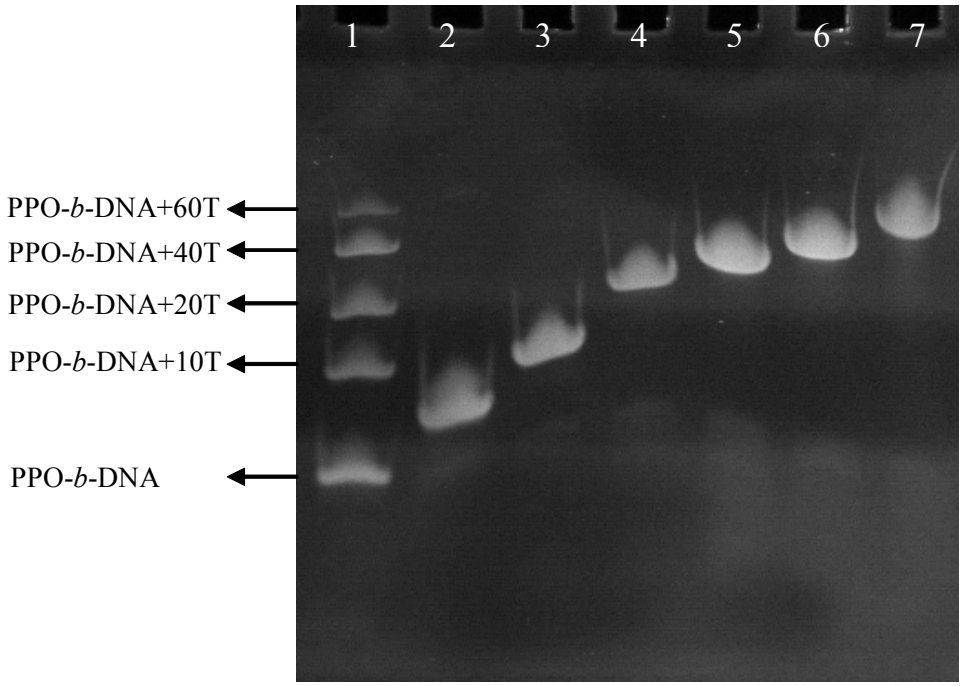

Figure 8.5 *Gel electrophoretic analysis of the DNA block copolymers extended by the enzyme TdT. Lane 1 represents the DNA-b-PPO ladder. Lanes 2, 3, 4, 5, 6 and 7 contain the DNA-b-PPO afterenzymatic extension for 15, 30, 60, 180, 300 and 9600 min, respectively.*

Incubation of 15 and 30 min with TdT generated nanoparticles with an average 4 and 11 additional nucleotides, respectively (**Figure 8.5, Lanes 2** and **3**). One-hour reaction time with the enzyme resulted in micelles with 22 added thymidine residues (**Figure 8.5** Lane 4). Incubating the amphiphilic block copolymers for 3 and 5 hours generated nanoobjects with 35 and 43 additional bases, respectively (**Figure 8.5, Lanes 5** and **6**). Finally, the extension with TdT for 16 hours yielded DNA-*b*-PPO nanoparticles with 56 thymidines added (**Figure 8.5, Lane 7**).

The size of block copolymer micelles is usually adjusted by the lengths of the constituent polymer blocks. However, a post-synthetic extension of the constituent components of block copolymer aggregates is rather difficult. The method presented here offers easy control over the size of nanoparticles by employing template independent DNA polymerase under isothermal conditions. It was possible to significantly increase the micelle size by a factor of up to 2.5. Further studies will focus on the use of TdT on other nanoparticle systems such as DNA nanoparticles with an inorganic core.

Experimental Section

The synthesis and the visualization of DNA-b-PPO block copolymers are carried out as reported in *Chapter 3* and *5*, respectively.

Enzymatic Reaction

The enzymatic reactions were carried out by mixing 4µl reaction buffer, 1nmol of DNA-*b*-PPO block copolymers, 150 nmol of dTTP and 40-60 units of TdT. This mixture was incubated for different times at 37°C in a thermoshaker.

FCS Measurements

FCS was performed on a custom-built confocal microscope based on an Olympus IX71. An Argon ion (Spectra Physics) laser was used to excite the micelle solutions at 488 nm with 20 µW or 50 µW, respectively. In epi-fluorescence configuration, diffraction-limited excitation and fluorescence collection was achieved through a water immersion objective (UPlanSapo 60xW, 1.2 n.a., Olympus, Hamburg). A 50 µm pinhole blocked the out-of-focus fluorescence. Fluorescence in the spectral range between 500 and 570 nm was separated from scattered light by an interference filter (HQ 532/70, AHF, Tübingen) and split in two channels by a polarizing beam splitter. The signals of the two single photon counting avalanche photodiodes (SPCM AQR-14, Perkin-Elmer) were fed into the autocorrelator card (ALV-5000/E, ALV, Langen) in cross-correlation configuration and in parallel to a set of synchronized, fast counter cards (SPC-152, Becker&Hickl, Berlin) for software-based autocorrelation.[18] A diluted Rhodamine-110 solution in pure water was used as the reference to yield the optical parameters of the confocal detection volume.

The kinetics of the nucleotide addition by TdT to the 3’ OH group of the nucleic acid unit of the DNA-*b*-PPO micelles was monitored by FCS. ss DNA-*b*-PPO micelles were hybridized with the complementary sequence which was functionalized with Alexa488 (Invitrogen, USA) at the 5’ end. The ratio of ss DNA-*b*-PPO to ODN carrying the dye was adjusted to be 4 % so that the predominant form of DNA within the corona remains single stranded. To maintain the micelles during the FCS measurements, the concentrations were kept well above the critical micelle concentration resulting in 50 to 100 fluorescently labeled micelles in the diffraction-limited confocal detection volume.

For spherical micelles the diffusion time can be directly related to the hydrodynamic radius, r_H (**Equation 8.1**):

$$r_H = kT (4 \tau_D) / 6\pi \eta \omega^2 \qquad \text{(Equation 8.1)}$$

where k is the Boltzmann constant, T is the temperature, η is the viscosity of the solution, and ω is the approximated axial $1/e^2$ radius of the confocal volume.

Fitting the autocorrelation function of rhodamine 110 in water yielded the axial radius ω = 220 nm of confocal volume using a diffusion coefficient D = 2.8 10^{-6} cm^2/sec.[21] The corresponding effective hydrodynamic radius of 0.77 nm for rhodamine 110 is similar as reported previously.[22] Accordingly, the diffusion times of the micelles were used to calculate the respective radii. The diameter increased from 9.9 nm for a TdT reaction time of 15 minutes up to 23 nm after 16 hours reaction time. The kinetics of micelle growth could be described by a logarithmic time dependence with an initial growth rate of about 1.6±0.1 nm / h.

References

[1] D. Distler, *Waessrige Polymerdispersionen : Synthese, Eigenschaften, Anwendungen*, Wiley-VCH, Weinheim ; Chichester, **1999**.

[2] T. Kietzke, D. Neher, K. Landfester, R. Montenegro, R. Guntner, U. Scherf, *Nature Materials* **2003**, *2*, 408.

[3] C. Zhisheng, S. L. Cooper, *Adv. Mater.* **2000**, *12*, 843.

[4] A. C. Grimsdale, K. Mullen, *Angew. Chem., Int. Ed.* **2005**, *44*, 5592.

[5] S. Forster, V. Abetz, A. H. E. Müller, *Adv. Polym. Sci.* **2004**, *166*, 173.

[6] I. W. Hamley, *Nanotechnology* **2003**, *14*, R39.

[7] F. E. Alemdaroglu, A. Herrmann, *Org. Biomol. Chem.* **2007**, *5*, 1311

[8] K. Ding, F. E. Alemdaroglu, M. Boersch, R. Berger, A. Herrmann, *Angew. Chem., Int. Ed.* **2007**, *46*, 1172.

[9] J. H. Jeong, T. G. Park, *Bioconjugate Chem.* **2001**, *12*, 917.

[10] Z. Li, Y. Zhang, P. Fullhart, C. A. Mirkin, *Nano Lett.* **2004**, *4*, 1055.

[11] F. E. Alemdaroglu, K. Ding, R. Berger, A. Herrmann, *Angew. Chem., Int. Ed.* **2006**, *45*, 4206.

[12] M. Delarue, J. B. Boule, J. Lescar, N. Expert-Bezancon, N. Jourdan, N. Sukumar, F. Rougeon, C. Papanicolaou, *EMBO J.* **2002**, *21*, 427.

[13] J. D. Fowler, Z. Suo, *Chem. Rev.* **2006**, *106*, 2092.

[14] K. I. Kato, Goncalve.Jm, G. E. Houts, F. J. Bollum, *J. Biol. Chem.* **1967**, *242*, 2780.

[15] H.-M. Eun, *Enzymology primer for recombinant DNA technology*, Academic Press, San Diego ; London, **1996**.

[16] D. Magde, W. W. Webb, E. Elson, *Phys. Rev. Lett.* **1972**, *29*, 705.

[17] M. Kinjo, R. Rigler, *Nucleic Acids Res.* **1995**, *23*, 1795.

[18] M. G. Düser, N. Zarrabi, Y. Bi, B. Zimmermann, S. D. Dunn, M. Börsch, *Proc. SPIE-Int. Soc. Opt. Eng.* **2006**, *6092*, 60920H.

[19] A. Armbruster, C. Hohn, A. Hermesdorf, K. Schumacher, M. Borsch, G. Gruber, *FEBS Lett.* **2005**, *579*, 1961.

[20] M. Diez, M. Borsch, B. Zimmermann, P. Turina, S. D. Dunn, P. Graber, *Biochemistry* **2004**, *43*, 1054.

[21] M. Borsch, P. Turina, C. Eggeling, J. R. Fries, C. A. M. Seidel, A. Labahn, P. Graber, *FEBS Lett.* **1998**, *437*, 251.

[22] G. Porter, P. J. Sadkowski, C. J. Tredwell, *Chem. Phys. Lett.* **1977**, *49*, 416.

9 DNA-templated Synthesis in Three Dimensions: Introducing a Micellar Scaffold for Organic Reactions*

"… our brain is organized in three dimensions.
We live in a 3-D world; why not use the third dimension? "

Dr. Raymond Kurzweil, 2000

Nowadays, a large variety of organic reactions and conversions can be carried out in a DNA-templated format.[1-9] Based on these developments, applications employing the concept of nucleic acid templated synthesis have already been realized. These include nucleic acid detection,[8, 10, 11] sequence specific DNA modifications,[12-15] screening of libraries of synthetic molecules,[3, 4, 16] and the discovery of new reactions.[17] These successful examples are based on three different nucleic acid template architectures, the A+B+A'B'-, A+BB'A'- and A+A'-templates. A/B and A'/B' denote complementary ODNs whereas + symbols indicate separate molecules. This basic set of templates was complemented by the so called Ω- and T-architectures, which allow distance dependent reactions and transformations involving three functional groups to proceed efficiently in a DNA-templated fashion.[18] Beside these ss templates the DNA-double helix itself was exploited as a reaction scaffold by using major- or minor grove binding motifs for the prearrangement of the reactants.[19, 20] Both ss- and ds templates represent one dimensional objects, whereas the so-called Y-shaped template, which catalyzed the coupling of three different ODNs to a tris-linker molecule, can be regarded as a two dimensional scaffold.[21]

* Parts of this chapter were published: *Angew. Chem. Int. Ed.* **2006**, *45*, 4206.

In this chapter, a novel template architecture is introduced which allows DNA-templated organic reactions to proceed in three dimensional space. The template consists of amphiphilic DNA-block copolymer micelles with a hydrophobic core and a ss DNA-shell. Instead of Watson-Crick base pairing, aggregation of hydrophobic polymer blocks aligns the DNA of the corona to act as a template in DNA-templated organic synthesis. The ss DNA of the corona is hybridized with ODNs which are equipped with different reactants. Depending on functionalization of either the 5' or 3' ends various organic reactions are performed sequence specifically on the surface of the micelles (5') or at the hydrophobic/hydrophilic interface (3'). The three-dimensional template architecture is of great importance for the advancement of nucleic acid templated synthesis because it allows DNA-templated reactions to occur while potentially shielded from the aqueous environment.

In dilute aqueous solutions, polyelectrolyte block copolymers self-assemble into three dimensional spherical micelles with a charged corona and a hydrophobic core.[22] Such nano-containers composed of amphiphilic block copolymers have found importance as drug delivery vehicles when lipophilic drugs are incorporated into their hydrophobic interior.[23] Recently, new types of micellar aggregates were introduced that consist of a ss DNA corona and a PLGA or a PS hydrophobic core.[24, 25] These micelles were applied for the delivery of ASOs[24] and for the selective hybridization with DNA-coated gold nanoparticles.[25] Both organic polymer blocks, PLGA and PS, as constituents of these DNA-block polymer architectures exhibit relative high T_G (T_G (PS) = 90°C, T_G (PLGA) = 30°C), which is known to prevent direct dissolving in aqueous solution[26] and hinders investigation of the micellar properties because the "frozen" micelles do not reach the state of thermodynamic equilibrium.[22] In this study, DNA-*b*- PPO polymers (T_G (PPO) = -70°C) were prepared to overcome these shortcomings as well as to provide a polymer with proven biocompatibility toward different cell types when administered as a constituent component of amphiphilic block copolymer micelles.[27]

DNA-*b*-PPO block copolymers were synthesized on the solid phase using a DNA synthesizer as outlined in *Chapter 3*. Briefly, hydroxyl-terminated PPOs were reacted with phosphoramidite chloride to yield the corresponding phosphoramidite-PPO derivatives. The activated PPOs were then coupled to the 5' end of an ODN (22mer, sequence: 5'-CCTCGCTCTGCTAATCCTGTTA-3') on a solid support using a DNA-synthesizer. After deprotection and purification by PAGE the DNA-*b*-PPOs were obtained. Coupling

efficiencies of the large polymer moieties were remarkably high with yields reaching 41 % and 32 % for PPO polymers with molecular weights of 1,000 and 6,800 g/mol, respectively.

Since it is well accepted for polyelectrolyte block copolymers that the polyelectrolyte chains within the corona of the micelle are well ordered and almost completely stretched,[28] it was hypothesized that these bioorganic nano-particles could serve as supramolecular scaffolds for DNA-templated organic reactions. In our initial studies, we investigated reactions proceeding at the rim of the corona (**Figure 9.1a**). The DNA-*b*-PPO was dissolved in buffer solution and hybridized with equimolar amounts of ODNs (22mer, sequence: 5'-TAACAGGATTAGCAGAGCGAGG-3') that were equipped with different reactants at the 5' end including sulfhydryl, amino, carboxylic acid, and malimide groups. With this set of reactants, three different reactions were carried out (**Figure 9.2**). First, a trimolecular coupling between a ss-thiol, a ss-amine and a free *o*-phthalaldehyde was accomplished to produce a fluorescent isoindole[29, 30] on the surface of the micelles. The desired product was confirmed by a gel-shift mobility assay (**Figure 9.3a, lane 1**) and fluorescence measurements (characteristic emission maxima at 440 and 460 nm). This novel, fluorogenic DNA-templated reaction turned out to be a highly efficient tool for optimizing reaction conditions for DNA-templated organic synthesis and to monitor the different control reactions that were necessary to prove the applicability and efficiency of the new micellar template architecture. As controls, similar reaction protocols were carried out as above but with the following alterations: with a complementary sequence but without terminal amino and sulfhydryl groups (**Figure 9.3a, lane 2 and 3**), with mismatching ODNs modified with amino and sulfhydryl functionalities (**Figure 9.3a, lane 4 and 5**), without free *o*-phthalaldehyde (**Figure 9.3a, lane 6**), without micelles composed of **DNA-*b*-PPO(6.8K)** (**Figure 9.3a, lane 7**), with the sequence of the template but without PPO attachment (**Figure 9.3a, lane 8**) and with the concentration of the hybrid being below the critical micelle concentration (CMC) (**Figure 9.3a, lane 9**). For all of these control reactions, no fluorescence signal and no band corresponding to the reaction product in the gel could be detected. These results impressively demonstrate the efficiency of the micellar template to increase the apparent molarities of the reaction partners, which in turn helps the chemical conversion proceed.

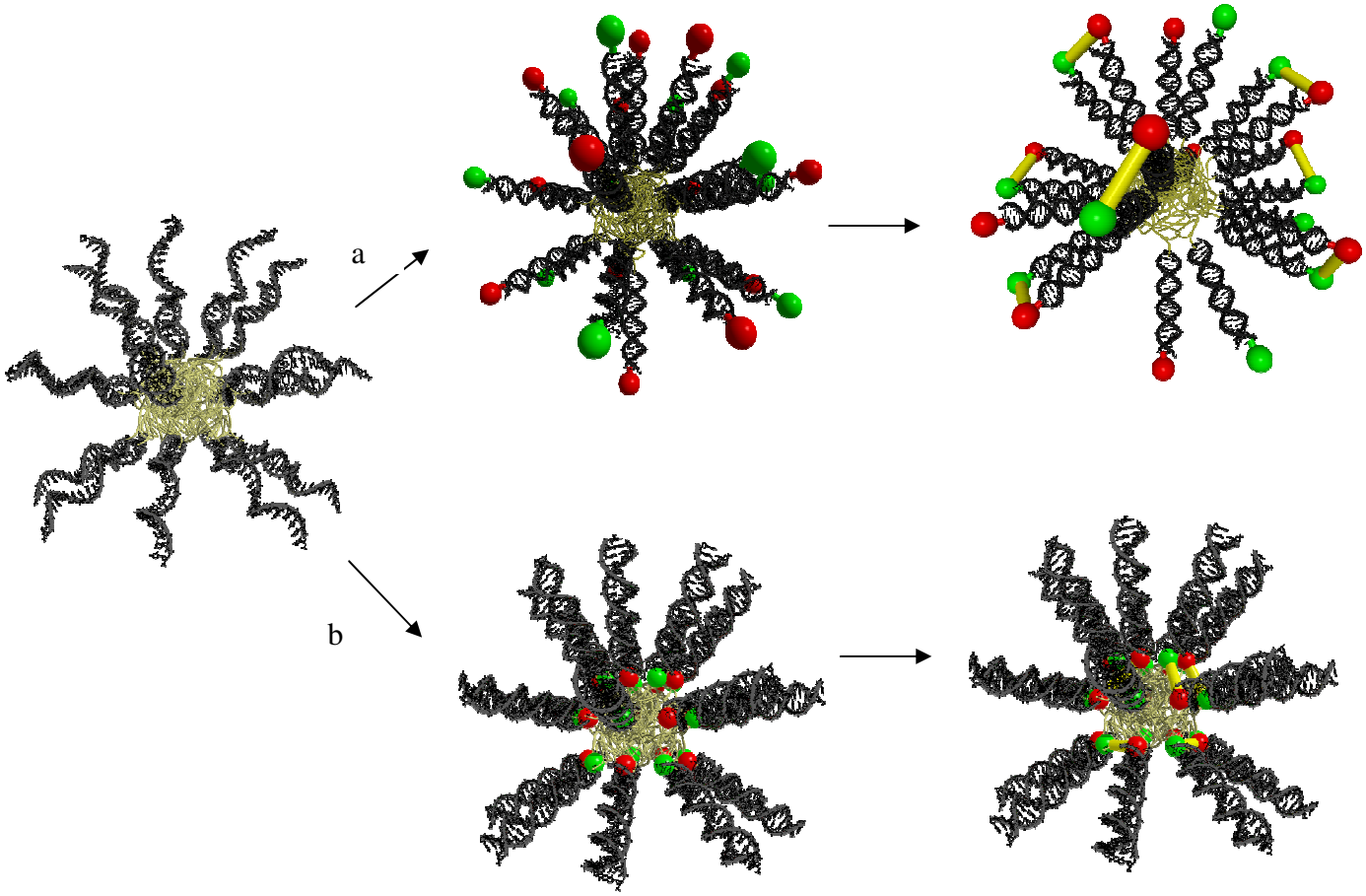

Figure 9.1 *Schematic representation of DNA-templated synthesis applying DNA block copolymers. The micelles resulting from these polymeric architectures consist of a hydrophobic core and a shell of DNA. Single stranded micelles can be either hybridized with oligonucleotides that are equipped with reactants at the 5' and 3' ends. The subsequent chemical reaction proceeds either (a) at the rim of the micelle or (b) at the hydrophobic/hydrophilic interface, respectively.*

Interestingly, the yield of fluorophore formation on the micelle scaffold was 41 %, which was higher than that obtained with the A+B+A'B'-, the A+BB'A'- and the A+A'-architectures for the same reaction (see Experimental). As a second DNA-*b*-PPO scaffold supported transformation, amide bond formation was carried out on the surface of the micelles by hybridization with carboxyl- and amine-functionalized ODNs in the presence of EDC and NHS as activation reagents. The yield for peptide bond formation was 72 %, which is comparable to yields achieved by Liu *et al* for the same reaction using an A+A'-template.[3]

Finally, to further prove the generality of the DNA block copolymer scaffold and its sequence specific chemistry at the surface, the Michael-addition between a thiol- and a malimide-modified ODN was performed. The yield was again very high (74 %) and was comparable to results achieved previously with A+BB'A'- and A+A'-templates.[4] For the amide bond formation and the Michael-addition the same controls as for the fluorogenic reaction were carried out but again did not show any product formation as confirmed by PAGE (see Experimental Section).

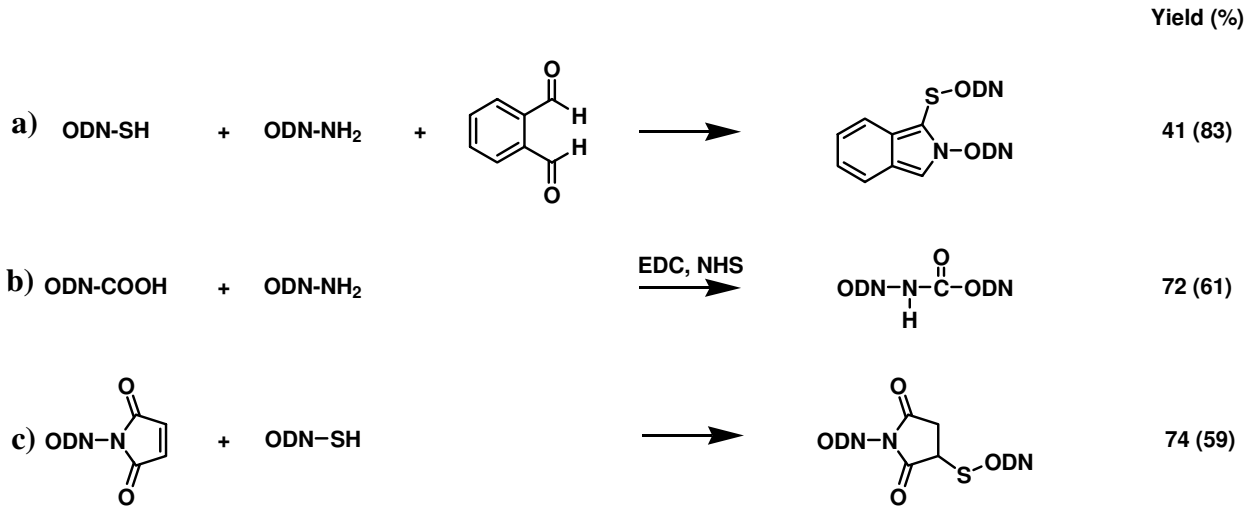

Figure 9.2 *DNA-templated reactions carried out either on the surface or within the interior of the DNA block copolymer micelles. a) Isoindole formation, b) amide bond formation and c) Michael addition. The numbers in parentheses indicate the yields achieved inside the micelles.*

To fully exploit the potential of the DNA-*b*-PPO micelles for templated transformations, reactions at the interface of the hydrophobic core and the hydrophilic corona were investigated using the same set of reactions described above. To conduct these experiments, a simple change to 3' modified ODNs was required (**Figure 9.1b**). After hybridization of the micelles with the appropriately functionalized ODNs, isoindole (**Figure 9.3b, Figure 9.4**) and amide bond formation as well as Michael addition were all detected by means of fluorescence and/or PAGE.

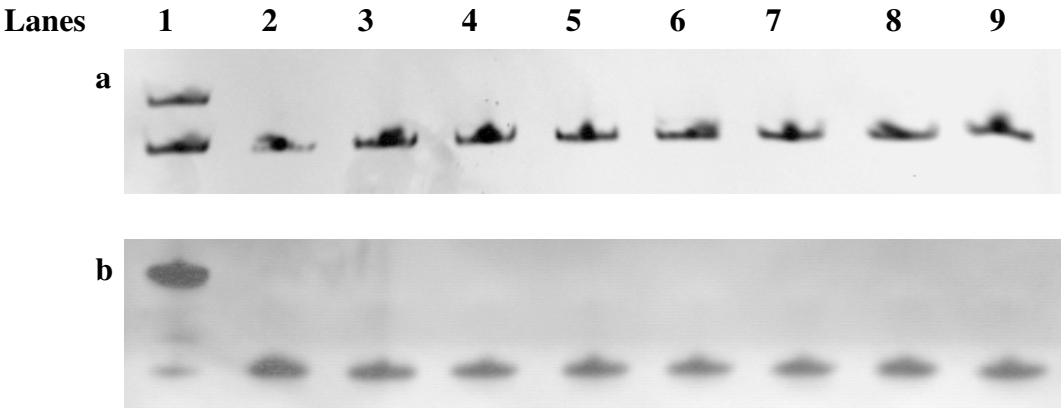

Figure 9.3 *Analysis by denaturing PAGE of the DNA-templated isoindole formation using the micellar scaffold a) at the surface of the micelles and b) at the interface of the biological and the organic polymer segment. Lane 1 shows the fully matching reaction conditions that resulted in product formation represented by the band with lower electrophoretic mobility. Lane 2 – 9 contained the control experiments where reaction conditions were modified in contrast to lane 1 accordingly. Lanes 2 and 3: Use of complementary sequences in regard to the template but without terminal amino and sulfhydryl groups, respectively. Lanes 4 and 5: Application of mismatching ODNs in respect to the template modified with amino and sulfhydryl functionalities. Lane 6: Reaction without o-phthalaldehyde. Lane 7: Reaction without the micelles composed of* ***DNA-b-PPO****. Lane 8: Conversion with the template sequence but without PPO attachment. Lane 9: Applying the DNA block copolymer* ***DNA-b-PPO*** *as a template below the CMC.*

The reactions proceeded with yields of 83, 61 and 59 %, respectively, in a sequence selective manner as demonstrated by comparison with the control experiments. It is noteworthy that the isoindole formation worked much more efficiently at the hydrophilic/hydrophobic interface than at the rim of the micelle. The *o*-phthalaldehyde might accumulate within the hydrophobic core leading to significant higher reaction yields when reactants were directed to the centre of the micelle. Since the DNA block copolymer ***DNA-b-PPO(6.8K)*** efficiently catalyzes DNA-templated organic reactions, the structural properties of the micelles were elucidated in more detail. Micelles of ***DNA-b-PPO(6.8K)*** with a ss DNA-corona exhibited a diameter of 11.3 ± 2 nm as detected by DLS.

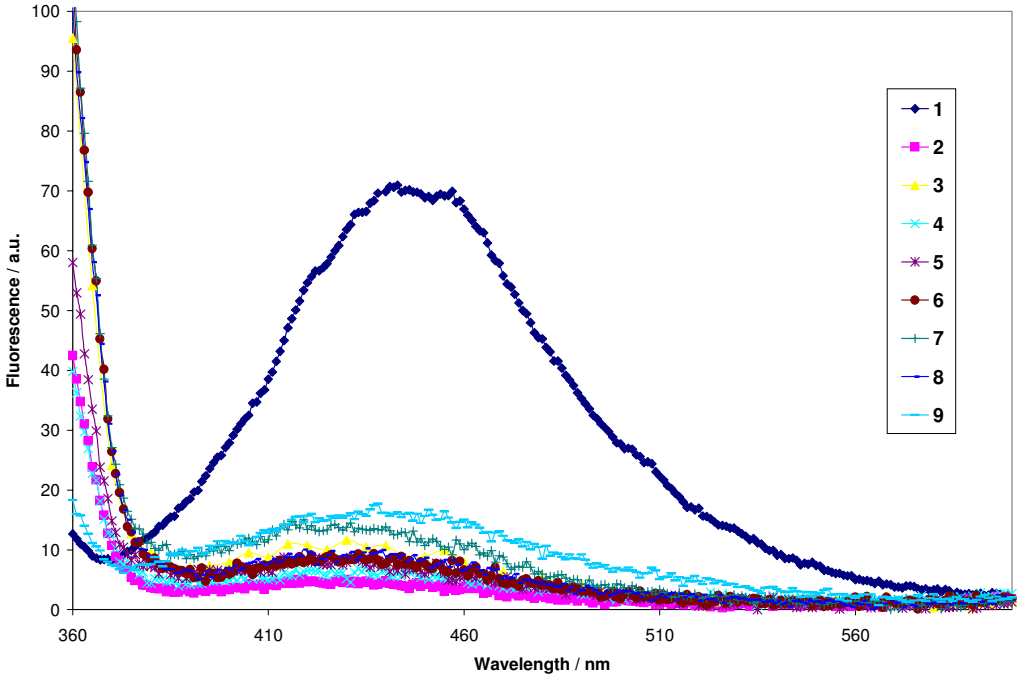

Figure 9.4 *Fluorescence spectroscopic analysis of the isoindole formation at the hydrophilic/hydrophobic interface of the micelles. A fluorescence signal was only obtained for fully matching reaction conditions (1). The corresponding control experiments (2-9) resulted in low emission intensities. Spectra 2 and 3: Use of complementary sequences in regard to the template but without terminal amino and sulfhydryl groups, respectively. Spectra 4 and 5: Application of mismatching ODNs in respect to the template modified with amino and sulfhydryl functionalities. Spectrum 6: Reaction without o-phthalaldehyde. Spectrum 7: Reaction without the micelles composed of* ***DNA-b-PPO(6.8K)****. Spectrum 8: Conversion with the template sequence but without PPO attachment. Spectrum 9: Applying the DNA block copolymer* ***DNA-b-PPO(6.8K)*** *as a template below the CMC. Excitation wavelength was 350 nm.*

To investigate if hybridization and chemical bond formation influenced the structural features of the micelles, they were visualized by scanning force microscopy (SFM) before and after amide bond formation. The SFM image before the DNA-templated reaction showed spherical micelles, which were visualized by soft tapping mode in the reaction buffer on a mica surface (**Figure 9.5a**). Inspection of the micelles by SFM after addition of the bond forming reagents resulted in very similar images (data not shown). Histograms of the height distribution before and after the reaction were also evaluated (**Figure 9.5b and 9.5c**). The height of the micelles ranged from 6 to 18 nm with an average height of 10.4 ± 1.8 nm before the reaction and 11.0

± 2.0 nm after amide bond formation. Upon the chemical reaction, no significant changes in the height distributions were detected. This indicates that the bond formation does not influence the structural properties of the micelles.

Cross linking reactions within micelles, either in the corona[31-34] or in the core,[35-37] are known and were mainly used to stabilize their spherical shapes. Unfortunately, conventional cross linking moieties need to be incorporated during the preparation of the block polymers and the subsequent transformations are usually not very well defined. Alternatively, the approach described herein represented a significant advancement in respect of performing chemistry in micelles. Aggregates of amphiphilic DNA block copolymers are a novel, highly modular platform of programmable objects that allow functionalization of micelles *post* synthesis with virtually any chemical moiety through DNA hybridization and the execution of chemical reactions within predetermined submicellar compartments.

In conclusion, DNA-*b*-PPO polymers formed spherical micelles in aqueous solution, which were characterized by light scattering and SFM, exhibiting a hydrophobic core and a ss DNA polyelectrolyte shell. It was demonstrated for the first time that various chemical reactions can be performed in a perfectly controlled and programmed manner within the volume of the micelle representing a spherical three-dimensional object. The DNA strands of the corona were organized by hydrophobic interactions of the organic polymer segments in such a fashion that several DNA-templated organic reactions proceeded in a sequence specific manner either at the surface of the micelles or at the interface between the biological and the organic polymer blocks. The yields of reactions employing the micellar template were equivalent or better than existing template architectures. Furthermore, hydrophobic reactants can accumulate within the core of the micelle to produce much higher yields than achieved with conventional templates. Finally, with the help of a novel fluorogenic reaction, the DNA-templated organic reaction was detected by fluorescence spectroscopy allowing easy optimization of reaction conditions for new template architectures.

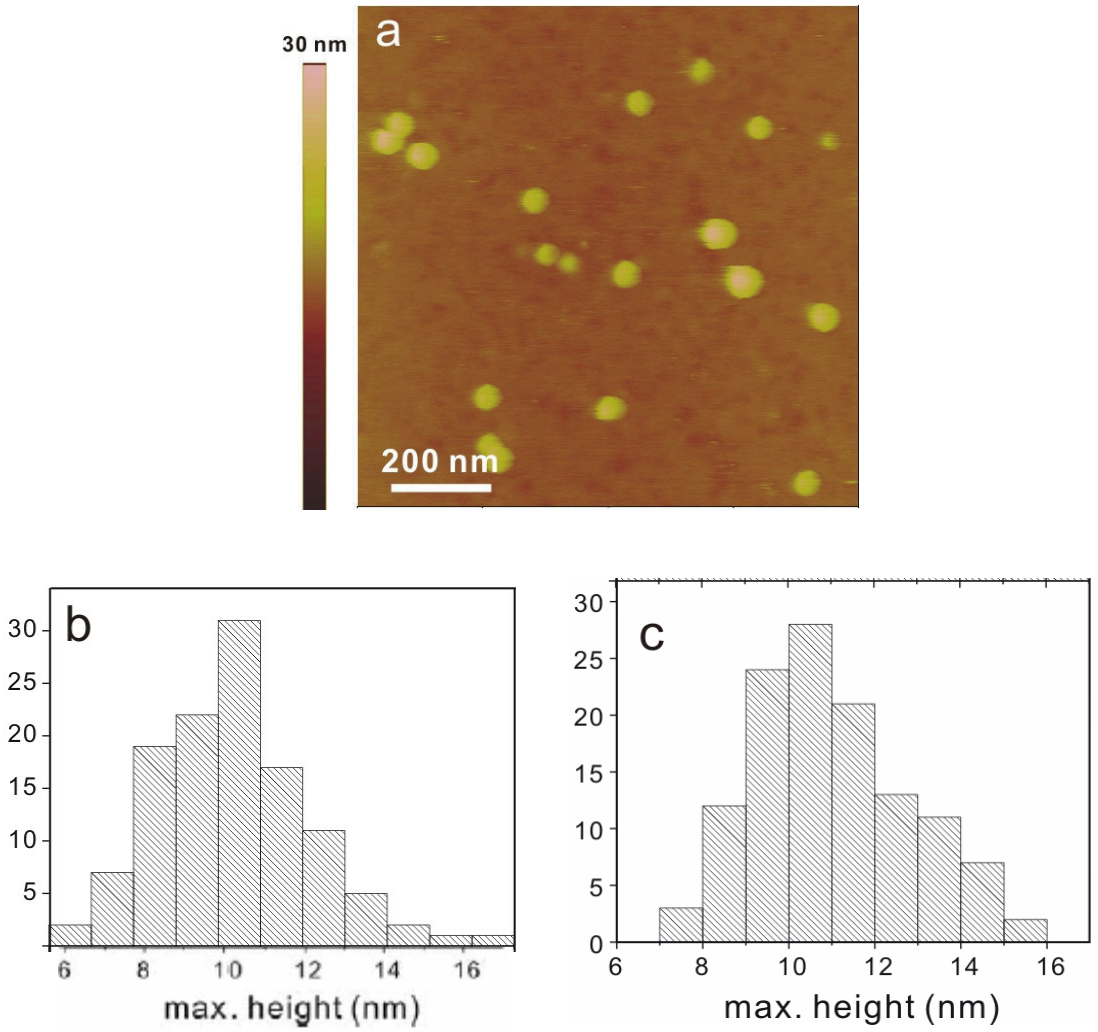

Figure 9.5 *Structural properties of the DNA block copolymer micelles investigated by Scanning Force Microscopy. a) SFM topographical image of double stranded micelles of* ***DNA-b-PPO(6.8K)*** *hybridized with amino- and carboxyl-modified ODNs before amide bond formation. The height is indicated with a color scale bar on the left. The z-scale in this image is 30 nm. The height of the micelles was expressed in histograms before b) and after c) the chemical reaction occurred.*

In the future, the application of the fluorogenic reaction will be investigated in regard to DNA detection and the potential for the identification of single nucleotide polymorphisms. The unique micellar template will further be investigated for its suitability in carrying out DNA-templated reactions that can not proceed in aqueous environment but within the hydrophobic environment of the core. DNA block copolymer micelles are also appealing candidates to carry out chemical synthesis in living cells since reactions might be allowed to take place shielded from the cellular environment.

Experimental Section

I. Formation and Characterization of Micelles

Micellization

Two different methods were employed for preparing DNA block copolymer micelles: the direct dissolution method and the dialysis method.[23] In the first method, DNA-*b*-PPO solutions (100 - 1000 mg/L) either containing deionized water or buffer medium (100 mM NaCl, 80 mM 3-(*N*-morpholino)propanesulfonic acid (MOPS)) were heated to 90 °C and were then cooled to room temperature overnight. In the dialysis method, the DNA-*b*-PPO was dissolved in dimethylformamide (1 g/L) and the resulting solution was dialyzed against deionized water for 4 days.

Characterization of DNA-PPO block copolymer Micelles

The effective hydrodynamic diameter of the micelle was measured by DLS at 25 °C using a dynamic light scattering photometer (ALV 5800, Avalanche Photodiode) equipped with He-Ne laser at a wavelength of 632 nm (**Figure 9.6**). The data were gathered and processed using the ALV 5000/E software. The samples, which were prepared in buffer medium, were dialyzed against deionized water before the measurement. The measurements were carried out in triplicate.

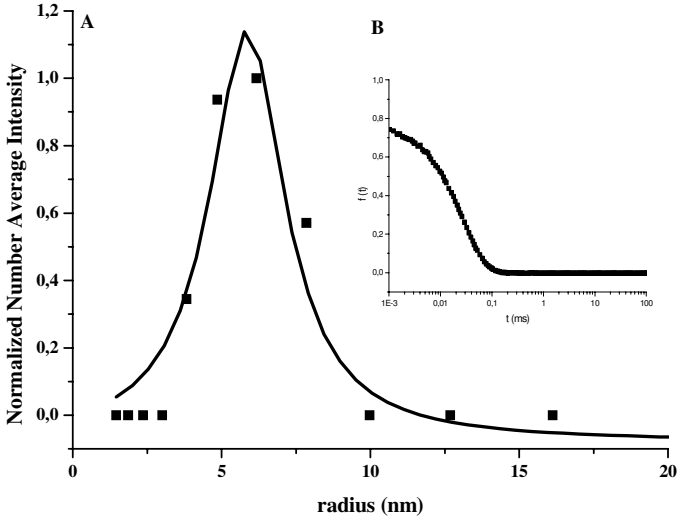

Figure 9.6 *Dynamic light scattering data of micelles of* ***5b****. A) Lorentzian size distribution. B) Correlation function.*

Measurement of CMC

The critical micelle concentration was determined by the well established fluorescence probe technique using pyrene as a chromophore.[24, 38] Several solutions of pyrene in acetone were allowed to evaporate for 3 h at 45°C yielding a final amount of 6.0 x 10^{-7} M in eppendorf tubes. By using a stock solution of DNA-*b*-PPO varying polymer concentrations ranging from 0.0005 to 5.0 g/L were prepared. The solutions were heated to 95 °C and slowly cooled to room temperature for 18 h. Fluorescence spectra were recorded at room temperature using an excitation wavelength of 339 nm. Excitation spectra were obtained at a wavelength of 390 nm. The CMCs of diblock copolymers with molecular weight of 1000 and 6800 g/mol were determined as 6 mg/L and 5 mg/L, respectively.

II. DNA-Templated Synthesis

a) DNA Templated Synthesis using the Conventional Templates (A+B+A'B'-, A+BB'A'- and A+A'). Reactions were carried out by mixing equimolar quantities of the reactant and the template in buffer containing 80 mM MOPS pH 7.5 and 100-250 mM NaCl at room temperature. Concentrations of the reactants and templates were adjusted to 90 nM. Following dilution, the reactions were analyzed by denaturing PAGE followed by ethidium bromide or SYBR safe staining. The yields were quantified by charge coupled device (CCD)-based densitometry of the product and template bands. Fluorescence spectra of the product were recorded on a fluorescence plate reader as additional structural proof. Representative compounds were characterized by MALDI-TOF MS.

DNA Sequences: The DNA sequences, which were used with the A+B+A'B'-, A+BB'A'- and A+A' templates for the fluorogenic reactions are listed below. For the A+BB'A' template: 5`-GAACTCGAAGTAGCCTCGATATCGATATCGA-SH-3' and 5'-$NH_2$-GCTACTTCGAGTTC-3'; For the A+A' template: 5'-$NH_2$ –ATCTTTAGT TTAGCCTAGTATATATCTTGC-3' and 5`-GCAAGATATATACTAGGCTAAACTAA AGAT-SH-3'; For the A+B+A'B' template: 5'- GCAAGATATATACTAGGCT AAACTAAAGAT-3`, 5'-$NH_2$-TAGTATATATCTTGC-3` and 5`-ATCTTTAGTTT AGC-SH-3'. The control experiments were carried out with the following sequences: For the A+A' template: 5'-ATCTTTAGTTTAGCCTAGTATATATCTTGC-3' was used without amino modification (**Figure 9.8**, Lane 2) and 5'-TACGATTACATCGTCA TGTCCGATTTCTGC-

SH-3' as mismatching sequence (**Figure 9.8**, Lane 4); For the A+BB'A' template: 5'-TACGATTACATCGTCATGTCCGATTTCTGC-SH-3' was applied as mismatching sequence (**Figure 9.8**, Lane 6); For the A+B+A'B' template: 5'-HS-GCTTTTCTACGATCG-3' and 5'- CAAGACTCAGTTAA- NH_2-3' sequences were used as non-matching sequences (**Figure 9.8**, Lane 8).

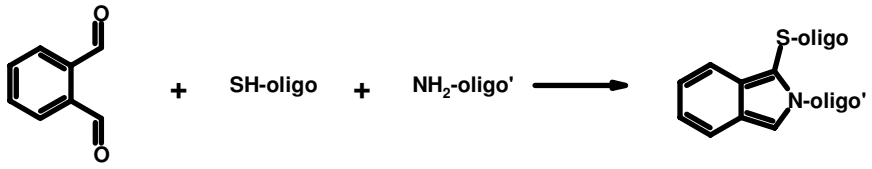

Figure 9.7 *DNA-templated isoindole formation.*

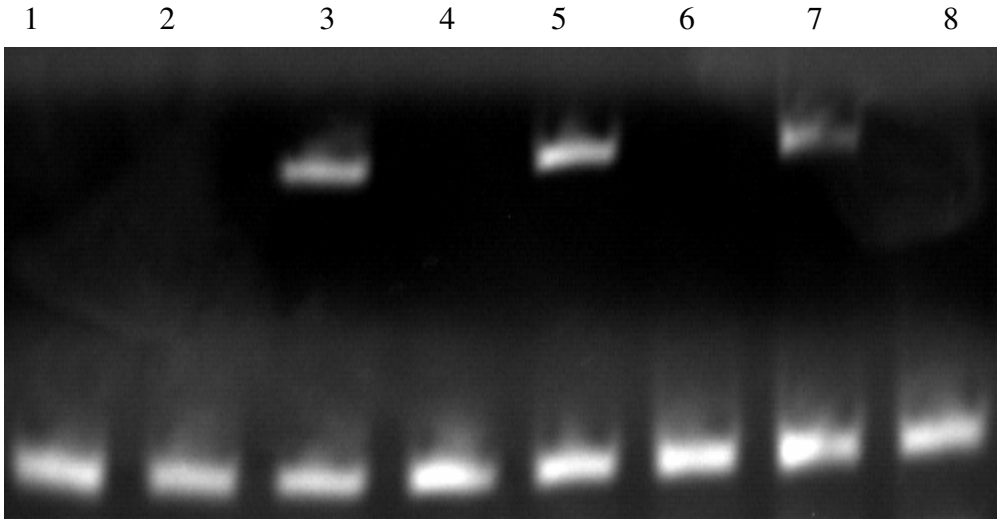

Figure 9.8 *Analysis by denaturing PAGE of the DNA-templated isoindole formation using the conventional templates. Lane 1 shows the A+A' template. Lane 2 gives the reaction where the oligonucleotide was not functionalized with an amino group. Lane 3 shows the reaction with the A+A' template applying matching conditions which resulted in product formation represented by the band with lower electrophoretic mobility (Yield: 32%). Lane 4 shows the reaction with mismatching sequences in the A+A' template configuration, which resulted in no product formation. Lane 5 and 6 represent the A+BB'A' template with matching and mismatching templates, respectively (Yield: 14%). Lane 7 shows the reaction with A+B+A'B' template resulting in 12% yield. Lane 8 represents the reaction using mismatching sequences for the A+B+A'B' template.*

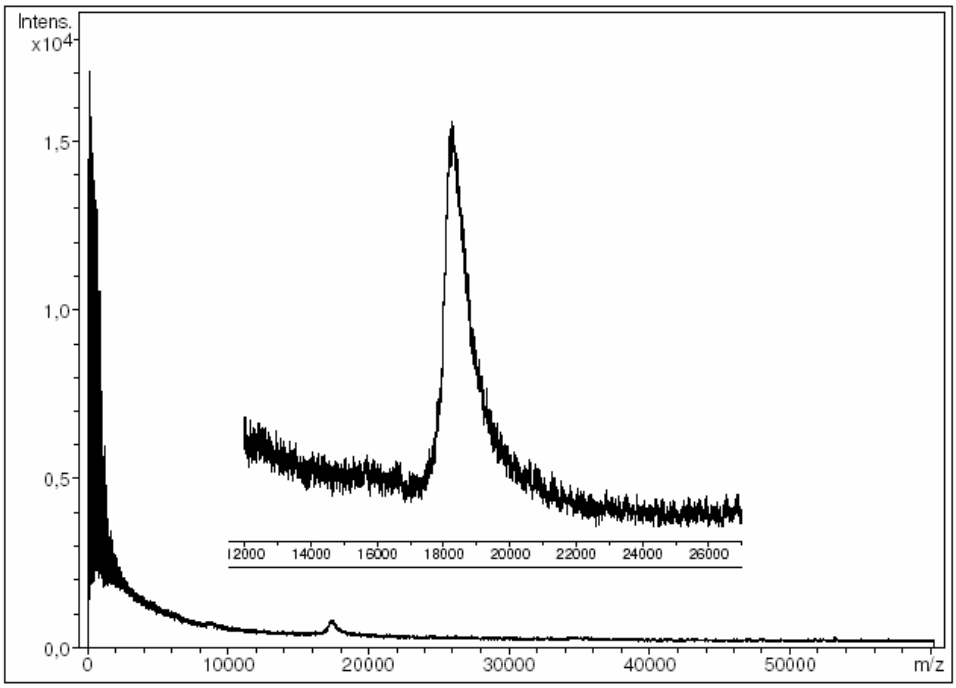

Figure 9.9 *MALDI-TOF spectrum of the purified reaction of the A+A' template (**Lane 3**) using 3-hydroxypicolinic acid as the matrix. Mass: 18,789 (found) and 18,856 (calculated)*

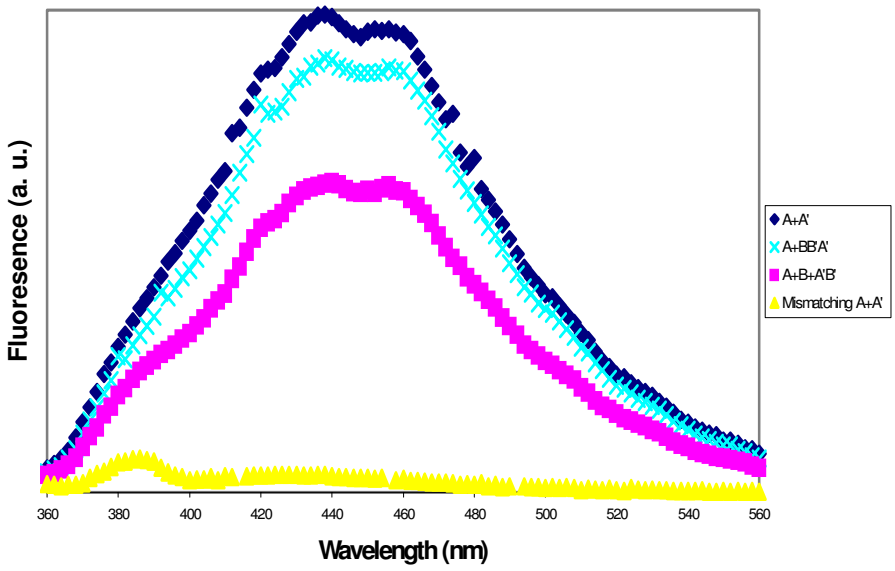

Figure 9.10 *Fluorescence spectra of the isoindole formation by DNA-templated synthesis using A+B+A'B'-, A+BB'A'- and A+A'-templates. Yellow line represents a mismatching A+A' template configuration.*

DNA-Templated Synthesis using the Micelle Template

DNA-templated synthesis. Reactions with the 3-D template were carried out by mixing the DNA-PPO diblock copolymer micelles composed of ***DNA-b-PPO(6.8K)*** with equimolar quantities of the reactant functionalized ODNs. The functional groups were adjusted to a 1/1-ratio. In the case of the isoindole formation, the *o*-phthaldialdehyde was used in two-fold excess. Concentrations of the micelle template were 250-550 nM in a reaction buffer containing 80 mM MOPS pH 7.5 and 100-500 mM NaCl. The following sequences were used and are written in the 5' to 3' direction. ***DNA-b-PPO(6.8K)***: CCTCG CTCTGCTAATCCTGTTA, matching reactants: TAACAGGATTAG CAGAGCGAGG, non-matching reactants: GCAGATTCTTGGAACTATGCTT, AAAACACAGTGACGG CCTAGCC. The reactions were analyzed by denaturing PAGE followed by ethidium bromide or SYBR safe staining. The yields were quantified by CCD-based densitometry of the product and template bands. For the isoindole formation, fluorescence spectra of the product were recorded on a fluorescence plate reader (SpectraMax M2, Molecular devices) as additional structural proof.

Michael Addition at the Rim of the Micelles:

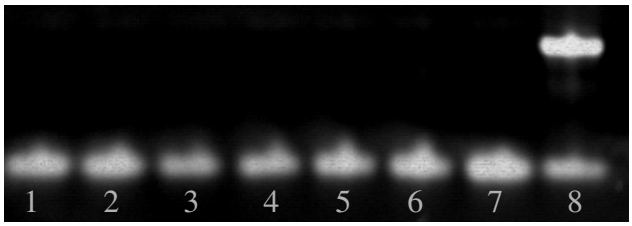

Figure 9.11 *Analysis by denaturing PAGE of the DNA-templated Micheal addition at the rim of the micelles. Lanes 1-7 contain the control experiments where reaction conditions were modified in contrast to lane 8 accordingly. Lanes 1 and 2: Use of complementary sequences in regard to the template but without terminal sulfhydryl and maleimido groups. Lanes 3 and 4: Application of mismatching ODNs in respect to the template modified with thiol and maleimido functionalities. Lane 5: Reaction without the micelles composed of* ***DNA-b-PPO(6.8K)****. Lane 6: Conversion with the template sequence but without PPO attachment. Lane 7: Applying the DNA block copolymer* ***DNA-b-PPO(6.8K)*** *as a template below the CMC. Lane 8 shows the fully matching reaction conditions, which resulted in product formation represented by the band with lower electrophoretic mobility. (Yield: 74%)*

Michael Addition at the hydrophobic/hydrophilic Interface:

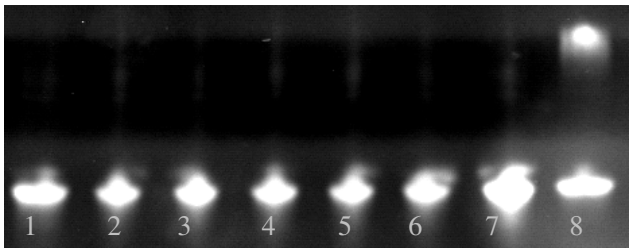

Figure 9.12 *Analysis by denaturing PAGE of the DNA-templated Micheal addition at the interface of the biological and the organic polymer segment of the micelles. Lanes 1-7 contains the control experiments where reaction conditions were modified in contrast to lane 8 accordingly. Lanes 1 and 2: Use of complementary sequences in regard to the template but without terminal sulfhydryl and maleimido groups. Lanes 3 and 4: Application of mismatching ODNs in respect to the template modified with sulfhydryl and maleimido functionalities. Lane 5: Reaction without the micelles composed of* ***DNA-b-PPO(6.8K)****. Lane 6: Conversion with the template sequence but without PPO attachment. Lane 7: Applying the DNA block copolymer* ***DNA-b-PPO(6.8K)*** *as a template below the CMC. Lane 8 shows the fully matching reaction conditions, which resulted in product formation represented by the band with lower electrophoretic mobility. (Yield: 59%)*

Amide Formation at the Rim of the Micelles:

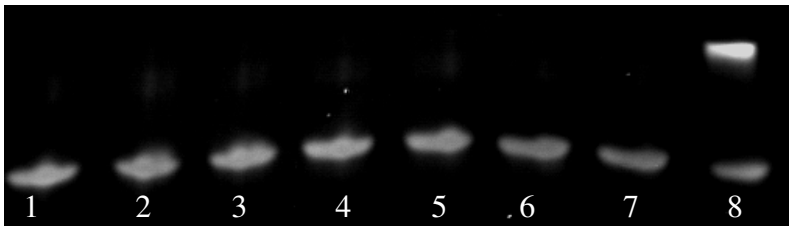

Figure 9.13 *Analysis by denaturing PAGE of the DNA-templated amide formation at the rim of the micelles. Lanes 1-7 contain the control experiments where reaction conditions were modified in contrast to lane 8 accordingly. Lanes 1 and 2: Use of complementary sequences in regard to the template but without terminal carboxyl and amino groups. Lanes 3 and 4: Application of mismatching ODNs in respect to the template modified with carboxyl and amino functionalities. Lane 5: Reaction without the micelles composed of* ***DNA-b-PPO(6.8K)****. Lane 6: Conversion with the template sequence but without PPO attachment. Lane 7:*

*Applying the DNA block copolymer **DNA-b-PPO(6.8K)** as a template below the CMC. Lane 8 shows the fully matching reaction conditions, which resulted in product formation represented by the band with lower electrophoretic mobility. (Yield: 72%)*

Amide Formation at the hydrophobic/hydrophilic Interface:

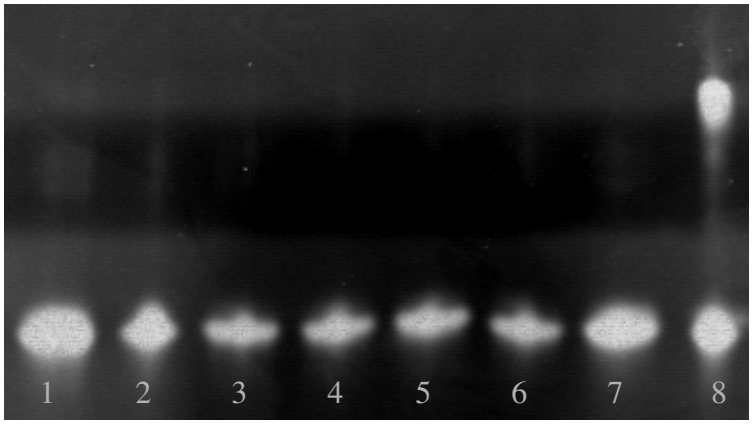

Figure 9.14 *Analysis by denaturing PAGE of the DNA-templated amide formation at the interface of the biological and the organic polymer segment of the micelles. Lanes 1-7 contain the control experiments where reaction conditions were modified in contrast to lane 8 accordingly. Lanes 1 and 2: Use of complementary sequences in regard to the template but without terminal carboxyl and amino groups. Lanes 3 and 4: Application of mismatching ODNs in respect to the template modified with carboxyl and amino functionalities. Lane 5: Reaction without the micelles composed of **DNA-b-PPO(6.8K)**. Lane 6: Conversion with the template sequence but without PPO attachment. Lane 7: Applying the DNA block copolymer **DNA-b-PPO(6.8K)** as a template below the CMC. Lane 8 shows the fully matching reaction conditions, which resulted in product formation represented by the band with lower electrophoretic mobility. (Yield: 61%)*

III. SFM Measurements

Twenty microliters of a 100 mg/l DNA-block-PPO solution in buffer (10 mM Tris PH 7.4, 1 mM $NiCl_2$) were deposited onto freshly cleaved mica (Plano GmbH, Germany). After 5 min incubation the samples were rinsed with 200 µl of buffer solution. The mica sheet was then mounted in the SFM keeping the surface always covered by buffer solution.

All images were recorded using a commercial SFM (Multimode, Nanoscope IIIa, Veeco Instruments, California USA) in soft tapping mode in liquid. Oxide-sharpened silicon nitride cantilevers (NP-S, Veeco Instruments, California; 115 µm long, 17 µm wide, 0.6 µnm thick) with an integrated tip (a spring constant of 0.32 N/m and a resonance frequency of 56 kHz in air) were used. The height of the tip was 2.5 to 3.5 µm. The tip radius was confirmed by scanning electron microscopy after having performed the SFM measurements. We found tip radii of curvatures < 20 nm in all cases. A piezoelectric E-scanner (Veeco Instruments, California) was used, which supplies a maximum x-, y-scan of 12.5 µm and a z-extension of 2.5 µm. The scanner was calibrated by imaging a rectangular grid of 1 µm × 1 µm mesh size.

In liquids, we selected a driving frequency between 8 – 10 kHz for imaging. SFM images (512x512 pixels) were recorded with a scan size of 1 x 1 μm^2 at a scan rate of 1 Hz. The raw data has been modified by applying the first order "flatten" filter. The maximum height of individual micelles was calculated by means of local roughness analysis. Height values determined from > 100 micelles obtained from 5 SFM pictures are plotted together in the histograms. A mean height of 10.4 ± 1.8 nm was calculated for micelles before the reaction. Additionally, analysis was performed after the chemical reaction, which resulted in a similar looking histogram having a mean height value of 11.0 ± 2.0 nm.

References

[1] X. Y. Li, D. R. Liu, *Angew. Chem. Int. Ed.* **2004**, *43*, 4848.

[2] D. Summerer, A. Marx, *Angew. Chem. Int. Ed.* **2002**, *41*, 89.

[3] Z. J. Gartner, M. W. Kanan, D. R. Liu, *Angew. Chem. Int. Ed.* **2002**, *41*, 1796.

[4] Z. J. Gartner, D. R. Liu, *J. Am. Chem. Soc.* **2001**, *123*, 6961.

[5] Z. J. Gartner, M. W. Kanan, D. R. Liu, *J. Am. Chem. Soc.* **2002**, *124*, 10304.

[6] J. L. Czlapinski, T. L. Sheppard, *J. Am. Chem. Soc.* **2001**, *123*, 8618.

[7] R. L. Letsinger, T. F. Wu, *J. Am. Chem. Soc.* **1994**, *116*, 811.

[8] Z. C. Ma, J. S. Taylor, *Proc. Natl. Acad. Sci. U. S. A.* **2000**, *97*, 11159.

[9] J. Brunner, A. Mokhir, R. Kraemer, *J. Am. Chem. Soc.* **2003**, *125*, 12410.

[10] Y. Z. Xu, N. B. Karalkar, E. T. Kool, *Nature Biotech.* **2001**, *19*, 148.

[11] A. Mattes, O. Seitz, *Angew. Chem. Int. Ed.* **2001**, *40*, 3178.

[12] A. Demesmaeker, R. Haner, P. Martin, H. E. Moser, *Acc. Chem. Res.* **1995**, *28*, 366.

[13] J. F. R. Ortigao, A. Ruck, K. C. Gupta, R. Rosch, R. Steiner, H. Seliger, *Biochimie* **1993**, *75*, 29.

[14] D. Magda, R. A. Miller, J. L. Sessler, B. L. Iverson, *J. Am. Chem. Soc.* **1994**, *116*, 7439.

[15] Q. B. Zhou, S. E. Rokita, *PNAS* **2003**, *100*, 15452.

[16] Z. J. Gartner, B. N. Tse, R. Grubina, J. B. Doyon, T. M. Snyder, D. R. Liu, *Science* **2004**, *305*, 1601.

[17] M. W. Kanan, M. M. Rozenman, K. Sakurai, T. M. Snyder, D. R. Liu, *Nature* **2004**, *431*, 545.

[18] Z. J. Gartner, R. Grubina, C. T. Calderone, D. R. Liu, *Angew. Chem. Int. Ed.* **2003**, *42*, 1370.

[19] K. J. Luebke, P. B. Dervan, *J. Am. Chem. Soc.* **1989**, *111*, 8733.

[20] A. T. Poulin-Kerstien, P. B. Dervan, *J. Am. Chem. Soc.* **2003**, *125*, 15811.

[21] L. H. Eckardt, K. Naumann, W. M. Pankau, M. Rein, M. Schweitzer, N. Windhab, G. von Kiedrowski, *Nature* **2002**, *420*, 286.

[22] S. Forster, V. Abetz, A. H. E. Muller, *Adv. Polym. Sci.* **2004**, *166*, 173.

[23] C. Allen, D. Maysinger, A. Eisenberg, *Colloids and Surfaces B-Biointerfaces* **1999**, *16*, 3.

[24] J. H. Jeong, T. G. Park, *Bioconjugate Chem.* **2001**, *12*, 917.

[25] Z. Li, Y. Zhang, P. Fullhart, C. A. Mirkin, *Nano Lett.* **2004**, *4*, 1055.

[26] J. Selb, Y. Gallot, *Makromolekulare Chemie-Macromolecular Chemistry and Physics* **1980**, *181*, 809.

[27] D. W. Miller, E. V. Batrakova, T. O. Waltner, V. Y. Alakhov, A. V. Kabanov, *Bioconjugate Chem.* **1997**, *8*, 649.

[28] L. F. Zhang, A. Eisenberg, *Science* **1995**, *268*, 1728.

[29] M. Roth, *Anal. Chem.* **1971**, *43*, 880.

[30] P. de Montigny, J. F. Stobaugh, R. S. Givens, R. G. Carlson, K.Srinivasachar, L. A. Sternson, T. Higuchi, *Anal. Chem.* **1987**, *59*, 1096.

[31] K. B. Thurmond, T. Kowalewski, K. L. Wooley, *J. Am. Chem. Soc.* **1996**, *118*, 7239.

[32] H. Y. Huang, E. E. Remsen, T. Kowalewski, K. L. Wooley, *J. Am. Chem. Soc.* **1999**, *121*, 3805.

[33] V. Butun, N. C. Billingham, S. P. Armes, *J. Am. Chem. Soc.* **1998**, *120*, 12135.

[34] J. F. Ding, G. J. Liu, *Macromolecules* **1998**, *31*, 6554.

[35] M. Iijima, Y. Nagasaki, T. Okada, M. Kato, K. Kataoka, *Macromolecules* **1999**, *32*, 1140.

[36] Y. Y. Won, H. T. Davis, F. S. Bates, *Science* **1999**, *283*, 960.

[37] Y. Kakizawa, A. Harada, K. Kataoka, *J. Am. Chem. Soc.* **1999**, *121*, 11247.

[38] M. Wilhelm, C. L. Zhao, Y. C. Wang, R. L. Xu, M. A. Winnik, J. L. Mura, G. Riess, M. D. Croucher, *Macromolecules* **1991**, *24*, 1033.

10 Shape Matters: Cellular Uptake of DNA Block Copolymer Micelles*

"Actually, nanotechnology has been around for over a hundred years. […] Nanoscience is a label given now to the new work emerging from the technology we have developed to manipulate, visualize and make atomic and molecular structures."

Dr. Peter Dobson, 2006

The cellular uptake of particles with sizes in the regime of nanometers is of great importance for two reasons. First, in biomedicine such particles have great potential as delivery systems for therapeutics or as carriers of imaging reagents. Second, with the incorporation of nanoparticles in commercial products, concerns have arisen about their toxicity and their influence on living matter. In the context of organic nanoparticle fabrication, polymers play an important role. Representatives of this class of materials are dendrimers,[1] polymer latices[2] and block copolymers.[3] When the latter consist of hydrophilic and hydrophobic segments these materials tend to form spherical micelles in aqueous solutions and thus can be regarded as nanoparticles. Recently, a special type of amphiphilic block copolymer with DNA as a water soluble segment and a hydrophobic organic polymer unit was introduced.[4, 5] The resulting spherical aggregates with a shell of ss DNA were employed to deliver ASOs,[6] to produce binary assemblies with DNA-coated Au-nanoparticles[7] and to act as programmable scaffolds for DNA-templated organic reactions.[8] Furthermore, the influence of hybridizing the ss DNA corona of the micelles with different sequences was investigated.[9] It turned out that hybridization with short sequences that are complementary to the corona does not change the structural properties of the micelles. However, when long DNA sequences that encode several times the complementary sequence of the corona were employed for hybridization,

* Parts of this chapter were submitted for publication.

highly uniform rod-like aggregates consisting of two parallel aligned DNA double helices were formed (**Figure 10.1**).

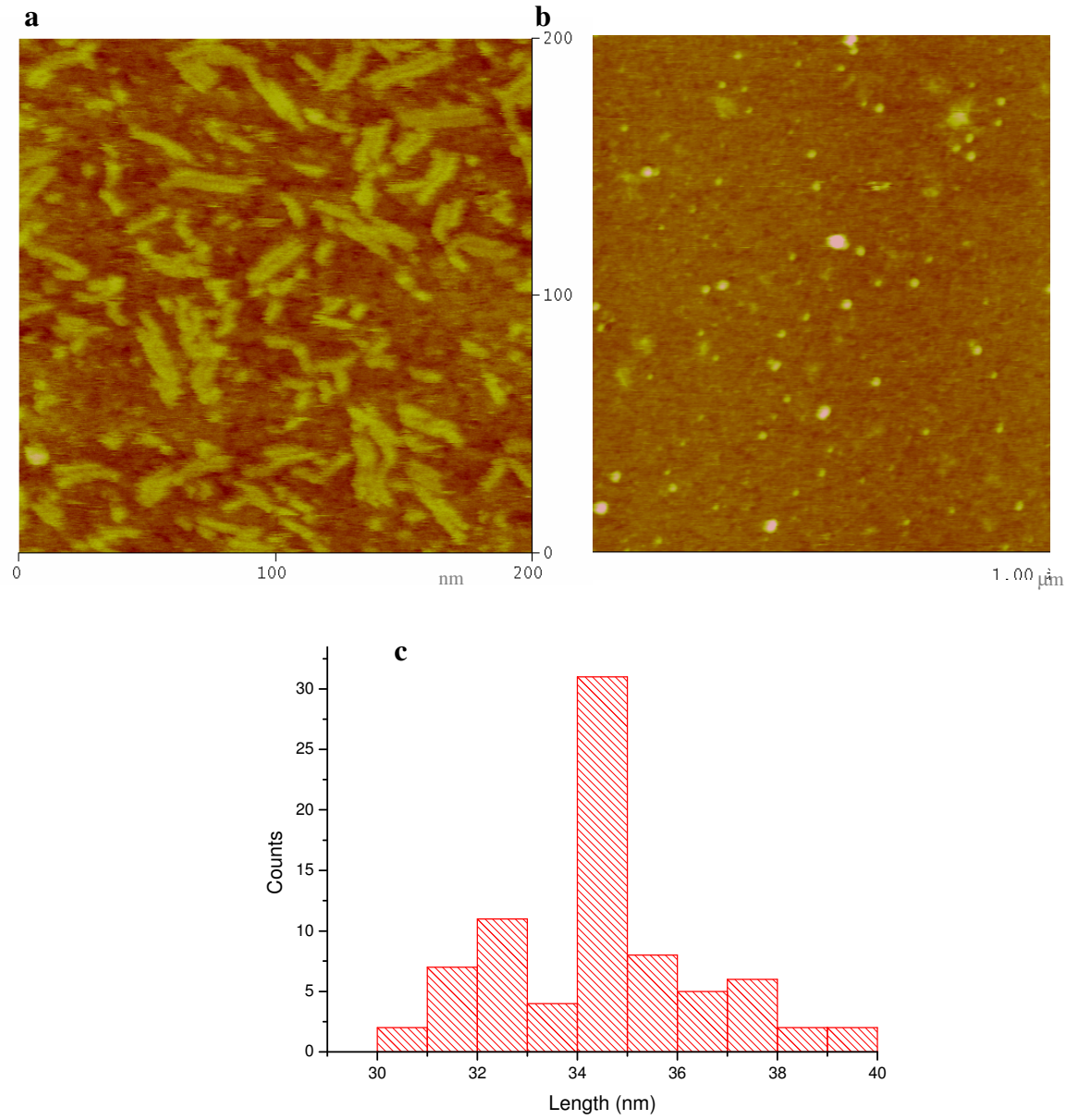

Figure 10.1 *SFM topography image of **a)** rod-like micelles and **b)** spherical micelles. **c)** The length of the rod-like aggregates was expressed in a histogram.*

Within this chapter we investigate the cellular uptake of DNA block copolymer aggregates with a ss and ds DNA corona as well as with different shapes. For spherical block copolymer micelles the influence of several physical parameters such as size and surface charge on the

entry into cells was investigated. These results suggest that it is also worthwhile to explore the morphology of the aggregates as an important structural feature. An amphiphilc DNA block copolymer combining a 22 mer ODN (sequence: 5'-CCTCGCTCTGCTAATCCTGTTA-3') with a PPO segment (MW= 6800 g/mol) in a covalent fashion was produced by employing an automated grafting onto strategy on the solid support as described in *Chapter 3*.[8] PPO was selected as the hydrophobic component to provide a polymer with proven biocompatibility toward different cell types when administered as a constituent component of amphiphilic block copolymer micelles. Ss micelles were obtained by dissolving DNA-*b*-PPO in HEPES buffer and heating. Ds DNA block copolymer aggregates were obtained by hybridization either with the complementary sequence T22 (sequence: 5'-TAACAGGATTAGCAGAGCGAGG-3') or with a ODN T110 (sequence: 5'-$(TAACAGGATTAGCAGAGCGAGG)_5$-3') five times encoding the complement of DNA-*b*-PPO, resulting in spherical micelles with a ds corona or rod-like micelles consisting of two parallel aligned doubles helices, respectively (**Figure 10.1**). Ss- and ds spherical micelles exhibited a diameter of 5.1 ± 1.8 nm and 5.4 ± 1.6 nm, respectively, as detected by DLS. For the rod-like particles a length and width of 37 ± 1 and 1.95 ± 0.1 nm was determined by scanning force microscopy, respectively (**Figure 10.1**).

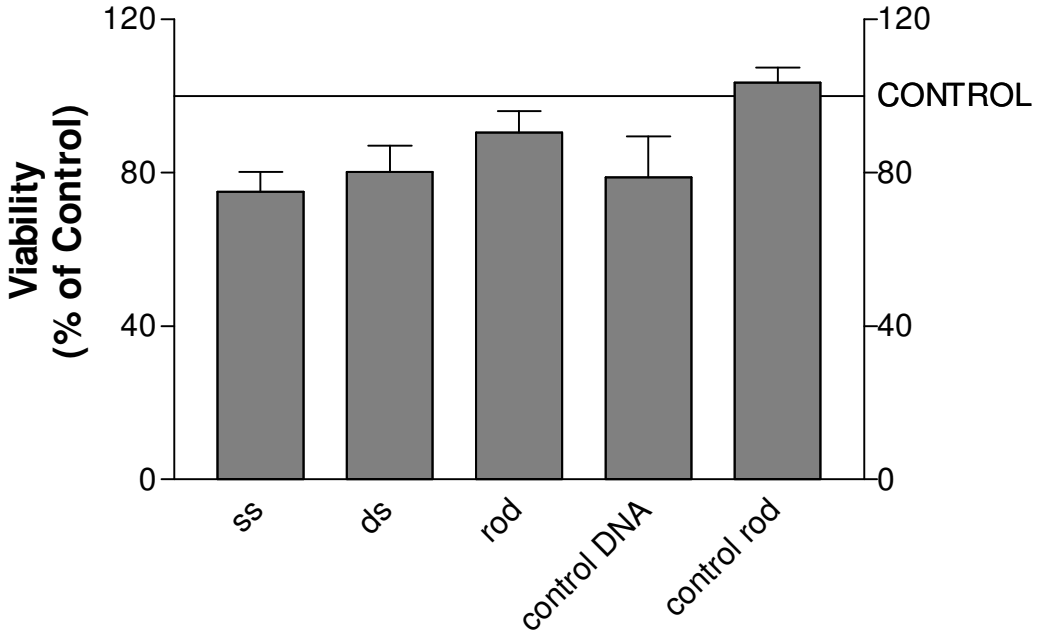

Figure 10.2 *XTT based toxicology assay.* **(***ss, ds and rod represent the corresponding micelles)*

Prior to the study of the uptake of the different nanoparticles, their cytotoxicity was assessed using an XTT *in vitro* proliferation assay together with *N.C. Alemdaroglu* in the group of *Prof. Dr. P. Langguth* from University of Mainz. Human colon adenocarcinoma cell line (Caco-2) cells showed a high viability when incubated with the different types of DNA block copolymer micelles as well as with DNA controls being non-modified by the organic polymer (**Figure 10.2**). Although, different nanoparticles showed varying toxicity, the viability of the cells were more than 75 % which might be considered non-toxic according to the literature.[10] Motivated by the harmless nature of the bioorganic hybrid materials, the uptake of the nanoparticles in the same cell line was investigated. For these experiments the micelles were labeled with a fluorophore. 5'-Alexa488-modified ODNs with the sequence of T22 or T110 were employed for hybridization with the micelles introducing the fluorescent reporter. Then the Caco 2 cells were incubated with the DNA block copolymer aggregates at a concentration of 300 μg/ml for 3 h. Similar conditions have been employed to study the uptake of polymer functionalized ODNs[11] and block copolymer aggregates.[6, 12] The internalization of the nanoparticles was investigated by confocal laser scanning microscopy (CLSM) and after lysis of the cells by fluorescence spectroscopy. The latter method allows comparative quantification of the uptake of the different DNA block copolymer aggregates. It turned out that the rod-like particles were internalized 12 times more efficiently than the spherical particles that were taken up similarly. The uptake of the pristine DNA controls was significantly less than for the micelle architectures (**Figure 10.3**).

CLSM has proven to be a powerful tool for acquiring high resolution images, 3-D reconstructions as well as for the visualization of internalization of nanoparticles. The fluorescence microscopy images show that the nanoparticles were distributed homogenously inside the cells and did not just adsorb to the surface (**Figures 10.4** and **10.5**). No distinct patterns of subcellular staining were observed. In the case of the spherical micelles CLSM revealed different degrees of uptake among the cells. While some of the cells were stained intensively others did not show any fluorescence. This may be explained by the heterogeneous population of Caco-2 cells leading to different uptake behavior of the cells in the same population.[13]

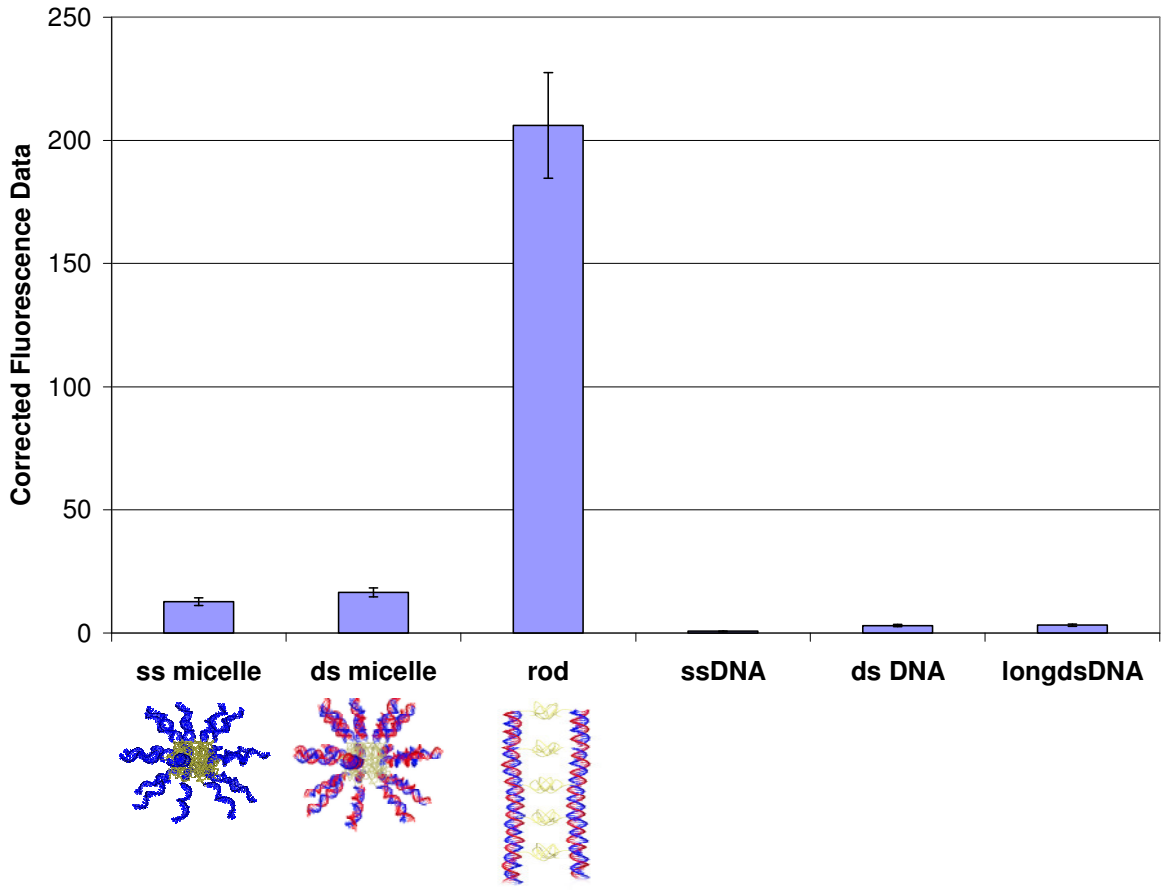

Figure 10.3 *Internalization of the nanoparticles monitored after lysis of the cells by fluorescence spectroscopy. The micelle aggregates were compared with the pristine DNA controls.*

The uptake of block copolymer aggregates has been studied intensively in the context of drug and gene delivery. However, these systems consisted exclusively of spherical nanosized objects; the internalization of rod-like block copolymer micelles has never been investigated. The uptake of rod-like nanoparticles was demonstrated for carbon nanotubes.[14] The only comparative study where nano-objects of different shape were employed deals with inorganic nanoparticles.[15] These experiments revealed lower uptake of rod-shaped Au-nanoparticles compared to their spherical counterparts. However, the Au-nanoparticles of different geometries varied in surface functionalization and the rod-shaped particles were contaminated with nonrod-shaped byproducts. In the experiments presented here contrary uptake behavior for DNA block copolymer nanoparticles was observed. Rod-like particles were internalized more efficiently than spherical particles. It should be pointed out here that the structures of the block copolymer aggregates were well defined.

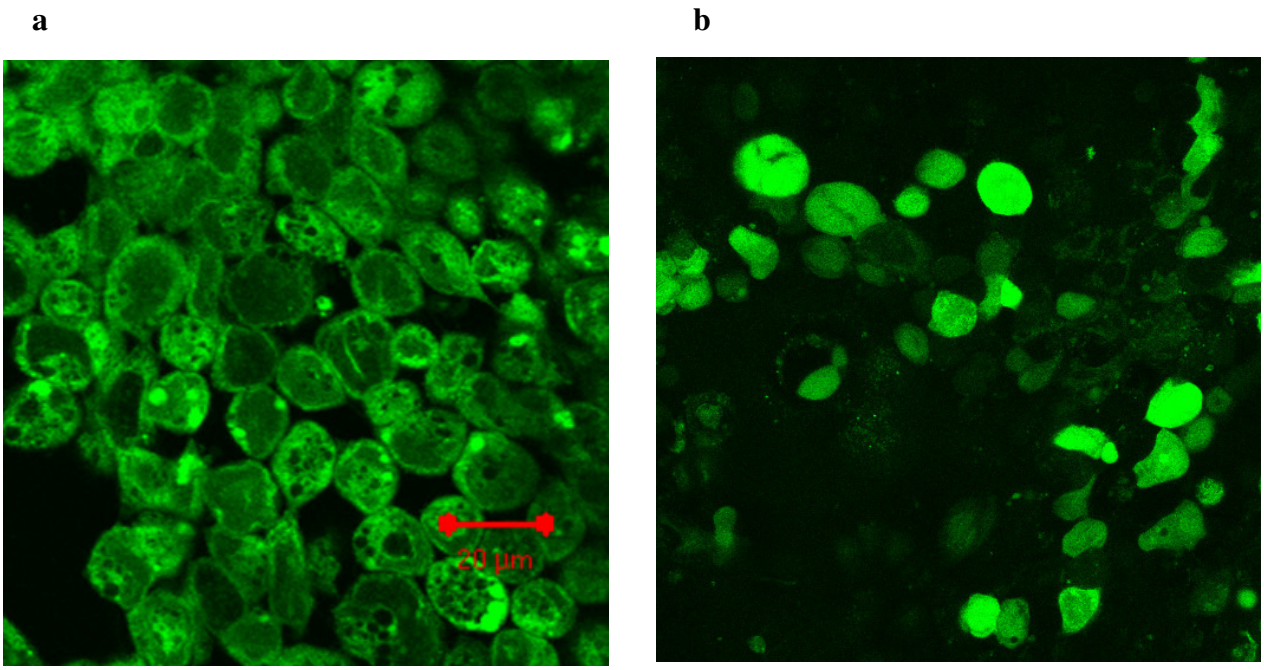

Figure 10.4 *CLSM image of the Caco-2 cells stained by labeled a) rod-like b)spherical micelles.*

A possible explanation for the shape-dependent uptake might be different uptake processes for nanoparticles with varying geometries. Since in the rod-like particles the hydrophobic PPO blocks that could interact with the cell membrane are less shielded than in the spherical particles, adsorptive endocytosis might play a major role. In contrast, the spherical micelles with the hydrophobic PPO buried in their interior might be taken up by fluid phase pinocytosis due to electrostatic repulsion of the negatively charged micelle corona and the cell surface as suggested for ODN-*b*-PLGA micelles.[6] The fact that the DNA block copolymer micelles were internalized more efficiently than the pristine DNA controls is in agreement with the literature and was also observed in uptake studies of ODN-*b*-PLGA aggregates.[6]

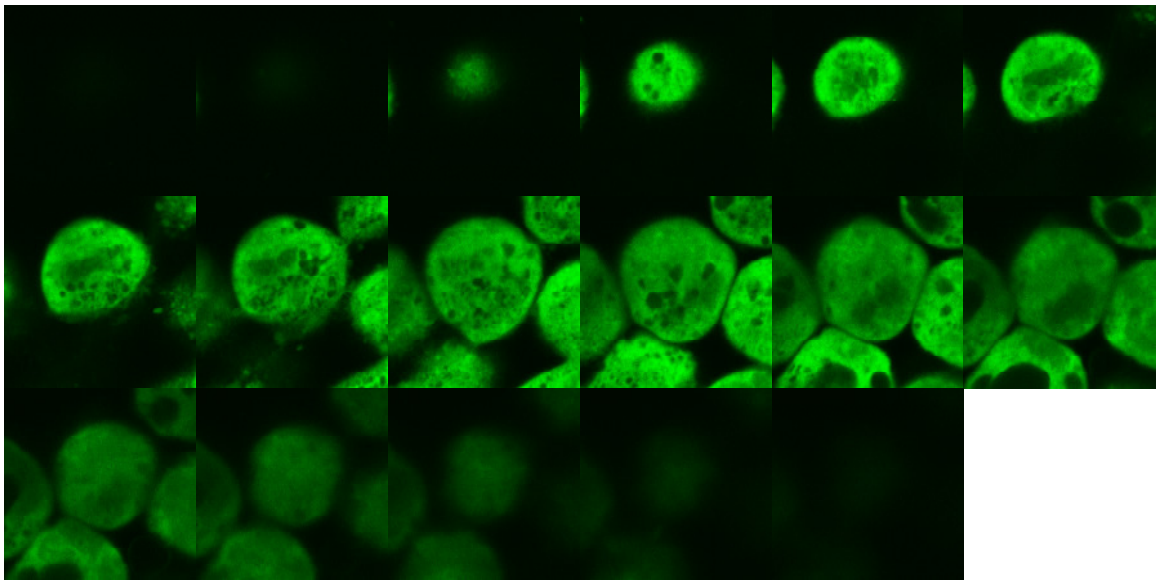

Figure 10.5 *3-D fluorescence picture shows the homogenous uptake behavior of the labeled rod-like nanoparticles into cells.*

In summary, the cellular uptake of DNA block copolymer aggregates with different shapes was investigated. It was found that rod-like nanoparticles were internalized to a much greater degree than were spherical particles although both types of self-assembled structures were built up from the same components. In future work, the uptake mechanism of these nano-objects will be elucidated in greater detail.

Experimental Section

Materials and Methods:

Caco-2 cells were from Deutsche Sammlung von Mikroorganismen und Zellkulturen GmbH (DSMZ), Braunschweig, Germany. All the cell culture media and supplements were purchased from Biochrom AG, Berlin, Germany. HEPES was provided from Merck, Darmstadt, Germany.

Preparation of Caco-2 monolayers for uptake studies

Caco-2 cells (passage number 45) were cultured at 37 °C in an atmosphere of 5% CO_2 and 90% relative humidity in 75 cm^2 cell culture flasks containing Dulbecco's modified Eagle's medium (DMEM) supplemented with 10% fetal bovine serum (FBS), 1% nonessential amino acids, 100 U/ml penicillin and 100 µg/ml streptomycin. The cells were routinely split and seeded into 6-well plates (Nunclon™ Multidishes, Life Technologies GmbH, Karlsruhe, Germany) with 800000 cells/well. The medium was changed three times a week. The development of the monolayers was examined under the microscope until the 16^{th} day. Then the monolayer cultures were used for uptake studies.

Cytotoxicity Assay

Prior to the uptake experiments, the cytotoxicity of the nanoparticles was checked using XTT in vitro toxicology assay kit following the procedure of the manufacturer (Sigma-Aldrich Chemie GmbH, Steinheim, Germany). The cytotoxicity of ss DNA of 22mer (control DNA) and the ssDNA 110mer (control rod) were compared with the ss, ds and rod-like nanoparticles.

Nanoparticle uptake studies

Uptake studies were performed on day 16. For the uptake studies, the growth medium was removed and the Caco-2 monolayer in each well was washed twice with the HBSS containing 5 mmol/l 4-(2-hydroxyethyl)-1-piperazineethanesulfonic acid (HEPES) adjusted to pH 7.4.

The wells were filled and incubated with 2 ml of PPO-*b*-DNA micelles hybridized with Alexa488-labeled complementary ODN added to attain a concentration of 300 µg/ml. After 3h incubation at 37 °C the medium was discarded and cells were washed five times with ice-cold buffer solution to remove non-specific binding as much as possible. The cell monolayers were then solubilized with 700 µl of 1.25 mM NaOH. Then the suspension was centrifuged to remove the cells and the fluorescence signal of the supernatant was measured.

Microscopy:

For the microscopy analysis, the Caco-2 cells were seeded at a density of 20000 cells/cm^2 on chamber slides (Lab-Tek, Germany). The cell monolayers were incubated with 300 µg/ml of the nanoparticles labeled with Alexa488 for 3 hours, washed 5 times with pH 7.4 Hank's balanced salt solution (HBSS) and subsequently, after the addition of sufficient volume of buffer, analyzed with confocal laser scnning microscopy (excitation 488nm).

References

[1] E. V. Andreitchenko, C. G. Clark, R. E. Bauer, G. Lieser, K. Müllen, *Angew. Chem. Int. Ed.* **2005**, *44*, 6348.

[2] J. M. Asua, *Polymeric Dispersions*, Kluwer Academic, Dordrecht, **1997**.

[3] S. Förster, V. Abetz, A. H. E. Müller, *Adv. Polym. Sci.* **2004**, *166*, 173.

[4] F. E. Alemdaroglu, M. Safak, J. Wang, R. Berger, A. Herrmann, *Chem. Commun.* **2007**, 1358.

[5] F. E. Alemdaroglu, A. Herrmann, *Org. Biomol. Chem.* **2007**, *5*, 1311

[6] J. H. Jeong, T. G. Park, *Bioconjugate Chem.* **2001**, *12*, 917.

[7] Z. Li, P. Fullhart, C. A. Mirkin, *Nano Lett.* **2004**, *4*, 1055.

[8] F. E. Alemdaroglu, K. Ding, R. Berger, A. Herrmann, *Angew. Chem. Int. Ed.* **2006**, *45*, 4206.

[9] K. Ding, F. E. Alemdaroglu, M. Börsch, R. Berger, A. Herrmann, *Angew. Chem. Int. Ed.* **2007**, *46*, 1172.

[10] M. Lucarelli, A. M. Gatti, G. Savarino, P. Quattroni, L. Martinelli, E. Monari, D. Boraschi, *Eur. Cytokine Netw.* **2004**, *15*, 339.

[11] S. Cogoi, M. Ballico, G. M. Bonora, L. E. Xodo, *Cancer Gene Therapy* **2004**, *11*, 465.

[12] Y. S. Nam, H. S. Kang, J. Y. Park, T. G. Park, S. H. Han, I. S. Chang, *Biomaterials* **2003**, *24*, 2053.

[13] S. Ferruzza, M. L. Scarino, G. Rotilio, M. R. Ciriolo, P. Santaroni, A. O. Muda, Y. Sambuy, *Am. J. Physiol.-Gastroint. Liver Physiol.* **1999**, *277*, G1138.

[14] N. Wong, S. Kam, Z. Liu, H. Dai, *Angew. Chem. Int. Ed.* **2006**, *45*, 577.

[15] B. D. Chithrani, A. A. Ghazani, W. C. W. Chan, *Nano Lett.* **2006**, *6*, 662.

11 DNA Block Copolymer Micelles – A Combinatorial Tool for Cancer Nanotechnology *

"Certainly, I hope that nanoparticles will be useful in targeting drugs for cancer treatment and many other diseases in the years to come."

Prof. Robert Langer, 2005

Selective drug targeting of a specific organ or tissue is a challenging task. This holds especially true for chemotherapeutic cancer treatment because most of the available anticancer agents cannot distinguish between cancerous and healthy cells, leading to systemic toxicity and undesirable side effects. One effective approach to address this problem is the application of polymeric nanoparticles equipped with targeting units for tumor-specific delivery.[1] For instance dendrimers, highly branched macromolecules, can be equipped with targeting units as well as with anticancer drugs due to their high number of surface functionalities.[2] Amphiphilic block copolymers, which self-assemble in dilute aqueous solutions into three-dimensional spherical micelles with a hydrophilic corona and a hydrophobic core, are another attractive option. These nanosized objects, with a typical size of 10 - 100 nm, are used to accommodate lipophilic drugs in their interior and alter their kinetics *in vitro* and *in vivo*.[3] Different polymeric systems such as shell cross-linked nanoparticles (SCKs),[4] PLGA-*b*-PEG,[5] poly(ethylene glycol-*b*-ε-caprolactone)[6] block copolymers and poly(N-isopropylacrylamide acrylic acid)[7] microgels have also been successfully utilized in combination with targeting units.

Folate receptors (FRs), which are highly expressed on the surface of various cancer cells, emerged as new targets for specific localization of chemotherapeutics incorporated into

* Parts of this chapter have been accepted for publication in *Advanced Materials*. (May 2007)

nanoparticle systems. The family of FRs currently consists of three known isoforms: FRα, FRβ and FRγ.[8] FRα is expressed primarily in cancer cells such as ovarian, testicular, breast, colon, renal and malignant nasopharyngeal carcinomas.[9-12] The process that mediates targeting of the folate-linked nanoparticle to the receptor and subsequent internalization is identical to that for the free folate.[1] As reviewed by Reddy *et al*., folates, after binding to their receptors, are taken up by the cells via the receptor-mediated endocytic pathway.[13]

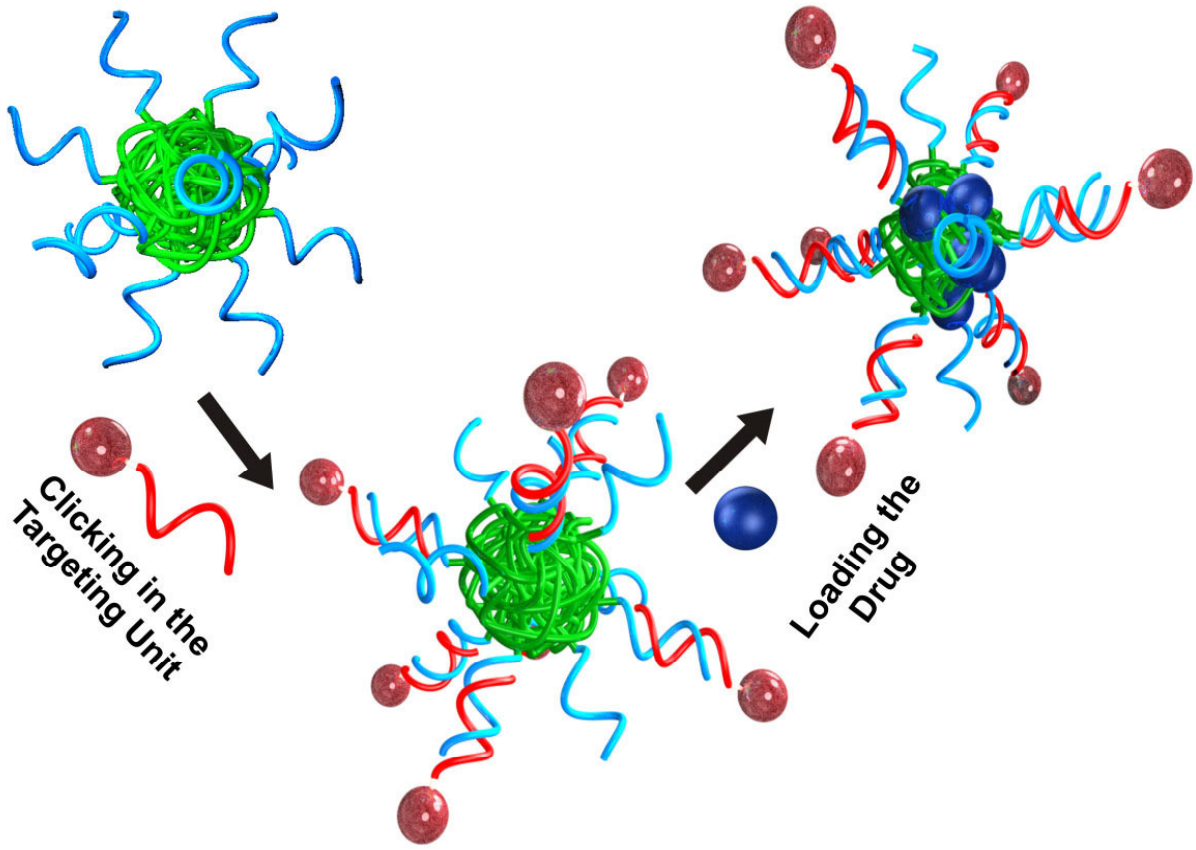

Figure 11.1 *Schematic representation of drug delivery system based on DNA block copolymers. Red and blue balls represent FA and Dox, respectively.*

Recently, a new type of amphiphilic block copolymers has emerged that comprises a hydrophobic synthetic polymer component and a biological segment consisting of an ODN sequence.[14-16] Micelles composed of these materials exhibit a corona of single ss DNA and have been utilized for the delivery of ASOs,[17] for the hybridization with DNA-coated gold nanoparticles[18] and as programmable, three-dimensional scaffolds for DNA-templated organic reactions.[19]

Here we introduce DNA block copolymer micelles as a highly modular system for chemotherapeutic drug delivery. ODN-modified targeting units were "clicked" into the micelle corona by hybridization, allowing perfect control of surface functionalities of the nanoparticle system. The interior of the micelles was loaded efficiently with a hydrophobic anticancer drug. Cell culture experiments revealed that cellular uptake strongly depends on the density of targeting units on the surface of the carriers. As a result, cancer cells were efficiently killed when targeting units and chemotherapeutic acted together within the DNA block copolymer drug delivery system (**Figure 11.1**).

PPO was selected as the hydrophobic component of the DNA block copolymer to provide a polymer with proven biocompatibility toward different cell types when administered as a constituent component of amphiphilic block copolymer micelles.[20] For the generation of the DNA-*b*-PPO copolymer, a phosphoramidite-functionalized PPO (M_n = 6800 g/mol) was synthesized and attached to the 5' terminus of the nucleic acid fragment (5'-CCTCGCTCTGCTAATCCTGTTA-3', 22mer, Mw = 6700 g/mol) via automated solid phase synthesis as reported in *Chapter 3*.[19] The resulting block copolymer was analyzed and purified by denaturing PAGE and the molecular weight confirmed by MALDI-TOF MS (Experimental Section). DLS measurements of the DNA block copolymer aggregates revealed the formation of uniform micelles of diameter 10.8 ± 2.2 nm consistent with previous findings.[16, 19] For equipping these micelles with targeting units 5'- and 3'-amino-modified ODNs that encode the complementary sequence of DNA-*b*-PPO were reacted with folic acid (FA) in the presence of DMT-MM[21] and purified by PAGE to generate the corresponding folic acid-functionalized ODNs in 65 % yield. These conjugates can be hybridized with the micelles so that the FA is either positioned at the periphery (5') or in the core (3') of the nanoparticle.

In order to study the effect of FA density and position within the nanoparticles on the targeting efficiency, DNA-*b*-PPO copolymers were hybridized in different ratios with the targeting unit-bearing oligonucleotides. This convenient procedure resulted in micelles with on average 2, 11 or 28 (fully hybridized) FAs either at the periphery or at the hydrophobic-hydrophilic interface of the micelles. The dimensions of the micelles were again assessed by DLS, which revealed maintenance of their narrow size distribution. Moreover, the diameter of the micelles was found to increase slightly with an increase in the number of FA units. For 2, 11 and 28 FA moieties at the rim, micelle diameters of 11.2 ± 1.6 nm, 13.2 ± 2.4 nm and 14.4

± 2.2 nm were measured, respectively. When FA is positioned inside, diameters of 11.2 ± 1.8 nm, 12.2 ± 2.4 nm and 12.2 ± 2.0 nm were detected for the same FA densities. Importantly, the nanoparticles were on the order of 10 nm, an important design criterion for efficient tumor cell-specific delivery.[22] Although it has been proven that polymer particles in the range of 100 nm exit the vasculature and enter tumor tissue through a process known as the enhanced permeability and retention effect,[23-25] it is in some cases favorable to make use of delivery independent of fenestrate pore cutoff size. This can occur when particles have a diameter of less than 10 nm, as do albumin molecules.[26] This is supported by recent computer simulations of cancer progression at the tumoral level.[27] It was demonstrated that nanoparticles with a size range of 1-10 nm diffuse directly and target the individual cell, which results in improved tumor response.

Caco-2 cells were employed as a cancerous cell line to study the uptake of the differently decorated DNA block copolymer micelles since they have already been used as a model to study nanoparticle uptake.[28] Moreover, their FA uptake has been characterized previously.[29] In the present study the availability of three known genes for folic acid transport, i.e. reduced folate carrier (RFC), FRα and FRβ, were examined and their relative gene expression levels measured by real-time PCR. These measurements were carried out by *N. C. Alemdaroglu* in the group of *Prof. Dr. P. Langguth* (see Experimental Section). Quantitative real-time PCR has become the most prevalent method for quantification of mRNA transcription levels due to its outstanding accuracy, broad dynamic range and sensitivity.[30] According to PCR experiments the three analyzed genes are expressed at different levels. The Caco-2 cells express a high level of FRα, which is consistent with previous findings.[8, 31] It should be added here that there was no apparent difference between the older and the younger passage, suggesting no loss of expression of the transporter genes by further splitting. FRα is also highly expressed in other solid epithelial tumors such as ovarian carcinoma and mesothelioma. Thus this cell line is well suited to act as a model to study the effect of targeting cancerous cells.

Before analyzing the uptake of DNA block copolymer micelles, we assessed their biocompatibility. *In vitro* cytotoxicity was determined based on a XTT cell proliferation assay. The Caco-2 cells were incubated with different concentrations of DNA-*b*-PPO copolymer and their FA-functionalized derivatives.

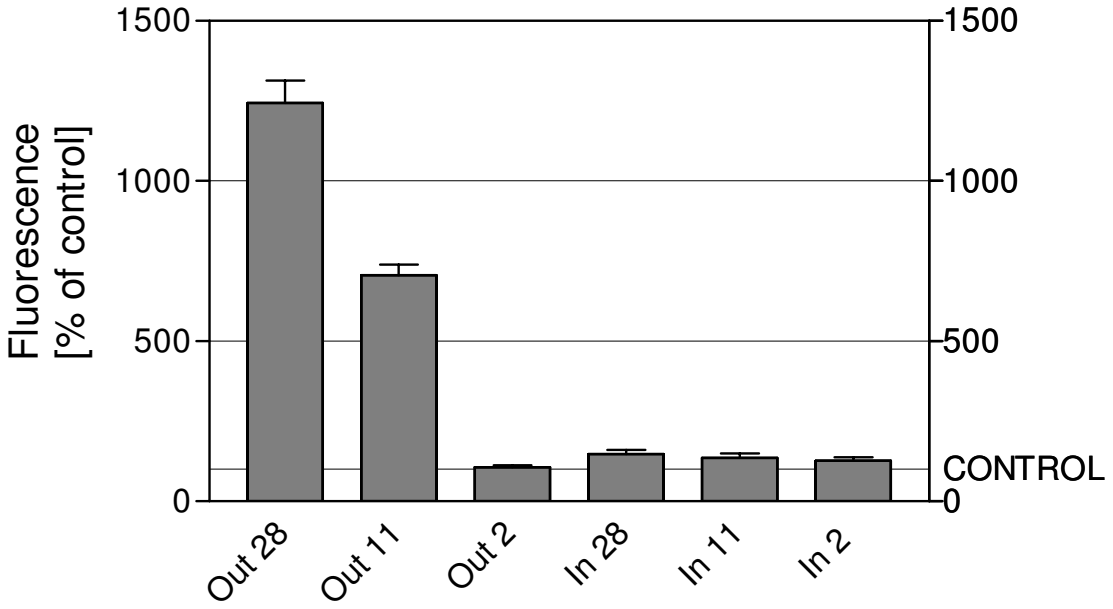

Figure 11.2 *Uptake of micelles that were decorated with folic acid into human Caco-2 cell monolayers incubated for 3 h. Out 28: DNA block copolymer micelles with 28 targeting units at the periphery of the micelle, Out 11: DNA block copolymer micelles with 11 targeting units at the periphery of the micelle, Out 2: DNA block copolymer micelles with 2 targeting units at the periphery of the micelle, In 28: DNA block copolymer micelles with 28 targeting units in the core of the micelle, In 11: DNA block copolymer micelles with 11 targeting units in the core of the micelle and In 2: DNA block copolymer micelles with 2 targeting units in the core of the micelle. Results are shown as the average values of triplicates ± SD.*

Toxicity of the DNA block copolymer was quantified spectrophotometrically at 450 nm and revealed that more than 75 % of the cells were viable (see Experimental Section for the viability of each nanoparticle). Motivated by the relatively non-toxic nature of the nanoparticles, we proceeded to study their uptake into Caco-2 cells. For tracking purposes 4% of the nanoparticles were additionally labelled with a fluorescent dye: PPO-*b*-DNA micelles were hybridized with 3'-Alexa488-functionalized oligonucleotides encoding the complementary sequence of the DNA corona so that the dye was located in the interior. These micelles were then administered to the folate receptor-bearing Caco-2 cells (see Experimental Section for details). The internalisation of the micelles was determined by CLSM and, after lysing the cells, by fluorescence spectroscopy. The latter method offers the possibility to quantitatively compare the uptake of nanoparticles. As shown in **Figure 11.2**, an increasing number of FA entities at the surface of the micelles strongly promoted internalisation. With

only 2 targeting units present the uptake into the cells was comparable to non-functionalized DNA block copolymer micelles. When the average number of targeting units was adjusted to 28, the uptake increased by a factor of 10 compared to the control. In contrast, when the targeting moieties pointed towards the interior of the micelles the uptake was comparable with bare DNA-*b*-PPO aggregates. From these experiments three important conclusions can be drawn. The uptake of DNA block copolymer micelles strongly depends on the number of targeting units at the rim. Furthermore, the higher the number of FA entities, the more efficiently the nanoparticles are internalized. Finally, when the targeting units are hidden inside the nanoparticles they cannot be "recognized" by the folate receptors, indicating that the micelles remain intact and do not dissociate into isolated block copolymers.

CLSM has proven to be a powerful tool for acquiring high resolution images, 3-D reconstructions and visualisations of internalization of nanoparticles.[32-35] **Figure 11.3** shows the CLSM image of Caco-2 cells after 3h incubation with DNA block copolymer micelles labelled with 28 targeting units at the surface that exhibited the most efficient uptake. 3-D slicing experiments showed that the nanoparticles were internalized homogenously and did not only adsorb on the membrane. No distinct patterns of subcellular staining were observed. It must be pointed out that the incubation experiments were performed in HBSS, which does not contain any protein that may interact with the nanoparticles. This visualization was carried out in collaboration with *Dr. K. Koynov*.

After the optimization of the targeting properties of the nanoparticles, the cytotoxicity of DNA block copolymer micelles loaded with the widely used anticancer drug Doxorubicin (Dox) was investigated. Dox is known to have side effects such as cardiotoxicity and myelosuppression, therefore targeted delivery is vital.[7] The preparation of Dox-loaded micelles and the determination of loading content were carried out according to the literature.[36] The drug payload was 5.6 % of the nanoparticle by weight. The viability of Caco-2 cells after 24h incubation with Dox-loaded DNA block copolymer micelles was compared with several control experiments.

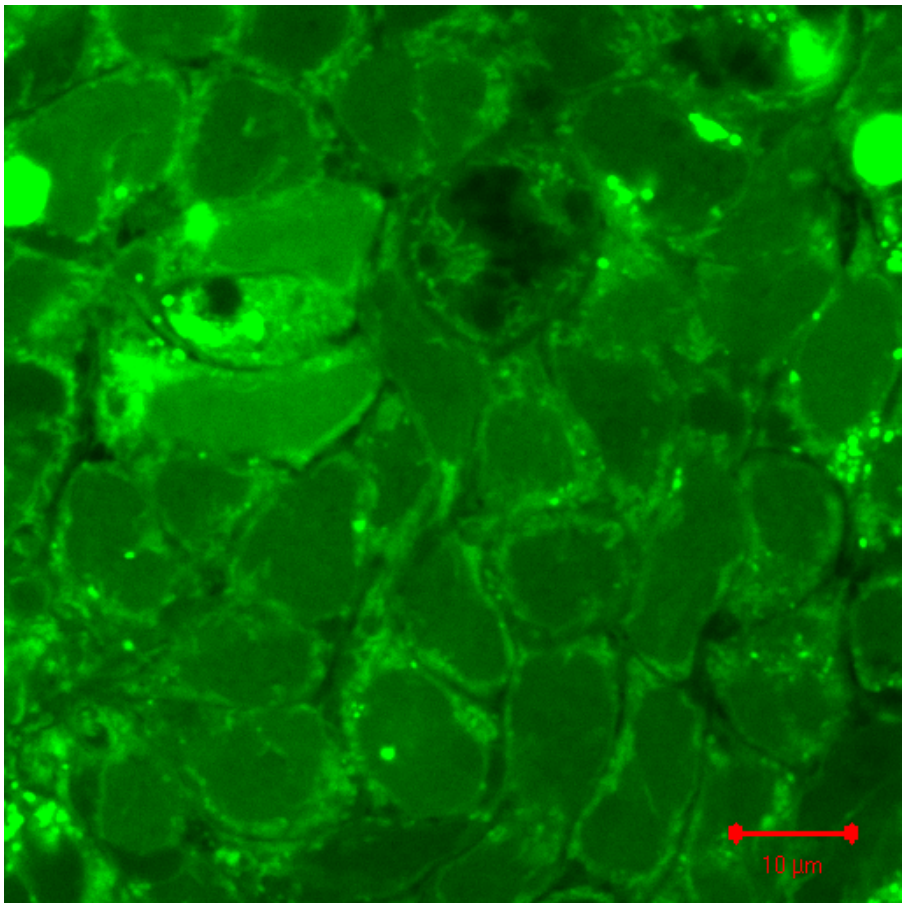

Figure 11.3 *CLSM image of the uptake of labeled micelles inside Caco-2 cells.*

The percentage of surviving cells was acquired using a XTT cell proliferation assay. **Figure 11.4A** shows that Caco-2 cells incubated with Dox-loaded micelles equipped with targeting units (on average 28 FA on the surface) had a viability of 24.1 ± 2.5 %. The controls consisted of Dox-loaded micelles in the presence of non-conjugated FA (**Figure 11.4B**), Dox-loaded micelles in the absence of any targeting unit, (**Figure 11.4C**) and folic acid-conjugated micelles in the absence of Dox, (**Figure 11.4D**) with viabilities of 63.5 ± 7.9 %, 68.3 ± 7.1 % and 75.9 ± 8.2 %, respectively. The cell mortalities of the control experiments were significantly lower than when the Dox-loaded micelles were outfitted with FA units, which strongly indicates efficient drug delivery into the tumor cells by the DNA block copolymer micelles with the aid of targeting moieties and thus the significant cytotoxicity of these nanoparticles.

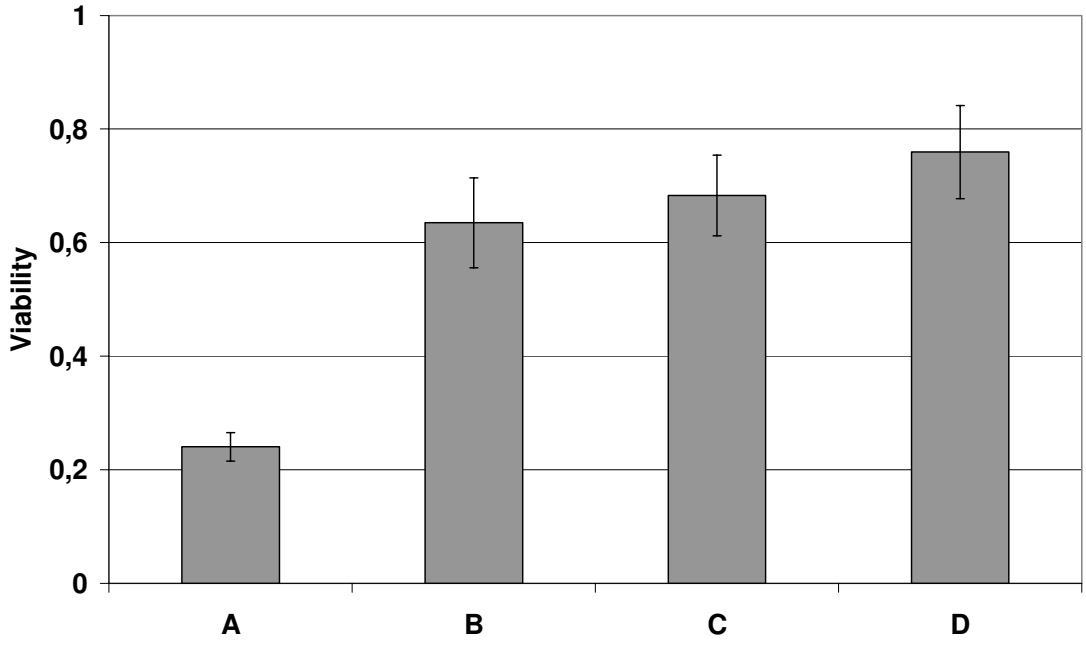

Figure 11.4 *The viability of cells after incubation with A) Dox-loaded micelles covalently linked to targeting unit, B) Dox-loaded micelles with but not covalently linked to folic acid, C) Dox-loaded micelles and D) folic acid conjugated micelles in the absence of dox.*

Although block copolymers have already been employed for drug delivery purposes,[37, 38] we believe that the nucleic acid/polymeric hybrid materials presented here represent a significant advantage in the field for several reasons. The DNA-*b*-PPO block copolymers that were synthesized in a fully automated fashion were structurally well-defined because the biological segment was monodisperse and contained defined end groups. Such a highly-defined structure is an important criterion for approval of a drug or a delivery system. Likewise, the resulting spherical micelles exhibited a narrow size distribution with dimensions in the range of 10 nm. In this regime delivery is independent of the compromised leaky vasculature of the tumor tissue. Most important, however, is the convenience of functionalizing these DNA block copolymer nanoparticles. Different amounts of targeting and reporter groups can be incorporated simultaneously at distinct positions on the nanoparticle by hybridization. A variety of 5'- and 3'-modified ODNs bearing different functional groups are commercially available allowing several coupling strategies for a wide range of ligands. In contrast, functionalization of conventional block copolymers with targeting moieties is demanding often requiring multi-step synthesis and separation of ligand-modified from unmodified

polymers.[39-41] Moreover, by employing negatively charged DNA with a persistence length of 50 nm as the hydrophilic block, surface exposition of the targeting moieties is guaranteed because, as is well accepted, the polymer chains of the corona in polyelectrolyte block copolymer aggregates are well-ordered and completely stretched.[42] When FA is conjugated to other block copolymer systems, e.g. exhibiting a corona of polyethylene glycol, this is not guaranteed to the same extent.[40]

In summary, a novel micelle platform consisting of amphiphilic DNA block copolymers was introduced for chemotherapeutic drug delivery, allowing for combinatorial testing of the drug carrier system. Prior to the investigation of the DNA block copolymer micelles, the presence of folate binding proteins in the cancerous cell line was confirmed and expression levels of three associated genes determined. The corresponding ligand-conjugated ODNs were introduced into the micelles as targeting units via hybridization. The incorporation of fluorescent reporter groups by the same procedure revealed that receptor-mediated endocytotic uptake of the nanoparticles with a diameter of approximately 10 nm was most efficient when the maximum number of ligands was present on the rim of the micelles. Loading Dox into the hydrophobic interior of the ligand-containing micelles resulted in efficient cytotoxicity and high mortality among the cancerous cells. Further studies will investigate targeting with different combinations and ratios of ligands as well as the incorporation of various hydrophobic cancer drugs into the DNA block copolymer micelles. Their potential as an anticancer drug delivery vehicle in *in vivo* experiments will also be assessed.

Experimental Section

I. Materials and Methods

Confocal laser scanning microscopy measurements were carried out with a LSM 510 laser scanning module coupled to a Zeiss Axiovert 200M inverted microscope. Caco-2 cells were obtained from DSMZ (Braunschweig, Germany). All the cell culture media and supplements were purchased from Biochrom AG (Berlin, Germany). HEPES was provided from Merck (Darmstadt, Germany). RNA STAT-60™ was purchased from Tel-Test Inc. (Friendswood, TX, USA). DNA-free™ purification kit was obtained from Ambion Ltd. (Cambridgeshire, UK). SuperScript™ First-Strand Synthesis System for reverse transcription (RT)-PCR, sense, and antisense primers were purchased from Invitrogen™ Ltd. (Paisley, UK). Expand™ High Fidelity PCR System Kit was provided from Roche Diagnostics GmbH (Mannheim, Germany). GeneRuler™ was purchased from Fermentas GmbH (Leon-Rot, Germany). QuantiTect Probe RT-PCR Kit and RNeasy Mini Kit were from Qiagen GmbH (Hilden, Germany). Sense and antisense primers and TaqMan probes for real-time PCR were purchased from Operon Biotechnologies (Cologne, Germany).

II. Synthesis of DNA-*b*-PPO Diblock Copolymers

The preparation of ss DNA-*b*-PPO diblock copolymers, and the formation of micelles were carried out as described previously.[1] These hybrids were characterized by MALDI-TOF MS and PAGE (**Figure 11.5**). Oligonucleotides were quantified spectrophotometrically at a wavelength of 260 nm.

A

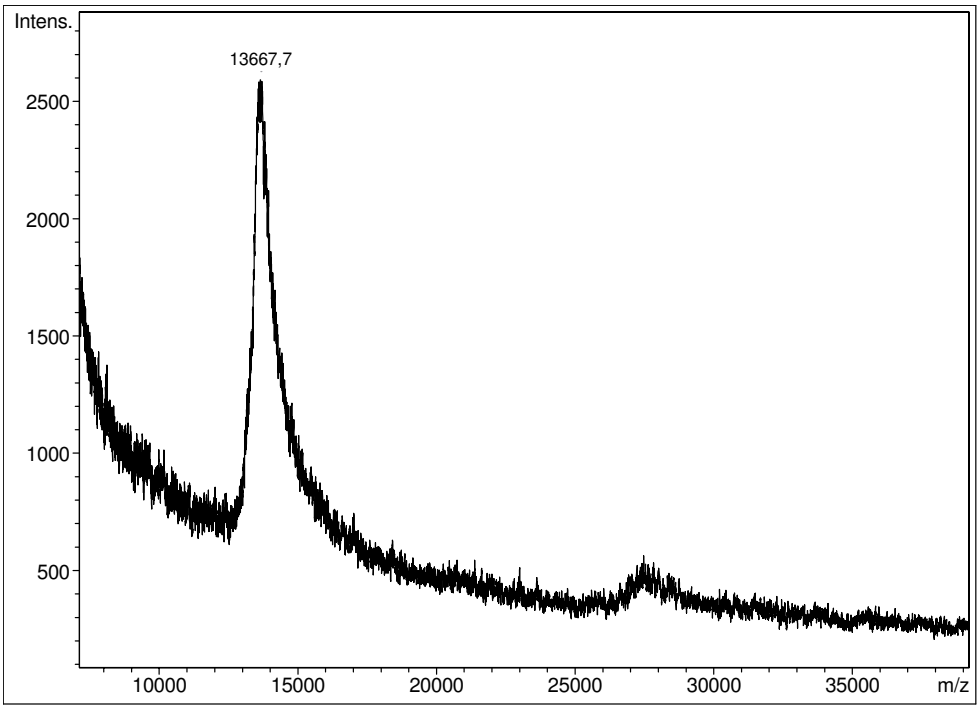

B

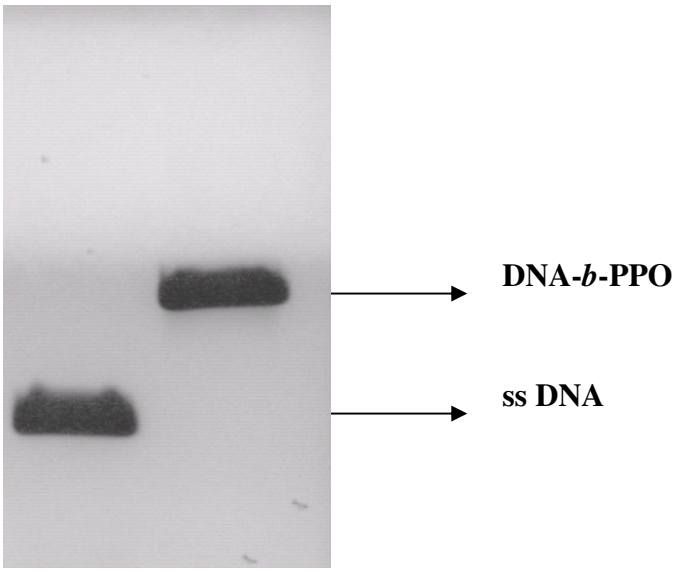

Figure 11.5 Characterization of DNA block copolymers by **(A)** MALDI-TOF MS and **(B)** PAGE.

III. Synthesis of Oligonucleotide-Folic Acid Conjugates

The synthesis of ss DNA-FA conjugates was carried out by mixing 5'-amino-modified oligonucleotide (TAACAGGATTAGCAGAGCGAGG, 22mer, MW = 6950 g/mol) (30 µmol) with folic acid (100 µmol) in the presence of DMT-MM (35µmol) in 1 ml of water. The mixture was allowed to react for 12 h at room temperature. The conjugate was purified using 20 % denaturing PAGE. After excision the bands were dialyzed against water for 24 hours. Subsequently, the DNA block copolymers were lyophilized yielding 60 % ss DNA-FA conjugate. Characterization of the products was carried out by PAGE and MALDI-TOF MS. (**Figures 11.6** and **11.7**)

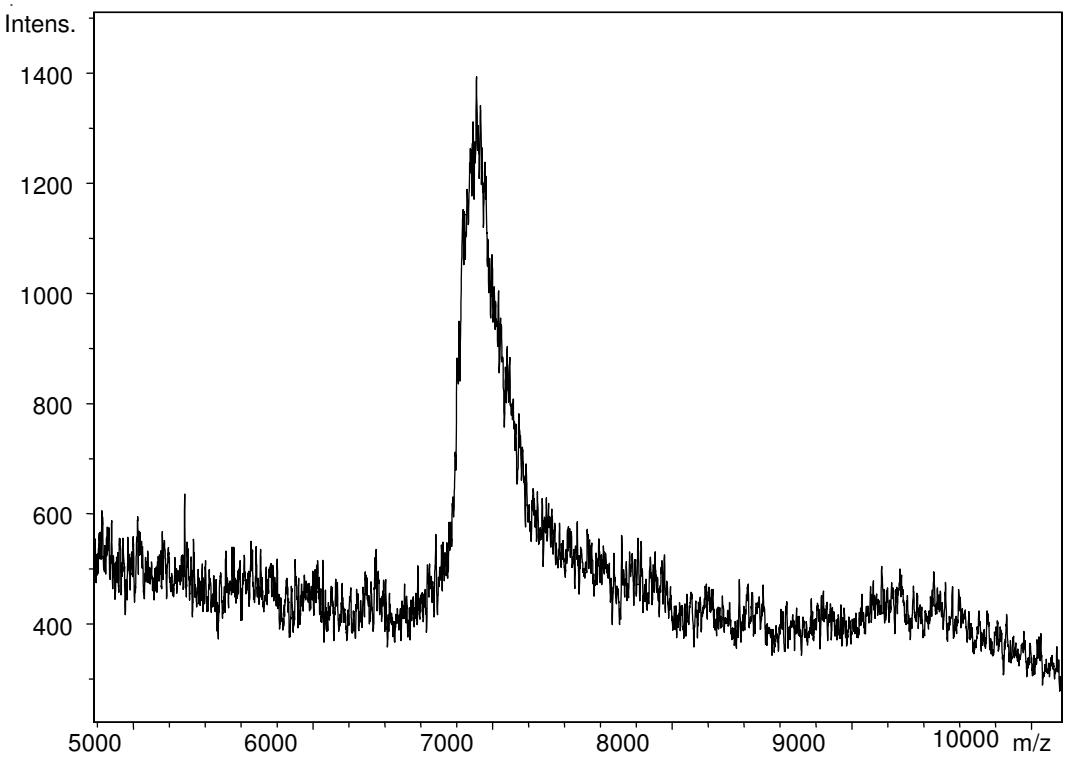

Figure 11.6 *The MALDI-TOF mass spectrum of ss DNA-FA conjugate (Found: 7385 g/mol, calculated: 7391 g/mol).*

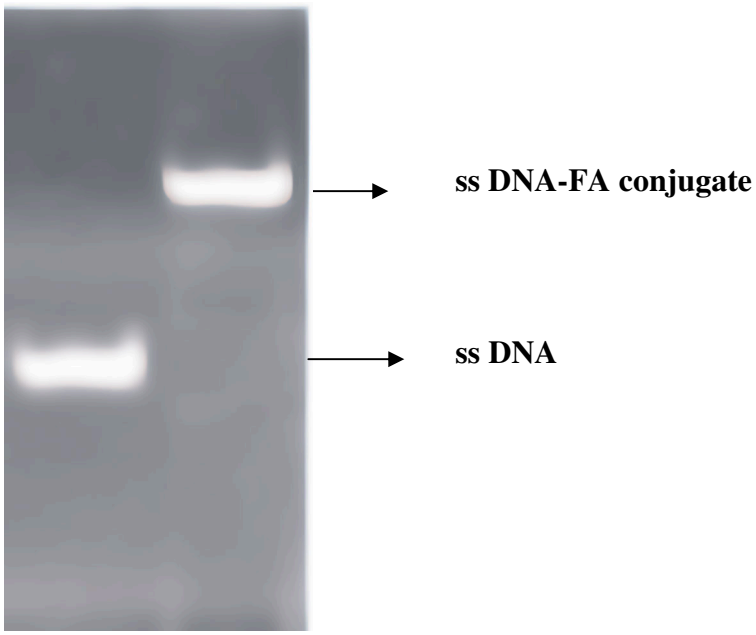

Figure 11.7 *Analysis of ss DNA and its folic acid conjugate in a 20 % polyacrylamide gel.*

IV. Functionalization of Micelles with Folic Acid and DLS characterization

DNA-b-PPO copolymers were hybridized in different ratios with the targeting unit-bearing oligonucleotides. The hybridization was carried out by dissolving ss DNA-*b*-PPO diblock copolymer and the ss DNA-FA conjugate in TAE buffer (20 mM tris(hydroxymethyl)aminomethane-HCl, pH 8.0; 10 mM acetic acid, 0,5 mM EDTA) containing Na^+ (100 mM) and Mg^{2+} (60 mM). The mixture was heated to 95°C and was slowly cooled to room temperature over the course of 3 days (1 degree per hour) by using a PCR thermocycler (Biorad, USA). The final concentration of DNA-*b*-PPO was between 200-500 μM.

Characterization of DNA-PPO block copolymer Micelles

The effective hydrodynamic diameter of the micelles was measured by DLS at 25 °C using a DLS photometer (ALV 5800, Avalanche Photodiode) equipped with He-Ne laser at a wavelength of 632 nm. The data were gathered and processed using the ALV 5000/E software. The samples were prepared in buffer medium and measured at a concentration of 2 mg/ml. For each micelle system the measurements were carried out in triplicate. (**Figure 11.8**)

A

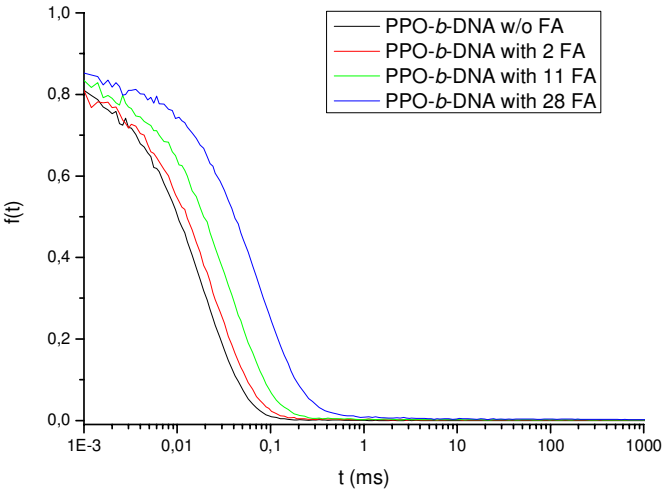

B

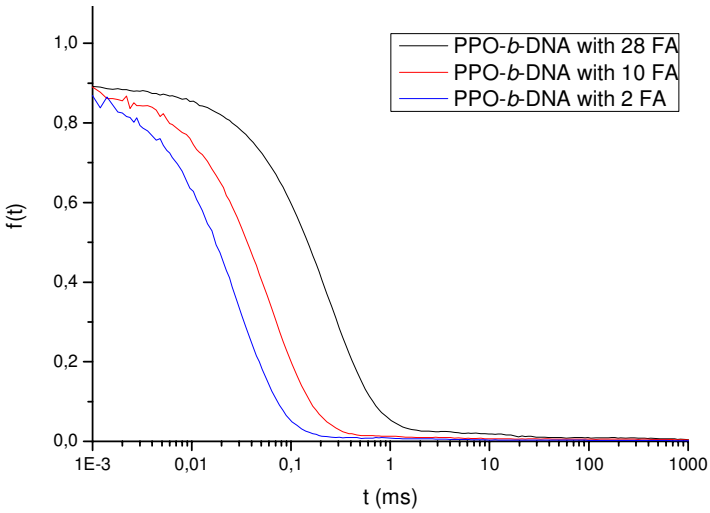

Figure 11.8 *Correlation function of the PPO-b-DNA diblock copolymers with increasing FA moieties (**A**) at the core and (**B**) at the corona of the micelle.*

V. Quantification of Relative Gene Expression Levels of Folate Receptors by Real-Time PCR

Preparation of the Caco-2 Monolayers for RT-PCR and Real-Time PCR

Caco-2 cells (passage 27, 54 and 62) were split and seeded into 24-well plates with a density of 100000 cells/well. The medium was changed three times a week. The development of the monolayers was examined under the microscope until the 16th day. Total cellular RNA both

for RT-PCR and for real-time PCR was isolated from Caco-2 monolayers on the 16th day post-seeding.

Isolation of Total Cellular RNA, Reverse Transcriptase Reaction, PCR and Gel Electrophoresis

For the investigation of some of the known transport routes of folates into the cells, and additionally the effect of passage number on the expression of the transport systems, one younger (passage 27) and one older (passage 62) passage was used. The RNA was isolated from the cells using RNA STAT-60^{TM} according to the company's protocol for RNA isolation. The obtained RNA pellet was dried by air-drying. 25 µl of RNase-free water was added to dissolve the RNA and was purified using a DNA-free^{TM} purification kit.
The integrity of the isolated RNA was checked by standard gel electrophoresis with 1% agarose. The total RNA was reversely transcribed into cDNA by using SuperScript^{TM} First-Strand Synthesis System for RT-PCR according to the manufacturer's guidance. cDNA obtained after reverse transcription was then amplified by PCR. The sequences of primers used in this study are shown in **Table 10.1**.

Table 10.1 *The sequences of the sense and antisense primers for RFC, FRα and FRβ (5' to 3') used in the RT-PCR reaction. "S" represents sense and "AS" represents antisense primers.*

OLIGO	***Sense and Antisense Primers (5' to 3')***
RFC-S	5'-TTTCAGATTGCATCTTCTCTGTCT-3'
RFC-AS	5'-GAAGTAGATGATGGACAGGATCAG-3'
FRα-S	5'-TTCTAGTGTGGGTGGCTGTAGTAG-3'
FRα-AS	5'-CACAGTGGTTCCAGTTGAATCTAT-3'
FRβ-S	5'-CTTATGCAAAGAGGACTGTCAGC-3'
FRβ-AS	5'-CTGACCTTGTATGAGTGACTCCAG-3'

The product sizes were 189 bp for RFC, 234 bp for FRα and 201 bp for FRβ. PCR was employed using the Expand^{TM} High Fidelity PCR system kit. Each reaction mixture contained 95 µl water, 20 µl 10x buffer, 40 µl enhancer, 4 µl dNTPs, 1 µl Taq polymerase and 20 µl

cDNA. PCR amplification consisted of 40 cycles of 1 min denaturation at 94°C, 1.30 min annealing at 58°C and 2 min extension at 72°C. Subsequently, the amplified PCR products were analyzed by 2% agarose gel electrophoresis with ethidium bromide staining along with a DNA ladder (GeneRuler^{TM}) (**Figure 11.9**).

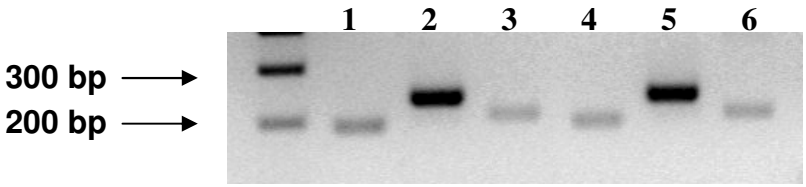

Figure 11.9 *Ethidium bromide-stained agarose gel of PCR products. P27: Lane 1, RFC; lane 2, FRα; lane 3, FRβ and P62: lane 4, RFC; lane 5, FRα; lane 6, FRβ. The gel electrophoresis of the PCR product clearly showed the similarity of younger and older passage by means of the three folate transport routes.*

Isolation of Total Cellular RNA, Quantification of Isolated RNA and Reverse Transcriptase Real-Time PCR Reaction

For this purpose, Caco-2 cells (passage 54) were seeded on 24-well plate with a concentration of 100,000 cells/well. On the 16th day, total RNA was extracted from Caco-2 cell monolayers using the RNeasy Mini Kit according to the instructions of the manufacturer. Quantification of isolated RNA was based on spectrophotometric analysis. 3 µl of isolated RNA together with 97 µl of RNase-free water was read at 260 nm wavelength against RNase-free water that served as blank. To perform the real-time PCR, a QuantiTect Probe RT-PCR Kit was used. The reactions were run in a real-time PCR instrument. The sequences of TaqMan probes, sense and ASOs are shown in **Table 10.2** and **Table 10.3**, respectively.

Table 10.2 *The sequences of the TaqMan probes for RFC, FRα and FRβ used in RT real-time PCR reaction.*

Protein Name	***Gene Symbol***	***TaqMan Probes (5' to 3')***
RFC	SLC19A1	5' FAM-TCCGCAAGCAGTTCCAGTTATACTCCG-TAMRA 3'
FRα	FOLR1	5' FAM-CATTTCTACTTCCCCACACCCACTGTT-TAMRA 3'
FRβ	FOLR2	5' FAM-TTGTTAACTCCTGAGGTCCAGTCCCAT-TAMRA 3'

Table 10.3 *The sequences of sense and antisense primers for RFC, FRα and FRβ used in RT real-time PCR reaction.*

Oligo	***Sense and Antisense Primers (5' to 3')***
RFC-S	5'-ACCATCATCACTTTCATTGTCTC-3'
RFC-AS	5'-ATGGACAGGATCAGGAAGTACA-3'
FRα-S	5'-ACTGGACTTCAGGGTTTAACAAG-3'
FRα-AS	5'-GTAGGAGTGAGTCCAGATTTCATT-3'
FRβ-S	5'-TATGCAAAGAGGACTGTCAGC-3'
FRβ-AS	5'-GGGAAGTAGGACTCAAAGGTG-3'
GAPDH-S	5'-AGCCTCAAGATCATCAGCAATG-3'
GAPDH-AS	5'-CACGATACCAAAGTTGTCATGGA-3'

Quantitative TaqMan PCR was performed in 96-well plates using a final volume of 25 µl. The components and volume of each component for the reaction were as shown in **Table 10.4**.

Table 10.4 *The components and volume of each component for Quantitative TaqMan PCR.*

Component	***Volume [µl]***
Sense primer [10 µmol/L]	2
Antisense primer [10 µmol/L]	2
Taqman probe [10 µmol/L]	1
RT-PCR Master Mix	12.5
QuantiTect Probe RT Mix	0.25
dNTPs	0.5
$MgCl_2$	1.75
Template RNA [0.1 µg/µl]	5
TOTAL	25

The reaction tubes were prepared as above and were placed in the real-time PCR instrument. The reaction was performed starting with a 30 min reverse transcription reaction at 50°C followed by the activation of Taq polymerase for 15 min at 95°C. 50 cycles of denaturation at 94°C for 15 s and combined primer annealing/extension at 60°C for 1 min were employed. The fluorescence increase of FAM was automatically measured during PCR. For normalization of the gene levels, glyceraldehyde-3-phosphate dehydrogenase (GAPDH) was used to correct for minor variations in the input RNA amount or inefficiencies in the reverse transcription. The relative expression level of the target gene was normalized to the endogenous control according to the equation below:

$$\Delta C_T = C_T(\text{target}) - C_T(\text{control})$$

where C_T is the cycle number at the threshold and ΔC_T is the difference between the C_T values of the target and the normalizer. SLC19A1 (RFC gene) was chosen as the reference for the comparison. The comparative $\Delta\Delta C_T$ is the difference between each sample`s $\Delta C_T$ and the reference`s ΔC_T. Accordingly, the comparative expression level was calculated with the formula: $2^{-\Delta\Delta C_T}$ (**Figure 11.10**).

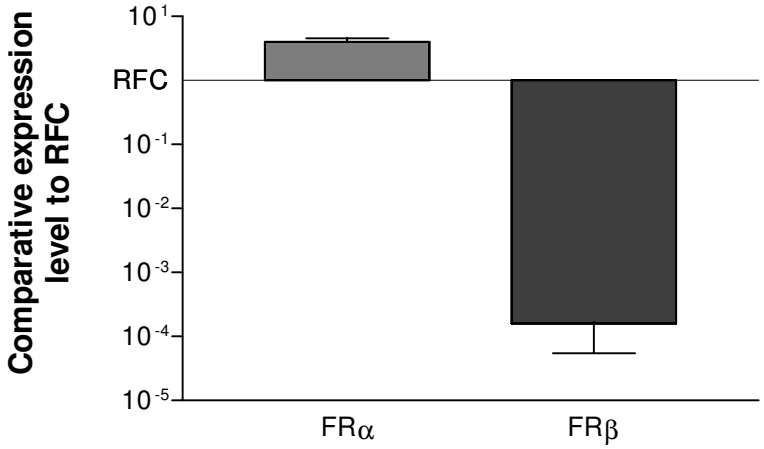

Figure 11.10 *Relative gene expression levels ($2^{-\Delta\Delta C_T}$) of FRα and FRβ to RFC which were normalized to GAPDH in Caco-2 cells. Values are shown as mean of three different reactions ± SD.*

VI. Cytotoxicity and Uptake Experiments

Culturing and Preparation of Caco-2 for uptake studies

Caco-2 cells (passage number 45) were cultured at 37 °C in an atmosphere of 5% CO_2 and 90% relative humidity in 75 cm^2 cell culture flasks containing DMEM supplemented with 10% FBS, 1% nonessential amino acids, 100 U/ml penicillin and 100 µg/ml streptomycin. The cells were routinely split and seeded into 6-well plates (Nunclon™ Multidishes, Life Technologies GmbH, Karlsruhe, Germany) with 800.000 cells/well. The medium was changed three times a week. The development of the monolayers was examined under the microscope until the 21st day. Then the monolayer cultures were used for uptake studies.

Cytotoxicity Assay

For the determination of the toxicity of the micelles, Caco-2 cells were seeded in 96-well plates at a concentration of 2500 cells/well. The cytotoxicity of the nanoparticles was checked using an XTT *in vitro* toxicology assay kit following the procedure of the manufacturer (Sigma-Aldrich Chemie GmbH, Steinheim, Germany). On the 21st day post-seeding, the cell monolayers were washed once with HBSS containing 5 mmol/L HEPES adjusted to pH 7.4. Cells were incubated with different micelle solutions at a DNA-*b*-PPO concentration of 325 µg/ml for 3 h at 37°C (in the case of dox-loaded micelles, 24 h of incubation time was employed). After the incubation period, the medium was removed, monolayers were washed once with the buffer solution and the reconstituted XTT was added into each well with a volume of 100 µl and incubated for 2 h at 37°C. Subsequently, absorbance was measured at a wavelength of 450 nm. A reference measurement was also taken at a wavelength of 690 nm and subtracted from the measurement at 450 nm. The cytotoxicity of folic acid conjugated nanoparticles were compared with the cells without any treatment (control). (**Figure 11.11**) Viabilities of all treatment groups were above 75%.

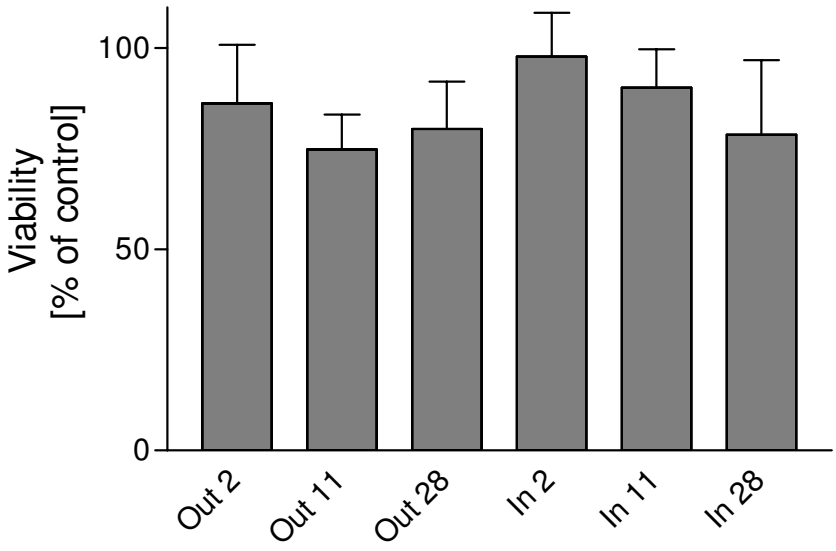

Figure 11.11 *Viabilities of Caco-2 cell monolayers exposed to different folic acid conjugated nanoparticles. Values are means of triplicates ± SD.*

Uptake experiment

Caco-2 cells with a passage of 57 were seeded on 6-well plates with a density of 800000 cells/well. The medium in each well was changed every other day. On day 21, the medium was removed and monolayers washed two times with HBSS containing 5 mmol/l HEPES adjusted to pH 7.4. Incubation mixtures were prepared in pH 7.4 HBSS buffer at a DNA-*b*-PPO concentration of 325 µg/ml for Out 28, Out 11, Out 2, In 28, In 11 and In 2. After incubating with 2 ml of micelle solutions for 3 h at 37°C on a rotating shaker at 50 rpm, incubation solutions were removed and the monolayers were washed five times with ice-cold HBSS (pH 7.4). Subsequently, cells in each well were lyzed with 0.6 ml of 1.25 mmol/l NaOH, cell lysates were transferred into eppendorf tubes and shaken overnight at room temperature. The next day, lysates were centrifuged and the fluorescence content of the supernatant in each tube was measured (Exc: 500 nm, Em: 595 nm). Experiments were carried out in triplicates and the resulting data were expressed as % of control (without any targeting unit).

CLSM Measurements

For the microscopy analysis, Caco-2 cells were seeded at a density of 20,000 cells/cm^2 on chamber slides (Lab-Tek® Chamber Slide System, Nunc, Germany). The cell monolayers were incubated with 325 µg/ml of the DNA-*b*-PPO labeled with Alexa488 for 3 h, washed 5 times with pH 7.4 HBSS and after the addition of 100 µl of buffer the monolayers were analyzed with confocal laser scanning microscopy (excitation 488nm).

References

[1] C. P. Leamon, J. A. Reddy, *Adv. Drug Delivery Rev.* **2004**, *56*, 1127.

[2] A. Quintana, E. Raczka, L. Piehler, I. Lee, A. Myc, I. Majoros, A. K. Patri, T. Thomas, J. Mule, J. R. Baker, Jr., *Pharm Res* **2002**, *19*, 1310.

[3] R. Savic, A. Eisenberg, D. Maysinger, *J. Drug Targeting* **2006**, *14*, 343.

[4] D. Pan, J. L. Turner, K. L. Wooley, *Chem. Commun.* **2003**, 2400.

[5] H. S. Yoo, T. G. Park, *J. Controlled Release* **2004**, *96*, 273.

[6] E. K. Park, S. Y. Kim, S. B. Lee, Y. M. Lee, *J. Controlled Release* **2005**, *109*, 158.

[7] M. Das, S. Mardyani, W. C. W. Chan, E. Kumacheva, *Adv. Mater.* **2006**, *18*, 80.

[8] L. Matherly, I. D. Goldman, *Vitamins and Hormones* **2003**, *66*, 403.

[9] H. Elnakat, M. Ratnam, *Adv. Drug Delivery Rev.* **2004**, *56*, 1067.

[10] G. Toffoli, C. Cernigoi, A. Russo, A. Gallo, M. Bagnoli, M. Boiocchi, *Int. J. Cancer* **1997**, *74*, 193.

[11] P. C. Elwood, *J. Biol. Chem.* **1989**, *264*, 14893.

[12] D. S. Theti, A. L. Jackman, *Clinical Cancer Res* **2004**, *10*, 1080.

[13] J. A. Reddy, V. M. Allagadda, C. P. Leamon, *Curr. Pharm. Biotechnol.* **2005**, *6*, 131.

[14] F. E. Alemdaroglu, A. Herrmann, *Org. Biomol. Chem.* **2007**, *5*, 1311.

[15] F. E. Alemdaroglu, M. Safak, J. Wang, R. Berger, A. Herrmann, *Chem. Commun.* **2007**, 1358.

[16] K. Ding, F. E. Alemdaroglu, M. Börsch, R. Berger, A. Herrmann, *Angew. Chem., Int. Ed.* **2007**, *46*, 1172.

[17] J. H. Jeong, T. G. Park, *Bioconjugate Chem* **2001**, *12*, 917.

[18] Z. Li, Y. Zhang, P. Fullhart, C. A. Mirkin, *Nano Lett* **2004**, *4*, 1055.

[19] F. E. Alemdaroglu, K. Ding, R. Berger, A. Herrmann, *Angew. Chem., Int. Ed.* **2006**, *45*, 4206.

[20] D. W. Miller, E. V. Batrakova, T. O. Waltner, V. Y. Alakhov, A. V. Kabanov, *Bioconjugate Chem.* **1997**, *8*, 649.

[21] M. Kunishima, C. Kawachi, K. Hioki, K. Terao, S. Tani, *Tetrahedron* **2001**, *57*, 1551.

[22] L. Serpe, in *Nanotechnologies for the Life Sciences, Vol. 6* (Ed.: C. S. S. R. Kumar), Wiley-VCH Verlag, Weinheim, **2006**.

[23] T. Tabata, Y. Murakami, Y. Ikada, *J. Controlled Release* **1998**, *50*, 123.

[24] Y. Matsumura, H. Maeda, *Cancer Res.* **1986**, *46*, 6387.

[25] K. Uchiyama, A. Nagayasu, Y. Yamagiwa, T. Nishida, H. Harashima, H. Kiwada, *Int. J. Pharm.* **1995**, *121*, 195.

[26] S. K. Hobbs, W. L. Monsky, F. Yuan, W. G. Roberts, L. Griffith, V. P. Torchilin, R. K. Jain, *Proc. Natl. Acad. Sci. U. S. A.* **1998**, *95*, 4607.

[27] X. Zheng, S. M. Wise, V. Cristini, *Bull. Math. Biol.* **2005**, *67*, 211.

[28] P. Pietzonka, B. Rothen-Rutishauser, P. Langguth, H. Wunderli-Allenspach, E. Walter, H. P. Merkle, *Pharm. Res.* **2002**, *19*, 595.

[29] M. L. Vincent, R. M. Russell, V. Sasak, *Hum. Nutr. Clin. Nutr.* **1985**, *39C*, 355.

[30] A. Radonic, S. Thulke, I. M. Mackay, O. Landt, W. Siegert, A. Nitsche, *Biochem. Biophys. Res. Commun.* **2004**, *313*, 856.

[31] S. W. Lacey, J. M. Sanders, K. G. Rothberg, R. G. W. Anderson, B. A. Kamen, *J. Clin. Invest.* **1989**, *84*, 715.

[32] N. S. White, R. J. Errington, *Adv. Drug Delivery Rev.* **2005**, *57*, 17.

[33] S. Mao, O. Germershaus, D. Fischer, T. Linn, R. Schnepf, T. Kissel, *Pharm. Res.* **2005**, *22*, 2058.

[34] Y. H. Lin, C. K. Chung, C. T. Chen, H. F. Liang, S. C. Chen, H. W. Sung, *Biomacromolecules* **2005**, *6*, 1104.

[35] S. Ito, H. Aoki, *Adv. Polymer Sci.* **2005**, *182*, 131.

[36] X. T. Shuai, H. Ai, N. Nasongkla, S. Kim, J. M. Gao, *J. Controlled Release* **2004**, *98*, 415.

[37] V. P. Torchilin, *Pharm. Res.* **2007**, *24*, 1.

[38] N. Nishiyama, K. Kataoka, *Adv. Polymer Sci.* **2006**, *193*, 67.

[39] Y. Nagasaki, K. Yasugi, Y. Yamamoto, A. Harada, K. Kataoka, *Biomacromolecules* **2001**, *2*, 1067.

[40] S. L. Eun, N. Kun, H. B. You, *J. Controlled Release* **2003**, 103.

[41] S. Vinogradov, E. Batrakova, S. Li, A. Kabanov, *Bioconjugate Chem.* **1999**, *10*, 851.

[42] L. F. Zhang, A. Eisenberg, *Science* **1995**, *268*, 1728.

12 SUMMARY

The last decades have witnessed significant and rapid progress in polymer chemistry and molecular biology. The invention of PCR and advances in automated solid phase synthesis of DNA have made this biological entity broadly available to all researchers across biological and chemical sciences. Thanks to the development of a variety of polymerization techniques, macromolecules can be synthesized with predetermined molecular weights and excellent structural control. In recent years these two exciting areas of research converged to generate a new type of nucleic acid hybrid materials, consisting of oligodeoxynucleotides (ODNs) and organic polymers. By conjugating these two classes of materials, DNA block copolymers (DBCs) are generated exhibiting engineered material properties that cannot be realized with polymers or nucleic acids alone.

Due to the fact that synthetic methods for the generation of linear DBCs were rather limited, a major part of this work was dedicated to the development of robust strategies towards such structures. Special attention is paid for achieving the synthesis of amphiphilic DBCs with high yields. Different synthetic routes in solution and on solid phase were employed to obtain DNA di-, tri- or pentablock copolymers. The methods described in this thesis are based on grafting-onto strategies or the self-recognition properties of DNA. These preparation methods afforded DBCs with any given composition and length of nucleic acid segments ranging from tens of bases to more than 1000 bp. Techniques of organic chemistry, polymer chemistry and molecular biology were synergistically combined to produce novel functional biological organic hybrid materials.

DBCs of higher complexity like multiblock architectures have never been achieved. This synthetic challenge in block copolymer synthesis has been approached for the first time by exploiting the self-recognition properties of DNA. Hybridization of ss DBCs bearing complementary sequences was successfully employed to generate PEG-*b*-ds DNA-*b*-PEG triblock architectures with a monodisperse central nucleic acid segment. For the construction of more complex structures, an ss DNA-*b*-PEG-*b*-ss DNA triblock building block was synthesized on the solid phase. Employing this triblock copolymer in the hybridization

process with two equivalents of a ss DNA diblock copolymer generated pentablock copolymer architectures with a well-defined block topology. These multiblock architectures were analyzed by gel electrophoresis and MALDI-TOF MS. Furthermore, preliminary studies towards the morphology of these multiblock copolymers revealed that triblock copolymers formed inverse micelles with a DNA fragment as the core and PEG at the periphery when they were drop-casted from dichloromethane solution.

The DNA block copolymers known to date are restricted with respect to the length of their nucleic acid segments when compared to plasmid or genomic DNA. This synthetic limitation has been overcome by transferring polymerase chain reaction (PCR) into polymer chemistry. This method provided a simple technique to build well-defined multiblock copolymers with extended DNA segments. The use of one ss DNA-PEG-ss DNA triblock copolymer primer and a conventional ODN primer in the amplification process resulted in double stranded (ds) DNA triblock copolymers. When the primer set consisted of the ss triblock copolymer and a ss DNA diblock copolymer, ds DNA pentablock architectures were obtained. The tri- and pentablock copolymers exhibited a block topology of type ds DNA-PEG-ds DNA and PEG-ds DNA-PEG-ds DNA-PEG where the PEG and DNA segments have high and variable molecular weights. The lengths of the DNA blocks, which ranged from tens of bp to more than 500 bp, were adjusted by the annealing sites of the primers on the template. Common to all architectures are the high molecular weight and the monodispersity of the nucleic acid units. This is a significant achievement in the context of block copolymer synthesis: complex, structurally well-defined, high molecular weight hybrids can be prepared in one step without any of the demanding conditions involved in other polymerization techniques. DNA multiblock copolymers were characterized by gel electrophoresis, restriction analysis with sequence specific endonucleases and by scanning force microscopy (SFM). Furthermore, these nanostructures were manipulated by the SFM tip to investigate their mechanical properties on the single molecule level.

After establishing the synthetic routes for preparing DBCs, the morphology of these novel architectures was investigated. Among several examples, amphiphilic DBCs have found promising biomedical and biotechnological applications due to their self-organization behavior and the formation of nanoscale objects. The morphologies of DNA-*b*-PS block copolymer hybrids were characterized on different substrate surfaces by SFM. Depending on the processing conditions, spherical micelles or novel microscale DNA arrays with nanoscale

features were observed. Dendritic architectures were detected on silicon as well as on mica substrates. It should be noted that structure formation originates from driving forces other than conventional Watson-Crick base pairing. Salient features of this novel class of 2D materials covering surface areas of several square micrometers are the straightness and periodicity of the nanoscopic dendritic patterns, the bending of rectilinear topologies, and the unidirectional growth of dendrons. These morphologies offer great future potential for the construction of more sophisticated nanostructures and functions. The single stranded DNA present in these self-assembled structures could be equipped with different functionalities by hybridization.

For the DNA-*b*-PS diblock copolymer system mentioned above, the morhologies could be altered by different processing conditions. However, for the DNA-*b*-PPO copolymer system a very mild stimulus for structure manipulation was employed which is based on molecular recognition. The specific hydrogen bonding of the nucleic acid segment in DNA block copolymers offered the possibility to change such morphologies sequence specifically. It was described how DNA block copolymer morphologies can be varied by hybridization with long ss DNA sequences. Employing a long template which encodes the complementary sequence of the DBC altered the morphology from spheres to rod-like micelles. Even the length of the resulting rod-like micelles could be precisely adjusted by the number of nucleotides of the templates. The resultant nanostructures were visualized by SFM on a substrate surface and further characterized by FCS in solution.

In addition to switching the morphologies of DNA block copolymer micelles, it was demonstrated how the size of the spherical nanoparticles could be adjusted by an enzyme. For this purpose a template independent polymerase, TdT, was employed to adjust the size of DNA nanoparticles. By incubating DNA-*b*-PPO micelles for different reaction times, the sizes of these nanoobjects were increased from 10 nm to 25 nm with perfect control over the diameter of the spherical particles. The growth of the micelles was visualized by AFM, which undoubtedly proved the increase in size. In order to measure the exact dimensions of the DNA nanoparticles, dye labeled micelles were further investigated by FCS in the reaction buffer. This study also verified the growth of micelles. Furthermore, the number of nucleotides attached by the enzyme was correlated to the size of the nanoparticle using a molecular weight marker. A ladder of DNA-*b*-PPO block copolymer was prepared consisting of the

starting sequence and an additional thymidine segment of variable length attached at the 3' end.

Besides altering and adjusting the shape and the size of nanoparticles, DNA block copolymer micelles were successfully employed as scaffolds for DNA templated synthesis. The template consisted of amphiphilic DNA-block copolymer micelles with a hydrophobic core and a ss DNA-shell. Reactant DNA can be "clicked in" by hybridization into the micelles with a single stranded corona either at the surface or in the interior. Both arrangements led to high yields of the organic conversions compared to conventional templates. Due to the close proximity of the functionalities, a variety of chemical transformations like a Michael addition or a peptide bond formation are significantly accelerated. These novel 3D nanoobjects are of great importance for DNA-templated chemistry because they may allow sequence specific programmable reactions to occur while protected from the environment, as in a cellular system.

Alongside its physical properties, an important criterion for a bioorganic hybrid is its biocompatibility. We have investigated the toxicity of DBCs in Caco-2 cells. Motivated by the non-toxic nature of the DNA block copolymer micelles, uptake studies were carried out to investigate the shape effect of the internalization of nanoparticles. For this purpose, spherical micelles with ss and ds nucleic acid segments as well as rod like micelles were used. It was observed that rod-like nanoparticles were internalized 12 times more efficiently than the spherical counterparts. This result might have important consequences in regard to the toxicology of nanoparticles since uptake into cells is a critical issue.

Inspired by these experiments, the DNA block copolymer nanoobjects were employed as drug delivery vehicles to target an anticancer drug to tumor cells. Caco-2, a widely used cell model for intestinal absorption, was chosen as the cancerous cell line because these cells express surface receptors for folic acid. For efficient and specific internalization, the nanoparticles were functionalized with targeting units by hybridizing complementary sequences carrying folic acid entities. This facile route of nanoparticle functionalization allowed studying the effect of targeting unit density on the uptake efficacy. Additionally, these micelles were loaded with the anticancer drug, doxorubicin, and then applied to the tumor cells. The viability of the cells was measured in the presence and absence of targeting unit. It was

demonstrated that the tumor cells showed a high mortality when the targeting unit and the anticancer drug acted together within the novel DNA nanocarriers.

List of Publications

A. Peer-Reviewed Articles

1. F. E. Alemdaroglu, K. Ding, R. Berger, and A. Herrmann: **DNA-templated Synthesis in Three Dimensions: Introducing a Micellar Scaffold for Organic Reactions.**
   Angew. Chem. **2006**, *118*, 4313-4317; *Angew. Chem. Int. Ed.*, **2006**, *45***,** 4206–4210. "Highlighted as *Hot Paper* by Editors"

2. K. Ding, F. E. Alemdaroglu, M. Boersch, R. Berger, A. Herrmann: **Engineering the Structural Properties of DNA Block Copolymer Micelles by Molecular Recognition.**
   Angew. Chem. **2007**, *119*, 1191-1194; *Angew. Chem. Int. Ed.*, **2007**, *46*, 1172-1175.

3. F. E. Alemdaroglu, M. Safak, J. Wang, R. Berger, A. Herrmann: **DNA Multiblock Copolymers.**
   Chem. Commun. **2007**, *13*, 1358-1359.

4. F. E. Alemdaroglu, A. Herrmann: **DNA meets synthetic polymers—highly versatile hybrid materials.**
   Org. Biomol. Chem., **2007**, *5*, 1311-1320. „Cover page". „Highlighted in *Chemical Science*"

5. M. Safak, F. E. Alemdaroglu, E. Ergen, A. Herrmann: **PCR as an Efficient Tool for Block Copolymer Synthesis.**
   Adv. Mater., **2007**, *19*, 1499-1505. "featured as very important article"

6. F. E. Alemdaroglu, N. C. Alemdaroglu, P. Langguth, A. Herrmann: **DNA Block Copolymer Micelles – A Combinatorial Tool for Cancer Nanotechnology.**
   Adv. Mater., **2007**, *accepted*. "will be featured as very important article"

7. F. E. Alemdaroglu, W. Zhuang, L. Zöphel, J. Wang, R. Berger, J. P. Rabe, A. Herrmann: **Generation of Multiblock Copolymers by PCR: Synthesis, Visualization and Nanomechanical Properties.**
   Angew. Chem. Int. Ed., 2007 (submitted)

8. F. E. Alemdaroglu, J. Wang, M. Boersch, R. Berger, A. Herrmann: **Controlling the Size of Nanoparticles by an Enzymatic Reaction**
   J. Am. Chem. Soc. (submitted)

9. F. E. Alemdaroglu, N. Ceren Alemdaroglu, P.Langguth, A. Herrmann: **Cellular Uptake of DNA Block Copolymers with Different Shapes**
   Small (submitted)

B. Patent:

European Patent Application; *DNA Block Copolymer Micelles – A Combinatorial Tool for Cancer Nanotechnology*; 2007; Müllen, Klaus (DE); Alemdaroglu, Fikri E. (TR); Herrmann, Andreas (DE); Alemdaroglu, N. Ceren (TR); Langguth, Peter (DE) ; MAX PLANCK GESELLSCHAFT (DE)

C. Presentations (Selected)

1. F. E. Alemdaroglu, A. Herrmann, **Functional Nanoparticles from DNA Block Copolymers**, 2007 American Chemical Society in Boston, USA.-oral presentation

2. F. E. Alemdaroglu, A. Herrmann **DNA Block Copolymers: From Synthesis to Drug Delivery** 2007 European Science Foundation SONS Conference, Strasbourg, France – Awarded the Best Poster Award and Travel Grant.

3. F. E. Alemdaroglu, A. Herrmann, **Amphiphilic DNA Block Copolymer Architectures**, 2006. European Chemical Congress in Budapest, Hungary.-oral presentation

4. A. Herrmann, F. E. Alemdaroglu, E. Ergen **DNA Hybrid Materials for Surface Patterning and Nucleic Acid Detection** , 2005, Minerva Student Symposium Rehovot, Israel.

5. F. E. Alemdaroglu, E. Ergen, A. Herrmann, K. Müllen, **Multichromophoric 2D- and 3D- Architectures Based on DNA-Organic Hybrid Materials**, 2004, CNRS Summer School on DNA, Cargese, France.

6. F. E. Alemdaroglu, C. Zhang, A. D. Schlüter, **Synthesis of high molecular weight poly(para-phenylenes) for studying their nanoscale assemblies**, 2003. American Chemical Society National Meeting in New York (USA).-poster presentation